A DECISION-SUPPORT SYSTEM FOR THE DESIGN OF A GREEN-HYDROGEN PRODUCTION SYSTEM IN A HYDROPOWER PLANT

David Jure Jovan

Doctoral Dissertation
Jožef Stefan International Postgraduate School
Ljubljana, Slovenia

Supervisor: Asst. Prof. Dr. Gregor Dolanc, Jožef Stefan Institute, Ljubljana, Slovenia

Evaluation Board:
Asst. Prof. Dr. Damir Vrančić, Chair, Jožef Stefan Institute, Ljubljana, Slovenia
Prof. Dr. Danjela Kuščer Hrovatin, Member, Jožef Stefan Institute, Ljubljana Slovenia
Prof. Dr. Mihael Sekavčnik, Member, Faculty of Mechanical Engineering, University of Ljubljana, Slovenia

MEDNARODNA PODIPLOMSKA ŠOLA JOŽEFA STEFANA
JOŽEF STEFAN INTERNATIONAL POSTGRADUATE SCHOOL

David Jure Jovan

A DECISION-SUPPORT SYSTEM FOR THE DESIGN OF A GREEN-HYDROGEN PRODUCTION SYSTEM IN A HYDROPOWER PLANT

Doctoral Dissertation

SISTEM ZA PODPORO ODLOČANJU PRI ZASNOVI SISTEMA ZA PROIZVODNJO ZELENEGA VODIKA V HIDROELEKTRARNI

Doktorska disertacija

Supervisor: Asst. Prof. Dr. Gregor Dolanc

Ljubljana, Slovenia, March 2024

To my wife, my daughter, my parents, and my family!

Acknowledgments

First of all, I would like to express my sincere gratitude to my employer, the Department of Systems and Control at the Jožef Stefan Institute in Ljubljana, for funding this doctoral dissertation. I would like to take this opportunity to thank you for your trust and willingness to support me in achieving my goals.

I would like to thank the following individuals for their contribution and support during the course of this dissertation:

I am deeply indebted to Asst. Prof. Dr. Gregor Dolanc for his excellent academic support and supervision throughout my doctoral research. Your unwavering academic guidance and mentorship have been invaluable. Your insightful feedback and thought-provoking discussions have significantly shaped the direction of my research. Thank you for your dedicated supervision.

I would like to express my sincere appreciation to Dr. Boštjan Pregelj for his valuable contributions to my dissertation. Your expertise in modelling and simulation has significantly improved the quality of my work. Thank you very much for sharing your knowledge and insights with me.

I would like to extend my sincere gratitude to all the staff at the department for their support and for fostering a collaborative and intellectually stimulating environment. Our interactions, seminars and shared experiences have enriched my academic journey.

My deepest and sincere gratitude also goes to my family for their constant and unrivalled love, help and support. They have been a great source of motivation throughout this process.

Abstract

This dissertation combines academic research and the application of its results to a real benchmark process.

With the emerging electro-energetic systems that have a large share of renewable sources, hydrogen is becoming an important energy carrier that contributes to the storage and usage of surplus green energy and thus reduces air pollution, climate change and can be used as a feedstock in a variety of industrial processes. Therefore, hydrogen production from renewable energy sources (known as green hydrogen) is important where a hydropower plant, as the most stable renewable electrical energy source, can play an important role. But today's green-hydrogen production is barely economically viable due to the current price of technological equipment for its production, which is not yet mass produced. This prevents green-hydrogen technologies from being widely adopted.

The basic aims of the dissertation are to address the potential for green-hydrogen production in a run-of-river hydropower plant during its regular operation and an evaluation of the economics of the cogeneration of electricity and hydrogen. The hypothesis is that the development of an appropriate decision-support tool can lead to a better hydrogen-system design and its inclusion in a hydropower plant for green-hydrogen production. Namely, the proper sizing of the equipment by simultaneously taking into account the available water resources and the techno-economic aspects (e.g., current electricity prices, the selling price of hydrogen) leads toward a better selection of the hydrogen system's components. It is expected that the developed decision-support tool will contribute to (i) efficient simulation scenarios for the evaluation of the techno-economic aspects of the hydrogen system's operation, (ii) a reduction of the investment costs for the hydrogen system's installation, (iii) lowering the hydrogen-production costs and (iv) increasing the financial sustainability of investment in a hydrogen system.

To verify the hypothesis, in the first part of the dissertation we developed a model of the hydropower plant's operation, the model of the hydrogen system and the economic model, which describes the link between the equipment type and size, on one hand, and related capital investment costs (CapEx) and operating costs (OpEx) on the other. The economic model also estimates the resulting costs of hydrogen production and the economic outcome of the operation of the entire system. These models were used to set up the simulation environment in a MATLAB/Simulink programming platform to conduct the various simulation runs and present the simulation results.

In the second part of the dissertation, we demonstrate the use of the developed models and the simulation environment in the evaluation of various scenarios for hydrogen production in the case-study hydropower plant. We demonstrated that the use of this tool helps to reduce the investment costs for the installation of a hydrogen system, to lower the production price of hydrogen and to make the investment in a hydrogen system profitable.

Povzetek

Disertacija združuje akademske raziskave in uporabo pridobljenih rezultatov na vzorčnem testnem procesu.

Z nastajanjem elektroenergetskih sistemov z visokim deležem obnovljivih virov vodik postaja tudi pomemben energetski nosilec, ki omogoča shranjevanje presežkov energije, zmanjšuje onesnaženost zraka in podnebne spremembe ter se uporablja kot surovina v različnih industrijskih procesih. Zato je proizvodnja vodika iz obnovljivih virov energije (zeleni vodik) pomembna tema, kjer ima lahko hidroelektrarna, kot najbolj stabilen vir obnovljive električne energije, pomembno vlogo. Vendar je današnja proizvodnja zelenega vodika težko ekonomsko upravičena zaradi trenutne cene tehnološke opreme za njegovo proizvodnjo, ki še ni predmet masovne proizvodnje. To preprečuje široko uporabo vodikovih tehnologij.

Osnovna cilja disertacije sta obravnava možnosti za proizvodnjo zelenega vodika v pretočni hidroelektrarni med njenim rednim obratovanjem in ocena ekonomske upravičenosti soproizvodnje električne energije in vodika. Hipoteza je, da lahko razvoj ustreznega orodja za podporo odločanju vodi do bolj optimalne zasnove vodikovega sistema in njegove vključitve v proizvodnjo zelenega vodika v hidroelektrarni. Pravilno dimenzioniranje opreme vodikovega sistema namreč ob hkratnem upoštevanju razpoložljivih vodnih virov in tehnično-ekonomskih vidikov (npr. trenutne cene električne energije, prodajna cena vodika) vodi k optimalnejši izbiri komponent vodikovega sistema. Pričakuje se, da bo uporaba razvitega orodja za podporo odločanju prispevala k (i) učinkovitim simulacijskim scenarijem za vrednotenje tehnično-ekonomskih vidikov delovanja vodikovega sistema, (ii) zmanjšanju investicijskih stroškov izgradnje vodikovega sistema, (iii) znižanju proizvodnih stroškov vodika in (iv) povečanju finančne vzdržnosti naložbe v vodikov sistem.

Za preverjanje hipoteze smo v prvem delu disertacije razvili model obratovanja hidroelektrarne, model vodikovega sistema in ekonomski model, ki opisuje povezavo med vrsto in velikostjo opreme na eni strani ter s tem povezanimi stroški investicije (CapEx) in operativnimi stroški (OpEx) na drugi strani. Ekonomski model ocenjuje tudi nastale stroške proizvodnje vodika in ekonomski rezultat delovanja celotnega sistema. Ti modeli so bili uporabljeni za nastavitev simulacijskega okolja v programski platformi MATLAB/Simulink za izvajanje različnih simulacijskih potekov in predstavitev rezultatov simulacije.

V drugem delu disertacije prikazujemo uporabo razvitih modelov in simulacijskega okolja pri vrednotenju različnih scenarijev proizvodnje vodika v vzorčni hidroelektrarni. Dokazali smo, da uporaba tega orodja pripomore k znižanju investicijskih stroškov vgradnje vodikovega sistema, nižji proizvodni ceni vodika in donosnosti naložbe v vodikov sistem.

Contents

List of Figures

List of Tables

Abbreviations

AEL	... alkaline-water electrolysis
AEM	... anionic exchange membrane
ANSI	... American National Standards Institute
ARSO	... Slovenian Environmental Agency
BoP	... balance of plant
CapEx	... capital investment costs
CF	... criterion function
CSA	... Canadian Standards Association
CV	... criterion variable
CCS	... carbon capture and sequestration
CH_4	... methane
CO	... carbon monoxide
CO_2	... carbon dioxide
DOE	... US Department of Energy
EES	... electro-energetic system
EHC	... electrochemical hydrogen compressor
ENTSO-E	... European Network of Transmission System Operators for Electricity
FCH-JU	... European Fuel Cells and Hydrogen Joint Undertaking
GHG	... greenhouse gas
GHP	... green-hydrogen production
GUI	... graphical user interface
HGV	... hydrogen gas vehicle
HPP	... hydropower plant
IEA	... International Energy Agency
IRENA	... International Renewable Energy Agency
KPI	... key performance indicator
LCHS	... levelized cost of hydrogen storage
LCOH	... levelized cost of hydrogen
NZE	... Net Zero Emissions (by 2050 Scenario)
OP	... optimisation parameter
OpEx	... operating costs
P2G	... power-to-gas (also PtG)
P2X	... power-to-x
PBP	... payback period
PC	... production cost
PEM	... proton exchange membrane
PSO	... particle swarm optimisation
PV	... photovoltaic
RES	... renewable energy sources
RMS	... root mean square
SCADA	... supervisory control and data acquisition

SMR ... steam methane reforming
SoC ... state of charge
SOEC ... solid-oxide electrolyser cell
TEA ... techno-economic assessment
TRL ... technology readiness level
WPEB ... wind-photovoltaic-electrolysis-battery

Symbols

A	... area [m^2], unit to ampere [A]
c	... hydrogen system utilisation rate [%]
C	... specific electrical energy consumption [kWh/kg], carbon
d	... denivelation [m], unit to days [d]
e^-	... electron
E	... energy [kWh]
g	... acceleration due to gravity [m/s^2], gain
h	... head [m]
H	... hydrogen
H^+	... proton
I_{DC}	... direct electric current [A]
J	... electric current density [A/m^2]
J_S	... solar irradiance [W/m^2]
k	... user-specified weight, inclination factor
K_L	... compression loss coefficient
m	... mass [kg]
$\dot{m}$	... mass-flow rate [kg/h]
M	... molar mass [g/mol]
n	... compression loss exponent
$\dot{n}$	... molar flow rate [mol/s]
N_A	... Avogadro's number [mol^{-1}]
N_{CELL}	... number of electrolyser stack cells
n_e	... number of electrons in one molecule
O	... oxygen
p	... pressure [bar]
P	... electrical power [kW]
Q	... volumetric flow rate [m^3/s]
q_{EL}	... electric charge of an electron [C]
R	... universal gas constant [J/(mol K)]
t	... time [s]
t_A	... hydrogen-system lifetime if not operated [h]
t_L	... hydrogen-system lifetime [h]
T	... absolute temperature [K]
T_F	... time constant
U_{DC}	... voltage of the electrolysis cell [V]
V	... volume [m^3], unit to voltage [V]
y	... unit to year [y]
γ	... compression factor
η	... energy efficiency [%]
ρ	... density (at STP) [kg/m^3]

Chapter 1

Introduction

The world is facing increasing energy consumption, air pollution and climate changes. In response the European Union is reducing the use of carbon-based fossil fuels and moving towards renewable energy sources (RESs) as a bases for energy supply. These decisions, supported by policy initiatives [1] and legislative packages [2] of the European Commission, and by national energy and environment plans [3], should enable the sustainable, environmentally acceptable and carbon-free development of the European Union.

These decisions inevitably lead to the so-called "green transformation" of the energy-supply sector, including the electrical power system, which is demonstrated by the European Network of Transmission System Operators for Electricity (ENTSO-E) association [4]. The integration of RESs, e.g., wind, photovoltaic and hydropower, is an effective way to deal with these problems [5]. Some European countries also envisage nuclear power generation as a non-renewable but carbon-free energy source. By 2050, the entire energy supply should be carbon-free and based on RESs.

Hydrogen has the potential to accelerate the process of scaling up clean and renewable energy, but its integration into electrical power systems remains under-studied [6]. However, research on the topic of using hydrogen-related technologies is becoming more intensive, particularly during the last decade [7].

Hydrogen technologies can be used to convert electrical energy into the chemical energy of hydrogen and vice versa, and to store and transport hydrogen. Electrical energy generation by renewable power sources (hydro, wind and solar) very much depends on the time of day, the season and the weather, and it cannot follow electrical energy demands. One possibility to balance energy generation and consumption is energy storage; however, the technical possibilities are very limited and expensive. One option is the conversion of any excess electrical energy into the chemical energy of hydrogen using water electrolysis. The generated hydrogen can then be stored and used for various purposes (feedstock, fuel) or it can be converted back to electrical energy by, e.g., fuel cells or other types of generators.

In the field of worldwide electricity production, hydropower is one of the largest sources of renewable energy. In 2020, hydropower generated one-sixth of global electricity, making it the third-largest energy source after coal and natural gas [5], [8]. Hydropower's contribution is more than half that of nuclear power and greater than that of all the other renewable energy sources combined. It should also be noted that compared to wind turbines and photovoltaic fields, hydropower plants (HPPs) are the least weather dependent and so they remain the backbone of low-carbon electricity generation, providing almost half of it today.

As the most stable renewable electrical energy source, hydropower in connection with hydrogen usage can play the central role in the decarbonisation of our society. The

introduction of hydrogen system/power-to-gas (P2G) technology [9], [10], [11] into a HPP operation enables hydrogen generation, which can be used in carbon-free transport, as feedstock in various chemical industries, or as a source of renewable chemicals (e.g., methanol, ammonia, synthetic natural gas). The hydrogen produced with electricity from hydropower and other RESs has a special value because its production is carbon dioxide (CO_2) emission free and, consequently, it is called green hydrogen [12].

But today's green hydrogen production is barely economically viable due to the current price of the technological equipment for its production, which is not yet mass produced. This prevents green hydrogen technologies from being widely adopted. Many articles and studies have addressed this issue and claim that the transition to RESs would inevitably need subsidies in the short-to-medium term [13], [14], [15], [16], [17], [18]. These supporting policies must be accompanied by lower costs to make the technologies a realistic future alternative. The authors in [19] state that if a wind or hydropower plant is upgraded with a hydrogen system, the economic viability is increased. The engineering and economic analysis [20] suggests that the green hydrogen economy will be a profitable option for industrial decarbonisation. It will be more viable in cases where carbon taxes are foreseen, and it will become more profitable when hydrogen production equipment costs start to fall relative to the current market price. In [21], the author summarises that green hydrogen is seen by investors, developers, and politicians as a strong enabler to meet net-zero targets and that a market for green hydrogen is opening up, but cost competitiveness remains a barrier to scaling up.

Despite the indisputable advantages of using green hydrogen in various fields, the technological feasibility of hydrogen systems, and above all their economic viability, still remain open issues. This also applies to HPPs with the ambition to produce green hydrogen.

1.1 Hydrogen Production and Use

Green hydrogen of very high purity (99.999% and better), produced in the process of water electrolysis using electrical energy from RESs, will play an increasingly important role in the coming years [22]. It is present in all eight net-zero greenhouse gas emission scenarios of the European Commission up to 2050 (A Clean Planet for all: A European long-term strategic vision for a prosperous, modern, competitive and climate neutral economy, [23]). The proposed strategy is meant to set the direction of travel for EU climate and energy policy, and to frame what the EU considers as its long-term contribution to achieving the Paris Agreement's temperature objectives in line with UN Sustainable Development Goals, which will further affect a wider set of EU policies.

Despite the fact that hydrogen is recognised as a promising energy vector/carrier, today's prevailing production method, i.e., steam reforming of natural gas (SMR), is not in line with long-term climate and energy goals since such production is not CO_2-emission free, as it uses natural gas and generates CO_2 emissions ("grey hydrogen"). Therefore, a hydrogen production process base on electrolysis using the energy from RESs ("green hydrogen") thus has added value and as such it could make a key contribution to reducing CO_2 emissions, reducing local pollution, ensuring energy independence and helping to achieve sustainable goals, as shown in Figure 1.1.

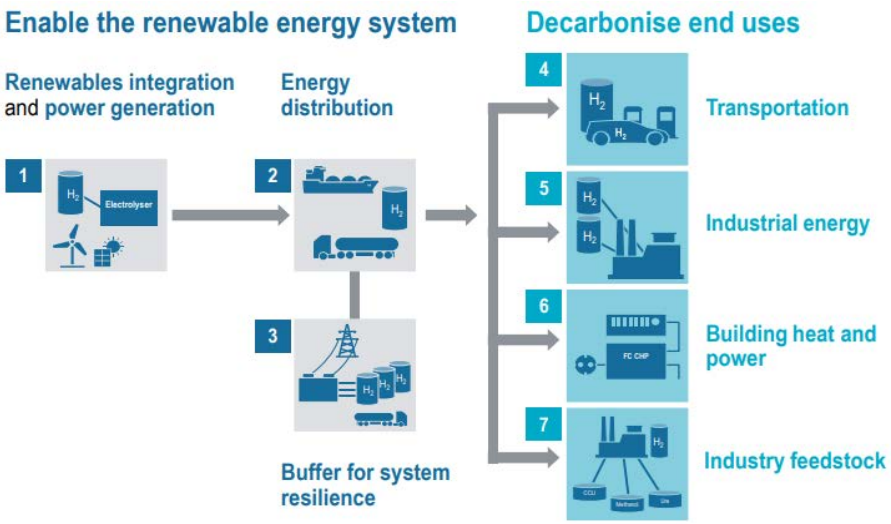

Figure 1.1: Potentials for the introduction of hydrogen technologies [24].

Over the past few years, several EU countries and others (Japan, China, USA, GB, etc.) have adopted their hydrogen strategies and already implemented policies that increase the role of hydrogen in a variety of applications. These and other drivers will increase the worldwide demand for hydrogen from around 80 million tons per year in 2020 to over 183 million tons per year in 2050 [25], [26], [27], as shown in Figure 1.2.

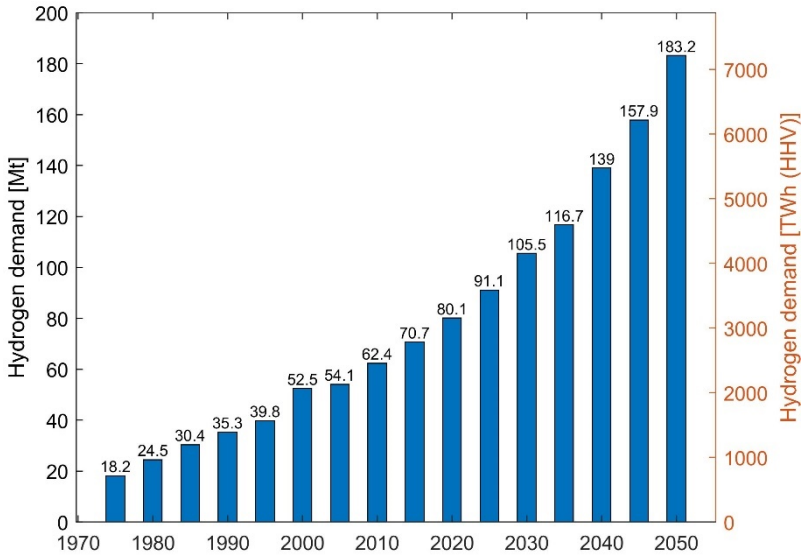

Figure 1.2: Outlook for world hydrogen demand in millions of tons per year.

However, the introduction of green hydrogen as an energy vector/carrier is not only a technological challenge, but also requires the coordination and convergence of the goals of many political and socio-economic factors. Political will, improved regulation and appropriate financial support are the instruments that will be needed to promote the use of green hydrogen. Green hydrogen has many benefits, but policy initiatives are also needed to help reduce production costs and remove market barriers.

The systematic initiatives needed are mainly those that:

- *reduce local emissions;*
- *reduce global greenhouse-gas (GHG) emissions;*
- *increase energy security through the use of local sources and alternative energy sources;*
- *develop new technological areas and thus new jobs (develop and produce equipment for hydrogen technologies).*

In addition to political decisions, the ability of industry to reduce the cost of manufacturing hydrogen and using the building blocks of hydrogen technologies will be extremely important for the future of the hydrogen economy. In this way, the conditions for the mass production of green hydrogen and its use will be met.

1.2 Hydrogen System

A hydrogen system encompasses equipment for the production, storage and utilisation of hydrogen as an essential component of our clean energy future. Designing and dimensioning a hydrogen system involves several considerations to ensure its efficiency and effectiveness. This section examines the key background information and inputs required for the dimensioning of such a system.

1.2.1 Hydrogen Taxonomy

In this subsection, different types (described as colours) of hydrogen are presented, differentiated according to the production method, feedstock and energy source, and CO_2 generation during production. This dissertation is focused on *green hydrogen*, which is produced from water by electrolysis using RESs [8], [28], [29]. It is called green because no CO_2 emissions are generated during its production and no fossil fuels are employed. Unlike other kinds of hydrogen, this kind is fully in line with the goals of a green transition. There are several other types of hydrogen. *Blue hydrogen* is produced from fossil fuels. The process involves carbon (CO_2) capture and sequestration (CCS) to avoid the release of CO_2 into the atmosphere. *Grey hydrogen* is produced from natural gas and normally uses the steam methane reforming (SMR) process, where natural gas is used as both the feedstock and the energy source. This process produces CO_2 and eventually releases it into the atmosphere. The options for hydrogen production that are based on thermal energy (pyrolysis of natural gas) result in *turquoise hydrogen*. *Brown and black hydrogen* are produced from coal via the gasification method. However, this is a very polluting process that produces CO_2 and carbon monoxide (CO) as by-products and releases them into the atmosphere. The literature also contains some less common hydrogen colours such as yellow, red, purple, orange and white, but these are not always used consistently. The selected hydrogen colour codes and associated production methods are summarised in Table 1.1.

Table 1.1: Hydrogen colour codes and associated production methods [30], [31].

Colour code	Source of energy	Source of hydrogen	Production process	CO_2 emissions [kg CO_2eq/kg H_2]
Green hydrogen	Renewable energy	Water	Electrolysis	0
Blue hydrogen	Electricity from non-renewable energy	Natural gas/Biomass	Steam methane reforming with CCS	0.5–4
Grey hydrogen	Electricity from non-renewable energy	Natural gas	Steam methane reforming	9–11
Turquoise hydrogen	Electricity from non-renewable energy	Natural gas	Pyrolysis	0
Brown hydrogen	Electricity from non-renewable energy	Lignite coal/Biomass	Gasification	18–20
Black hydrogen	Electricity from non-renewable energy	Bituminous coal	Gasification	18–20

The methods described for producing hydrogen use either one or a combination of the following primary energy sources: electrical, thermal, photonic and biochemical. Electrical and thermal energy can be derived from renewable energy, biomass, nuclear power or fossil fuels. The electrical and thermal energy source has a major impact on the emissions of the corresponding methods. If the electricity is obtained from RESs, the CO_2 emissions are lower or even non-existent. The individual production methods also differ significantly in terms of the production costs of hydrogen.

Today, SMR is the most common and cost-effective method for hydrogen production [32]. As this technology is mature and production equipment is well developed, fluctuations in the cost of produced hydrogen today mostly depend on the price of natural gas [33]. However, SMR generates CO_2 emissions, so in the future this process should be replaced by green methods.

1.2.2 Systems for Electrical Energy Conversion

Hydrogen systems belong to a broader class of systems that store electrical energy in synthesized gaseous or liquid fuel (e.g., pure hydrogen, synthetic methane, methanol, ammonia, etc.). These kinds of systems that convert electrical energy into another energy vector are referred to as “electrical energy-x” (P2X), where X is the end product of the energy conversion. The term “electrical energy-gas” describes a variety of systems where the end product is a gaseous fuel, usually hydrogen or synthetic methane. The term P2G thus refers to the process in which electrical energy is converted into chemical energy via gas production. Originally, power-to-gas (P2G or PtG) describes the conversion of renewable electricity into renewable synthetic methane gas [34], [35], [36]. The production combines two core processes: water electrolysis and CO_2 methanation [37], as seen in Figure 1.3.

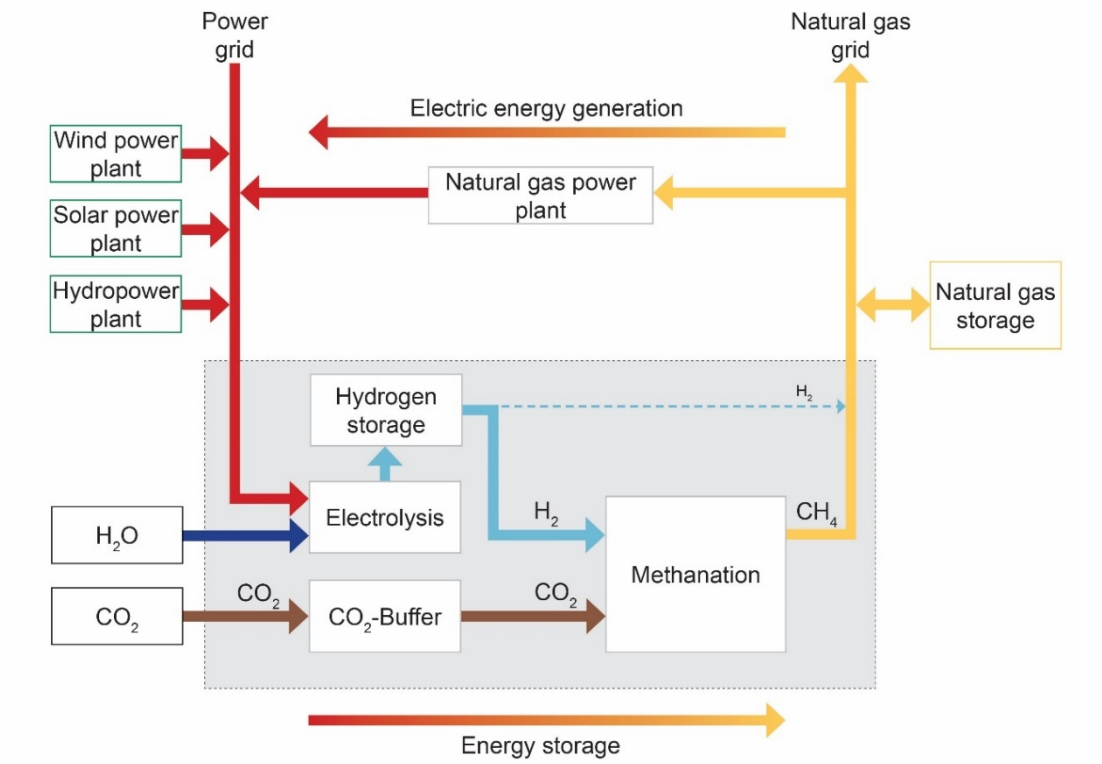

Figure 1.3: Scheme of a typical P2G installation (first published in 2009 [38]).

The common point of P2G or P2X systems is the green-hydrogen production method. Green hydrogen is usually produced from water by electrolysis, driven by green renewable electrical energy (hydro, wind, solar power source). The resulting hydrogen can be directly used or it can be, for example, converted into synthetic methane (CH_4) by a methanation process using CO_2. Methane is the main constituent of natural gas and thus the generated synthetic methane is a substitute of natural gas that can be fed and stored in the natural-gas grid without limitations. In [39], a worldwide overview of power-to-gas projects producing hydrogen or a renewable substitute is elaborated. The article [34] sets out the conceptual aspects that are necessary to include power-to-gas facilities in a more comprehensive analysis framework for the operation of an electrical system in various sectors.

P2G systems represent a way to integrate green electrical energy into electrical power grid and replace the use of fossil fuels in different sectors (transport, heat production for buildings and industrial processes, etc.). More specifically, P2G systems can help balance the electricity grid. When there is an excess of green electrical energy, the surpluses can be converted to synthetic fuels, thus balancing the electrical energy production and consumption. This becomes increasingly important since the green transition requires the installation of numerous new, renewable energy sources. Renewable energy sources very much depend upon the weather and do not follow the demands for electrical energy. Thus, grid balancing becomes more and more important and P2G systems represent one possible solution. On the other hand, the resulting green, renewable synthetic fuels can help decarbonise the sectors that cannot be directly electrified and are traditionally powered by fossil fuels. In these sectors, fossil fuels can be replaced by synthetic green and renewable fuels, generated by P2G systems. Further discussion can be found in, e.g., [40].

Electrolysis technology (described in Section 1.2.3) and electrolyser manufacturing capacities strongly affect the possibilities for green or low-emission hydrogen production and the further production of synthetic fuels, as discussed, e.g., in IEA report [41]. Electrolysis offers a sustainable, high-purity method of producing hydrogen [42]. Accelerated by green-transition plans, electrolysis capacity is growing from a low base and needs to accelerate to keep pace with the Net Zero Emissions by 2050 (NZE) scenario, which requires an installed electrolysis capacity of more than 550 GW by 2030 [43]. The realisation of all the planned projects could lead to an installed electrolyser capacity of 170–365 GW by 2030 [41]. Similarly, another source estimates that more than 230 GW of electrolyser capacity will be commissioned globally by 2030 [44].

In general, P2G systems can generate income from various sources, as follows:

- *Income from produced hydrogen or related synthetic fuel (sold as fuel or feedstock),*
- *Income from electricity-grid balancing services (ancillary services paid by electricity grid operators or participation and trading in short-term electrical energy markets).*

The operation of P2G plants can be economically acceptable and even profitable in certain cases. It can assure the clean production of feedstock for industrial processes [45], an affordable solution for storing larger amounts of electrical energy in an economically viable way [37], [46] and also provide a strong link between the gas grid and renewable electrical energy.

1.2.3 Structure of the Hydrogen System

This subsection is focused on the hydrogen system (a subsystem of P2G, presented in Figure 1.3), which consists of an electrolyser and hydrogen storage.

The electrolyser generates the hydrogen from water using electrical energy. Today, four main electrolyser technologies are in use [42], [47], [48], [49], [50], [51], [52]:

- *Alkaline electrolysis (AEL),*
- *Proton-exchange-membrane (PEM) electrolysis,*
- *Solid-oxide electrolysis (SOEC),*
- *Anionic-exchange-membrane (AEM) electrolysis.*

The advantages and disadvantages of the individual types of electrolysers are summarised in Table 1.2. Further details about electrolysis can be found in [50].

Table 1.2: Summary of electrolysis technologies.

TYPE	AEL	PEM	SOEC	AEM
Advantages	Mature technology High and long-term stability Catalysts without platinum group metals (PGMs) Low investment cost Megawatt range	Commercial technology High current density Compact High purity of hydrogen Simple design Fast response (start-up) time Dynamic operation High operating pressure Small plant layout	High current density Low energy consumption High efficiency of conversion Low capital loss No catalyst Inexpensive materials	Non-noble-metal catalysis Non-corrosive electrolyte Compact cell design Low cost Absence of leaking High operating pressure
Drawbacks	Gas permeation Low current densities Slow dynamics Low operating pressure Corrosive electrolyte Large plant layout Exhibit lower energy conversion efficiency (compared to PEM)	High cost of components Acidic, corrosive components Possible low durability Requires noble-metal catalysts Stack limited to around MW range	Currently in demonstration stage Small volume production Short durability (e.g., delamination of electrodes) Safety issues Instability of electrodes Problematic sealing	Currently at laboratory stage Low current density Short durability Membrane degradation Excessive catalyst loading

During the electrolysis of water, hydrogen and oxygen gases are produced according to the following electro-chemical reaction:

$$2H_2O\ (l) + electricity + heat \rightarrow 2H_2(g) + O_2(g) \tag{1.1}$$

The half reaction of the anode and cathode can be expressed as:

$$\begin{gathered} 2H_2O \rightarrow O_2 + 4H^+ + 4e^-\ (anode) \\ 4H^+ + 4e^- \rightarrow 2H_2\ (cathode) \end{gathered} \tag{1.2}$$

In PEM water electrolysis, water is electro-chemically split into hydrogen and oxygen at their respective electrodes: hydrogen at the cathode and oxygen at the anode. PEM water electrolysis is accrued by pumping water to the anode where it is split into oxygen (O_2), protons (H^+) and electrons (e^-). These protons travel via the proton-conducting membrane to the cathode side. The electrons exit from the anode through the external power circuit, which provides the driving force (cell voltage) for the reaction. At the cathode side, the protons and electrons re-combine to produce the hydrogen, following the mechanism as depicted in Figure 1.4 [53].

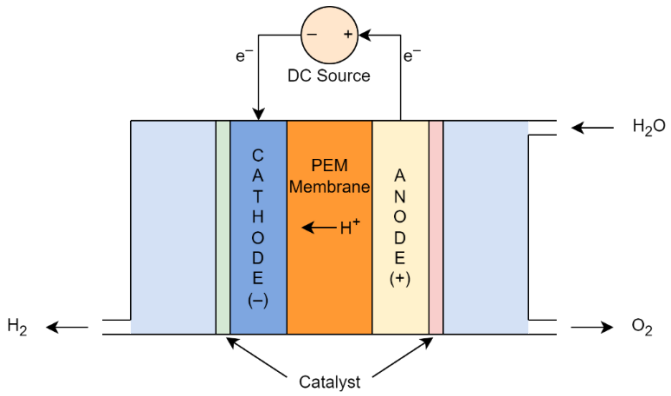

Figure 1.4: Basic illustration of PEM water electrolyser.

Generated hydrogen usually needs to be stored for a short or long period. There are several hydrogen-storage technologies: hydrogen compression, liquefaction, adsorption (metal hydrides, LOHC) or chemical storage (conversion into ammonia, methanol). In this dissertation, we focus on storage in compressed gaseous form, which is the simplest solution and requires a hydrogen compressor and a pressurised hydrogen-storage tank. Further details on hydrogen storage can be found in [54], [55], [56], [57], where the main features of each storage method for use in heating, mobility, industry and power are discussed in detail.

A typical hydrogen system is shown in Figure 1.5.

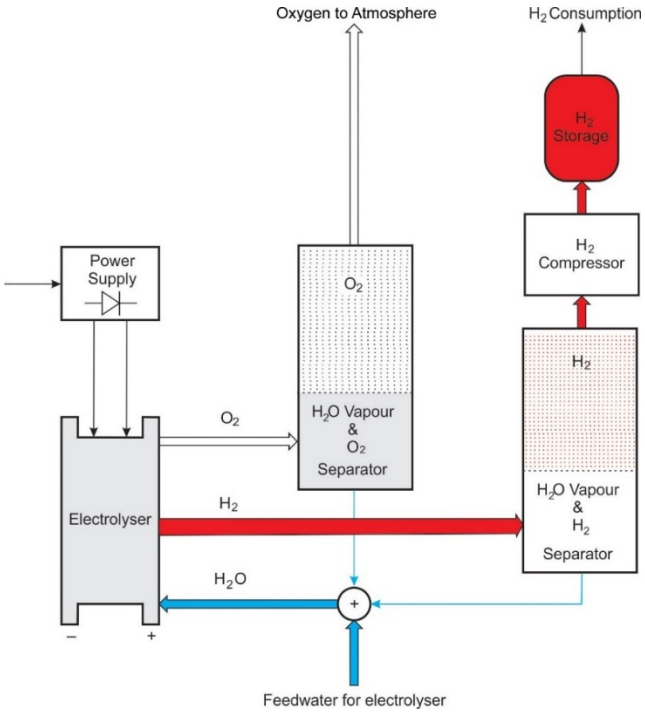

Figure 1.5: Basic components of hydrogen system.

In the following subsections, the state-of-the-art of the hydrogen-system equipment is analysed. This is needed to develop the technical and economic models of the hydrogen system.

1.2.4 Designing a Hydrogen System

Designing a hydrogen system means selecting the proper type and size of the system's components. As follows from the previous sections, the main system components are an electrolyser, hydrogen storage and a hydrogen compressor. In general, the capital and operating costs (CapEx, OpEx) of components increase with their sizes and capacities. To optimise the economic sustainability of hydrogen systems, costs must to be minimised since they directly affect the production price of hydrogen (see Section 1.2.6) and the financial sustainability of the hydrogen system.

1.2.4.1 Equipment Type Selection

The electrolyser type (AEL, PEM, SOEC, AEM) is selected on the basis of two parameters: required purity of the produced hydrogen, and the fluctuation in the rate of hydrogen production.

Hydrogen-purity requirement: If the produced hydrogen is to be converted back to electricity with a fuel cell, then "fuel-cell-grade hydrogen purity" is required. This level of purity can only be achieved by PEM electrolysers, while hydrogen produced by AEL electrolysers requires additional purification to remove residues of the electrolyte. SOEC and AEM electrolysers are still in the R&D phase, but the manufacturers expect a similar degree of hydrogen purity as with PEM electrolysers. In the case of the AEM electrolyser, an additional drying process is required to achieve a higher hydrogen purity.

Fluctuation of the hydrogen-production rate: When the hydrogen is to be produced at a steady and constant production rate, AEL type electrolysers can be used. On the other hand, when the hydrogen-production rate changes rapidly over time (e.g., due to the fluctuating available electrical power of the RESs or due to participation in ancillary services for electricity grid stabilisation), the PEM technology should be used since it enables ramping up and down (load change) between minimum and maximum power in seconds. The PEM type also facilitates rapid stat-up.

1.2.4.2 Equipment Sizing

The most important sizing parameters are the production capacity of the electrolyser [kg H_2/h], the hydrogen-storage capacity [kg] and the storage pressure [bar]. In general, the hydrogen production task can be solved by different combinations of component sizes, but the goal is to find the optimal combination in terms of costs (cost minimisation). Due to the many variables involved and the nonlinear relations between the variables, the problem cannot be solved analytically.

In this dissertation the problem is approached by mathematical modelling of the process (hydropower plant model, hydrogen system model, economic model) and simulating the mathematical model with different combinations of component sizes that fulfil operating conditions and demands. The optimal solution is found through simulation by performing the following steps:

- *Create the mathematical model.*
- *Define the cost function (e.g., price of the equipment, degradation, etc.).*
- *Define the* range *and* step change *of a particular parameter.*
- *Simulate the model with all combinations of parameters.*

- *Calculate the cost function for each parameter combination.*
- *Select the parameter combination with the minimum value of the cost function.*

In the dissertation, the procedure is enhanced by an optimisation algorithm and represents a decision support in the designing of a hydrogen system.

1.2.5 Capital and Operating Costs of Hydrogen System

The investment costs of hydrogen technologies represent a central challenge for the realisation of energy systems based on renewable hydrogen. In general, the technological equipment of a hydrogen system is not yet mass produced and consequently the associated costs are high. In Chapter 1.3 we analyse the current prices of the individual components of a hydrogen system in the MW range, considering the effects of plant size and the expected technological developments. In this subsection, we identify the categories of costs of purchasing and operating the necessary equipment for hydrogen production for a case study of a HPP. For further calculations, technical specifications of one of the commercially available P2G systems [58] are used.

On the basis of commercial providers of hydrogen systems and literature data [9], [11], [47], [59], [60], [61], [62], [63], [64], [65], [66], [67], [68] the main estimated costs for the implementation of a 1-MW PEM-based hydrogen system were already elaborated in [69] and are listed in Table 1.3. The assumed hydrogen storage has the following characteristics: the maximum storage pressure (p_{H2_MAX}) is 50 bar, the maximum storage capacity for hydrogen (m_{H2_MAX}) is 400 kg. A 25-kW compressor with a hydrogen compression flow (Q_{H2}) between 20–35 kg/h from the initial pressure (p_{IN}) of 2 MPa to the target pressure, (p_{H2}) of 5 MPa, is assumed for the compression of the hydrogen before storage.

Table 1.3: Estimated costs of the components for proposed hydrogen system.

Equipment or service	Estimated cost
Project documentation	100,000 €
Electrolyser	1,600,000 €
Hydrogen storage	200,000 €
BoP[1] components	120,000 €
Electrical connection to HPP	100,000 €
Construction and assembly works	80,000 €
Total costs	2,200,000 €

[1] BoP: balance-of-plant components (various supporting and auxiliary components)

Using the data from Table 1.3, capital expenditure costs (CapEx) and operating costs (OpEx) for the 1 MW hydrogen system installation and operation can be estimated.

Investment costs (CapEx) are 2,200,000 €. Operation costs (OpEx) are manpower (e.g., operator to run the hydrogen system), consumables (parts that must be replaced on periodic basis, purified water – a feedstock for hydrogen production), maintenance services, and similar costs. The estimation of exact OpEx costs depends on the operating conditions of the equipment and many other factors and is thus difficult to determine [59], [61], [66]. In the literature, it varies from 1.5 to 5% [70]. Since the exact OpEx costs are not known, it is assumed that these annual costs equal 5% of the CapEx costs, which means 110,000 €/year.

Another important factor is the lifetime of the equipment, in particular the lifetime of the electrolyser. In general, lifetime depends on operating conditions, there are events and

conditions that additionally reduce the lifetime (frequent starts and stops, rapid power change). If these events are avoided or their frequency reduced, then the expected lifetime of the hydrogen system is estimated to be 15 years.

1.2.6 Green-Hydrogen Production Costs

The hydrogen production cost has a decisive influence on the economic viability of green hydrogen and the use of hydrogen technologies [71]. It can be expressed either per unit of mass [€/kg] or per unit of energy [€/kWh]. The own price of green hydrogen consists of three main cost components:

Table 1.4: Hydrogen-production cost components.

Cost component	Description
C_1	This cost component resulting from the investment costs (CapEx) for hydrogen-production equipment (electrolyser, hydrogen storage and related equipment). The contribution of this component to the cost of hydrogen production depends strongly on the utilisation rate of the equipment and its lifetime.
C_2	This cost component results from the operating costs (OpEx), such as labour costs, equipment-maintenance costs and material costs consumed in hydrogen production.
C_3	This cost component results from the cost of the electrical energy used to produce hydrogen through electrolysis. The main component is the electricity consumption of the electrolyser (typically 50 kWh/kg H_2), including other external components of the hydrogen-production process that also consume electricity (estimated up to 5 kWh/kg H_2).

Cost component C_1

The cost component (C_1) can be expressed as the quotient of the total investment costs for green-hydrogen production equipment (CapEx) and the total mass of hydrogen produced during the lifetime of the system (m_{TOT}):

$$C_1\left[\frac{€}{kg}\right] = \frac{CapEx\ [€]}{m_{TOT}[kg]} \tag{1.3}$$

The mass of hydrogen produced during the lifetime of the system can be expressed as the product of the lifetime of the production system (t_L [h]), the production capacity (Q_{H2} [kg/h]) and the utilisation rate of the hydrogen system (c [%]):

$$m_{TOT}[kg] = Q_{H2}[kg/h] \cdot t_L[h] \cdot c[\%] \tag{1.4}$$

It can be seen that for a low value of the price component C_1, a high utilisation rate of the electrolyser or the production system is required.

Cost component C_2

Similar to the cost component C_1, the cost component of operating costs during the lifetime of the system $C2$ can be expressed as the quotient of the overall OpEx operating costs (f_{OpEx}-estimated at 5% of CapEx per year) and the total mass of hydrogen produced during

the lifetime of the system and multiplied with t_L [y], which denotes the overall lifetime of the system:

$$C_2\left[\frac{€}{kg}\right] = \frac{t_L[y] \cdot OpEx\ [€]}{m_{TOT}[kg]} = \frac{t_L[y] \cdot f_{OpEx}\ [1/y] \cdot CapEx\ [€]}{m_{TOT}[kg]} \tag{1.5}$$

Cost component C_3

Component C_3 represents the electricity costs for the production of green hydrogen and is directly dependent on the selling price of excess electricity SP_{EL} and the electricity consumption per mass unit of hydrogen produced E_{EL_SYS}:

$$C_3\left[\frac{€}{kg}\right] = SP_{EL}\left[\frac{€}{kWh}\right] \cdot E_{EL\_SYS}\left[\frac{kWh}{kg}\right] \tag{1.6}$$

Hydrogen-production cost PC_{H2} [€/kg] can thus be expressed as:

$$PC_{H2} = C_1 + C_2 + C_3 = \frac{CapEx \cdot (1 + t_L \cdot f_{OpEx})}{m_{TOT}} + SP_{EL} \cdot E_{EL\_SYS} \tag{1.7}$$

where we assumed that in case of choosing an electrolyser with different nominal power, the CapEx costs are in proportion with a production capacity of the system.

Total cost of hydrogen production

The total production cost of green hydrogen is the sum of all three cost components ($C_1 + C_2 + C_3$) and is expressed in [€/kg H_2].

The production cost of hydrogen can also be expressed in terms of a cost per unit of energy containing hydrogen. The relationship between the mass of hydrogen and the amount of its energy is defined by the calorific value of hydrogen. There are two different heating values:

- *Lower heating value of hydrogen E_{H2_LHV} (33.32 kWh/kg).*
- *Higher heating value of hydrogen E_{H2_HHV} (39.39 kWh/kg).*

The lower calorific value takes into account the fact that the water produced during combustion does not condense and remains in vapour form. The higher calorific value, on the other hand, takes into account that the latent heat of water condensation is recovered and added to the total heat released during combustion. The price of hydrogen per unit of contained energy PC_{H2_kWh} is relevant for applications where hydrogen is used as an energy source.

$$PC_{H2\_kWh}\left[\frac{€}{kWh}\right] = PC_{H2}\left[\frac{€}{kg}\right] \cdot \left(E_{H2\_HHV}\left[\frac{kWh}{kg}\right]\right)^{-1} \tag{1.8}$$

For an example, assume a hydrogen-production system with a 1 MW PEM electrolyser, and the following data:

Table 1.5: Hydrogen production system symbols and parameters.

Variable	Symbol/parameter description	Estimation
CapEx	Investment (project documentation, 1 MW PEM electrolyser, high-pressure hydrogen storage and compression, various supporting and auxiliary components, electrical connection, construction and assembly works)	2,200,000 €
f_{OpEx}	Operating costs factor, estimated as a part of CapEx costs per year (this means 5 % of 2,200,000 €, i.e., 110,000 €/year)	0.05
c	Electrolyser utilisation rate (estimated at 45 %, which means 3942 hours of the available 8760 hours per year)	45%
t_L	Overall lifetime of the hydrogen system in hours	131,400 h
E_{EL_SYS}	Electrolyser system electrical energy consumption at full capacity	50 kWh/ kg
Q_{H2}	Production capacity of the system at full power (which can be achieved by a 1 MW electrolyser with electricity consumption of 50 kWh / kg H_2)	20 kg H_2/h
P_{EL_SYS}	Nominal power of the electrolyser system	1 MW
m_{TOT}	The amount of hydrogen produced per year considering utilization rate (365 [d] · 24 [h/d] · 45 [%] · 20 [kg/h])	78.84 t/year
SP_{EL}	Selling price of excess electrical energy	50 €/MWh

Table 1.6 shows the individual components of the production cost of hydrogen for an assumed 1 MW system as a function of the electricity cost.

Table 1.6: Hydrogen production cost in relation to the consumed electrical energy.

N°	Electricity costs [€/MWh]	C_1 [€/kg]	C_2 [€/kg]	C_3 [€/kg]	Total hydrogen-production cost [€/kg]	Total hydrogen production cost [€/MWh]
1	0	1.86	1.40	0.00	3.26	82.76
2	30			1.50	4.76	120.84
3	60			3.00	6.26	158.92
4	120			6.00	9.26	235.09
5	180			9.00	12.26	311.25

Value-added tax (VAT) and possible other charges are not considered.

Cost components C_1 and C_2 decrease if the amount of hydrogen produced is close to the maximum theoretically possible with the electrolyser operating continuously at maximum output. The production of hydrogen from surplus electricity with a low or even zero cost therefore does not lead to a low production cost of hydrogen, as the electricity surplus only occurs occasionally, resulting in a low utilisation of the electrolyser and consequently a high-cost component C_1 and C_2.

In the case-study presented in the dissertation (Section 4.1), the HPP is contractually obliged to supply electricity on a regular annual basis at the fixed cost and according to the prescribed timetable and is not involved in short-term electricity markets or ancillary services. Even in this case, the HPP can make additional profit with the additional production of hydrogen, which is limited by the amount of excess hydropower or/and the final capacity of the PV installation.

Assuming that the HPP would have more options to deviate from the prescribed timetable, it is interesting to analyse in which cases hydrogen production is more profitable than electricity production. For example, assume an electrolyser with a nominal power of 1 MW and electricity consumption of 50 kWh/kg H_2, an average utilisation rate of 0.45, a hydrogen selling price of 8 €/kg H_2, and a selling price of 50 €/MWh for the supplied electrical energy production (see Table 1.7).

Table 1.7: Variables and their assumed values.

Variable	Variable description	Assumed value
P_{EL_SYS}	Nominal power of the electrolyser system	1 MW
c	Factor of hydrogen system exploitation (or utilisation rate of 1 MW hydrogen system)	0.45
E_{EL_SYS}	Electrolyser system electrical energy consumption at full capacity	50 kWh/kg
PC_{H2}	Production cost of hydrogen (the cost of excess electrical energy is 0 €)	3.26 €/kg
SP_{H2}	Selling price of hydrogen	8 €/kg
SP_{EL}	Selling price of excess electrical energy	50 €/MWh

An important quantity is the difference between the cash flow generated by hydrogen production and the cash flow generated by selling excess electrical energy. The maximal revenue from invested 1 MWh of electrical energy into hydrogen production is expressed as:

$$Revenue\ \left[\frac{€}{MWh}\right] = \frac{SP_{H2}}{E_{EL\_SYS}} \tag{1.9}$$

and the cash flow as:

$$Profit\ [€/h] = c \cdot P_{EL\_SYS} \cdot \left(\frac{(SP_{H2} - PC_{H2})}{E_{EL\_SYS}} - SP_{EL}\right) \tag{1.10}$$

For the case above, the profit from hydrogen generation versus electricity production turns positive with an extra profit of 20.16 €/h (see Figure 1.6). With a market selling price of hydrogen under 5.76 €/kg H_2, it makes more sense to produce additional electricity if we manage to sell it on the energy market at a price of 50 €/MWh of electrical energy.

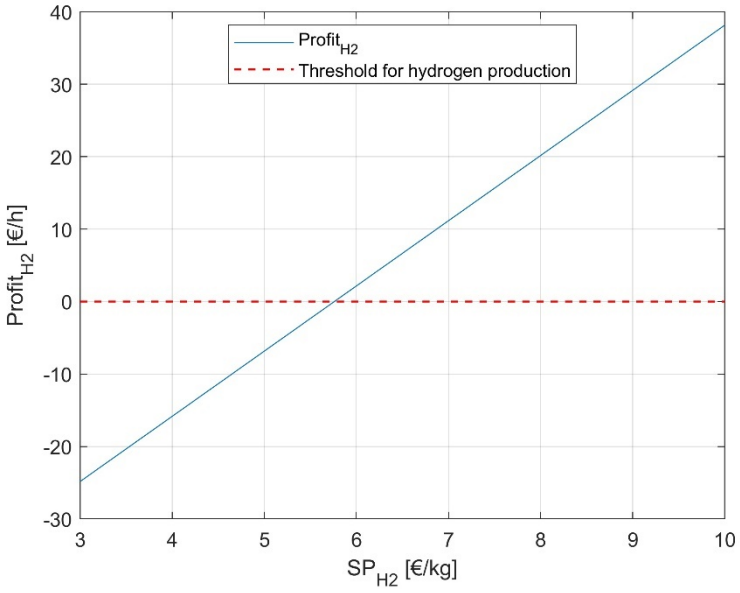

Figure 1.6: Profit of hydrogen production as a function of selling price.

1.3 State of the Art

In this section, an overview of research activities and demonstration projects on the field of renewable hybrid system and its subset, namely hydrogen system, is given. The first subsection gives the overview of state-of-the-art on hydrogen system control and sizing optimisation, while the next subsection deals with the issues connected with green-hydrogen production and related production costs. The section follows with a description of the necessary equipment, a techno-economic assessment of green hydrogen production and presents some already-completed demonstration projects in the area of green hydrogen production.

1.3.1 Hydrogen System Control and Sizing Optimisation

During the last decade many studies and literature have been published in the areas of hybrid system or hydrogen system control and proper sizing optimisation. Some of them also include techno-economic issues for the design of an optimised hybrid system.

Appropriate control of a hybrid system is one of the factors for its successful implementation. Three control strategies were proposed in [72] based on operating modes and combining technical-economic aspects for the energy management of the hybrid system. They have been designed, primarily, to satisfy the load power demand and, secondarily, to maintain certain conditions in the hydrogen tank (hydrogen energy reserve), and an adequate state of charge of the battery bank to extend its life, also taking into account a techno-economic analysis. Another control strategy is proposed in [73] and is based on a power-decoupling strategy of the power sources. This energy-management strategy fulfils the fast energy demands if the load respects the integrity of each source. The modelling and simulations are performed using MATLAB/Simulink and *SimPowerSystems* packages and the results are presented to verify the effectiveness of the proposed system. Another approach of hybrid hydrogen energy system control is given in

[74]. The work deals with the control of an autonomous hydrogen-production system consisting of a solar panel array supplying an alkaline electrolyser. The controller is proposed that meets the maximum power capture objective for the solar array and the power constraints of the electrolyser. The developed controller is designed using concepts of hybrid control theory, which is very powerful to cope with the nonlinear and hybrid dynamics inherent in the system's behaviour.

More authors deal with grid-tied hybrid systems, such as the paper [75] that deals with the optimal control of a hydrogen-production system supplied by photovoltaic solar energy and assisted by the grid. For that, the authors proposed a simple dynamic model accounting for the main features of the system, where the electrolyser current is used as the control variable. In this way, the control law is obtained that optimises the grid's energy consumption despite the solar energy's variability. An important constraint with the obtained solution are the physical limitations of the hydrogen-storage tank, which results in a non-smooth and non-continuous problem. Simulation results are presented to illustrate the effectiveness of the proposed control design.

In [76] the author states that one of the key system control parameters is the operational mode of the electrolyser. The author suggested that the electrolyser should operate in a variable power mode, rather than in a fixed power mode and that the set point for switching on the electrolyser should be as high as possible (depending on constraints). The article also claims that finding an optimal solution requires performing a combined techno-economic optimisation that takes into account both system design (sizing of components) and the control strategy.

Similarly, the authors in [77] conclude that the interaction between the hydrogen producer and the energy market is crucial for keeping the modern energy transition on track. The article considers a system of a renewable energy producer that jointly interacts with the electricity market and a hydrogen market under different hydrogen-offtake agreements and distribution options. The authors claim that by solving the system to optimality this would allow them to derive the profit-maximising behaviour of the operators of the considered system.

A recent overall review of control strategies for a hydrogen renewable-energy power system is given in [78]. The review presents a comprehensive examination of the current challenges related to the control aspects of integrating hydrogen energy-storage technologies into modern power grids.

During recent years, the interest in the dimensioning/sizing of hydrogen systems using models and optimisation has also increased. Optimal sizing is defined by the determination of the parameters of the system components by which the load demand is met, and the total cost is minimised. The optimised design of a hydrogen system's equipment is also important for its reliability and cost efficiency. Over sizing can lead to high initial costs and low utilisation rate, while under sizing it can lead to operating limitations and energy shortfalls, despite lower initial costs. These facts meant that the sizing of hybrid systems including hydrogen energy storage have received much attention recently.

Four sizing methods for a stand-alone hybrid generation system integrating renewable energies (photovoltaic panels and wind turbine) and storage system based on battery and hydrogen (fuel cell, electrolyser and hydrogen-storage tank) are described [79]. In the first case, the sizing is based on basic equations, and in the second case, an optimal technical sizing is achieved using Simulink Design Optimisation. The other two methods perform an optimal techno-economical sizing by using the hybrid-system optimisation software HOMER and HOGA, respectively. A MATLAB/Simulink model of the hybrid system was used to simulate the annual performance of a hybrid system designed by each method.

The authors in [80], [81] suggest that a common methodological approach is to use commercial software designed for hybrid system optimisation, such as HOMER Pro or

HOGA. However, the reliance on commercial simulation software can reduce the degrees of freedom in model customisation and, therefore, some authors use more general modelling methods for their system.

The authors in [82] presented a list of implemented optimisation methods for equipment sizing. They concluded that for these purposes the HOMER software has some limitations (like black-box coding, different working platforms, and inflexibility regarding optimisation techniques) and suggested that modern artificial-intelligence techniques have the potential to improve the process of optimisation. Some researchers have already used a particle-swarm-optimisation (PSO) method as an intelligence algorithm [83] to find the optimum values of design parameters. The authors found that the PSO algorithm is very suitable for solving this type of problem as it can solve it with high speed and accuracy.

In [84], the authors evaluate the performance of seven different algorithms for optimum sizing of a hybrid system to continuously satisfy the load demand with the minimal total annual costs. Among these algorithms, three well-known heuristic algorithms, namely, particle swarm optimisation, tabu search and simulated annealing, and four recently improved metaheuristic algorithms, namely, improved particle-swarm optimisation, improved harmony search, improved harmony-search-based simulated annealing, and artificial bee-swarm optimisation, are applied to the system and the results are compared in context of the total operating costs. The article finds that from the optimisation viewpoint, the artificial bee-swarm optimisation method yields more promising results than the other algorithms and it is also the most robust.

An optimal sizing of components is an important subject for researchers to explore the optimal design of the system. But the authors in [85] suggest that besides techno-economic objectives some other objectives should also be taken into account during the optimisation process, like reducing the air pollution, increasing the reliability, boosting the customer satisfaction, decreasing the excess energy in the system etc. The article presents a survey on the state of the art in the multi-objective optimal design of hybrid stand-alone or grid-connected energy systems, where the applied objective functions, design constraints and decision variables in the optimisation of hybrid energy systems are addressed. It is found that the recent objective functions (like customer satisfaction and grid dependency) need further investigation in the multi-objective design process.

1.3.2 Green-hydrogen Production

Due to green transition goals, the research on GHP has become more intensive, especially during the last decade. One of the promising options for green-hydrogen production, which is also investigated in the context of the present dissertation, is the cogeneration of electrical energy and green hydrogen at a hydropower plant. Cogeneration is defined as the generation of two different forms of useful energy from a single primary energy source [86]. In our context thus cogeneration means the production of both electrical energy and green hydrogen in a HPP from the available hydro energy.

Although the possibilities and methods for hydrogen production in a HPP were presented a long time ago [87], this topic has not attracted much attention in the academic sphere. During the last decade, most of the conditions for increasing hydrogen production in an ecologically acceptable and efficient way have been established (i.e., a consensus for environment decarbonisation, maturity of the technological equipment for hydrogen production-P2G systems, increased hydrogen consumption in industry, the emergence of the electrical energy market with a significant share of RESs, increased dynamics of the electrical energy sector, requirements for greater profitability of power facilities), so these topics received more attention from research and engineering.

In [35], the authors present a study on the option to decarbonise hydrogen production using hydropower at the European level. The results show that such a transformation is possible and compatible with the ongoing transition towards carbon-neutral power systems in the European Union. Also, other countries, especially those rich in hydropower, are also intensively involved in its use for hydrogen production [88], [89], [90], [91], [92], [93]. Some articles define the role of P2G systems in future electro-energetic systems with a high share of RESs. The authors in [10], [11], [94], [95] found that P2G technology is a feasible option for storing energy for the long term, but the cost reduction of electrolysis is essential to make P2G attractive. The article [39] gives a worldwide overview of several P2G projects producing hydrogen or renewable substitute natural gas in Germany, Denmark, the United States and Canada. The results show substantial cost reductions for electrolysis during the recent years and a further price decline to less than 500 €/kW electrical power input for P2G technology until 2050 if the cost projection follows the current trend.

It should be noted that today green hydrogen technologies (P2G systems, fuel cells) are hardly economically viable. The reason is the technological equipment for green-hydrogen production, storage and distribution is expensive, since it is not mass produced. This leads to high capital expenditures for systems based on green-hydrogen technologies, which results in a high price for the generated green hydrogen. This reduces hydrogen's economic competitiveness in comparison to other fuels, particularly natural gas, and prevents green-hydrogen technologies from being widely adopted. To accelerate the adoption of green-hydrogen technologies under current conditions, particular applications must be identified where green hydrogen could be competitive due to its low environmental impact, leading to lower environmental taxes. Many studies have addressed this issue and claim that the transition to RESs will inevitably need subsidies in the short and medium terms [13], [14], [15], [16], [17], [18]. These supporting policies must be accompanied by reduced costs to make the technologies a realistic alternative for the future. A similar opinion is expressed in [96], where the authors report that green hydrogen for road transport (in China) could be competitive against grey hydrogen in terms of cost, but new market mechanisms and appropriate policies would be necessary. The authors of [19] note that in a hybrid system where P2G provides a real option between the electricity and hydrogen markets, hydrogen values greater than 4 €/kg are required to provide an equal or greater net present value than an offshore wind farm producing only electricity. An engineering economic analysis [20] suggests that the green-hydrogen economy will be a viable option for industrial decarbonisation. It will be more profitable in cases where carbon taxes are levied and when the unit hydrogen production cost starts to decline from 9 €/kg. In [21] the author concludes that green hydrogen is seen by investors, developers, and politicians as a strong enabler to meet net-zero targets and that a market for green hydrogen is opening up, but cost competitiveness remains a barrier to scaling up.

1.3.3 Equipment for Hydrogen Production

The following is an overview of the equipment for green-hydrogen production by water electrolysis.

1.3.3.1 Electrolyser

Today, four main electrolyser technologies are developed and used: AEL, PEM, AEM, SOEC (see Table 1.2). Within each technology there are many variations, with the most radical differences being cell design, component variation and technology maturity. Each technology has its own challenges, from critical materials to performance, durability and maturity. SOEC and AEM have high potential, but are much less mature technologies,

with only a few companies and original equipment manufacturers involved in their manufacture and commercialisation.

AEL technology

AEL electrolysers are the oldest and most best-known technology and they have been available for industrial purposes for decades. They are characterised by the use of aqueous alkaline solutions, which are extremely corrosive.

The different sizes of alkaline electrolysers cover a wide range of power (from tens of kW to a few MW) and they are characterised by different plant layouts [97], [98], see Table 1.2.

However, some drawbacks still have to be overcome [99], concerning:

- *The minimum load. The minimum load usually falls within 10–40% of nominal power* [100]*. This means that if the input is lower than these limits, the electrolyser has to be switched off.*

- *Transient operation is possible with this technology, but some problems can arise* [34]*. In fact, the typical response time is seconds or minutes, but according to* [100]*, these performance characteristics result from the fact that industry never demanded a flexible operation of alkaline electrolysers, so the technology has never been designed to operate as such. Currently, with the integration of intermittent sources, the demand for flexible operation arises.*

- *The relatively long electrolyser cold-start time (around 10 min), which mainly depends on the required hydrogen purity* [100].

- *The long electrolyser restarting time after shutdown. This is an important drawback, because the electrolyser takes 30–60 minutes before it can be switched on again (due to purging operations with nitrogen).*

Currently, such a system costs about 1400 €/kW [67], whereas the entire system has a lifetime of 15–30 years [98], [99]. It should also be noted that the purity of the hydrogen production lies within the 99.8–99.9% range and on occasion can even reach 99.999% with an additional purification system [98].

PEM technology

The PEM technology for water electrolysers was developed in 1966 and was put on the market in 1978 [98]. It is based on the use of a polymer membrane as an electrolyte [48], and because of the acidic regime provided by the proton-exchange membrane, noble materials (basically platinum-group metals) have been successfully adopted as catalysts. This aspect is a drawback as far as the cost is concerned, because it has been estimated to be at least double (> 2000 €/kW) that of the alkaline technology [10], [34].

However, the better exploitation that can be achieved with noble materials (usually platinum-group metals) could lead to a cost reduction [48] and the development of a technology based on rare materials can lead to material-availability constraints, and alternative materials, such as nickel, could be valid substitutes [101]. The operating temperature lies within the 20–100 °C range [48].

PEM electrolysers allow a high-pure hydrogen ($> 99.99\%$) to be produced, without the need for any further purification equipment [98]; this can be confirmed from the data available on the manufacturers' websites, where a higher purity level than 99.998% is indicated. With appropriate drying PEM water electrolysers can produce pressurised

hydrogen with a purity of at least 99.9995% on a constant basis, due to the stoichiometry of the generation process [102].

Furthermore, PEM electrolysers can be completely ramped up and down in just a few seconds and they can work in the 0–100% range; moreover, a cold start can be completed in just minutes.

As a final remark, it is important to point out that the lifetime of a system based on the PEM technology is shorter than that of a system based on alkaline technology (AEL) [47].

There are several studies focused on the characteristic of electrolysers [9], [34], [47], [48], [103], [104], [105], [106]. In a report [107], a detailed assessment of electrolysers is described, together with opportunities and potential challenges for each type of electrolyser.

Electrolyser models are an essential tool in electrolyser development because they allow us understand the influence of different parameters on the electrolyser's performance enabling an efficient simulation, design and optimisation of the electrolyser [108]. The literature provides models with varying degrees of complexity. Analytical models are a satisfactory tool to identify the effects of the main variables on the performance of the electrolyser, based on simplified considerations to simulate a fairly accurate polarisation curve. Empirical/semi-empirical models allow the prediction of the electrolyser's behaviour as a function of the operating conditions (e.g., pressure, temperature) based on simple empirical equations. The main disadvantage is that the application of this type of model is generally limited to the range of operating conditions studied and to the specific electrolyser design. Mechanistic models use differential and algebraic equations, which are derived taking into account the electrochemical phenomena occurring in the electrolyser and are solved numerically using various methods. These models, which require extensive calculations, accurately predict the polarisation curve and the flux and concentration of several species in the electrolyser, but this leads to simulation times that are considered too long for real-time applications.

In [108], the authors presented a review of PEM electrolyser modelling especially useful for beginners in this area. The main equations to predict cell voltage, including reversible voltage, activation losses, ohmic losses and mass transport losses are presented. Special sections are devoted to dynamic behaviour, two-phase flow effects and the inclusion of thermal effects in model development.

A bibliographic analysis in [109] was carried out to identify existing models. The authors claim that only a few models considers the dynamics of the whole system including balance of the plant. Therefore, they developed a model under Bond Graph formalism that is suitable for control and model-based diagnostic.

A recent review of the literature on this topic is given in [110]. Analytical, semi-empirical and mechanistic models are presented and further clustered depending on their scope which is mainly classified as (i) membrane and electrode modelling and material properties, (ii) cell model, (iii) stack model, (iv) module and system model.

In [111] the authors show a novel model that combines the Tafel equation and an original model for Faradaic efficiency tested on real data. The authors claim that the model estimated hydrogen consumption more accurately than the "Linear Model" habitually used in the industry. It also emphasized the importance of an optimised control scheme for minimising hot standby losses. The authors also observed that pressurisation during start-up, purging and pressure-driven fluctuations also contributed significant losses and scatter when inspecting minute-by-minute data.

A review of the modelling and operation of the hydrogen system for renewables integration with suggestions on relevant future research is given in [40]. Based on the summarised features, this paper put forward suggestions on the future research directions

of hydrogen system modelling and operations as follows: hydrogen-system control for regular grid regulation; hydrogen-system control for special operating situations; comprehensive integrated model of hydrogen systems; locating and sizing of hydrogen systems; combined operation of multi-energy network with hydrogen systems.

It should be noted that electrolyser models are often either too detailed to be computationally efficient in the context of a whole system model or too inaccurate in times of low renewable energy production [112]. The most detailed models are used to study what happens in the sub-components of the electrolyser (e.g., membrane and electrode, material properties, cell, stack, etc.). On the stack/system level, the transients of the stack and BoP components are essential. Moreover, there are models for macroscopic simulations, where a lumped model of components is used, often described by static relations only. For the purpose of the present study, such models (i.e., the production rate of the PEM electrolyser as a function of the power load) is used for electrolyser. The characteristics of the electrolyser were obtained from renowned electrolyser manufacturers such as NEL, H-TEC Systems and ITM Power [58], [113], [114].

After reviewing the literature on electrolyser modelling, we found that although there are many microscopic models in the literature, they describe the electrolyser stack in detail depending on the geometric coordinates, which is computationally demanding and does not contribute to the decision-support system we envisioned. Therefore, we developed a simplified and reduced-order macroscopic model that describes the mass and energy flows, and the energy efficiency based on the polarisation curve and consumption of the balance of plant components.

1.3.3.2 Hydrogen Storage

Hydrogen storage is one of the key-enabling factors for the establishment of a hydrogen economy.

The low volumetric energy density of hydrogen can be increased by using one of the available technologies such as hydrogen compression, liquefaction, adsorption (metal hydrides, liquid organic hydrogen carriers-LOHC) or chemical storage (ammonia, methanol). A comprehensive assessment of hydrogen-storage options is presented in [55], [56], [115].

Among the hydrogen-storage technologies, compressed gas (above and underground) and liquid are the widely used methods to store hydrogen [116].

For compressed hydrogen storage, pressurisation is required before the hydrogen enters a buffer or storage tank. Since most PEM electrolysers operate at about 30 bars, the produced hydrogen can be directly sent into hydrogen-storage tank [117].

The classification of compressed hydrogen gas vehicle fuel containers is well studied in [118]. The ANSI/CSA standards for hydrogen fuel cover both vehicle fuel systems and the hydrogen fuel station.

Hydrogen storage for large and long-term effects is a major bottleneck faced in recent times, and it remains untested [119]. Large-scale storage facility types for compressed hydrogen are presented in [120]. The authors classified them as a storage vessel with its different types, geological storage, and other underground storage alternatives.

Compressed hydrogen is considered the dominant storage technology for stationary and mobile applications, as the available solutions have very good scalability and the highest technology readiness level (TRL) for all solutions [121]. Therefore, for our study we considered a pressurised hydrogen tank, which is a common type of hydrogen storage in industrial practice. In general, tanks come in various shapes and sizes, ranging from smaller tanks for on-site storage to massive tanks used on an industrial scale. Their design,

manufacture, use and maintenance are regulated by various standards with well-defined safety guidelines [120].

According to [29] the initial cost of hydrogen storage with a capacity of 0.1–10 MWh (or 2.5–254 kg H_2) is 220–365 €/kg. In [59] the authors estimate the cost of storing hydrogen at 50 bar to be 632 €/kg.

Finally, [122] states that the levelized cost of hydrogen storage (LCHS) of above-ground storage of compressed hydrogen gas for a daily and 4-month storage cycle length is ∼0.31 € and ∼23.50 € per kg H_2, respectively.

1.3.3.3 Hydrogen Compression

Compression has proven to be the most straightforward and a very effective technique to increase hydrogen density and storage capacity. For this reason, storing hydrogen as a compressed gas in metal cylinders at various pressures is currently the most commonly used method [123].

When hydrogen-gas compression is required, mechanical compressors are the industrial standard [124]. Compressors with an output pressure of 20–200 bar are required for various operations in this industry [125]. Only reciprocating and centrifugal compressors can handle the capacity (high volume flows) required. The disadvantages of such compressors include vibrations and noise due to the moving parts.

An alternative solution is the use of electrochemical hydrogen compressors (ECHCs). Recent advances and perspectives in the diagnostics and degradation of electrochemical hydrogen compressors are described in [126]. This paper provides a literature review of the progress and current state of the art in electrochemical hydrogen compressors, emphasizing their performance diagnostics, durability testing methods, and possible degradation mechanisms that could affect the desired performance. The paper also critically identifies current technological shortcomings and challenges, especially with regard to current EHC health-testing procedures, but also suggests potential development ideas for perspective improvements. Another advantage of an electrochemical hydrogen compressor is that they can provide an alternative solution, as these devices can electrochemically purify and compress hydrogen in a single device [127]. However, to be competitive, electrochemical hydrogen compressors must operate in very intensive conditions (high current density and low cell voltage) that can only be reached if their core materials, e.g., the membrane and the electrodes/electrocatalysts, are optimised [128]. The basic model of a hydrogen compressor is presented in [129].

1.3.4 Techno-Economic Assessment of Hydrogen Production

By definition, a techno-economic assessment (TEA) is a methodological framework for examining the technical and economic performance of a process, product, or service and includes a study of the economic impact of the technology [130], it is a cost-benefit comparison that considers technological and economic factors.

Ideally, a techno-economic model represents the best current understanding of the system being modelled. Such a model can then help allocate planned budget and investment resources, set achievable research and development targets, understand the process and its value chain, or convince investors of the sustainability of the process (both economic and environmental).

For the purposes of this analysis, the cost components, including capital expenditure (CapEx), operating expenditure (OpEx) and other influencing parameters/variables of the electrolyser, compression station and hydrogen storage (designed as a buffer tank for the short-term storage of hydrogen production) are evaluated below.

CapEx and OpEx are the most important costs in a techno-economic assessment [130]. The main problem is to minimise the CapEx and OpEx of different hydrogen-production systems while increasing the production volume. This can reduce the cost of producing hydrogen from different energy sources. The expenses associated with the construction of a new plant are called CapEx. OpEx stands for the various expenses that occur through their day-to-day system operation, such as the cost of raw materials, operating labour, maintenance and utilities. Annual expenses are considered based on items related to operating costs and general and administrative expenses. As the size and capacity of the plant increases, so do the investment costs (CapEx). However, since the price of the equipment usually increases more slowly than the production capacity, the production costs per unit of hydrogen are therefore lower. Additional equipment (compressor, storage, etc.) also leads to an increase in CapEx.

According to [131], the key cost drivers of electrolysers are stack, power electronics, gas conditioning (drying) and balance of plant components. All these costs will be further considered as electrolyser CapEx.

To make green hydrogen the fuel source of the future, it needs to be competitive with fossil-fuel prices. A recent review of the literature on this topic [132] provides clear insights into a techno-economic analysis of various hydrogen-production platforms. Steam reforming of natural gas for hydrogen production has drawn the attention of many researchers and policymakers due to the high efficiency in hydrogen production (70–85%) with low operating, feedstock (0.28 €/kg of hydrogen) and production (1.2–3.2 €/kg of hydrogen) costs. However, this technology comes with the cost incurred in the process and the catalyst cost. But the study IRENA predicts a decline in green-hydrogen costs by up to 85% by 2050 [48], making it the dominant hydrogen source [133].

When it comes to opportunities for the cost reduction [131] of hydrogen generation by water electrolysis, the following parameters have to be improved: electrical energy consumption per unit of production (i.e., kg of hydrogen), electrolyser lifetime, electrolyser size, load range, start-up time, use of scarce materials and scale of industrial production. Very importantly, the price of the equipment (electrolysers, compressors, storage) has to be reduced, since it is directly incorporated into the hydrogen's price.

There is a considerable amount of literature on hydrogen techno-economic from which we can extract a price breakdown for a proposed hydrogen system, as shown in Table 1.4. Comprehensive reviews on the hydrogen system's main components CapEx, OpEx and BoP costs can be found in [59], [61], [62], [47], [134], [135], [136], [137], [138]. A detailed compilation of past and expected AEL and PEM electrolysis plant cost in €/kW is given in [139]. Future technology cost assessment and outlook towards 2030 for AEL and PEM electrolysers in the MW-to-GW range is presented in [140].

The US Department of Energy (DOE) and the European Fuel Cell Hydrogen-Joint Undertaking (FCH-JU) indicated that the investment cost of a PEM must be decreased from current 1000–1500 €/kW to 250–600 €/kW [141], [142].

In [138] authors suggest that a CapEx of 750 €/kW is realistic for a single stack 2 MW system. The electrolytic hydrogen production is shown to be around 3 €/kg, which is within the range estimated for renewable hydrogen (i.e., 2.5–5.5 €/kg) [143]. While the IEA forecasts that current green-hydrogen production costs of 2.83–7.4 €/kg will fall to 1.2–4.2 €/kg in 2030 and 0.9–2.8 €/kg by 2050 [29], [144].

The cost of P2G systems shows a decreasing trend that will most probably continue [145], especially if the P2G plant components are manufactured in standardised sizes and series.

Another important factor in achieving an efficient hydrogen-production price is the location of the plant. In [146], the authors present the levelized cost of hydrogen (LCOH) calculations for promising locations worldwide. A literature review [147] shows that the

cost of hydrogen in Europe can be reduced by around 10 €/MWh (or 0.3939 €/kg) if the hydrogen consumption is positioned strategically in regions with good conditions for wind and solar power. The authors also claim that the potential cost savings that can be obtained from full temporal flexibility of hydrogen consumption are three times higher than that linked to strategic localisation of the hydrogen consumption. The cost of hydrogen per kg increases, and the value of flexibility diminishes, as the size of the hydrogen demand increases relative to the traditional demand for electricity and the available variable renewable-energy resources. Low-cost hydrogen is, thus, achieved by implementing efficiency and flexibility measures for hydrogen consumers, as well as an increasing acceptance of variable renewable energy.

In [148], the authors present the techno-economic feasibility of the wind-photovoltaic-electrolysis-battery (WPEB) power system and its capability for curtailment reduction. A flexible hydrogen-demand curve is well suited to boost the hydrogen production of the WPEB system, which adapts to the seasonal and daily variation of renewable power generation. A flexible hydrogen demand profile enables higher hydrogen production.

For our needs, a techno-economic assessment of equipment costs was made according the methodology described in Section 3.4 and included into the economic part of the entire model.

1.3.5 Demonstration Projects

Hydropower has played an important role in the production of green hydrogen for more than 100 years [149], [150]. The 167-MW historic hydropower-based hydrogen production by electrolysis in Rjukan, Norway, which operated from 1919–1988, is now possibly the oldest plant of its kind in the world. Another 135-MW historic hydroelectric and electrolysis-based hydrogen production plant operated in Glomfjord, Norway, 1953–1991. Industrial research and development to improve the economic performance of the method have continued to today.

More recent coverage on current hydrogen production and the prospects for developing the production of green hydrogen using RESs in various countries around the world that are leaders in this field can be found in [151]. The potential of hydrogen energy in countries and regions such as Australia, the European Union, India, Canada, China, the Russian Federation, the United States of America, South Korea, the Republic of South Africa, Japan and the northern countries of Africa is considered. Of the 109 regions in Europe associated with hydrogen production, 88 regions have a surplus of potential electrical energy generation from RESs after meeting the annual demand for electrical energy in all sectors and hydrogen production.

In Europe, there are already some ongoing projects that use hydropower for the production of green hydrogen, mainly in Switzerland. One of the demonstration plants is located at the Gösgen hydropower plant [152]. With a capacity of 2 MW, it is the largest plant in Switzerland for the production of green hydrogen for commercial use in zero-emission heavy-duty transport. The plant can produce up to 300 tonnes of green hydrogen per year and thus ensure an annual consumption of around 40–50 fuel-cell electric trucks or 1700 fuel-cell passenger cars. Another hydrogen-production plant is being built at the Schiffenen dam hydropower plant [153]. Following the building permit procedure, Axpo and Rhiienergie started construction of the 2.5-MW hydrogen production plant at the Reichenau hydropower plant on 23 January 2023. The hydrogen system's installation will be connected to the Reichenau hydropower plant. The hydrogen system will produce about 350 tonnes of green hydrogen annually. The third plant with a smaller capacity for the production of green hydrogen is located in Aarau, Switzerland [154]. The plant is located at the run-of-the-river plant of IBAarau. The green hydrogen is planned for use as fuel for

vehicles. The electrolyser plant supplies enough hydrogen for the annual consumption of approximately 170 fuel-cell cars.

Similarly, a green-hydrogen production plant is being built in Iceland at the 16-MW Ljósifoss Hydropower Station near Reykjavík [155]. The facility will be housed in a 700 m^2 building that will be sufficient for maximum production at 10 MW, although the electrolysis will be built out in phases, increasing in capacity as demand increases. At full capacity, the station will produce enough green hydrogen to power the Reykjavík area's entire public transportation fleet.

To realise a modern water electrolysis plant for the production of green hydrogen as reality on an industrial scale, the ThyssenKrupp company is working with the Canadian company Hydro-Québec to install an 88-MW water-electrolysis plant following the successful completion of a feasibility study [156]. Hydro-Québec, a state-owned company, is one of the largest hydropower suppliers in North America due to the enormous hydraulic energy resources in the province of Quebec. The water electrolysis plant will be built in Varennes, Quebec, and is expected to produce 11,100 tonnes of green hydrogen annually. Both the hydrogen and the oxygen, a by-product of the electrolysis process, will be used in a biofuel plant to produce biofuels from residual waste for the transportation sector. With a capacity of 88 MW, this plant will be one of the world's first and largest production facilities for green hydrogen. Commissioning is planned for the end of 2025 [157].

Chapter 2

The Aim and Goals of the Dissertation

The main purpose of the dissertation is to investigate both the technical and economic aspects of the integration of a hydrogen system into the operation of a hydropower plant. Namely, the necessary equipment of hydrogen systems is currently not yet mass produced and is therefore expensive, which leads to a challenge with the profitability of the cogeneration of electricity and green hydrogen in hydropower plants. Profitability can be improved by optimal sizing of the components of the hydrogen system by taking into account an expected demand for hydrogen and available electrical energy to generate hydrogen. The next challenge is control and coordination of the hydrogen system with the hydropower plant's operation, the prediction of available hydropower and the conditions in the electro energetic system and hydrogen market demands. The upgrade of a hydropower plant with a hydrogen system thus represents a complex challenge, where numerous operating and weather-dependent parameters must be considered. For this reason, an appropriate decision-support system for design and operation would be a benefit, and the development of such a system is the main target of this dissertation.

Therefore, the main goal is to develop a decision support tool for hydrogen system design and operation that takes into account both (i) technical and operating input parameters such as the hydropower plant's operating power, the dynamics of water inflow to the hydropower plant and current water accumulation, the dynamics of electricity consumption and anticipated hydrogen consumption and (ii) economic aspects of hydrogen production, such as the quantity of hydrogen produced, the amount of required electricity for its production, the sizing of the relevant hydrogen system, the investment and operating costs of the hydrogen system's equipment, the production and sales prices of electricity and hydrogen, and the income from the sale of electricity and hydrogen.

The decision-support tool is based on the developed mathematical model of the entire system, presented in Figure 2.1. The complete model consists of the following sub-models:

- *Process model of a hydropower plant and hydrogen system,*
- *Economic model of the overall system,*
- *Control system that coordinates and controls the hydrogen production.*

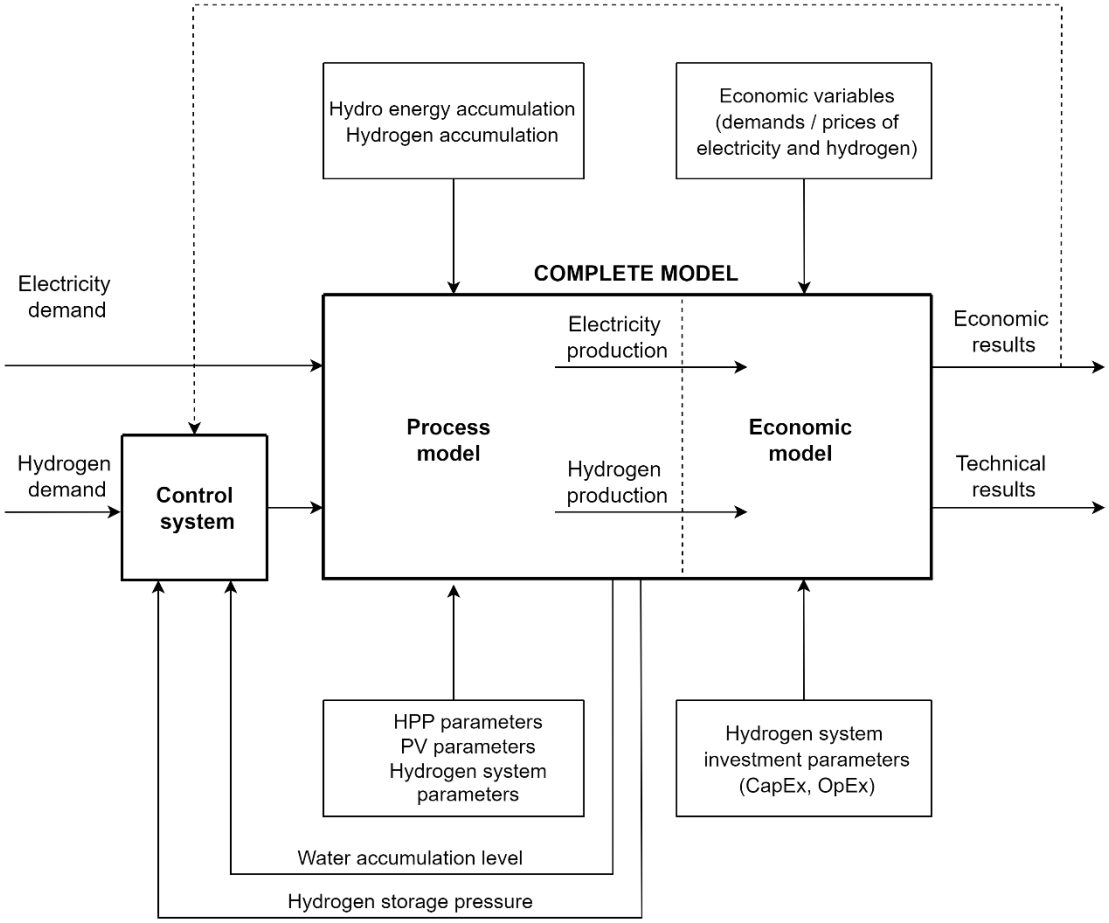

Figure 2.1: Conceptual scheme of the developed model.

The next goal is to use the developed decision-support tool and built-in mathematical models for evaluating various real-data-based scenarios for hydrogen production on the case-study hydropower plant. The specific goal is to determine the optimal hydrogen system's configuration, evaluate the possibility of a cogeneration of electricity and hydrogen, investigate the possibility of hydrogen production from excess hydro energy and assessing the amount of hydrogen produced and related financial outcome.

The design of the decision-support system requires the implementation of several tasks, the most important are:

- *Design the mathematical model of a hydropower plant (relation between water flow, water level and generated electrical power, considering the number and types of hydropower generators);*
- *Design the mathematical model of the hydrogen system (relation between input electrical power and flow of generated hydrogen including basic dynamics, energy efficiency of the components, etc.);*
- *Design the prototype control system (control algorithm), which determines under which circumstances and in what amount the hydrogen is produced;*
- *Design the economic model, which describes the link between the equipment type and size, on one hand, and the related capital investment costs (CapEx) and operating costs*

(OpEx), on the other hand. The economic model also estimates the resulting hydrogen production costs and the economic outcome of the operation of the entire system (hydropower plant and linked hydrogen system);

- *Setting-up the simulation environment to conduct the simulation experiments and present the simulation results;*
- *Providing the historical data for simulation and testing (time series of available hydro energy, demands for electrical energy and hydrogen generation, prices of electrical energy and hydrogen);*
- *Estimation of the potential amount of daily hydrogen consumption to support green transition (hydrogen use for transport/traffic, heat generation in buildings and industry, industrial use as feedstock);*
- *Verification of both developed models on the data from the chosen case-study hydropower plant.*

Once developed and verified, the decision-support tool can then be used to complete the following tasks, related to the design and operation:

- *Simulation of different electricity and hydrogen cogeneration scenarios for a chosen case-study hydropower plant (use of hydrogen in transport, for heating, as an excess energy for water accumulation levelling, etc.);*
- *Determination of the optimal design parameters (sizes, capacities) of all necessary components for a hydrogen system (electrolyser, hydrogen storage, hydrogen compression unit);*
- *Evaluation of the economic effects of cogeneration scenarios (based on built-in economic model, estimated hydrogen prices and estimated needs for green hydrogen in transportation, industry and heating).*

In the dissertation, we investigated the hypothesis that the usage of the developed decision-support tool can lead to more optimal hydrogen-system design for green-hydrogen production in hydropower plants. The proper sizing of the hydrogen system equipment by simultaneously considering the available water resources and techno-economic aspects (e.g., current electricity prices, the selling price of hydrogen) leads to a more optimal selection of the hydrogen system's components in a cogeneration process. It is expected that the use of this decision-support tool will contribute to:

- *Simulating the techno-economic aspects of hydrogen system operation in advance (hydrogen production quantities, economic effects, degradation of the hydrogen system, estimation of remaining lifetime, etc.);*
- *Reduction of investment costs of hydrogen systems;*
- *Lowering the hydrogen-production price;*
- *Increasing the financial sustainability of investment in the hydrogen system.*

2.1 Structure of the Dissertation

This dissertation is structured as follows.

Chapter 1 gives a brief introduction to the subject matter. It gives a preview of the content along with the background of hydrogen production and use. First a classification of hydrogen types is made based on production methods, feedstock, energy sources and CO_2 generation during production. Then the typical structure and main components of the hydrogen system are investigated, followed by an examination of the investment and operation costs for hydrogen production. A comprehensive review of the literature relevant to the scope of the dissertation is then provided. Based on this overview, conclusions were drawn about the type and size of hydrogen-production systems and their price together with the electricity and hydrogen market price to be incorporated into the future process model.

Chapter 2 defines the problem and the objectives of the dissertation. In addition, a concept of the complete system model to be developed is defined.

Chapter 3 addresses the mathematical modelling of the entire system. Several mathematical sub-models were developed and implemented in MATLAB/Simulink. Inputs, outputs and general characteristics are described. The section ends with a presentation of the complete developed process model.

Chapter 4 demonstrates the application of the developed process model in the case-study HPP. The section begins with a detailed description of the case-study HPP. Then the developed model is adjusted to the case-study HPP, followed by steps for data preparation and initial model verification.

Chapter 5 presents a series of simulation experiments for model verification. After verification, this model is used for the simulation-based exploring and optimisation of the hydrogen system connected to the case-study HPP. To simplify the visualisation of the simulation results and to determine the optimal system configuration, a Hydrogen-System-Configuration Explorer was developed with the MATLAB Application Designer. It enables a manual search for the optimal hydrogen-system parameters for a given objective function. To automate the search, an additional system-design tool named Hydrogen System Configuration Optimiser was developed.

Finally, a series of simulations were carried out in MATLAB/Simulink based on the developed process model to estimate the financial impact of integrating the hydrogen system into the regular operation of the HPP and to properly dimension the hydrogen system.

Chapter 6 contains the original contributions, summarises the main conclusions and describes the future research lines.

The References section lists the literature cited and used in the dissertation.

Chapter 3

The Developed System Model

The subject of this chapter is a description of the developed mathematical model of a complete system as shown in Figure 2.1. This kind of model is needed to simulate the operation of the system over the desired time interval and to evaluate the techno-economic effects of operation.

The developed model serves as a basis for a series of simulation experiments in which we will realistically assess the idea of cogeneration by using real data on the case-study HPP's operating conditions, electrical energy and hydrogen-production requirements, their current market prices and some additional parameters. The developed model uses a combination of first principle and real-data modelling.

The model enables an optimum sizing of hydrogen system's elements (electrolyser nominal power, storage tank volume and maximum pressure). This is a complex task since many parameters, scenarios and operation modes need to be considered. Furthermore, the model allows through simulation runs various kinds of sensitivity analysis (influence of technical parameters and market conditions on financial effects of HPP operation).

The goal of the system model is to simulate the operation of the process and to evaluate the technical and economic impacts. The process consists of a HPP operation and hydrogen production and includes the control system that coordinates the hydrogen production considering the power plant's limitations. In addition, the degradation model of the electrolyser is also considered as it allows the evaluation of effect of different modes of operation on the shortening of equipment lifetime, which in turn influences the profitability. All these sub-processes are modelled with sufficient accuracy to describe the mass and energy balances, dynamic operation and energy efficiency. On the other hand, the complexity of the model is limited in order to avoid a high computational effort during simulation and optimisation.

The complete structure of the developed process model follows the structure of the process and consists of the following sub-models/modules:

- *The input data module uses historical data and generates real data on water inflow and outflow (available head) and solar irradiation (see* Table 3.1*) as a function of time in the year, which are adjusted for further use. It also provides the hydropower plant's "timetable" defined by the electricity-grid operator. The timetable is the demanded production of electrical energy as a function of time.*

- *The hydropower plant model consists of a simplified model of the power plant's operation by taking into account the basic relations between the potential energy of the water and the electrical energy produced.*

- *The electrolyser model describes basic mass balances, energy balances, efficiencies and basic dynamic phenomena of the electrochemical conversion of electrical energy and water into hydrogen.*
- *The hydrogen-storage model is based on the storage of hydrogen in a tank. It defines the basic relation between the amount of hydrogen and the pressure in the hydrogen tank and evaluates the energy required for hydrogen compression.*
- *The photovoltaic field model estimates the electrical energy generation of the PV field based on the measured solar irradiation data and the size of the PV field.*
- *The remaining useful life (RUL) model evaluates the degradation rate of electrolysers depending on the operating mode (dynamic or static operation, number of on/off cycles, ageing, etc.).*
- *The economic model calculates the financial variables of the operation of the HPP and the hydrogen production by the hydrogen system. The financial flows are calculated using the quantities and prices of the electrical energy and hydrogen produced, as well as the capital and expenditure costs associated with financing and operating the plants.*
- *The control system module is an important part of the process, as it is designed to balance the requests for predicted electricity and hydrogen production (load-following). It takes into account the demand for electrical energy and hydrogen on the market, the available hydropower (water flow in the accumulation), the state of charge of the hydrogen storage and the limits of the HPP and the electrolyser.*

3.1 Input-Data Module

The input-data module generates a time profile of water inflow, available head, solar irradiation and required electrical energy to be generated and delivered to the grid, determined by the grid operator. The data are based on past operation. The past data usually has a non-uniform format and time resolution (sampling time). One task of the input-data module is therefore to standardise the format and time resolution of the data through normalisation, resampling, interpolation and extrapolation.

A list of the components of the input-data module with their inputs, outputs and parameters can be found in Table 3.1.

Table 3.1: Input data module variables.

Input	Description	Unit
/	Files with historic data (time profiles) of: • water inflow, • water head, • required electrical power generation (timetable), • solar irradiation.	/
Output variables	Description	Unit
Q_{IN}	HPP water reservoir inflow	m^3/s
h	Current head (the head is the height difference between where the water enters into the hydro system and where it leaves it measured in metres)	m
P_{TT}	HPP required electrical power given by system operator timetable	MW
P_{PV}	Electrical power generated by photovoltaic field	MW
Parameters	Description	Unit
P_{PV_INST}	Nominal power of photovoltaic field	MW

The data originates from the supervisory control and data acquisition (SCADA) system of the case-study HPP (see Section 3.1). For the purposes of this work, an annual amount of data was exported. The data were pre-processed and organised in the form of a matrix suitable for further use in the MATLAB/Simulink environment. From more than 100 different recorded attributes/variables, data on inflow, outflow, overflow (flow through spillways) and water flow to individual electrical power generators and their sums were selected to recalculate the electrical power generation profile (timetable). The data were extracted in monthly columns. Missing values were regenerated and outliers were smoothed. Some missing values or measurement intervals were replaced and finally the months were merged and synchronised to obtain the entire annual data set. No inflow data was available for the case-study HPP, so some data had to be resampled and synchronised with the outflow data of the HPP upstream in a cascade of five HPPs originating from a different source. The water inflow to the reservoir of the case-study HPP (which is now a delayed and smoothed outflow from the previous HPP in the chain) was calculated with compensation for evaporation and precipitation in the river downstream to the reservoir. Then, uniformly sampled (equidistant) and time-adjusted data were created (time series) to perform a simulation with arbitrary start date and duration.

The owners of the case-study HPP plan to install a photovoltaic (PV) system with a nominal capacity of 6 MW. For this reason, the input-data module also contains the simulated data of the PV power output for 1 year. The predicted electrical power generated by the PV field was calculated based on the solar irradiation data obtained from [158], the website of the Slovenian Environmental Agency (ARSO).

3.2 Hydropower Plant Model

After reviewing the relevant literature in the field of run-of-river hydropower plant modelling [90], [159], [160], [161], [162], [163], [164], [165], [166], we did not find a suitable

model in the MATLAB/Simulink programming environment that would meet our needs. Therefore, we developed simplified HPP's operation model and a hydrogen-system model. The outputs of these models (electricity and hydrogen production) serve as the inputs to the (i) developed economic model and (ii) the developed control system. The complete model makes it possible to verify the possibilities of cogeneration of both electrical energy and hydrogen in a run-of-river hydropower plant and the resulting financial effects [167].

The developed model of the hydropower plant (HPP) is composed of several sub-models:

- *Water-accumulation mass balance model,*
- *Water-accumulation geometric model (relation between mass and volume of accumulated water on one side and water level on the other side),*
- *Bypass-flow model (overflow from the water accumulation to limit the water level),*
- *Power-generation model (relation between generated electrical power on one side and water flow and level on the other side),*
- *Lower-water-level model.*

The structure of the overall HPP model and the interconnection between sub-models are shown in the following figure:

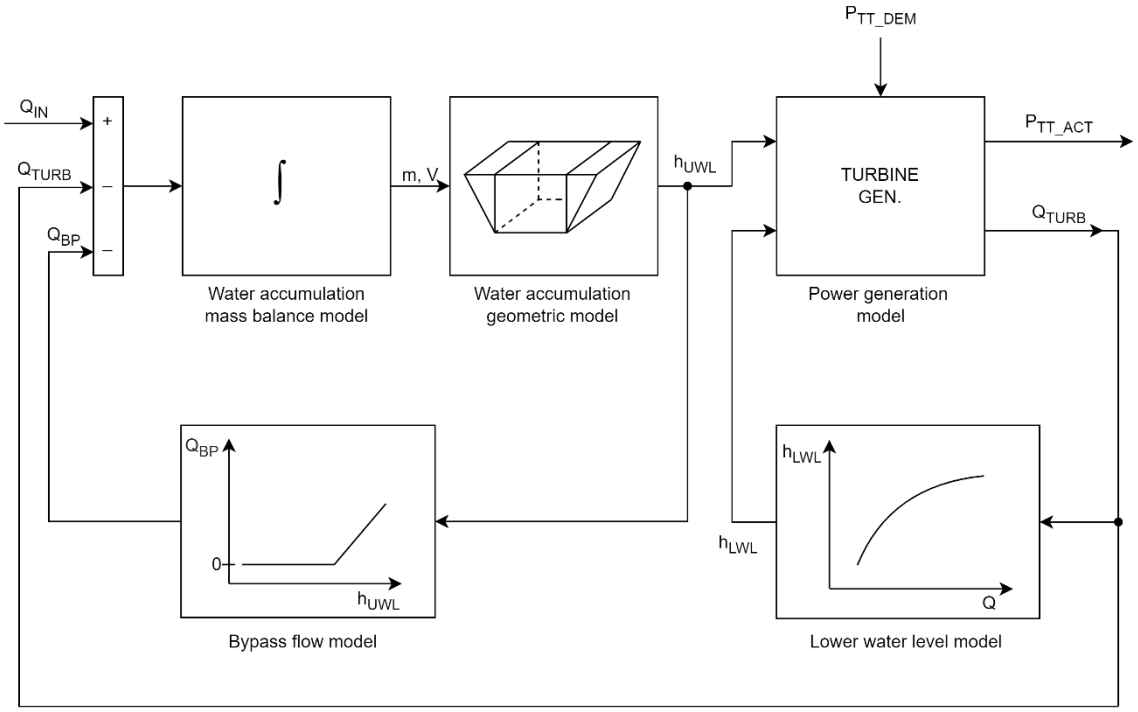

Figure 3.1: Hydropower plant model.

A list of variables of the HPP model can be found in Table 3.2 and are shown in Figure 3.2 and Figure 3.3.

Table 3.2: Variables of the hydropower plant.

Input variables	Description	Units
Q_{IN}	HPP water reservoir inflow	m^3/s
P_{BP}	HPP electrical energy production according to the HPP's timetable	m^3/s
P_{TT_DEM}	Electrical power demanded according to the timetable	MW
Output variables	Description	Units
P_{TT_ACT}	Actual generated electrical power according to the timetable	MW
Internal variables	Description	Units
Q_{TURB}	Water flow through turbines	m^3/s
Q_{BP}	Overflow from the water accumulation	m^3/s
h_{UWL}	Upper water level	m.a.s.l.
h_{LWL}	Lower water level	m.a.s.l.
Parameters	Description	Units
η	Efficiency function parameters $\eta = f(P, h)$	%
ρ	Density of water (1000 kg/m^3)	kg/m^3
g	Acceleration due to gravity (9.81 m/s^2)	m/s^2
V_{ACCUM_MAX}	Maximum reservoir volume (3,400,000 m^3)	m^3

The subsections that follow describe a particular sub-model of the HPP.

3.2.1 Water-Accumulation Mass-Balance Model

The HPP is equipped with a water-accumulation reservoir, which is filled by the river flow (Q_{IN}) and emptied by the water flow through turbines (Q_{TURB}) that generate electrical power and bypass flow (Q_{BP}), i.e., the flow that bypasses the turbines and does not generate electrical power.

The operation of the HPP can lead to rapid and frequent changes in the water flow rates, usually as a result of turbines being controlled in response to changes in electrical load [168]. To explain the relationships between the variables, a simple drawing of a HPP, a water reservoir and the inflow and outflow of the river is shown in Figure 3.2.

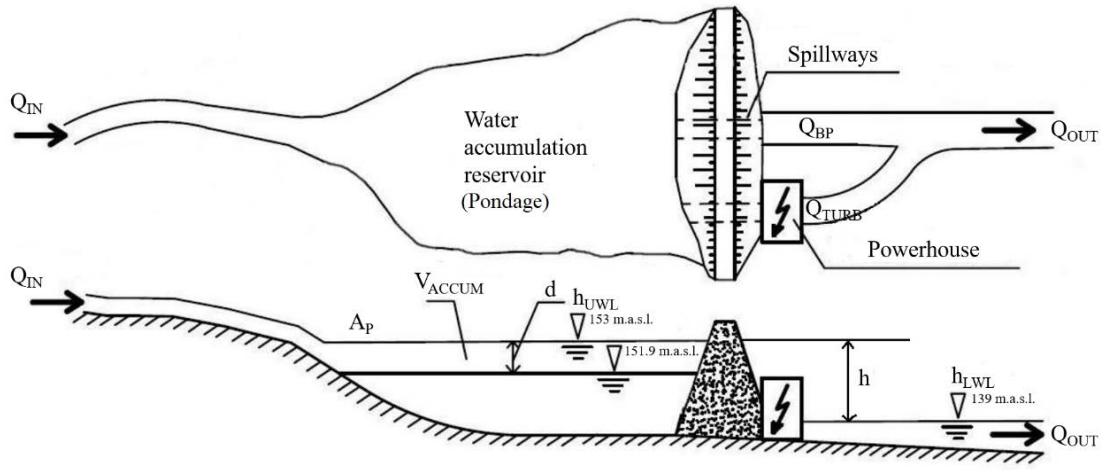

Figure 3.2: River flow distribution in a HPP scheme [168].

The mass balance of the hydropower plant accumulation reservoir can be expressed as follows:

$$Q_{IN} - Q_{TURB} - Q_{BP} - A_P(h) \cdot \frac{dh}{dt} = 0 \tag{3.1}$$

Here, the variables have the following meanings:

- Q_{IN} - *flow entering the HPP water reservoir,*
- Q_{TURB} - *flow entering the HPP generators,*
- Q_{BP} - *flow leaving the HPP water accumulation reservoir via spillways,*
- h - *state of head,*
- $A_P(h)$ - *reservoir surface area as a function of h.*

This means that, ideally, the difference between the input flow (Q_{IN}), the output flow ($Q_{TURB} + Q_{BP}$) and the rate of change of the water volume in the reservoir should be zero. However, since the accuracy of the model is limited, the sum of the terms mentioned is not zero, but can be referred to as Q_{RE} (residual flow):

$$Q_{IN} - Q_{TURB} - Q_{BP} - A_P(h) \cdot \frac{dh}{dt} = Q_{RE} \tag{3.2}$$

3.2.2 Geometric Model

The subchapter defines three possible geometric models of the water level in a water accumulation reservoir. Figure 3.3 defines the water-level situation in the whole system of both reservoir and HPP turbine generator.

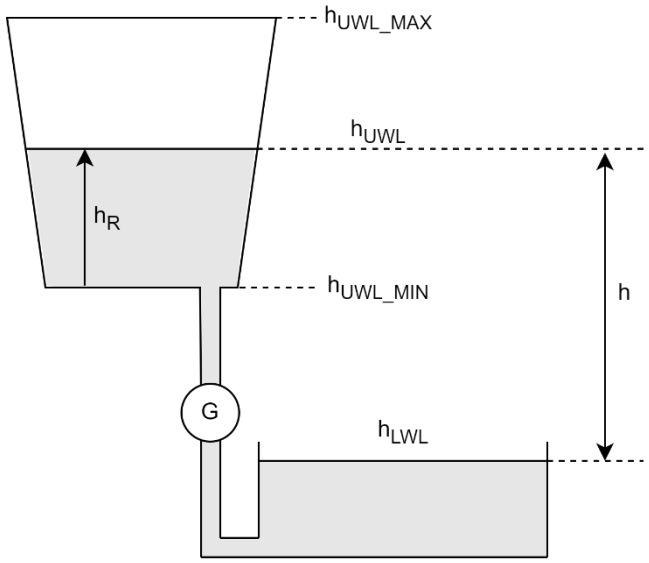

Figure 3.3: Definition of water levels.

There are several important water levels identified in the figure, see Table 3.3.

Table 3.3: Parameters describing water levels.

h_{UWL_MAX}	Upper water level maximum (accumulation reservoir full)	m.a.s.l.
h_{UWL}	Upper water level (actual level in the accumulation reservoir)	m.a.s.l.
h_{UWL_MIN}	Upper water level minimum (accumulation reservoir empty)	m.a.s.l.
h_{LWL}	Lower water level (near the exit of the turbine generator)	m.a.s.l.
h	Water head ($h_{UWL} - h_{LWL}$) that generates electrical power	difference
h_R	Water level in the reservoir measured from the minimum level ($h_{UWL} - h_{UWL\_MIN}$)	difference

m.a.s.l. = metres above sea level

The models are useful when the geometry of the accumulation reservoir and its volume (V_{ACCUM}) are known and there is a need to calculate a resulting denivelation. The cross-section of the reservoir determines the relation between the water level (h_R) and the current volume of water in the accumulation reservoir (V_{ACCUM}). A trapezoidal cross-section is assumed, see Figure 3.4. This results in a relationship between the surface area, the water level and the volume in the reservoir, whereby the surface area and the volume increase with level. V_{ACCUM_MAX} is the maximum volume of the reservoir, A_{ACCUM_MAX} is the corresponding maximum surface area and d_{MAX} is the maximum variation of the water level of the reservoir/denivelation.

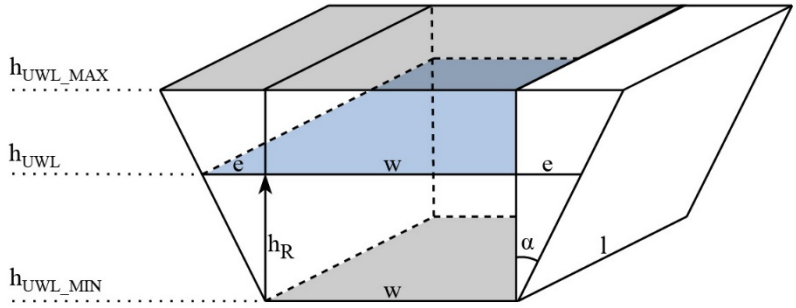

Figure 3.4: Geometry of a reservoir.

To create a simplified model for the assumed morphometry of the case-study HPP reservoir, it was modelled as the volume of three bodies, a rectangular box and two prisms.

The volume is calculated as follows:

$$V_{ACCUM} = w \cdot h_R \cdot l + e \cdot h_R \cdot l = \\ = {h_R}^2 \cdot (k \cdot l) + h_R \cdot (w \cdot l) \tag{3.3}$$

where h_R *and* e *are*

$$h_R = h_{UWL} - h_{UWL\_MIN} \tag{3.4}$$

$$e = h_R \cdot tg\alpha = h_R \cdot k \tag{3.5}$$

and k is the inclination factor:

$$k = tg\alpha. \tag{3.6}$$

Eq. (3.3) can be rewritten as

$${h_R}^2 \cdot (k \cdot l) + h_R \cdot (w \cdot l) - V_{ACCUM} = 0 \tag{3.7}$$

The solution of quadratic Eq. (3.7) is a positive value of Eq. (3.7):

$$h_R = \frac{-w \cdot l \pm \sqrt{w^2 \cdot l^2 + 4 \cdot k \cdot l \cdot V_{ACCUM}}}{2 \cdot k \cdot l}, \quad \alpha > 0. \tag{3.8}$$

The product $w \cdot l$ represents the surface of the reservoir's bottom (A_{BOTTOM}) and the product $k \cdot l$ can be derived from Eq. (3.9) for the surface of the reservoir and maximum denivelation (d_{MAX})

$$A_{ACCUM\ MAX} = A_{BOTTOM} + 2 \cdot k \cdot l \cdot d_{MAX}. \tag{3.9}$$

Eq. (3.8) can thus be rewritten in a different form as

$$h_R = \frac{-A_{BOTTOM} + \sqrt{{A_{BOTTOM}}^2 + 2 \cdot \frac{A_{ACCUM\ MAX} - A_{BOTTOM}}{d_{MAX}} \cdot V_{ACCUM}}}{\frac{A_{ACCUM\ MAX} - A_{BOTTOM}}{d_{MAX}}}, \quad \alpha > 0. \tag{3.10}$$

We can also define the part of the reservoir's surface (p_{TRAP}) over its trapezoidal part regarding the total reservoir's surface A_{ACCUM_MAX} as

$$p_{TRAP} = \frac{A_{ACCUM\ MAX} - A_{BOTTOM}}{A_{ACCUM\ MAX}}. \tag{3.11}$$

By knowing the estimation for p_{TRAP}, Eq. (3.3) can be rewritten in the form

$$h_R = \frac{A_{ACCUM\_MAX} \cdot (p_{TRAP} - 1) + \sqrt{{A_{ACCUM\_MAX}}^2 \cdot (p_{TRAP} - 1)^2 + 2 \cdot \frac{p_{TRAP} \cdot A_{ACCUM\ MAX}}{d_{MAX}} \cdot V_{ACCUM}}}{\frac{p_{TRAP} \cdot A_{ACCUM\ MAX}}{d_{MAX}}}, \quad \alpha > 0 \tag{3.12}$$

The availability of data determines which of these three models (Eqs. (3.8), (3.10), (3.12) is reasonable to choose for modelling the HPP's water reservoir.

3.2.3 Bypass-Flow Model

In a real HPP, the water level in the accumulation reservoir cannot exceed h_{MAX} due to overflow. When the level reaches h_{UWL_MAX}, overflow occurs and prevents the level from further rising. In the model, this is implemented by the following relation:

$$\begin{aligned} &h_{UWL} \leq h_{UWL\_MAX}: Q_{BP} = 0 \left[\frac{m^3}{s}\right] \\ &h_{UWL} > h_{UWL\_MAX}: Q_{BP} = k_{BP} \cdot \left(h_{UWL} - h_{UWL\_MAX}\right) \left[\frac{m^3}{s}\right] \end{aligned} \tag{3.13}$$

Q_{BP} represents the bypass flow, i.e., overflow. When the water level is below maximum, there is no overflow. When the water level is at the maximum or above, overflow is proportional to the level deviation over maximum. In the equation above, k_{BP} represents the flow coefficient in units [m^2/s].

3.2.4 Power-Generation Model

A simplified static model is used to simulate a HPP's operation. The use of a static model instead of a dynamic model is justified by the fact that the transition phenomena of a HPP during a power change are much shorter than the simulation and observation step, which is typically between 15 and 30 minutes.

The basic model establishes the relationship between water flow and water level on one hand, and resulting generated electrical power, on the other hand. A simplified model of the energy efficiency is also integrated into the model.

In the HPP simulation, two forms of models, "direct" and "inverse" are possible. The direct model calculates the generated electrical power (P) based on the actual water head (h) and the water flow (Q_{TURB}) to the HPP, taking into account the turbine and generator efficiency (η).

The direct model is given by the following basic equation, which determines the generated electrical power (P) as a function of the water inflow (Q_{TURB}) and the water head (h) (source [163], [164], [8], [162]):

$$P = Q_{TURB} \cdot h \cdot g \cdot \rho \cdot \eta \tag{3.14}$$

An inverse model is needed in the case when the demanded generated electrical power is given and the corresponding water flow rate has to be determined. For the inverse model, the inverted equation is used:

$$Q_{TURB} = \frac{P}{h \cdot g \cdot \rho \cdot \eta} \tag{3.15}$$

The efficiency factor (η) is not constant, but depends on the operating power (P) and the water head (h). The typical shape of the function $\eta = f\,(P,\ h)$ is shown in Figure 3.5 and represents the total efficiency of the turbine and generator [169], [170].

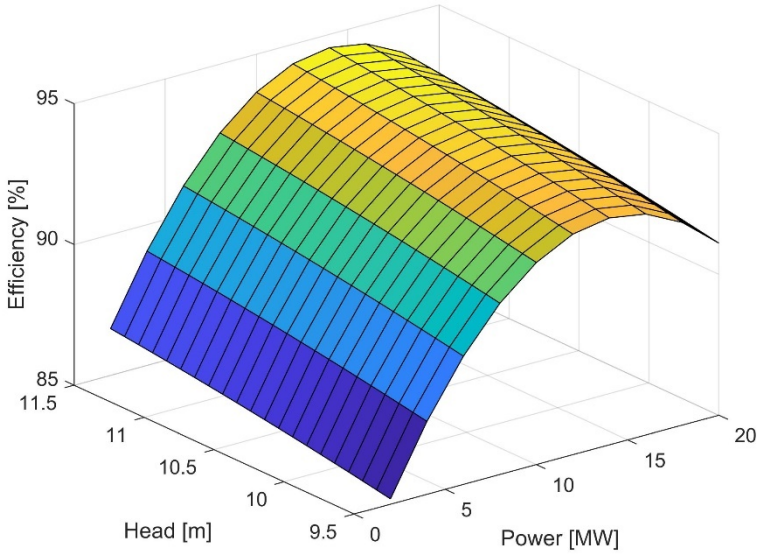

Figure 3.5: Generator efficiency as a function of power (P) and head (h).

The efficiency can be determined experimentally or derived from the literature and can be approximated by the following quadratic relation:

$$\eta\,(P,h) = a_1 + a_2 h + a_3 P + a_4 h^2 + a_5 P^2 \tag{3.16}$$

From Eq. (3.15), we can derive an inverse value of water flow:

$$Q_{TURB}{}^{-1} = \frac{1}{P} \cdot (h \cdot g \cdot \rho \cdot \eta) \tag{3.17}$$

By inserting relation (3.16) into (3.17), we get:

$$Q_{TURB}{}^{-1} = g \cdot \rho \cdot \left(\frac{h}{P} \cdot (a_1 + a_2 h + a_3 P + a_4 h^2 + a_5 P^2) \right) \tag{3.18}$$

After further manipulation we get:

$$Q_{TURB}{}^{-1} = g \cdot \rho \cdot \left(a_1 \frac{h}{P} + a_2 \frac{h^2}{P} + a_3 h + a_4 \frac{h^3}{P} + a_5 hP \right) \tag{3.19}$$

As the gravitational acceleration (g) and water density (ρ) are constants, we can introduce new coefficients (q_i):

$$q_i = a_i \cdot g \cdot \rho \qquad (i = 1 \ldots 5) \tag{3.20}$$

Then, Eq. (3.19) can be rewritten as:

$$Q_{TURB}{}^{-1} = q_1 \frac{h}{P} + q_2 \frac{h^2}{P} + q_3 h + q_4 \frac{h^3}{P} + q_5 hP \tag{3.21}$$

or:

$$Q_{TURB}{}^{-1} = q_1 \cdot h^1 P^{-1} + q_2 \cdot h^2 P^{-1} + q_3 \cdot h^1 P^0 + q_4 \cdot h^3 P^{-1} + q_5 \cdot h^1 P^1 \tag{3.22}$$

Finally, (Q_{TURB}) can be expressed in more compact form:

$$Q_{TURB} = \left(\sum_{i=1}^{5} (q_i \cdot h^{hi} \cdot P^{pi}) \right)^{-1} \tag{3.23}$$

The exponents hi and pi result directly from Eq. (3.20), while the set of coefficients (q_i) is taken from the literature [170], [169], see Table 3.4:

Table 3.4: Coefficients.

i	hi	pi	q_i
1	1	-1	6.3868E-03
2	2	-1	2.6564E-04
3	1	0	1.4992E-04
4	3	-1	-9.2174E-06
5	1	1	-5.3474E-06

The inverse model calculates the required water inflow (Q_{TURB}) to the power plant for the demanded electrical power (P) at an actual water head (h). The inverse model is used to determine the required water flow for the demanded electrical power, defined by operator timetable. It uses the real data of the actual water inflow into the reservoir and the actual water head (h). The module updates an overall water accumulation of the HPP and identifies the difference between the demanded electrical power according to the timetable (based on the system operator's model) and the electrical energy production that is actually possible (based on actual water inflows).

3.2.5 Lower-Water-Level Model

The lower water level (h_{LWL}) is the water level at the exit of the turbine generator. Together with the upper water level (h_{UWL}) it defines the water-level difference (h), which determines the amount of electrical power generated by the water flow through the turbine generator (Q_{TURB}). The lower water level is not a constant value and depends on many conditions; the most important one is the flow through turbines (Q_{TURB}).

The determination of a rating curve depends on a number of complicated factors, including the geometry of the riverbed and the uncertainty of the discharge measurements. The determination of the discharge rate is normally subject to high uncertainty. High water levels represent extreme conditions that are dangerous and unfavourable for measurements. It can therefore be difficult to create a reliable measurement curve. Extreme discharge conditions are particularly prone to errors.

The most common type of functional relationship in rating curves is a fairly simple power-type equation, e.g., Eq. (3.24), which can be used to simulate the relationship between the discharge and the lower water level can be found in [171], [172], [173]. The general mathematical description for the stage-discharge relationship is given as:

$$Q = a(h - h_0)^b \tag{3.24}$$

where Q is the stream discharge, [m^3/s], h is the water level [m], h_0 is the water level corresponding to zero discharge [m], and a and b are the parameters of the rating curve model.

The data-based model of the lower water level used in this dissertation is presented in Section 4.2.3.

3.3 Hydrogen-System Model

A developed hydrogen-system model consists of several sub-models: electrolyser, compressor, hydrogen storage. During modelling, the realistic technical characteristics and limitations of individual components were taken into account. The model enables an estimation of the amount of hydrogen produced and stored from the available electrical energy.

3.3.1 Electrolyser Model

A simple static model of the electrolyser was developed, which defines the relation between the input electrical energy to the electrolyser and the generated hydrogen flow. In general, the electrolysis process involves various kinds of losses. Theoretically, a 100% efficient electrolysis system would require 39.39 kWh of electrical energy to produce 1 kg of hydrogen at standard temperature and pressure, since 1 kg of hydrogen releases 39.39 kWh of energy when combusted. But due to losses, about 50 kWh of energy is required to produce 1 kg of hydrogen using commercial electrolysers available now.

The efficiency model was built on the basis of a particular industrial electrolyser, produced by the manufacturer NEL [58]. The manufacturer provides the data about the overall electrolyser system's efficiency and the stack efficiency. A stack represents a set of electrolyser cells, while the system also includes a number of BoP components (actuators for cooling, preheating, sensors, electronic control units, etc.), which also consume electrical power during operation. Table 3.5 provides data on the efficiency of a particular NEL electrolyser at a particular flow of generated hydrogen:

Table 3.5: Efficiency as a function of load.

Q_{H2} hydrogen flow rate		C_{STACK} consumption stack [kWh/kg]	C_{SYS} consumption system [kWh/kg]	η_{STACK} efficiency stack	η_{SYS} efficiency system
[%]	[kg/h]				
10	2.2	45.6	61.2	0.86	0.64
20	4.5	46.2	54.0	0.85	0.73
30	6.7	46.7	52.8	0.84	0.75
40	9.0	47.8	52.8	0.82	0.75
50	11.2	49.0	53.4	0.80	0.74
60	13.5	50.1	54.4	0.79	0.72
70	15.7	51.2	55.6	0.77	0.71
80	18.0	52.3	56.7	0.75	0.69
90	20.2	53.4	57.9	0.74	0.68
100	22.5	54.5	59.0	0.72	0.67

The data from the above table are shown graphically in Figure 3.6, where the x-axis represents the hydrogen flow (Q_{H2} [kg/h]) and the y-axis represents the specific electrical energy consumption (C [kWh/kg]) for hydrogen generation at a particular hydrogen flow. The bottom curve (blue line, symbol "$*$") represents the energy consumption of electrochemical cells (stack) only, while the upper curve (red line, symbol "$+$") represents the consumption of the entire system (stack and BoP components). It can be noticed that the system relative consumption increases and the efficiency decreases with the electrolyser load (flow rate of the produced hydrogen).

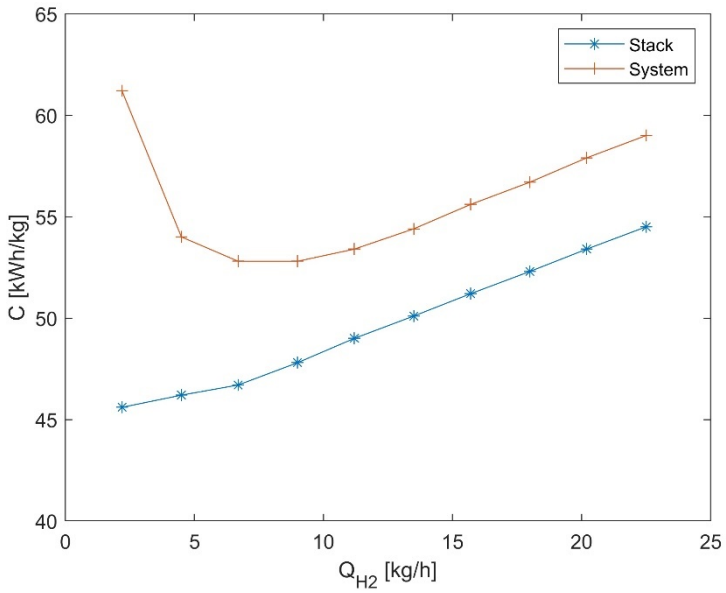

Figure 3.6: Electrical energy consumption as a function of hydrogen production rate.

An important feature of electrolysers (and fuel cells) is the polarisation curve, which characterises the operation of a single cell of the electrolyser. The polarisation curve is a

graph whose x-axis represents the cell current density [A/cm^2] and the y-axis represents the cell voltage [V] needed to generate the electric current. In the case of the electrolyser's manufacturer NEL, the polarisation curve is not expressed directly. Note that it is not needed for modelling either, as the consumption of the electrolyser at a given hydrogen production rate is explicitly defined in Table 3.5. However, for demonstration and comparison purposes, we extract the polarisation curve from the relationship resulting from Table 3.5.

The polarisation curve is determined using the following relationship. The mass-flow rate (Q_{H2} or $\dot{m}$), see Table 3.5, column 2, was converted to the molar-flow rate ($\dot{n}$) using Eq. (3.25), where (M_{H2}) is the molar mass of hydrogen. The factor 1000 is used to convert kilogrammes [kg] to grammes [g] and the factor 3600 is used to convert hours [h] to seconds [s].

$$\dot{n} = \frac{\dot{m}_{H2} \cdot 1000}{M_{H2} \cdot 3600}, \left[\frac{mol}{s}\right] \tag{3.25}$$

Next, the relationship (3.26) between hydrogen molar flow rate ($\dot{n}$) and electric current (I_{DC}) was introduced. The electric current is proportional to the hydrogen flow, and this originates from the simple fact that each hydrogen atom brings one electron, which is a carrier of the electric current. In the equation, (N_{CELL}) is the number of electrolyser stack cells, n_e is the number of electrons in one hydrogen molecule (hydrogen molecule is diatomic, so it has 2 electrons), (N_A) is Avogadro's number and (q_{EL}) is the electric charge of one electron.

$$I_{DC}[A] = \frac{\dot{n}\left[\frac{mol}{s}\right]}{N_{CELL}[1]} \cdot n_e \cdot N_A \left[\frac{1}{mol}\right] \cdot q_{EL}[As] \tag{3.26}$$

The next step in determining the polarisation curve is to calculate the electric current density (J), which is the electric current (I_{DC}) distributed over the cross-sectional area (A_{CELL}) of a single cell of the electrolyser:

$$J\left[\frac{A}{cm^2}\right] = \frac{I_{DC}[A]}{A_{CELL}[cm^2]} \tag{3.27}$$

The electrolyser cell voltage (U_{DC}) represents the y-axis of the polarisation curve. In our case, it was estimated from the expression for the electrical power of the electrolyser stack:

$$P_{EL\_STACK} = U_{DC} \cdot I_{DC} \cdot N_{CELL} \tag{3.28}$$

Cell voltage is then expressed by the relation above:

$$U_{DC} = \frac{P_{EL\_STACK}}{I_{DC} \cdot N_{CELL}} \tag{3.29}$$

Electrical power (P_{EL_STACK}) expressed in [kW] from the relationship above is simply derived from the specific consumed electrical power, see Table 3.5, column 3, multiplied by the hydrogen mass flow rate, see Table 3.5, column 2:

$$P_{EL\_STACK}[kW] = C_{STACK}(Q_{H2})\left[\frac{kWh}{kg}\right] \cdot Q_{H2}\left[\frac{kg}{h}\right] \tag{3.30}$$

Based on the current density (J) and the cell voltage (U_{DC}), the polarisation curve is generated (Figure 3.7).

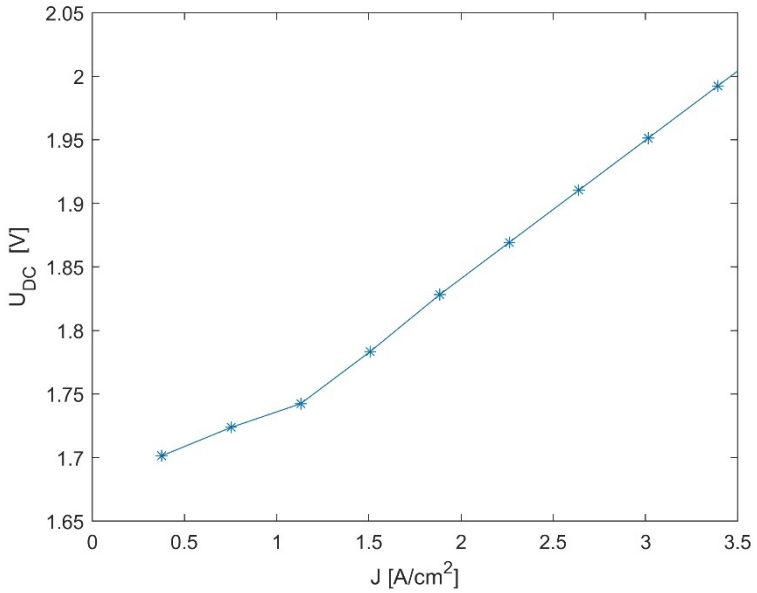

Figure 3.7: Polarisation curve.

The already mentioned characteristic value is the efficiency of "conversion" of the electrical energy into hydrogen (see Table 3.5). It is defined as the quotient between the thermal power (P_{H2_HHV}) of the produced hydrogen, and the electrical power consumed for hydrogen production. Two types of efficiency are observed:

- *stack efficiency (based on the energy consumption of the stack only);*
- *system efficiency (based on the energy consumption of the stack + the balance of the plant's components).*

Stack efficiency, see Eq. (3.31)

$$\eta_{STACK} = \frac{P_{H2\_HHV}}{P_{EL\_STACK}} \tag{3.31}$$

and system efficiency, see Eq. (3.32).

$$\eta_{SYS} = \frac{P_{H2\_HHV}}{P_{EL\_SYS}} \tag{3.32}$$

The thermal power of the produced hydrogen (P_{H2_HHV}) is proportional to the mass flow of hydrogen and the hydrogen high heating value (E_{H2_HHV}) of 39.39 kWh/kg H_2:

$$P_{H2\_HHV} = Q_{H2}\left[\frac{kg}{h}\right] \cdot E_{H2\_HHV}\left[\frac{kWh}{kg}\right] \tag{3.33}$$

The hydrogen-production electrical power of the stack only is expressed by Eq. (3.28). The electrical power of the entire system (stack + balance of plant components) is expressed as:

$$P_{EL\_SYS}[kW] = C_{SYS}(Q_{H2})\left[\frac{kWh}{kg}\right] \cdot Q_{H2}\left[\frac{kg}{h}\right] \tag{3.34}$$

The resulting efficiency curves are shown in Figure 3.8.

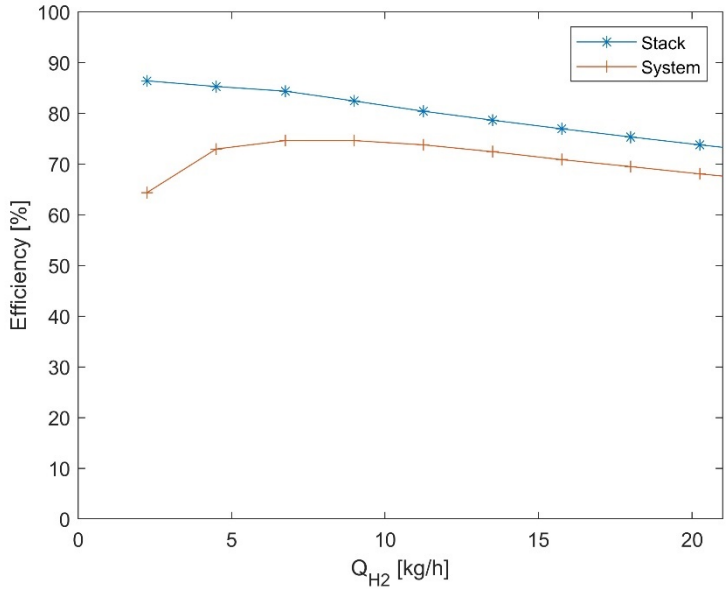

Figure 3.8: Efficiency curves.

The developed static model of the electrolyser describes the mass and energy balances of hydrogen production by water electrolysis.

3.3.2 Hydrogen-Compression Model

After generation, hydrogen must be stored for later use. Here, storage in pressurised form in tanks is considered. In general, the maximum pressure in the tanks can vary between e.g. 50 bar and up to 900 bar, depending on the tank shape and material used. Higher pressure means smaller geometrical dimensions of the tank, but the energy needed for hydrogen compression increases and can represent a significant portion of hydrogen's combustion energy, also known as the heating value (HHV or LHV). Therefore, in this subsection, we investigate the energy needed for hydrogen compression as a function of target pressure. Hydrogen can be compressed by mechanical compressors and also electrochemically by PEM membranes [174], [175]. For mechanical compression, the following equation estimates the compression energy [174]:

$$E_C = m \cdot \frac{R \cdot T}{M} \cdot \left(\frac{\gamma}{\gamma - 1}\right) \cdot \left(\left(\frac{p_{H2}}{p_{IN}}\right)^{\frac{\gamma-1}{\gamma}} - 1\right) \tag{3.35}$$

Variables in the equation have the following meanings:

- p_{IN} – *initial pressure [bar], i.e., pressure at the output of the electrolyser*
- p_{H2} – *target pressure [bar], i.e., pressure in storage tank*
- E_C – *energy [J] needed for compression from (p_{IN}) to (p_{H2})*

- *m – mass of hydrogen to be compressed [kg]*
- *M – molar mass of hydrogen (2.01588 10^{-3} [kg/mol])*
- *R – gas constant (8.314 [J/(mol K)])*
- *T – absolute temperature (293 [K])*
- *γ – compression factor (the adiabatic coefficient of hydrogen is $\gamma = 1.41$)*

For electrochemical compression, energy needed for compression can be expressed as:

$$E_C = m \cdot \frac{R \cdot T}{M} \cdot ln\left(\frac{p_{H2}}{p_{IN}}\right) \tag{3.36}$$

The figure below shows the dependence between the target (end) pressure (p_{H2}) and the required compression energy for adiabatic mechanical compression and electrochemical compression. In both cases the starting pressure and temperature are 1 bar and 20 °C, respectively.

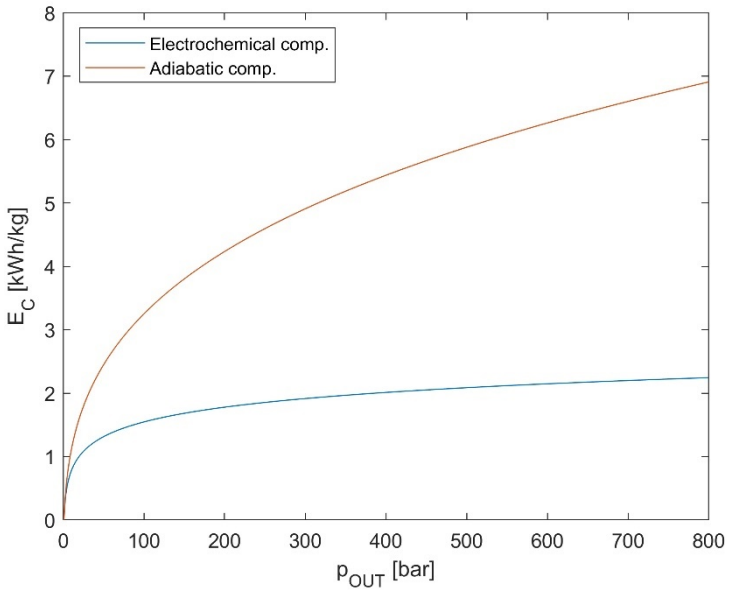

Figure 3.9: Hydrogen compression energy as a function of target pressure.

It can be seen that mechanical compression to 800 bar consumes almost 7 kWh per kg of hydrogen, which represents almost 18% of hydrogen internal energy HHV, which is 39.39 kW/kg.

Since hydrogen production and compression operates in a continuous way, compression power P_C is more interesting than energy and can be expressed for mechanical adiabatic compression:

$$P_C = Q_{H2} \cdot \frac{R \cdot T}{M} \cdot \left(\frac{\gamma}{\gamma - 1}\right) \cdot \left(\left(\frac{p_{H2}}{p_{IN}}\right)^{\frac{\gamma-1}{\gamma}} - 1\right) \tag{3.37}$$

and electrochemical compression:

$$P_C = Q_{H2} \cdot \frac{R \cdot T}{M} \cdot ln\left(\frac{p_{H2}}{p_{IN}}\right) \tag{3.38}$$

3.3.3 Required Electrical Power to Generate and Compress Hydrogen

As follows from the previous two subsections, the hydrogen system composed of electrolyser, compressor and storage consumes electrical power in two ways:

- *power P_G for hydrogen generation by electrolyser (Section 3.3.1,).*
- *power P_C for hydrogen compression (Section 3.3.2)*

The power component P_G depends on the flow rate of generated hydrogen (Q_{H2}) and it can be expressed in the following generalised form:

$$P_G = Q_{H2} \cdot C_{SYS}(Q_{H2}) = Q_{H2} \cdot a(Q_{H2}) \tag{3.39}$$

Here, $a(Q)$ is a non-linear function indicating the consumption [kWh/kg H_2] as a function of the flow of hydrogen generated by the electrolyser from NEL, see Table 3.5, column 4 (C_{SYS}).

The power component P_C depends on target pressure (p) and flowrate (Q_{H2}) of generated hydrogen, which needs to be compressed:

$$P_C = Q_{H2} \cdot b(p) \tag{3.40}$$

Equation (3.40) is a generalised form of equations (3.37) or (3.38). Here, $b(p)$ is a non-linear function that gives the consumption [kWh/kg] as a function of the final compression pressure ($p = p_{H2}$).

Total power required for the generation and compression (P_{GC}) of hydrogen with a flow rate (Q_{H2}) and a final pressure (p) can be expressed in generalised form:

$$P_{GC} = P_G + P_C = Q_{H2} \cdot (a(Q_{H2}) + b(p)) \tag{3.41}$$

For a given pressure p, the term $b(p)$ is a constant denoted by the symbol c; $c = b(p)$.

$$P_{GC} = Q_{H2} \cdot (a(Q_{H2}) + c) \tag{3.42}$$

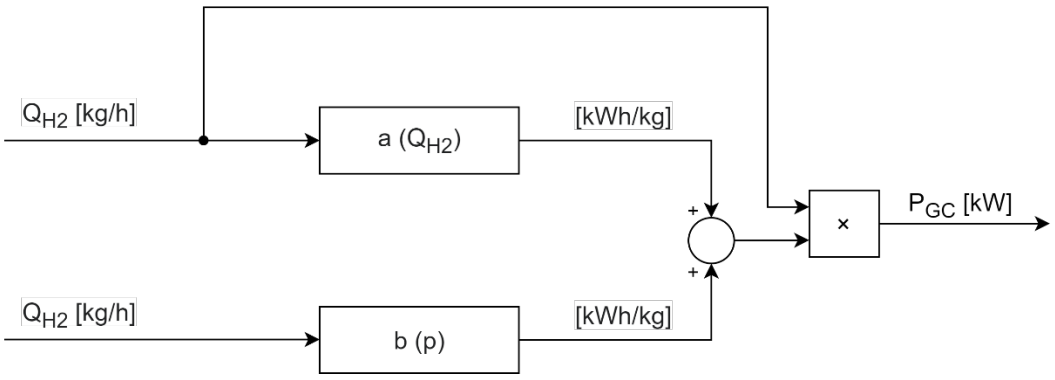

Figure 3.10: Direct model.

If the hydrogen flow rate Q_{H2} and current pressure p are given, then the calculation of the electrical power P_{GC} is a subject of direct calculation by equation (3.42), which represents direct model, illustrated also by Figure 3.10. But in the opposite case, if the available power (P_{GC}) for the generation and compression of hydrogen is given and the hydrogen pressure (p) is also defined, it is necessary to determine the hydrogen mass flow (Q_{H2}) at which the power (P_{GC}) is just sufficient to generate and compress hydrogen. It is therefore necessary to express the flow (Q_{H2}) from the equation (3.42). An analytical solution is not possible because $a(Q_{H2})$ is a non-linear function, which is tabulated in our case. Therefore, the solution must be found numerically by interpolation. The procedure is the following:

- *Based on given pressure* p *calculate* c = b(p).
- *Create initial hydrogen mass flow vectors* Q_{H2}*;* Q_{H2_min} ... Q_{H2_max} *with, e.g., 10 steps.*
- *Calculate the corresponding electrical powers* P_{GC} *using the equation* (3.42)*.*
- *Based on the given available power* P_{GC}*, calculate the hydrogen mass flow* Q_{H2} *using the linear interpolation function. In MATLAB, this can be implemented by the following code line:* Q_{H2} = interp1(P_{GC}, Q_{H2}, P_{GC}).

The procedure represents an inverse model, and is illustrated by Figure 3.11.

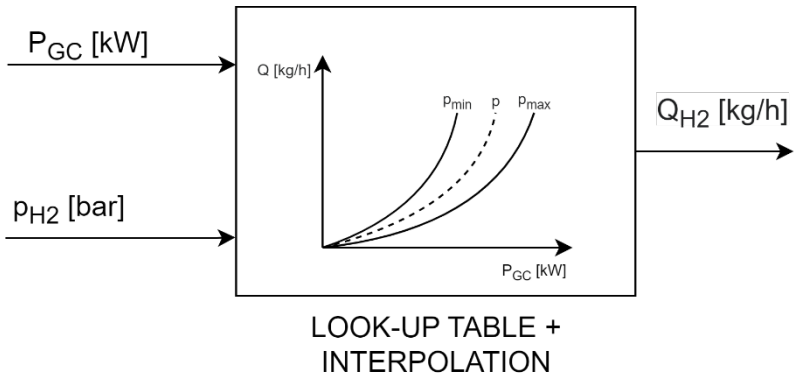

Figure 3.11: Inverse model.

Figure 3.12 shows the hydrogen generation power (P_G), compression power (P_C) and their sum (P_{GC}) as a function of the hydrogen flow (Q_{H2}) and the target compression pressure (p_{H2}).

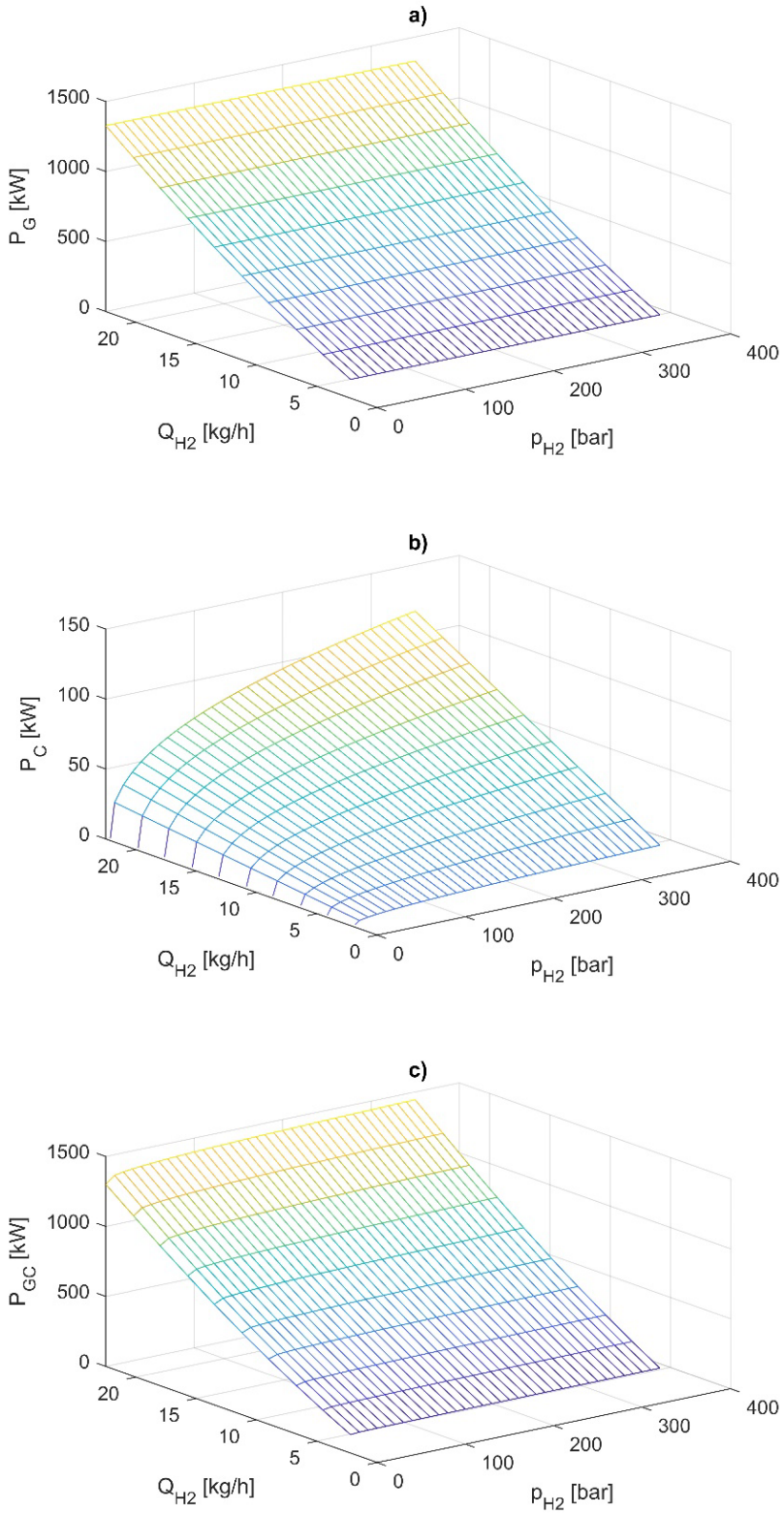

Figure 3.12: a) Generation, b) compression c) generation and compression power as a function of pressure and hydrogen mass-flow rate.

A list of model inputs, outputs and parameters can be found in Table 1.1.

Table 3.6: Electrolyser model variables.

Input variables	Description	Units
P_{GC}	Actual energy consumption for hydrogen generation and compression	MW
p_{H2}	Current pressure in the hydrogen storage tank	bar
Output variables	Description	Units
Q_{H2}	Generated hydrogen mass flow	kg/h
η_{SYS}	hydrogen system's operating efficiency	%
Parameters	Description	Units
E_{H2_HHV}	Energy content of 1 kg hydrogen (141.9 MJ, i.e. 39.39 kWh)	kWh
K_L	Compression-loss coefficient	/
n	Compression-loss exponent	/
P_C	Power losses for hydrogen compression	MW

3.3.4 Hydrogen-Storage Model

The hydrogen-storage model assumes hydrogen storage in pressurised tanks. The corresponding model defines the actual pressure in the hydrogen-storage tank according to the hydrogen production (inflow) and consumption (outflow). A list of the variables of the hydrogen-storage model with their inputs, outputs and parameters can be found in Table 3.7.

Table 3.7: Hydrogen-storage model variables.

Input variables	Description	Units
Q_{H2}	Input mass-flow rate to storage (produced hydrogen flow rate)	kg/h
$Q_{H2\_OUT\_DEM}$	Demanded output mass-flow rate of hydrogen	kg/h
$Q_{H2\_OUT\_ACT}$	Actual output flow mass rate of hydrogen	kg/h
Output variables	Description	Units
p_{H2}	Current pressure in the hydrogen storage tank	bar
Parameters	Description	Units
V_{GEO}	Hydrogen storage tank geometric volume	m^3
m_{H2}	Mass of hydrogen in the tank	kg
R_{H2}	Hydrogen specific gas constant (R_{H2} = 4124 J/(kg K) [176])	J/(kg K)
T_m	Mean temperature of stored hydrogen	K
p_{H2_MIN}	Minimum allowed tank pressure	bar

The model considers the hydrogen-storage pressure. If pressure is below minimum, which indicates empty storage, the hydrogen tank outflow is stopped. In this way, reaching zero or negative pressure is prevented, which is in accordance with physical laws:

$$\begin{aligned} &if\ (p_{H2} \geq p_{H2_{MIN}}) \\ &\quad Q_{H2\_OUT\_ACT} = Q_{H2\_OUT\_DEM} \\ &else \\ &\quad Q_{H2\_OUT\_ACT} = 0 \end{aligned} \tag{3.43}$$

The time-derivative of stored mass in tank can be expressed as the difference between inlet and outlet mass-flow rate (Q_{H2} [kg/s] and Q_{H2_OUT} [kg/s], respectively):

$$\frac{dm_{H2}}{dt} = \left(Q_{H2} - Q_{H2\_OUT\_ACT}\right) \tag{3.44}$$

By numeric integration of the derivative, current mass of hydrogen in the tank m_{H2} is calculated.

The relation between mass (m_{H2}) of stored hydrogen in the tank and hydrogen pressure in the tank (p_{H2}) is given by the well-known ideal gas law:

$$p_{H2} \cdot V_{GEO} = m_{H2} \cdot R_{H2} \cdot T_m \tag{3.45}$$

The values for (R_{H2}) and (T_m) are assumed to be constant. The block diagram of the hydrogen-storage model is shown in Figure 3.13.

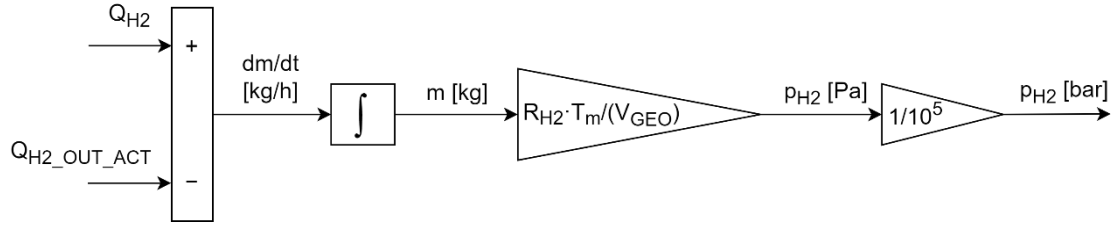

Figure 3.13: Hydrogen storage sub-model.

First, the model subtracts the mass flow (Q_{H2}) of hydrogen produced and the simulated hydrogen consumption ($Q_{H2\_OUT\_ACT}$). This is followed by integration resulting in the mass of stored hydrogen. Mass is then converted to pressure using the ideal gas law equation. Pressure is also converted from Pa to bar.

3.4 Photovoltaic-Field Model

A photovoltaic power-plant model has been developed for the case when the HPP is equipped with a photovoltaic (PV) field for additional electrical power generation. The PV model calculates the power of the PV field based on the actual solar irradiation data and area of PV field:

$$P_{PV} = J_S \cdot A_{PV} \cdot \eta_{PV} \tag{3.46}$$

Here, P_{PV} is the generated electrical power, J_S is the actual solar irradiation (function of time and geographical location), A_{PV} is area of photovoltaic field and η_{PV} is the efficiency of the conversion of solar irradiation to electrical power. An example of the resulting time profile of the generated electrical power is shown in Figure 3.14.

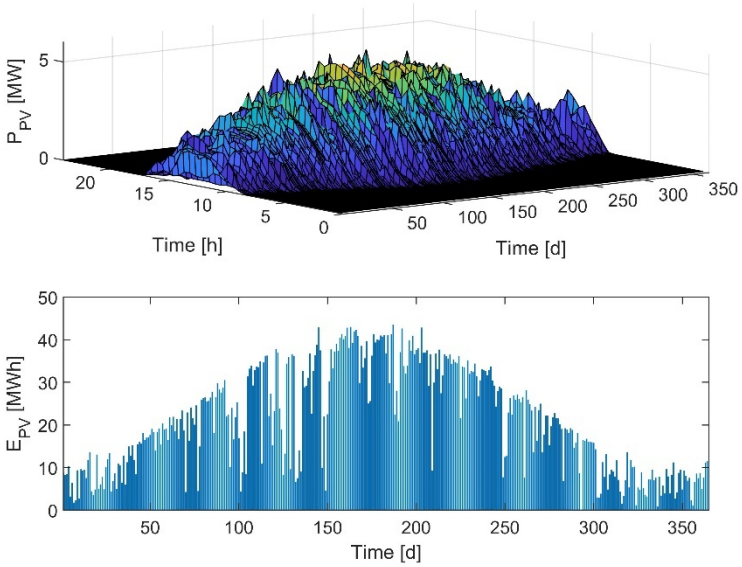

Figure 3.14: Simulated annual production of electrical energy from 6 MW PV field.

The data set for annual solar irradiation was created based on data from the Slovenian Environment Agency and used for the simulation of the PV field's electrical power generation. A list of the variables of the photovoltaic field model can be found in Table 3.8.

Table 3.8: Photovoltaic field model variables.

Inputs	Description	Units
J_S	Solar irradiance	W/m^2
Outputs	Description	Units
P_{PV}	Generated electrical power	MW
Parameters	Description	Units
A_{PV}	PV field area	m^2
η_{PV}	PV field efficiency (14.5 %)	%

Figure 3.15 shows a scheme of photovoltaic field model. The input to this model is the current measured solar irradiance (J_S). The model then calculates the power generated by the PV field (P_{PV}) using Eq. (3.46).

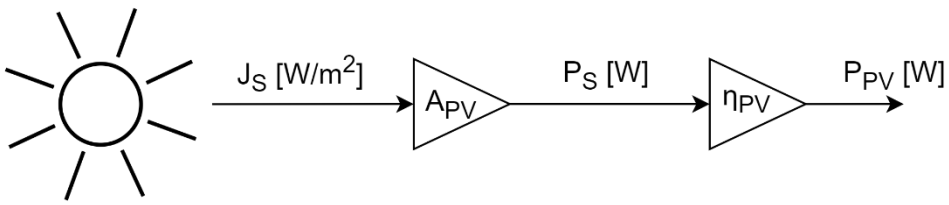

Figure 3.15: Structure of PV field sub-model.

3.5 Remaining-Useful-Life Model

This model is intended to estimate the remaining useful life (RUL) of an electrolyser. The RUL model is needed for the implementation of the economic model, addressed later in this section. The degradation process of the system and the reduction of its remaining useful life is driven by numerous complex mechanisms of materials and components degradation, which depends on many factors, such as system age, intensity and duration of the exploitation, number and duration of events with irregular process conditions (e.g. overload, overheating, contaminated input streams, etc.). Exact modelling of degradation and the remaining useful life is therefore extremely complex and demanding and exceeds the scope of this work. Instead, we propose a very simplified model, which assumes the following factors that reduce the RUL:

- *equipment ageing (some degradation progresses can occur while the system is not in operation, since material and components degrade due to environmental effects),*
- *amount of electrical energy used (when the system is in operation, material and components degrade due to the transport of material, catalyst degradation, etc.),*
- *number of system start-up events (each start-up event causes changes in temperature and thermal stress, which have a negative effect on the materials and components).*

The proposed structure of the RUL model is shown below:

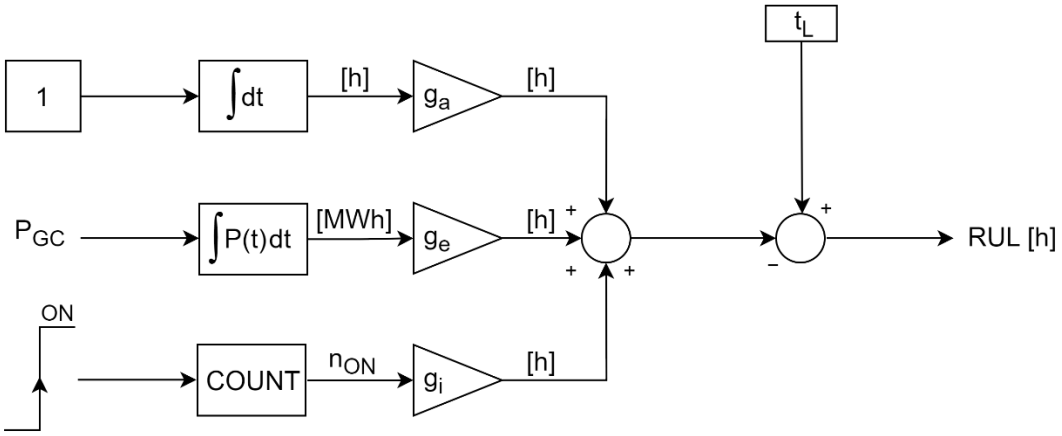

Figure 3.16: Structure of RUL sub-model.

- t_L *represents the total lifetime of the system (assumed e.g., 80,000 h).*
- *The upper branch with gain* g_a *represents degradation due to ageing. Gain* g_a *is the ratio between the lifetime* t_L *in the case of continuous operation and lifetime* t_A *in case the system is not used (*$g_a = t_L / t_A$*). Elapsed time from the beginning of life is multiplied by gain* g_a*.*
- *The middle branch with gain* g_e *represents the degradation due to exploitation (hydrogen production). This branch integrates the input electrical power of the electrolyser resulting in the total amount of electrical energy consumed, which is in close relation to the total mass of hydrogen produced. In general,* $g_e = 1 / P_{MAX}$*, where* P_{MAX} *represents the maximum electrical power of the hydrogen system.*

- *The bottom branch with gain* g_i *represents degradation due to intermittent operation (frequent start-up and stop). Gain* g_i *represents the lifetime reduction by each start-up event.*

A list of the variables of the degradation model can be found in Table 3.9.

Table 3.9: Degradation model variables.

Inputs	Description	Units
P_{GC}	Hydrogen generation and compression power	MW
Outputs	Description	Units
RUL	The remaining useful life of the hydrogen system	h
Parameters		
t_L	Hydrogen system's lifetime during continuous operation at nominal power	h
t_A	Hydrogen system's lifetime if not operated (pure ageing)	h
g_a	RUL reduction gain due to ageing	-
g_e	RUL reduction gain due to exploitation	MW^{-1}
g_i	RUL reduction gain due to intermittent operation	h

Note that the degradation of the hydrogen system actually manifests in two ways:

- *reduction of the remaining useful life (RUL),*
- *reduction of the energy efficiency.*

Both manifestations of degradation appear in parallel, but in this work, only the reduction of RUL is considered, but not the reduction of energy efficiency. In our model, energy efficiency is assumed to be unchanged during the entire lifetime of the electrolyser.

Note also that the typical hydrogen system consists of several major components: electrolyser, hydrogen compressor and hydrogen-storage tank. These components have different degradation models, but in our work, we only use one common degradation model for the entire system, which is not completely realistic.

Currently, the commercial electrolyser stacks have been in operation for more than 80,000 hours [51]. The authors also reported certain degradation of efficiency (loss of production). For example, a degradation rate of 0.125%/1000 h corresponds to a 10% increase in energy consumption over a 10-year lifetime for a system operating for 8000 hours per year. Commercial PEM electrolysers can operate in a wide current density range from 1 to 4 A/cm^2. Today, the typical degradation rate is about 0.15% every 1000 hours [177], [178]. Degradation increases with current density (potential) and temperature [179].

In one of the reported tests [180], a drop of voltage < 5 µV/h was measured for a stack operated continuously for 6865 h at 3 A/cm^2 and producing hydrogen at a pressure of 15 bar, corresponding to an efficiency loss of $< 2\%$ per year (8760 h). The FCH-JU-projected degradation target for PEM electrolysers by 2030 is expected to be less than 2.3 µV/h [179], which corresponds to an efficiency loss of 1% per year (8760 h).

At the current stage of development of PEM electrolysers, the focus is usually on durability and reliability rather than cost. Therefore, evidence of a lifetime without measurable degradation has already been provided, e.g., in the form of an increase in cell voltage over the operating time [181].

3.6 Economic Model

The main purpose of the economic model is to evaluate the financial results of the entire system operation by estimating both the generated incomes and the operating costs. Obviously, the economic model is a very important part of the overall model as it supports the techno-economic analysis of the operation under various system sizes, variants and operation scenarios.

The economic model developed in our study is strongly linked to the system process model (presented in Sections 3.2 and 3.4) and the model of the remaining useful life (represented in Section 3.5).

Let us first analyse the financial incomes generated by the system's operation. These can be divided into the following categories:

- *Income from the electrical energy, delivered to the electricity grid and the market;*
- *Income from the hydrogen, delivered to the consumers.*

Income (financial flow) from the electrical energy, delivered to the electricity grid and the market is proportional to the electrical power and the difference between the selling price of electrical energy and production cost of electrical energy:

$$CF_{EL}(t)\left[\frac{€}{h}\right] = P_{GRID}(t)[MW] \cdot \left(PR_{EL}(t)\left[\frac{€}{MWh}\right] - PC_{EL}(t)\left[\frac{€}{MWh}\right]\right) \tag{3.47}$$

In the equation, CF_{EL} represents corresponding financial flow or cash-flow, P_{GRID} represents electrical power delivered to the grid according to the prescribed timetable, and PR_{EL} denotes (dynamic) price of electrical energy, which in general varies with time.

Similarly, the income (financial flow) from the hydrogen delivered to the consumers can be calculated as:

$$CF_{H2}(t)\left[\frac{€}{h}\right] = Q_{H2}(t)\left[\frac{kg}{h}\right] \cdot PR_{H2}(t)\left[\frac{€}{kg}\right] \tag{3.48}$$

Here, (CF_{H2}) represents cash flow, (Q_{H2}) represents hydrogen flow delivered to the consumers, and (PR_{H2}) represents dynamic price of hydrogen, which can vary with time and market conditions. With a time integration of the financial flows over the desired time interval, the overall income [€] is calculated:

$$Income_{EL} = \int_{t_1}^{t_2} CF_{EL}(t) \cdot dt \tag{3.49}$$

$$Income_{H2} = \int_{t_1}^{t_2} CF_{H2}(t) \cdot dt \tag{3.50}$$

Besides income, the system also generates costs, which can be grouped into the following two categories:

- *Investment costs (CapEx) of the hydrogen system;*

- *Operation costs (OpEx) of the hydrogen system.*

There are several ways to incorporate CapEx and OpEx costs into the economic model. The simplest way (but not the most realistic) is to assume that both CapEx and OpEx are evenly distributed over the lifetime of the system. This method does not consider the fact that the system wears out more during use than when it is idle, and that the wear and degradation costs are therefore higher during operation than during idle or switch off periods. Assuming an even distribution of costs over time, the financial flow from CapEx and OpEx can then be simply calculated as:

$$CF_{COST}\left[\frac{€}{h}\right] = \frac{CapEx[€] + OpEx[€]}{t_L[h]}, \tag{3.51}$$

where (CF_{COST}) represents the financial flow or cash-flow due to costs, CapEx represents the total investment costs of hydrogen system, OpEx represents total operation costs during system's lifetime (t_L). In this case the CF_{COST} is a constant value over the entire lifetime of the system.

The more realistic way is to consider the proposed RUL model presented in Section 3.5, which assumes that wear and degradation of the system increase with its actual usage, i.e., hydrogen-production power. However, to some extent, the system also degrades when it is not operating. This is due to various kinds of chemical degradation and overall ageing.

$$CF_{COST}\left[\frac{€}{h}\right] = \left(\frac{CapEx + OpEx}{t_L}\right) \cdot \left(-\frac{dRUL}{dt}\right). \tag{3.52}$$

If in Figure 3.16 the bottom branch with gain g_i is neglected, then integration operation in branches g_a and g_e are neutralised by the derivation operation of RUL and cost cash flow can be expressed by the following simplified equation:

$$CF_{COST}\left[\frac{€}{h}\right] = \left(\frac{CapEx + OpEx}{t_L}\right) \cdot \left(\frac{P_{GC}}{P_{MAX}} + \frac{t_L}{t_A}\right). \tag{3.53}$$

An economic model is depicted in Figure 3.17.

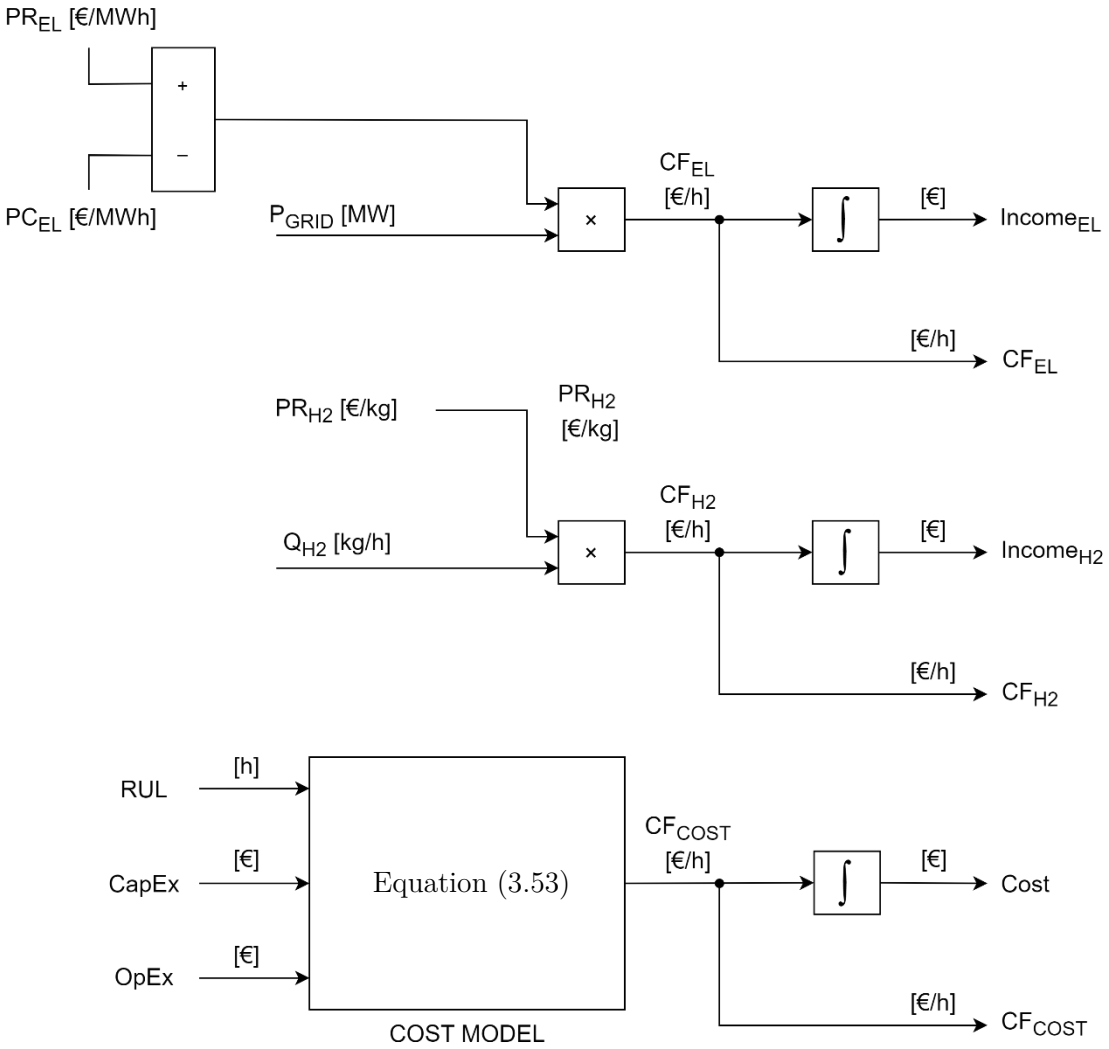

Figure 3.17: Structure of the economic model.

The variables of the economic model are listed in Table 3.10.

Table 3.10: Economic model's variables.

Input variables	Description	Units
P_{GRID}	Electrical power generated by HPP and PV and delivered to the grid according to the system operator's requirements (timetable)	MW
PR_{EL}	Selling price of electrical energy (e.g., 50 €/MWh)	€/MWh
PC_{EL}	Production cost of electricity (e.g., 35 €/MWh)	€/MWh
Q_{H2}	Mass flow of generated hydrogen	kg/h
PR_{H2}	Selling price of hydrogen (e.g., 8 €/kg)	€/kg
Output variables	Description	Units
CF_{EL}	Positive cash flow generated by selling electrical energy	€/h
$Income_{EL}$	Income generated by selling electrical energy	€
CF_{H2}	Positive cash flow generated by selling hydrogen	€/h
$Income_{H2}$	Income generated by selling hydrogen	€
CF_{COST}	Negative cash flow incurred by hydrogen sys. CapEx and OpEx	€/h
$Cost$	Cost incurred by hydrogen system CapEx and OpEx	€
Parameters	Description	Units
$CapEx$	Hydrogen system's capital expenditure	€
$OpEx$	Hydrogen system's operation expenditure	€
t_L	Hydrogen system's lifetime during continuous operation at nominal power	h

3.7 Control System

A basic control system was developed to determine the available electrical power P_{GC} for hydrogen generation and compression. The goal of the control system is twofold:

1. *To fulfil the demands for electrical energy generation, which is defined by the system operator's timetable (electrical power vs. time);*

2. *To fulfil the demands for hydrogen generation.*

To be able to fulfil the first goal, the electrical energy generation timetable must consider hydrogen generation. This means that the predicted available hydropower (proportional to the predicted water flow into accumulation) cannot be completely assigned for electrical power generation, but a certain part (e.g., a few %) must be assigned for hydrogen generation. Then, the control system determines the electrical power P_{GC} for hydrogen generation and compression based on the water-accumulation state of charge SoC_W (SoC_W in our case means the available amount of water in the accumulation given in m^3) and the p_{H2}, which is the hydrogen pressure in the hydrogen-storage tank, as illustrated in Figure 3.18.

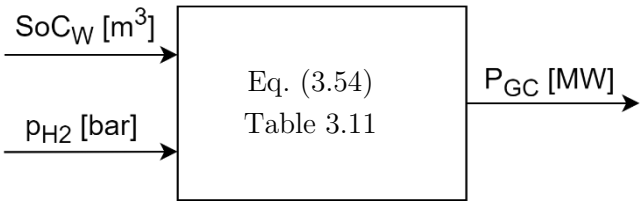

Figure 3.18: Control system.

In general, the electrical power P_{GC} is determined by Eq. (3.54):

$$P_{GC} = f_L \cdot P_{MAX} \tag{3.54}$$

Here, f_L is the load factor of the electrolyser and P_{MAX} is the maximum power of the hydrogen system. The load factor depends on the current SoC_W and p_{H2} according to the following logic:

- f_L *increases with* SoC_W *(if there is a significant amount of hydro energy stored in the accumulation, hydrogen production is increased),*
- f_L *decreases with pressure* p_{H2} *in the hydrogen-storage tank (if the amount of hydrogen in the storage tank is high, hydrogen-production rate is decreased).*

The described control law is formalised by the look-up table (Table 3.11).

Table 3.11: Control system look-up table (f_L as a function of SoC_W and p_{H2}).

	$SoC_W \leq 0.1$	$0.1 < SoC_W \leq 0.25$	$0.25 < SoC_W \leq 0.65$	$0.65 < SoC_W < 0.85$	$SoC_W \geq 0.85$
$p_{H2} \leq 0.5\ p_{H2\_MAX}$	0	0.2	0.5	0.8	1
$0.5\ p_{H2\_MAX} < p_{H2} < 0.95\ p_{H2\_MAX}$	0	0.2	0.5	0.8	1
$p_{H2} \geq 0.95\ p_{H2\_MAX}$	0	0	0	0	0

The thresholds in the look-up table are determined in a way that f_L stays most of the time in the range where the electrolyser operates most efficiently. The hydrogen system shuts down ($f_L = 0$) in cases of a very low water accumulation ($SoC_W \leq 0.1$) or when the hydrogen-storage tank is near full ($p_{H2} \geq 0.95\ p_{H2\_MAX}$).

A list of control system input, output and internal variables is given in Table 3.12.

Table 3.12: Control system's variables.

Input variables	Description	Units
SoC_W	State of charge of water accumulation	0…1
p_{H2}	Pressure in the hydrogen storage tank	bar
Output variables	Description	Units
P_{GC}	Electrical power of hydrogen generation and compression	MW
Internal variables	Description	Units
P_{MAX}	Maximum power of the electrolyser	MW
f_L	Current load factor of electrolyser	0…1
p_{H2_MAX}	Maximum allowed pressure in hydrogen tank	bar

Due to measurement noise in the signals SoC_W and p_{H2}, the load factor f_L can change frequently between two neighbouring values from Table 3.11. This causes frequent and significant changes of the electrolyser's power, which leads to increased degradation. This can be prevented by applying low pass filters or hysteresis elements to the signals SoC_W and p_{H2}.

3.8 Implementation of the Developed Model

Figure 3.19 shows the implementation of the complete model, which is implemented in MATLAB/Simulink environment.

The main inputs to the model are:

- *Electrical power demand according to the timetable (*P_{TT_DEM}*),*
- *Hydrogen demand (*$Q_{H2\_OUT\_DEM}$*),*
- *Water inflow to the water accumulation (*Q_{IN}*),*
- *Solar radiation (*J_S*).*

The developed model enables:

- *Simulation of the case-study HPP and hydrogen system in various set-ups,*
- *The collection of operating parameters (energy flows, mass flows, water accumulation level, pressure in hydrogen storage, hydrogen system efficiency, etc.),*
- *An economic evaluation of the electrical energy and hydrogen production, while considering investment and operating costs for the necessary equipment.*

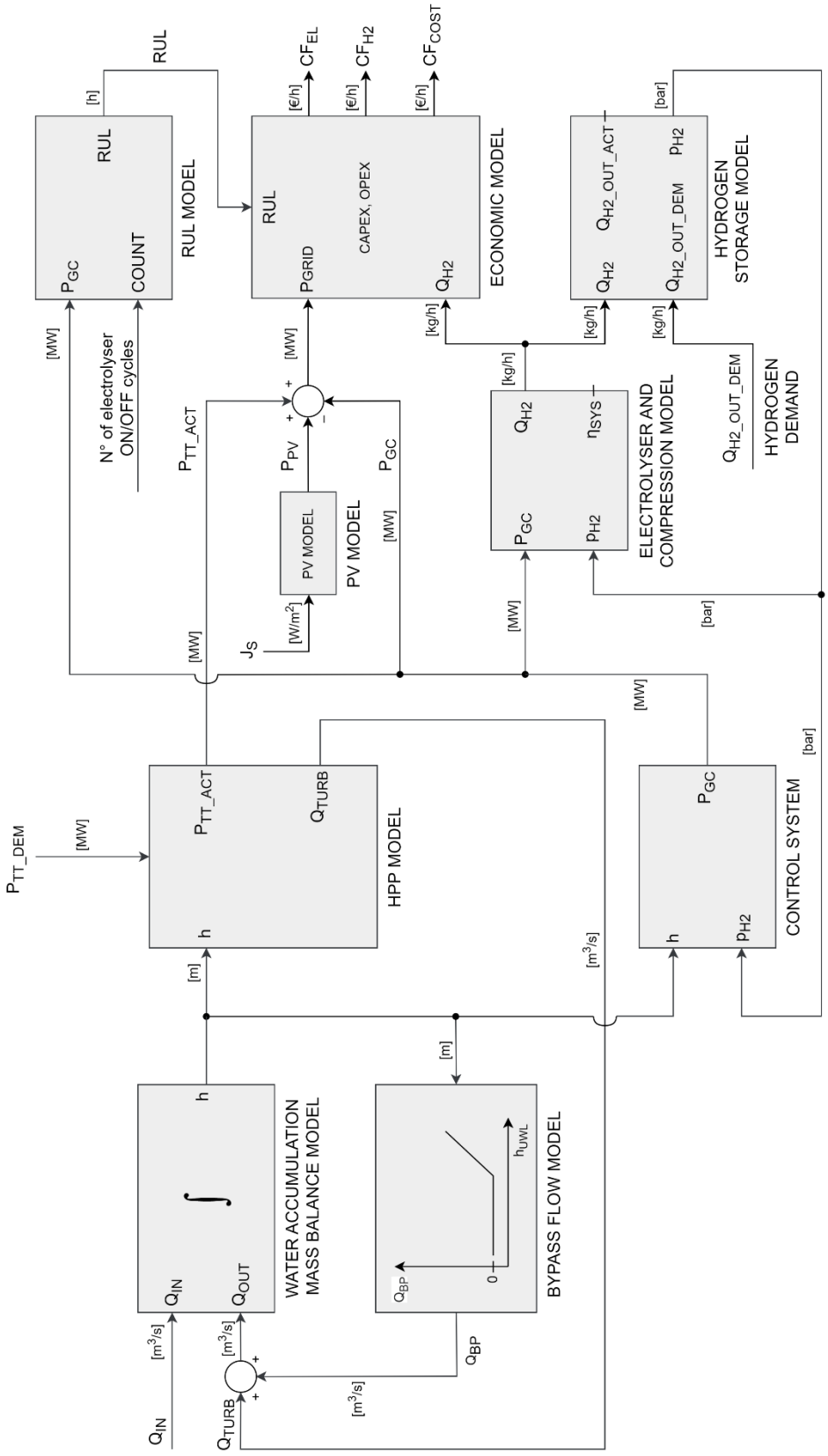

Figure 3.19: Implementation of complete model.

Chapter 4

Use of the Developed Process Model in Case-Study HPP

This chapter describes the use of the developed process model and parameter identification for the selected case-study hydropower plant, upgraded with an actual photovoltaic field and simulated hydrogen system.

In general, large systems can capture large amounts of energy, but most of the time they can be underutilised, resulting in high costs for hydrogen production and storage. It is therefore necessary to find a compromise, which cannot be calculated analytically due to the large number of design parameters and the complex dynamics of the elements of a hydrogen system. For proper sizing of the equipment, the following conditions must be taken into account:

- *costs of the components of a hydrogen system, in particular electrolyser and hydrogen storage,*
- *available excess electricity, which is obtained either from the excess hydro energy and/or from the PV field,*
- *selling price of hydrogen on the market,*
- *predicted amount and dynamics of hydrogen consumption.*

The effects of proper sizing of a hydrogen system are reflected in:

- *hydrogen-production costs,*
- *income from hydrogen production,*
- *utilisation rate of the hydrogen system,*
- *payback period of the hydrogen system.*

For adequate sizing of a hydrogen system, we developed a decision-support tool that considers the stated findings and gives a calculation of the relevant quantities according to the selected parameters of the hydrogen system. With this tool it is possible to optimise the selection of the hydrogen system's components by considering the existing constraints. Through the simulation runs, we can to test the operating efficiency when varying different parameters (nominal power of the hydrogen system, volume and maximum pressure of the hydrogen storage tank, different constraints of electricity grids). The results of the

simulation study serve as a decision support for the possible investment in the hydrogen system.

In developing the process model and decision support, we have considered (i) the technical characteristics and limitations of the individual components of the hydrogen system and (ii) the financial aspects of hydrogen CHP, as described in the following subsections.

4.1 Case-Study HPP

In general, hydropower plants can be constructed in a variety of sizes and with different characteristics. The following three categories can be considered as the main types of hydropower plants:

Reservoir hydropower plants: Reservoir (storage) hydropower plants have the ability to store a large amount of water behind the dam. In this way, it is possible to de-couple the generation of electricity from water inflows. So, they effectively act as an electricity storage system. As with other hydropower systems, the amount of generated electricity is determined by the volume of water flow and the amount of available water net head.

Pumped storage hydropower plants: Pumped storage hydropower schemes use off-peak electricity to pump water from a reservoir located after the tailrace to the top of the reservoir. In this way, the pumped storage hydropower plant can generate electricity at peak times.

Run-of-river hydropower plants: Run-of-river hydropower plants have no or limited storage capacity behind the dam and power generation strongly depends on the river flow rate. Run-of-river hydropower plants with storage are said to have "pondage". This allows short-term water storage (hourly or daily). Plants with a reservoir can regulate water flows to some extent and shift generation a few hours or more over the day to the period when it is most needed. This type of hydropower plant often occurs in a cascade, where the first power plant usually has a larger water accumulation, which is then used by the downstream hydropower plants.

The case-study HPP is a conventional run-of-river type HPP with a low-capacity water reservoir (see Figure 4.1). The theoretical annual production of this particular HPP is around 415 GWh, while the actual average production power is around 168 GWh, when operating with average power of 20.03 MW, due to the limitations in seasonal river water flow (see Table 4.1). This particular HPP accounts for approximately one percent of Slovenia's current annual electricity production.

Figure 4.1: Case-study HPP [182].

The main technical characteristics of the case-study HPP are given in Table 4.1.

Table 4.1: Basic technical characteristics of the case-study HPP [182], [183], [184].

HPP data	Values
Number of generating units	3
Turbine type	Double-regulated vertical Kaplan turbine
Installed plant capacity (P_{HPP})	47.4 MW (3 · 15.8 MW)
Rated plant discharge	500 m^3/s
HPP low-water point (h_{LWL})	139 m.a.s.l.
Rated head (h)	14 m
Average annual output	168 GWh
Maximum upper water level (h_{UVL_MAX})	153 m.a.s.l.
Maximum operating variation of water level (d_{MAX})	1.1 m
Mean annual discharge	207 m^3/s
Reservoir capacity	19,300,000 m^3
Reservoir live storage (V_{ACCUM_MAX})	3,400,000 m^3
Number of spillways	5

For the modelling of the case-study reservoir, we used the developed model described in Section 3.2. We used the following reservoir and downstream parameters, see Table 4.2.

Table 4.2: Reservoir and upstream characteristics.

Reservoir data	Values
Water surface of the reservoir (A_{ACCUM_MAX})	317 ha
Total length of embankments	13.67 km
Length of the river between the case-study HPP and the previous HPP in the chain upstream	12.95 km
Maximum width of the reservoir	680 m
The length of deepening of the downstream riverbed	3000 m
Total length of drainage channels	21.7 km
Total capacity of the spillway	5000 m^3/s
Nominal water power	53.96 MW
Average water power	22.34 MW
Actual average electrical power	20.03 MW
Capacity of usable water accumulation	101.92 MWh

The case-study HPP is also upgraded with a PV field with a nominal power of 6 MW (see Figure 4.2), which is connected to the HPP via a cable line and it is treated as an additional (fourth) generator unit of the HPP. The PV field consists of 11,232 modules, the estimated annual production of electrical energy by the PV field is about 6.8 GWh. Part of this additional energy can be used for hydrogen production.

Figure 4.2: Case-study PV field [185].

4.2 Model Adjustment to Case-Study HPP

4.2.1 Data Preparation and Analysis

To test the developed model and for further experimentation, real data from the case-study HPP were acquired and transformed into a form suitable for use in the simulation environment. Key steps include collecting, cleaning and labelling the raw data in a form acceptable for further use.

First, historical data from the HPP monitoring system were obtained. This data contains a lot of information about the internal processes, inputs and outputs of the considered HPP. From the more than 100 different variables recorded, we extracted only the data representative of the modelled process (such as water flows, electrical energy generation, set point (i.e., HPP timetable), water head and reservoir water level).

Due to some inconsistencies and even missing real-time data, it was necessary to process them by the procedure with the following steps:

- *Generation of missing data (interpolation),*
- *Data smoothing by filtering to remove noise,*
- *Identification and removing of outliers and inconsistencies,*
- *Resampling and synchronising the data obtained from different sources (e.g., from the upstream HPP in the chain),*
- *Collecting all data in a single spreadsheet.*

The data about water inflow to the accumulation reservoir of the case-study HPP were not available. Instead, it was estimated from the outflow from the upstream HPP in the chain by the combination of time-delay and smoothing operations. The effects of water evaporation and precipitation in the area between upstream HPP and case-study HPP were taken into account.

Furthermore, uniformly sampled (equidistant) and time-adjusted data (time series) were prepared to run a simulation with any start date and duration.

To evaluate the amount of additional electrical energy obtained from the PV field, which is coupled to the case-study HPP, historical solar irradiation data at the location of the PV field were obtained (see the PV model in Section 3.4).

The entire data preparation was implemented in the MATLAB/Simulink programming environment. The sampling time of the input data and the calculation of the output data were unified and cover a continuous time frame of 30 minutes. The simulation is performed with a variable integration step and the integration method is automatically selected by the numerical method built in the MATLAB/Simulink.

To estimate the annual distribution of HPP water flows we compare four important flows from the data spreadsheet: estimated inflow to the reservoir (Q_{IN}), estimated bypass flow of excess water from reservoir through spillways (Q_{BP}), estimated flow through three turbines necessary to generate electrical energy according to prescribed timetable (Q_{TURB}) and estimated outflow (Q_{OUT}), which is the sum of the bypass and the turbine flow. For annual flow regimes, see Figure 4.3 to Figure 4.6, which represent the situation for the observed year.

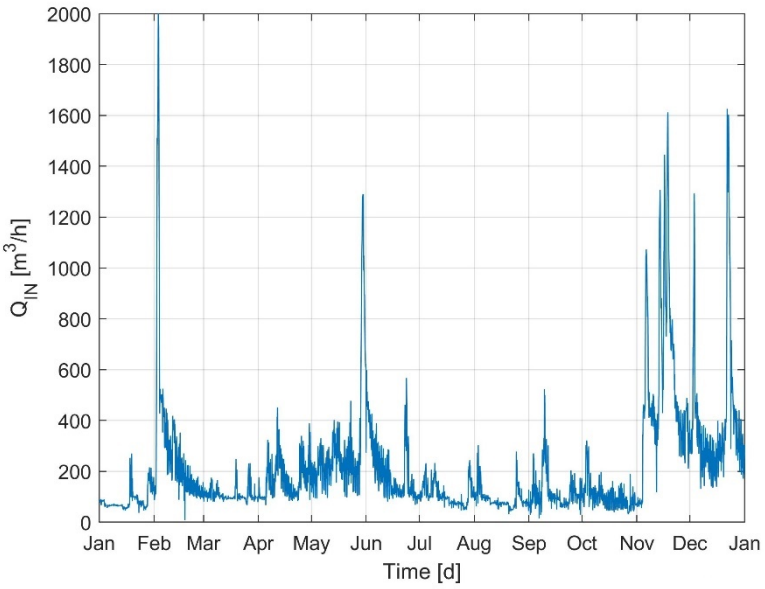

Figure 4.3: Annual inflow (Q_{IN}).

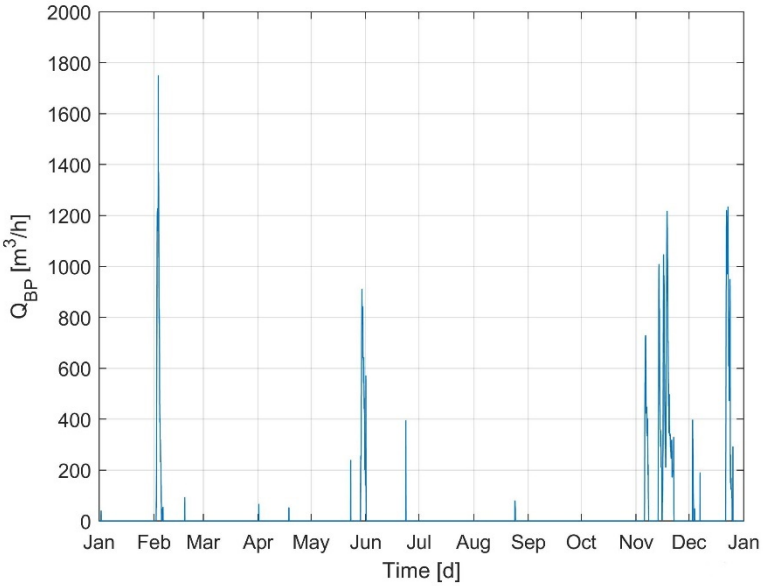

Figure 4.4: Annual bypass flow (Q_{BP}).

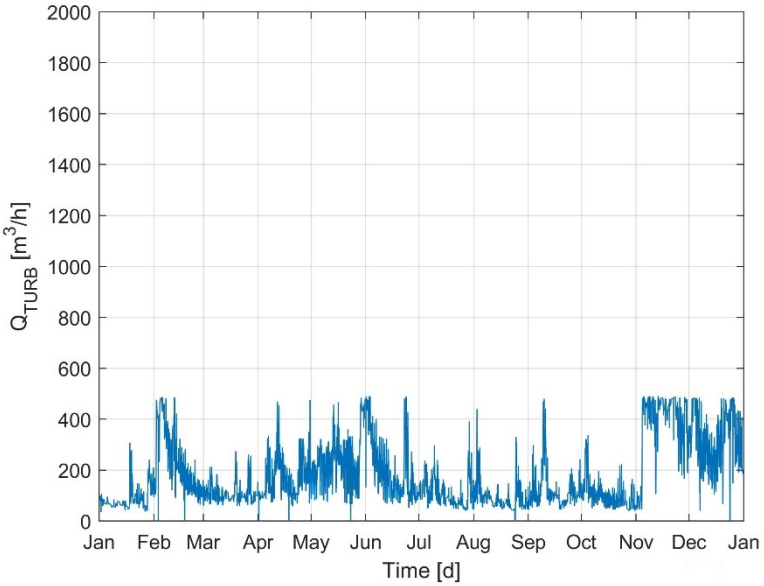

Figure 4.5: Annual flow through turbines (Q_{TURB}).

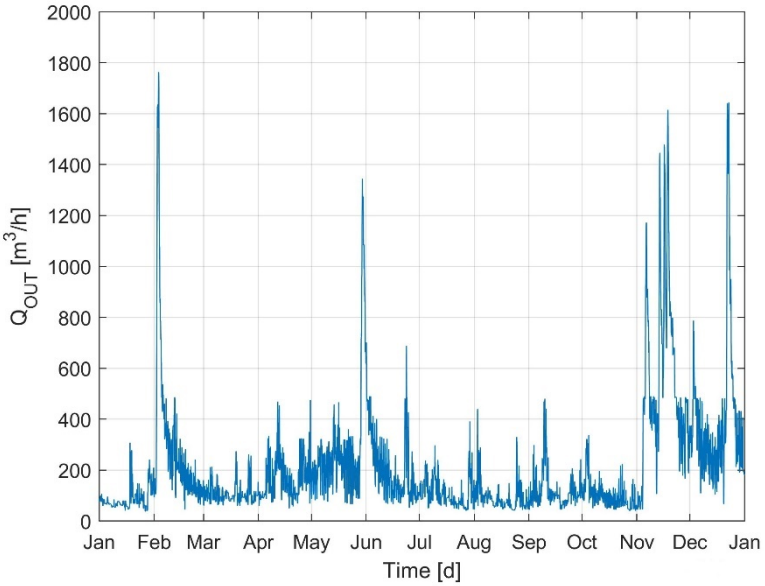

Figure 4.6: Annual outflow (Q_{OUT}).

The annual dynamics of the HPP's electrical energy production is shown in Figure 4.7. According to the timetable, the case-study HPP operates with an annual average power of 20.03 MW.

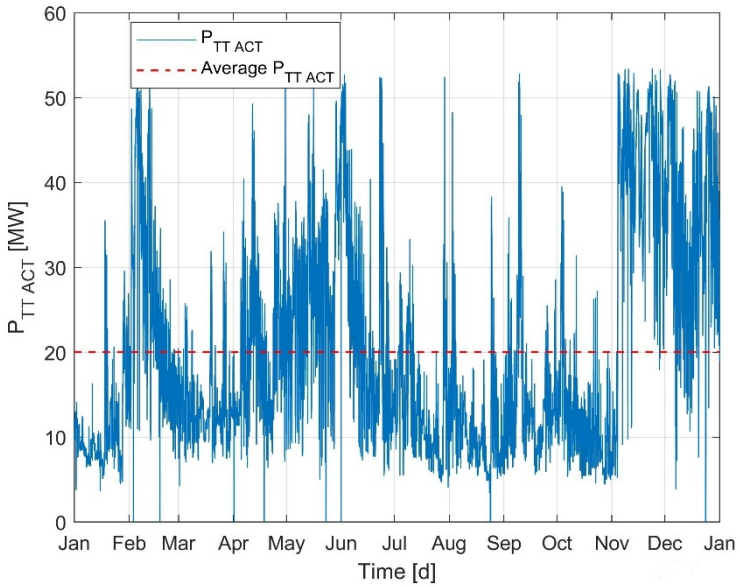

Figure 4.7: Annual HPP timetable (P_{TT_ACT}).

Another important information for further investigations is the change in water level of the reservoir (water denivelation). The annual denivelation (d) regime is shown in Figure 4.8. During normal HPP operation, the maximum-allowed denivelation is 1.1 m. Therefore, the actual level varies between 153 and 151.9 m.a.s.l. In the first half of October, the denivelation increases (upper water level decreases) due to maintenance procedures.

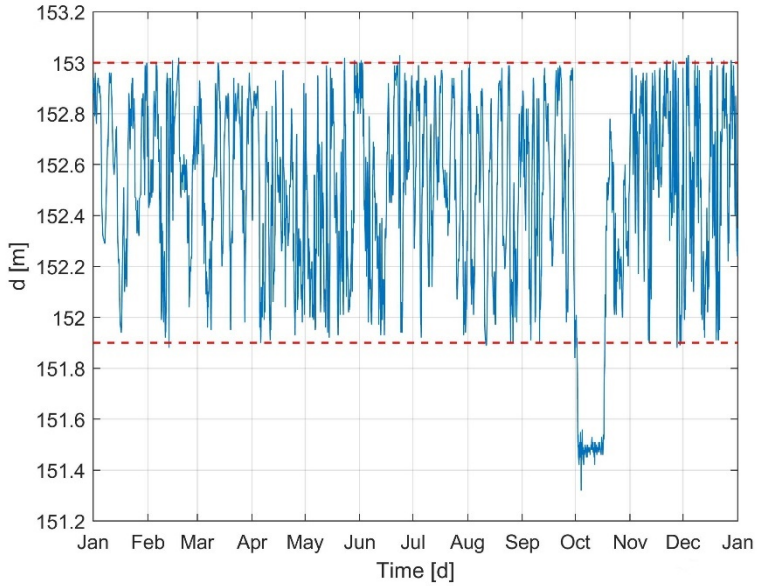

Figure 4.8: HPP annual water reservoir denivelation (d).

To verify the water mass balance Eq. (3.1) was used (see Section 3.2.1). The results are shown in Figure 4.9:

- *Upper graph: RES (absolute value),*
- *Bottom graph: RES/Inflow (value relative to current value of inflow).*

Notice that some rarely observed peaks occur during bypass activation. The reason lies in the fact that the water-bypass data were available only on an 8-hour period, while the dataset used for the simulation is unified and covers a continuous time frame of 30 minutes. Therefore, due to the missing water-bypass data inside an 8-hour period we were unable to represent the real situation within a 30-minute period.

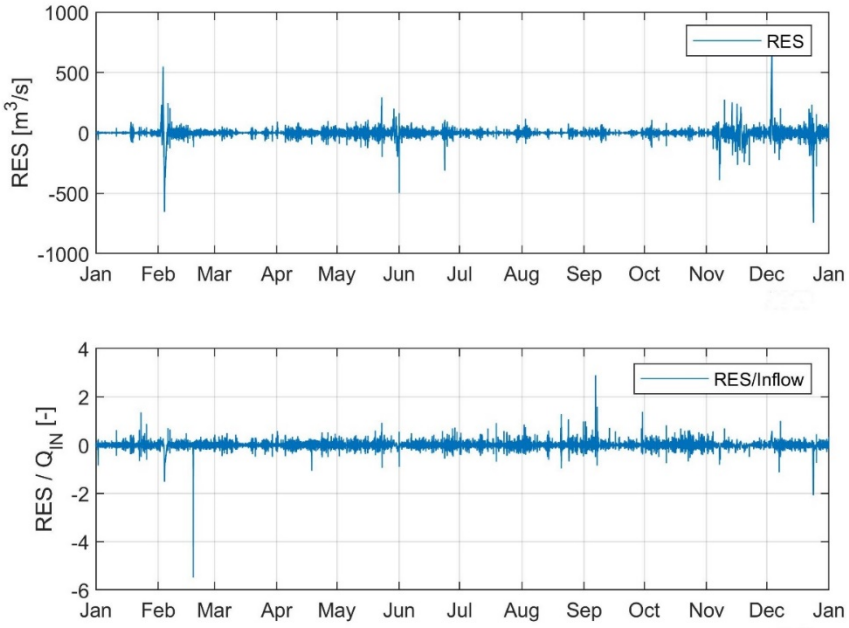

Figure 4.9: Residual time profile (RES).

In addition, the root-mean-square (RMS) value of the RES was calculated, and it is 15%, which is considered as acceptable. It should be taken into account that measurements of water flow and water level are either measured by sensors with limited accuracy or estimated.

4.2.2 Upper-Water-Level Limitations

In run-of-river HPPs, the predominant type of a dam design is a combination of a fixed spillway and slide gates, which are used to limit the maximum level in the reservoir. The slide gates limit the maximum level in the accumulation reservoir. In the particular case, the upper limit is set to 153 m for the input flow rates up to 800 m^3/s. For the flow rates above 800 m^3/s, the upper limit is reduced according to the operating curve presented in Figure 4.10 (red line). If the input flow (Q_{IN}) exceeds the flow through the turbines (Q_{TURB}), then the level in the reservoir increases. When the level reaches the upper limit, defined by the slide gates, then the water bypasses the turbine generator over the slide gates denoted by flowrate (Q_{BP}). In Figure 4.10, the red curve is the upper water-level limit, while blue dots represent the actual denivelation data over the period of 1 year by data sampling a time of 30 min.

In cases where blue dots are above the red denivelation curve, the water level exceeds the upper-level limitation and consequently the water flows over the slide gates (Q_{BP}).

The determination of the operating curve depends on the operating mode of the HPP and on the requirements or conditions at points along the reservoir that need to be protected against flooding (so-called critical points).

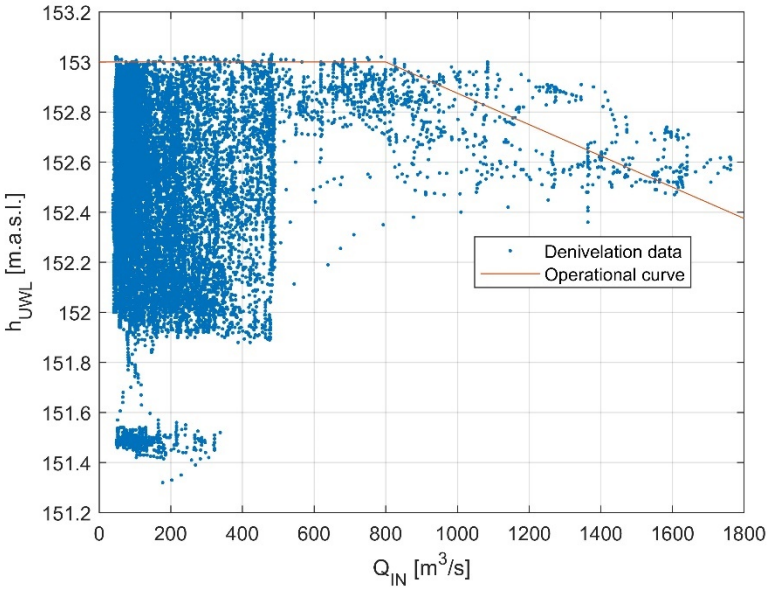

Figure 4.10: Annual denivelation data and estimated operating curve for the case-study HPP's inflow water data.

4.2.3 Lower-Water-Level Estimation

The lower water level (h_{LWL}) was also obtained from the real data of the case-study HPP. A simple mathematical function was constructed that best fits a set of h_{LWL} data points and approximated it with the following square-root function:

$$y = k \cdot \sqrt{x} + n \tag{4.1}$$

where the coefficients of the square root function are: $k = 0.1753$, $n = 137.2170$ and x are the h_{LWL} data points.

In the range of regular operation of the HPP between 0 and 500 m^3/s water flow, there is a considerable deviation from the estimated curve at some operating points, with deviations up to ± 1 m.a.s.l., see Figure 4.11.

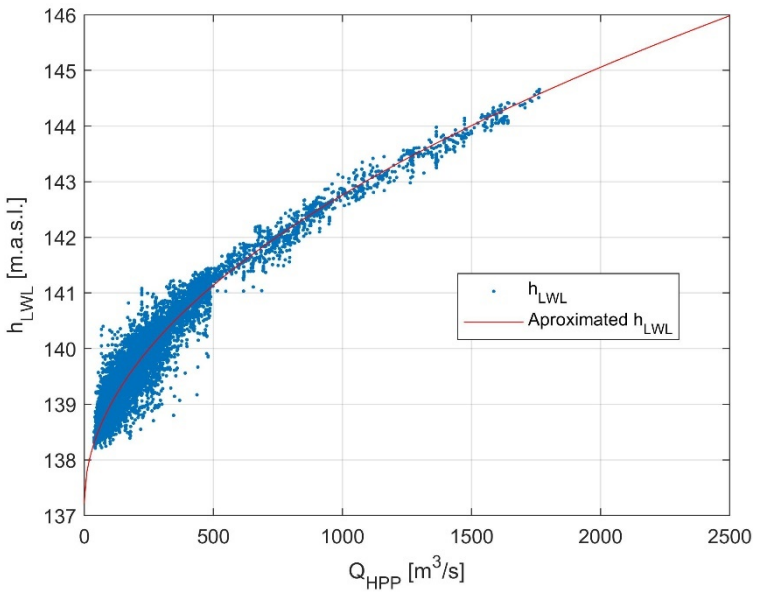

Figure 4.11: The h_{LWL} as a function of flow.

In case we calculate the actual water head from the difference between upper and lower water levels, this can lead to a deviation between the actual water head and the calculated water head. As a result, we observed a deviation of the flow at the desired output of the HPP. Therefore, we need to evaluate and account for this error. In our case, we have limited the accumulation integral at the lower bound to 0 and estimated the deviation on an annual basis.

From Figure 4.10 and Figure 4.11 it can be concluded that the actual water head of the case-study HPP is about 14 metres under normal operating conditions (i.e. at an average HPP output of 20.03 MW). This water head will decrease in the future as the construction of the next HPP in the chain is planned.

4.2.4 The Operation of HPP Generators

The case-study HPP can operate with three turbine-generators at the same time. Each generator has the same nominal electrical power and can be controlled individually in order to adjust the production of the HPP to the demands. During normal operation of the HPP, the load distribution of the HPP generators follows the regime described in Figure 4.12.

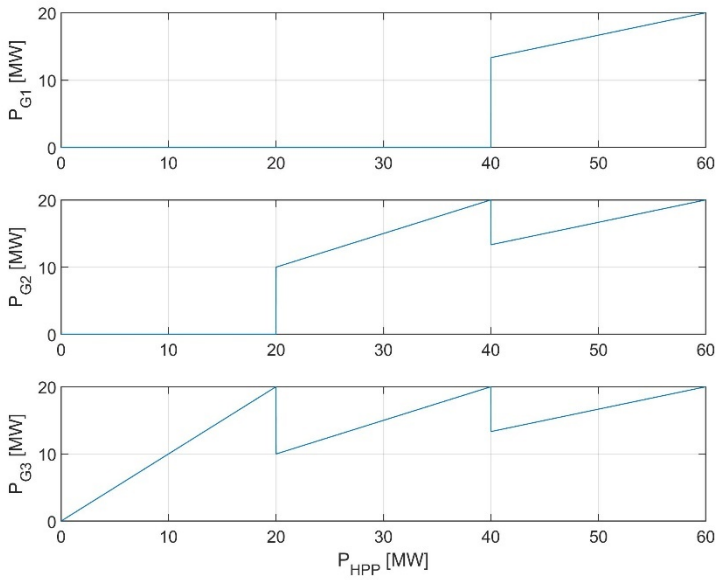

Figure 4.12: Generators G1, G2, G3 start-up sequence.

Figure 4.13 shows the actual operation of the three generators and confirms the load-distribution principle shown in Figure 4.14.

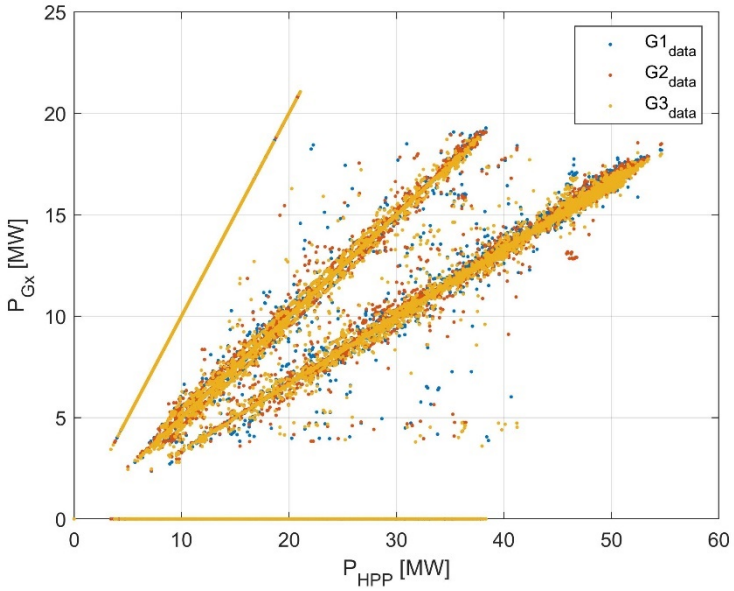

Figure 4.13: Electrical power production by generators G1, G2, G3.

The operating time range per generator (t_{OP_GX}) is shown in Figure 4.14. *X* represents the number of each generator from *G1* to *G3*.

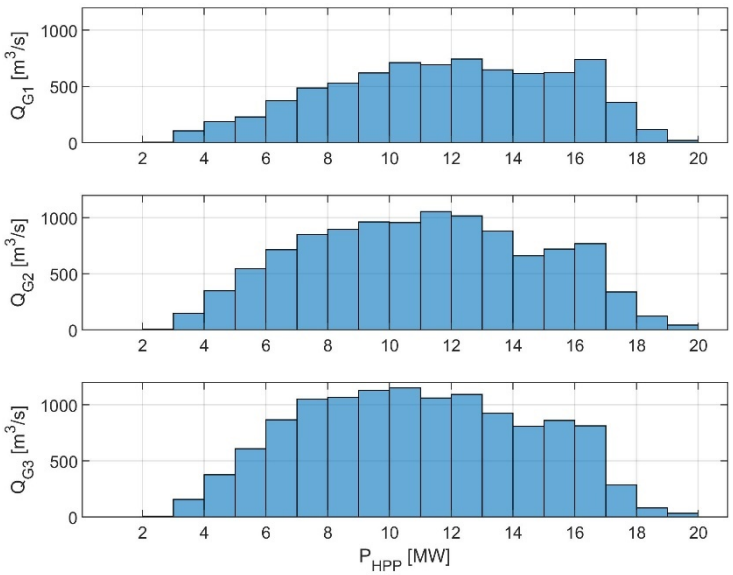

Figure 4.14: Operation histogram of generators *G1, G2, G3* in electrical power production.

It can be seen that the three generators operate most of the time between 8 and 14 MW. Generator *G3* is the first and most used, since the majority of time the HPP operates below 20 MW.

4.2.5 Simulated Hydrogen Consumption

As today there is no explicit need for hydrogen production in the case-study HPP, the hydrogen consumption for our simulation runs needed to be presupposed.

To position a hydrogen system in the case-study HPP environment for future useful operation, we considered some promising options:

- *City and/or intercity (long-distance) buses powered by hydrogen fuel cells.*
- *Use of hydrogen in a nearby nuclear power plant, where the hydrogen is used to internally cool the plant's electricity generators.*
- *Use of hydrogen for heating requirements in the nearby local community.*

For the case-study scenario, the first option was used (city buses), since city or intercity buses come very close to the ideal application for green hydrogen. This is because buses are only refuelled at one or a few dedicated refuelling stations, which greatly reduces the costs for the hydrogen-refuelling infrastructure. For economic reasons, city buses must run continuously, without long stops, so the possibility of quick refuelling is very important. Most importantly, vehicles running on green hydrogen have no emissions and produce much less noise than internal combustion engines running on hydrocarbons [186].

A typical hydrogen-fuel-cell-powered bus of 12 m length has a hydrogen consumption of around 9 kg per 100 km [187], [188] and has a hydrogen-storage capacity between 35 and 40 kg [189]. With an average driving distance of around 400 km per day, approximately 40 kg of hydrogen is needed for one bus every day. A hydrogen system capable of producing up to 320 kg of green hydrogen per day would allow the refuelling of eight buses each day. Figure 4.15 shows the time profile of hydrogen consumption. It is assumed that all the

buses are refuelled in the period 6–10 am. This means that the total daily hydrogen consumption only occurs in this period, which is a greater challenge from the point of view of dimensioning the hydrogen system and operating its control system than in the case of a more even daily hydrogen consumption.

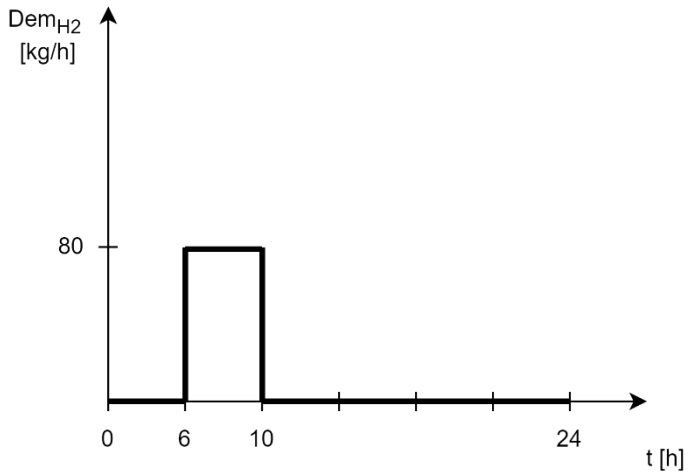

Figure 4.15: Daily hydrogen demand profile.

Chapter 5

Model Exploitation for Process Optimisation

This chapter shows how the developed process model can be used and what benefits it brings. The general idea is to use the model as a support tool for the design of hydrogen systems, in particular for a hydrogen system in connection with a hydropower plant. The goal is to find the optimal parameters of the hydrogen system that lead to the most economical system. This is achieved by optimising the size of the system's components to the minimum possible for the required operating parameters. This chapter is structured into three sections:

- *Section 5.1 shows how the model can be used to simulate and predict the results of the process operation for a given combination of process parameters. In this way, it is possible to estimate various cost functions or performance indicators, such as the amount of hydrogen produced, the income from the hydrogen produced and the electrical energy and many more. This allows a detailed evaluation of the technical and economic effects of the hydrogen system in the phase before the actual implementation.*

- *Section 5.2 focuses on process optimisation. The simulation of the developed model enables an assessment of the optimal size of the hydrogen system's elements and gives an economic effect for the cogeneration of electricity and hydrogen for the case-study HPP. In this case, the process is parametrised with a limited number of parameters (mostly sizes of the system components, the selling prices of hydrogen and the electrical energy or similar). The typical question is which combination of process parameters gives the best results. In this subsection, the problem is solved by simulating the process with all possible combinations of process parameters and finding the optimal combination(s). This approach leads to a high computational demand and long simulation times.*

- *Section 5.3 introduces a particle swarm optimisation method to find the optimal process parameters. This is motivated by the need to shorten the simulation time, optimise a larger number of parameters and obtain more accurate results. Instead of simulating all the combinations of process parameters, the particle swarm algorithm applies a more advanced search procedure that finds the directions in the parameter space that are more likely to lead to optimal solutions. In addition, the optimised parameters are not changed in predefined discrete steps, but via adaptive steps, which leads to higher accuracy.*

5.1 Model-Based System Simulator

This subsection presents how the developed process model from Chapter 3 can be used to perform simulation experiments. One of the purposes is to perform a series of initial simulation experiments for model verification. The experiments are characterised by:

- *Parameters of the hydrogen system and the hydropower plant;*
- *Inputs, such as time profiles of available hydro and solar power, demand and prices for electrical energy and hydrogen;*
- *Simulation start and end times and dates, simulation interval (time step).*

During the initial verification of the developed model, the simulations of the annual electricity generation with the developed HPP model (see Figure 5.1) resulted in 175.5 GWh/year, which corresponds to the actual amount of energy generated, see Table 4.1.

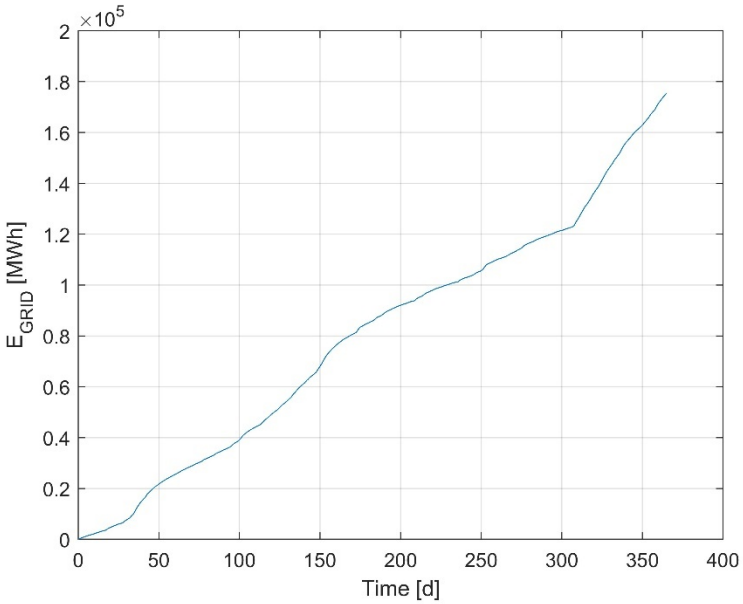

Figure 5.1: Annual electrical energy generated by HPP (without inclusion of the PV field).

If the 6 MW PV field is included in the electricity generation, 7645 MWh/year of additional electrical energy can be generated according to the developed PV model, see Figure 5.2 and Figure 5.3, for the annual and 10-day electrical power generation profiles. This means that the PV model result is also in accordance with the actual amount of expected energy production for the PV field, see Section 4.1.

As the 6-MW PV field produces 7645 MWh/year of electrical energy, the same configuration of the proposed 1 MW hydrogen system results in a theoretical production of up to 152,900 kg/year of hydrogen according to the developed process model for an electrolysis electrical consumption of 50 kWh/kg of generated hydrogen without considering compression.

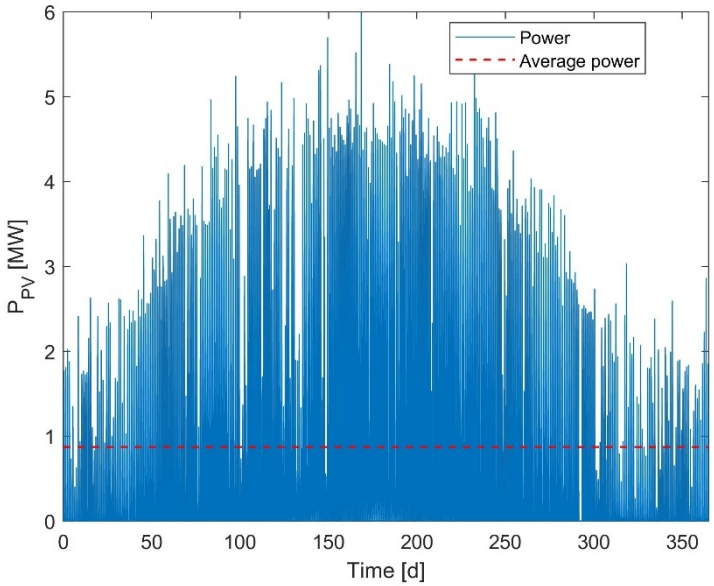

Figure 5.2: Annual electrical power generated by 6 MW PV field.

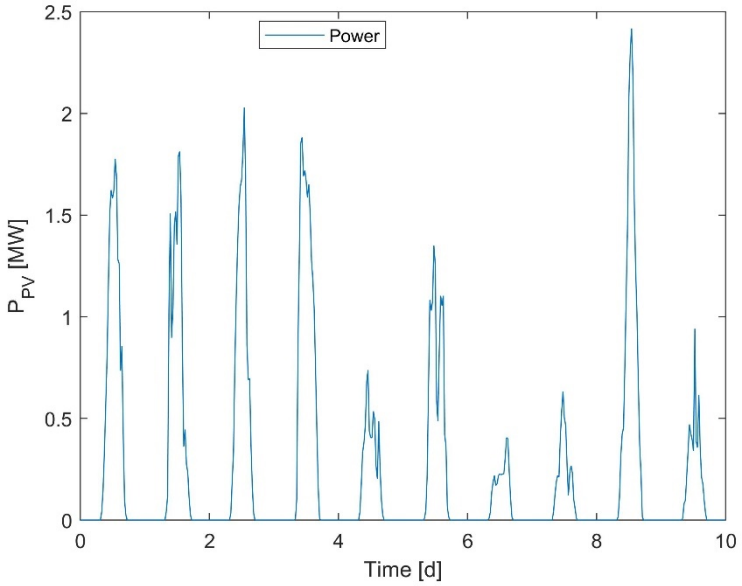

Figure 5.3: Example of 10-day time profile for generated electrical power from a 6-MW PV field.

Figure 5.4 shows that the total electrical energy generated by both the HPP and the 6-MW PV field can then be increased to 183.1 GWh/year.

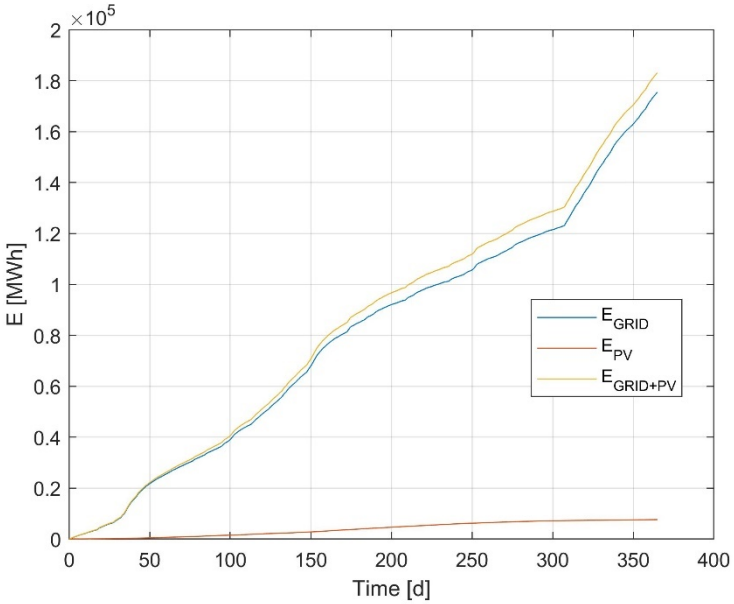

Figure 5.4: Comparison of the electrical energy generated by HPP and PV field.

Since the HPP's priority is to produce electricity according to the timetable, the production of hydrogen by exploiting some electrical energy from the PV field is only possible to a limited extent. To exploit the amount of excess energy in this case, the HPP can be upgraded with a properly sized hydrogen system.

The simulation environment uses a complete model, which includes the HPP, PV field and hydrogen system. To get an insight into the actual amount of hydrogen potentially produced from the available hydro energy during 1 year, we observe the operation of a 1-MW electrolyser and the amount of hydrogen produced in one year.

The demand for hydrogen consumption was assumed to be up to 320 kg/day.

For the hydrogen-storage tank, the following parameters were assumed: geometric volume of 30 m^3 and maximum pressure of 350 bar.

The electrolyser is controlled by the algorithm specified in Section 3.7.

For the purpose of the simulations, the CapEx for the electrolyser system ($CapEx_{EL\_SYS}$) is the same as described in Sections 1.2.5 and 1.2.6 with the annual OpEx estimated as 5%.

The CapEx value of the PV field ($CapEx_{PV}$) is estimated at 700,000 €/MW (i.e., the cost of the PV field per 1 MW of its nominal power), and the annual OpEx is estimated as 2% of PV CapEx.

The CapEx value of the storage tank ($CapEx_{H2\_STOR}$) is estimated at 20,000 €/m^3 (i.e., the cost of the tank per 1 m^3 of storage capacity), and the annual OpEx is estimated as 2% of the storage tank CapEx.

Taking into account the above CapEx, OpEx and system operating costs we considered several simulation scenarios and observed the impact on the overall hydrogen production. The scenarios are distinguished according to different sources of electrical power for hydrogen generation and compression:

1. HPP operation without hydrogen system (no hydrogen generation).

2. Electrical power generated by HPP using excess hydro energy.

3. Electrical power generated by HPP obtained by reducing the timetable for e.g., 5%.

4. Electrical power from 6-MW PV (all generated power).

5. Combination of cases 3 and 4.

These scenarios can be represented by the following table:

Table 5.1: Different sources of electrical energy for hydrogen production and compression.

	Energy source for hydrogen production		
	HPP Excess hydropower	HPP 5 % timetable reduction	PV All generated power
Scenario 1			
Scenario 2	✔		
Scenario 3	✔	✔	
Scenario 4	✔		✔
Scenario 5	✔	✔	✔

5.1.1 Scenario 1

The Scenario 1 simulation experiment assumes HPP operation without the hydrogen system. Figure 5.5: shows a) the annual water inflow (Q_{IN}), the turbine flow (Q_{TURB}) and the bypass flow (Q_{BP}), b) the upper water level (h_{UWL}), and c) the operating power of the HPP according to the prescribed timetable (P_{TT_ACT}).

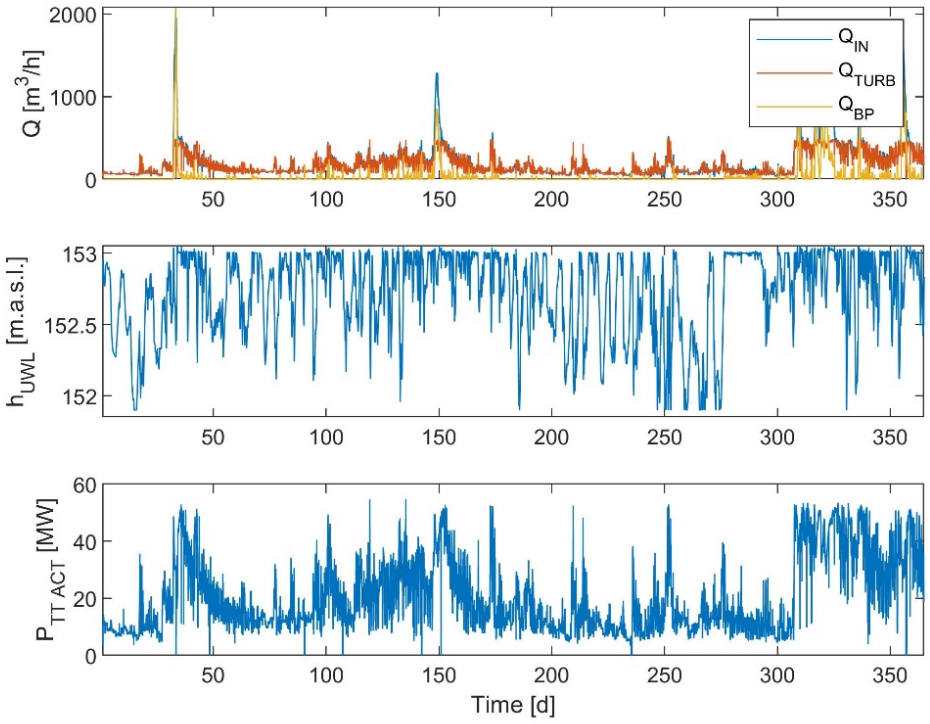

Figure 5.5: Annual HPP's operation.

Table 5.2 shows the summarised annual quantities of the HPP's water-regime conditions, the total amount of electrical energy produced and the resulting annual income.

Table 5.2: Cumulative annual HPP's operation data.

Parameter	Value	Unit
Total amount of water entering the accumulation (V_{IN})	6.5661e+09	m^3/y
Total amount of water passing through turbine (V_{TURB})	5.4279e+09	m^3/y
Total amount of water passing through bypass (V_{BP})	1.1488e+09	m^3/y
Total amount of generated electrical energy (E_{GRID})	1.7544e+05	MWh/y
The difference between selling price and production cost of electricity (SP_{EL} – PC_{EL})	15	€/MWh
Total amount of lost hydropower through bypass (E_{BP})	3.1843e+04	MWh/y
Total income from electrical energy delivered to the grid ($Income_{EL}$)	2.6316e+06	€/y

Figure 5.6 shows the operation of the hydrogen system: a) operating power of the electrolyser (P_{GC}), b) inflow (Q_{H2}) and outflow ($Q_{H2\_OUT\_ACT}$) from the hydrogen-storage tank, c) mass of the stored hydrogen (m_{H2}), d) pressure in the storage tank (p_{H2}). At the beginning of the simulation run, the annual hydrogen consumption is around 440 kg. This result is obtained because the model assumes that the hydrogen storage tank is 50% full at the start of the simulation. Thereafter, all values are constant throughout the year, as there is no excess of electrical energy and the hydrogen system is excluded.

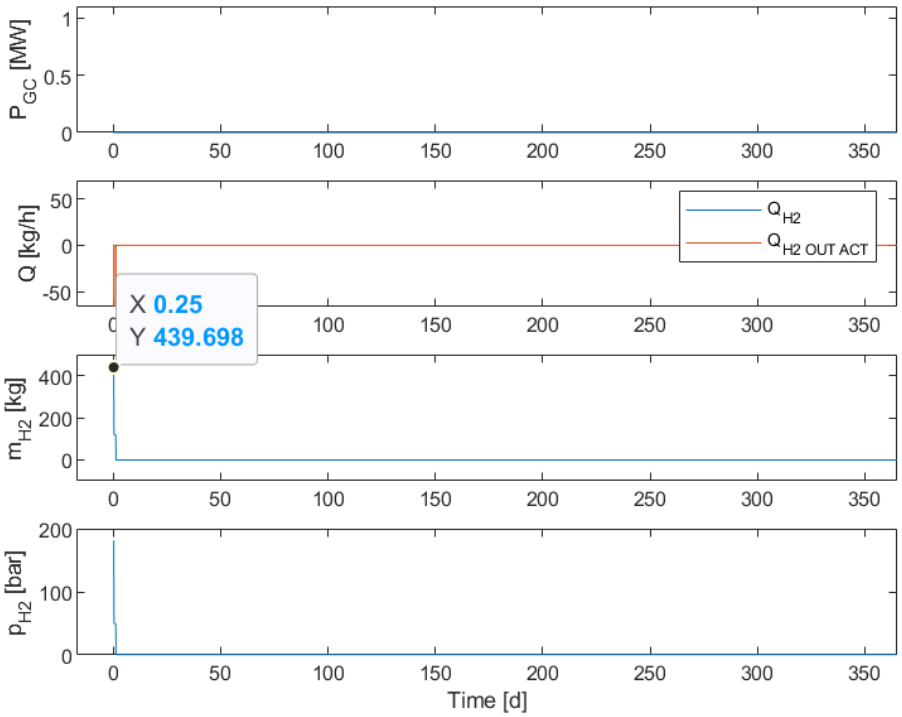

Figure 5.6: Annual hydrogen system's operation.

Table 5.3 shows the summarised annual quantities of the hydrogen system.

Table 5.3: Cumulative annual hydrogen system's operation data.

Parameter	Value	Unit
Total amount of electrical energy consumed for hydrogen generation (electrolysis + compression)	0	MWh/y
Total amount of electrical energy lost during electrolysis and compression	0	MWh/y
Total amount of produced hydrogen	0	kg/y
Total amount of consumed hydrogen (consumers)	439.6980	kg/y
Hydrogen selling price (SP_{H2})	8	€/kg
Total income from produced hydrogen	–6.7267e+05	€/y
Total system operation costs (*operCosts*)	6.7267e+05	€/y

5.1.2 Scenario 2

The Scenario 2 simulation assumes that the electrical energy for the operation of the hydrogen system comes only from excess hydropower inflow to the HPP.

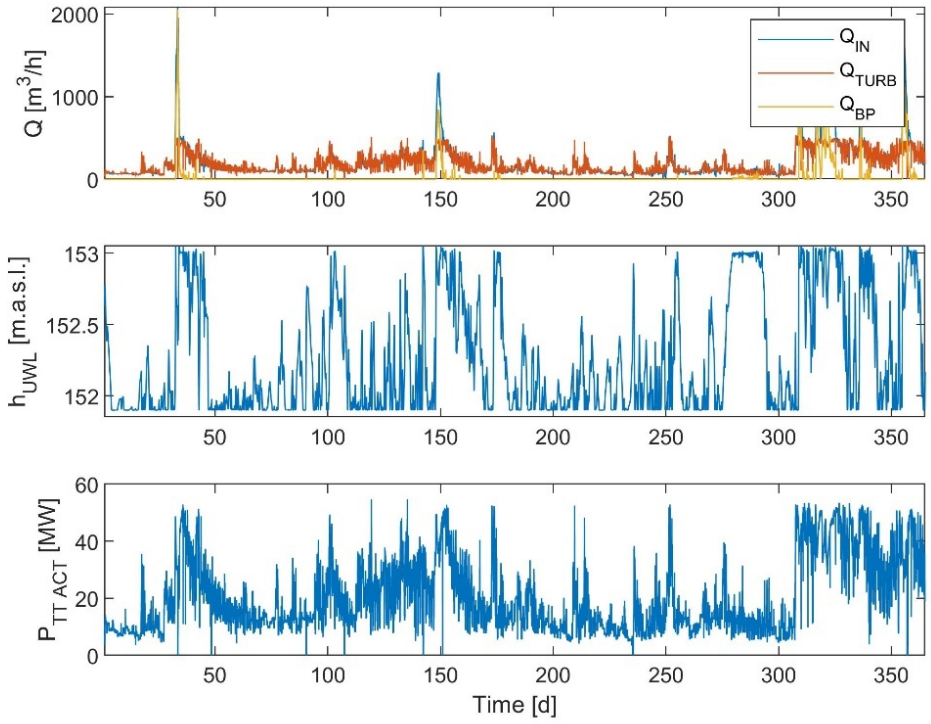

Figure 5.7: Annual HPP's operation

Table 5.4 shows the summarised annual quantities of the HPP's water-regime conditions, the total amount of electrical energy produced and the resulting annual income.

Table 5.4: Cumulative annual HPP's operation data.

Parameter	Value	Unit
Total amount of water entering the accumulation (V_{IN})	6.5661e+09	m^3/y
Total amount of water passing through turbine (V_{TURB})	5.7792e+09	m^3/y
Total amount of water passing through bypass (V_{BP})	9.7425e+08	m^3/y
Total amount of generated electrical energy (E_{GRID})	1.7544e+05	MWh/y
The difference between selling price and production cost of electricity (SP_{EL} – PC_{EL})	15	€/MWh
Total amount of lost hydropower through bypass (E_{BP})	2.5769e+04	MWh/y
Total income from electrical energy delivered to the grid ($Income_{EL}$)	2.6316e+06	€/y

Figure 5.8 shows the operation of the hydrogen system.

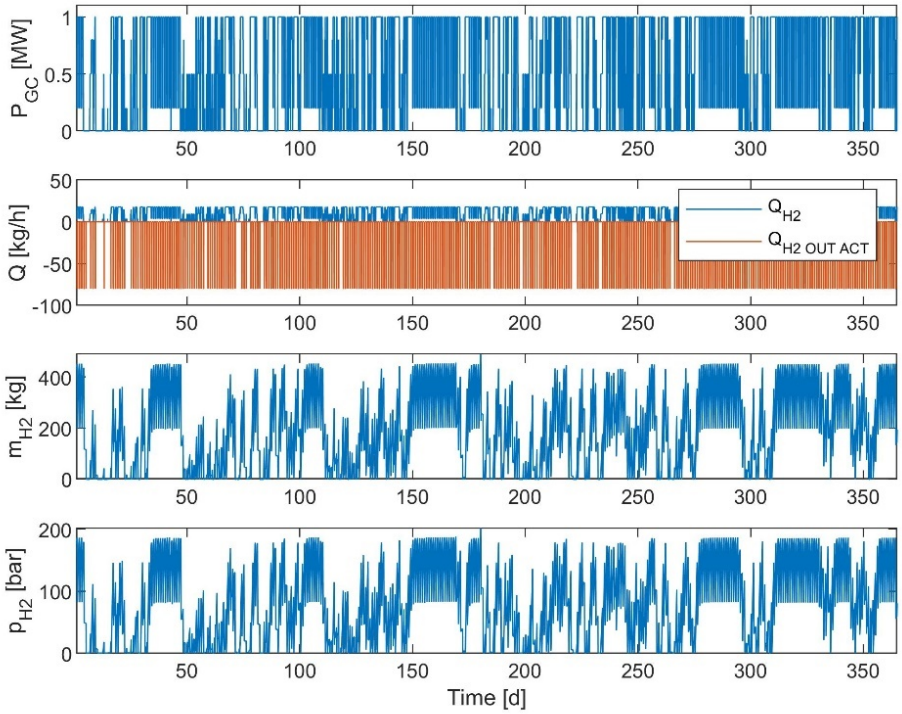

Figure 5.8: Annual hydrogen system's operation.

In Figure 5.8 / Figure 5.9, b) we can see that the outflow from the hydrogen tank, in general, follows a predefined hydrogen consumption, see Figure 4.15, except for the case when the hydrogen tank is empty. In this case there is no outflow from the tank.

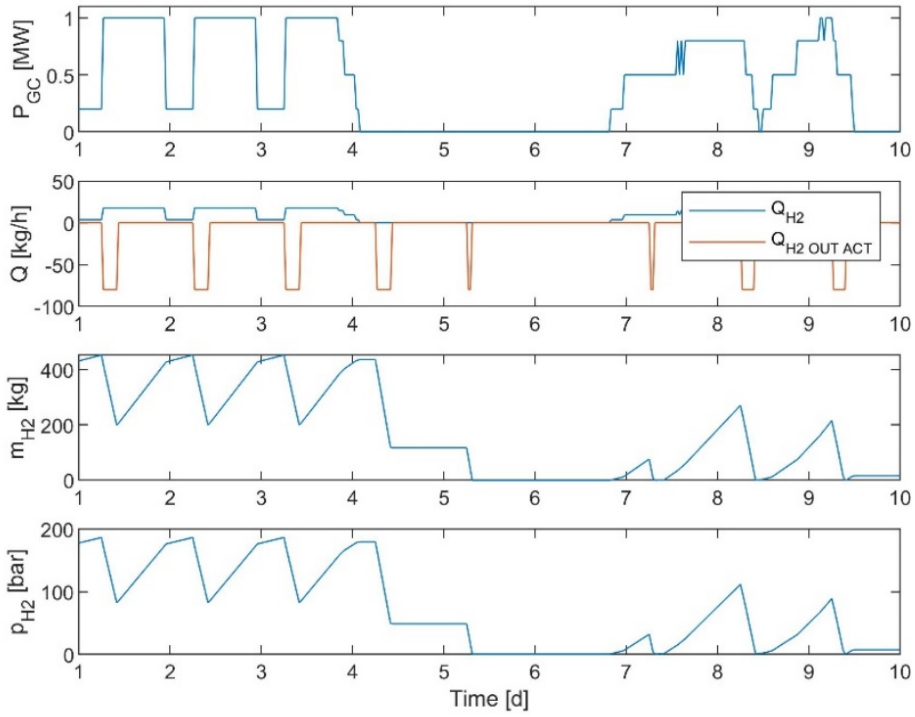

Figure 5.9: Daily hydrogen system's operation (10 days).

Table 5.5 shows the summarised annual quantities of the hydrogen system.

Table 5.5: Cumulative annual hydrogen system's operating data.

Parameter	Value	Unit
Total amount of electrical energy consumed for hydrogen generation (electrolysis + compression)	5.2494e+03	MWh/y
Total amount of electrical energy lost during electrolysis and compression	1.5561e+03	MWh/y
Total amount of produced hydrogen	93,729	kg/y
Total amount of consumed hydrogen (consumers)	93,975	kg/y
Hydrogen selling price (SP_{H2})	8	€/kg
Total income from produced hydrogen	7.7169e+04	€/y
Total system operation costs (*operCosts*)	6.7267e+05	€/y

Hydrogen demand ($Q_{H2\_OUT\_DEM}$ = 320 kg/day) cannot be completely fulfilled.

- *This is visible from the fact that the hydrogen tank occasionally reaches the empty state and, during these events, actual hydrogen supply does not meet the demands.*
- *The demand of 320 kg/day leads to annual hydrogen amount 116,800 kg. From Table 5.5 it follows that the total amount of produced hydrogen is 93,824 kg, which means that the demand is 80.3% fulfilled.*

5.1.3 Scenario 3

The Scenario 3 simulation assumes the hydrogen production using an additional electrical power due to a 5% reduction of the hydropower plant timetable.

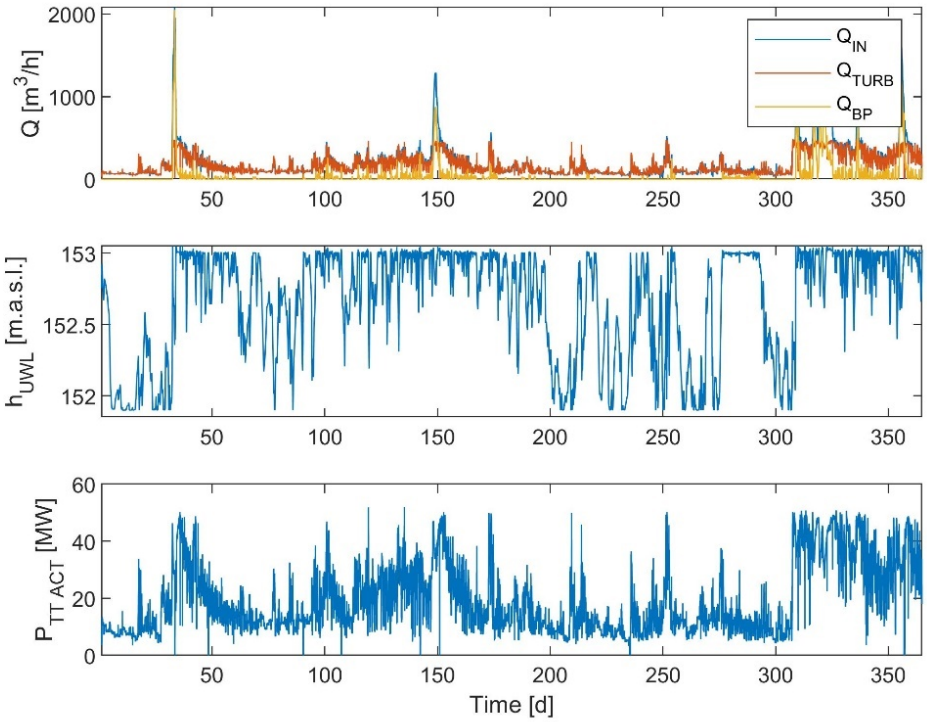

Figure 5.10: Annual HPP's operation.

Table 5.6 shows the summarised annual quantities of the HPP's water-regime conditions, the total amount of electrical energy produced and the resulting annual income.

Table 5.6: Cumulative annual HPP's operation data.

Parameter	Value	Unit
Total amount of water entering the accumulation (V_{IN})	6.5661e+09	m^3/y
Total amount of water passing through turbine (V_{TURB})	5.3461e+09	m^3/y
Total amount of water passing through bypass (V_{BP})	1.2456e+09	m^3/y
Total amount of generated electrical energy (E_{GRID})	1.6667e+05	MWh/y
The difference between selling price and production cost of electricity (SP_{EL} – PC_{EL})	15	€/MWh
Total amount of lost hydropower through bypass (E_{BP})	3.5003e+04	MWh/y
Total income from electrical energy delivered to the grid ($Income_{EL}$)	2.5000e+06	€/y

Figure 5.11 shows the operation of the hydrogen system.

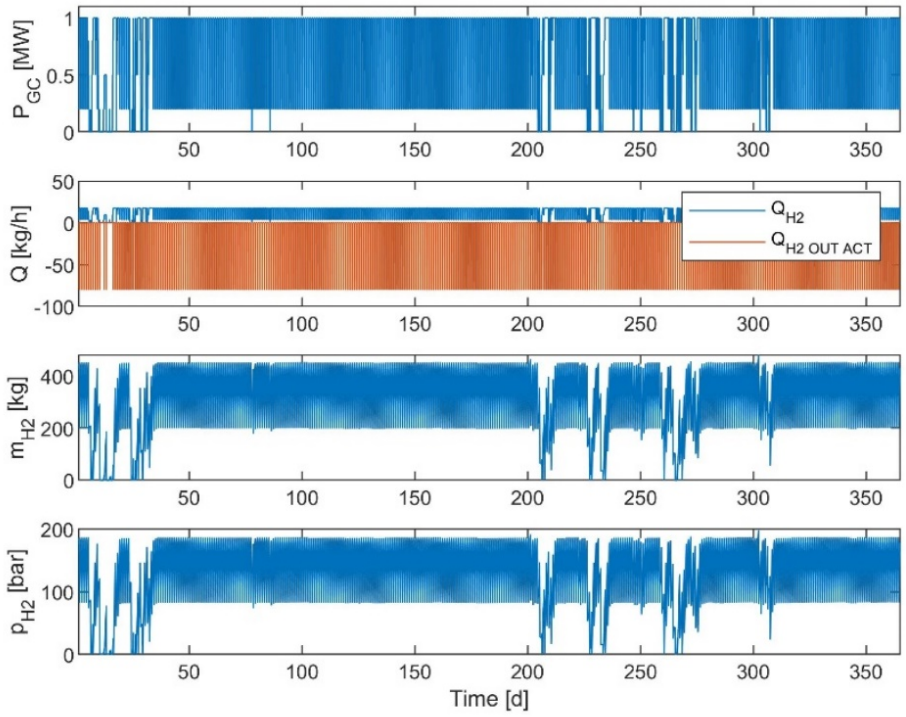

Figure 5.11: Annual hydrogen system's operation.

Table 5.7 shows the summarised annual quantities of the hydrogen system.

Table 5.7: Cumulative annual hydrogen system's operating data.

Parameter	Value	Unit
Total amount of electrical energy consumed for hydrogen generation (electrolysis + compression)	6.3763e+03	MWh/y
Total amount of electrical energy lost during electrolysis and compression	1.9088e+03	MWh/y
Total amount of produced hydrogen	113,324	kg/y
Total amount of consumed hydrogen (consumers)	113,325	kg/y
Hydrogen selling price (SP_{H2})	8	€/kg
Total income from produced hydrogen	2.3329e+05	€/y
Total system operating costs (*operCosts*)	6.7267e+05	€/y

In this scenario, the hydrogen demand is almost completely fulfilled. One can see that the amount of hydrogen in the tank varies between 200 and 420 kg, which means that the tank is almost never empty and the hydrogen demand can therefore almost always be fulfilled.

5.1.4 Scenario 4

The Scenario 4 simulation experiment assumes the hydrogen production using only the existing water surplus and additional electrical power from a 6-MW PV field.

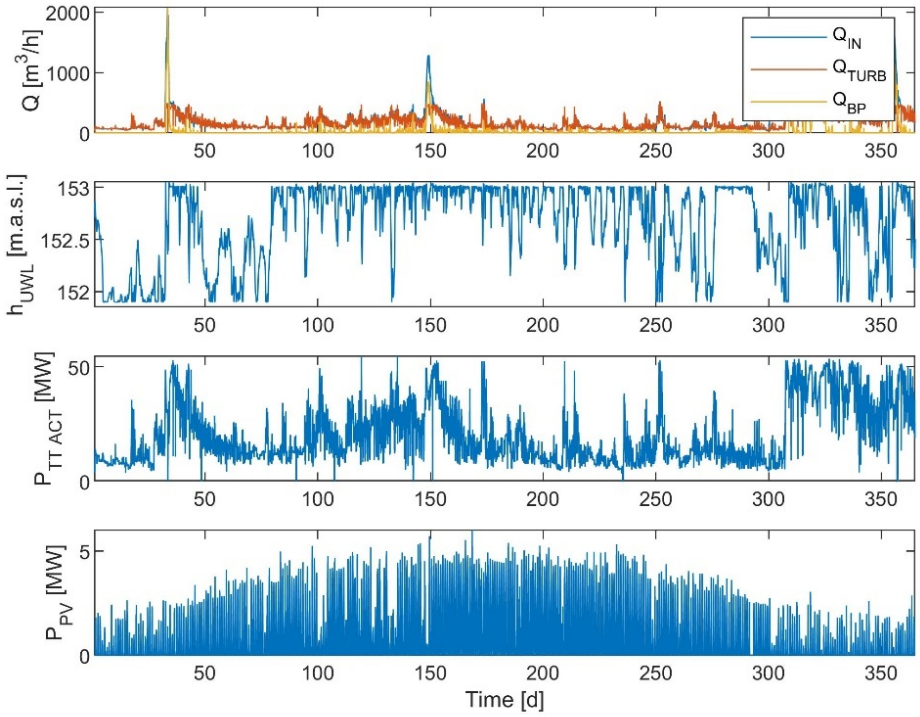

Figure 5.12: Annual HPP's operation and PV field power generation.

Table 5.8 shows the summarised annual quantities of the HPP's water-regime conditions, the total amount of electrical energy produced and the resulting annual income.

Table 5.8: Cumulative annual HPP's operating data.

Parameter	Value	Unit
Total amount of water entering the accumulation (V_{IN})	6.5661e+09	m^3/y
Total amount of water passing through turbine (V_{TURB})	5.4301e+09	m^3/y
Total amount of water passing through bypass (V_{BP})	1.1657e+09	m^3/y
Total amount of generated electrical energy (E_{GRID})	1.8309e+05	MWh/y
The difference between selling price and production cost of electricity (SP_{EL} – PC_{EL})	15	€/MWh
Total amount of lost hydropower through bypass (E_{BP})	3.2705e+04	MWh/y
Total income from electrical energy delivered to the grid ($Income_{EL}$)	2.6316e+06	€/y

Figure 5.13 shows the operation of the hydrogen system.

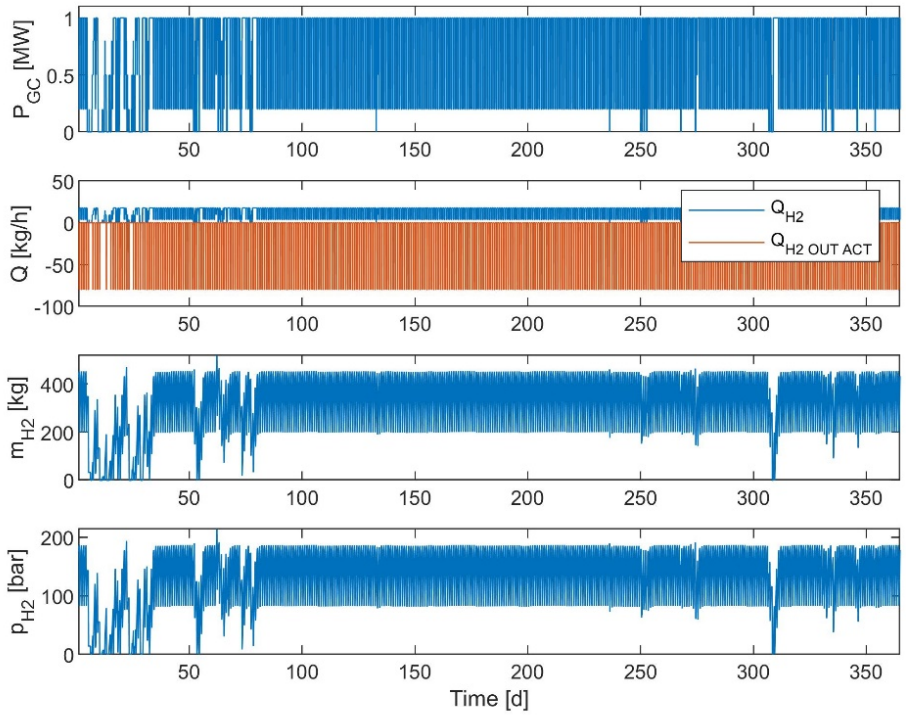

Figure 5.13: Annual hydrogen system's operation.

Table 5.9 shows the summarised annual quantities of the hydrogen system.

Table 5.9: Cumulative annual hydrogen system operating data.

Parameter	Value	Unit
Total amount of electrical energy consumed for hydrogen generation (electrolysis + compression)	6.3829e+03	MWh/y
Total amount of electrical energy lost during electrolysis and compression	1.9089e+03	MWh/y
Total amount of produced hydrogen	113,290	kg/y
Total amount of consumed hydrogen (consumers)	113,300	kg/y
Hydrogen selling price (SP_{H2})	8	€/kg
Total income from produced hydrogen	2.3365e+05	€/y
Total system operating costs (*operCosts*)	6.7267e+05	€/y

5.1.5 Scenario 5

The Scenario 5 simulation experiment assumes the hydrogen production using an additional 5% of electrical energy due to the prescribed timetable and additional electrical power from a 6-MW PV field.

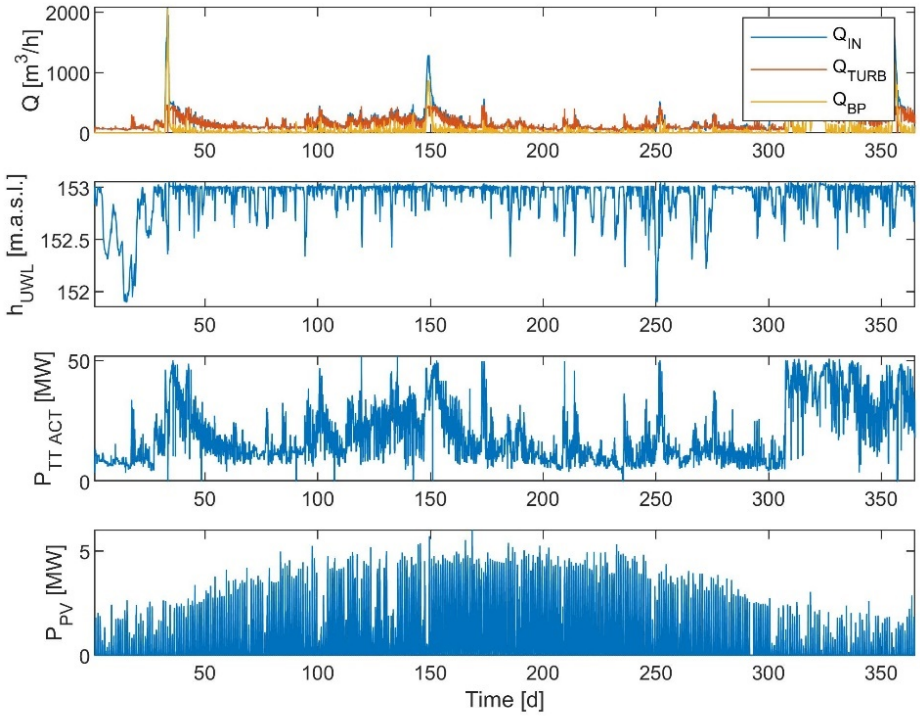

Figure 5.14: Annual HPP's operation and PV field power generation.

Table 5.10 shows the summarised annual quantities of the HPP's water-regime conditions, the total amount of electrical energy produced and the resulting annual income.

Table 5.10: Cumulative annual HPP's operating data.

Parameter	Value	Unit
Total amount of water entering the accumulation (V_{IN})	6.5661e+09	m^3/y
Total amount of water passing through turbine (V_{TURB})	5.0691e+09	m^3/y
Total amount of water passing through bypass (V_{BP})	1.5013e+09	m^3/y
Total amount of generated electrical energy (E_{GRID})	1.7431e+05	MWh/y
The difference between selling price and production cost of electricity (SP_{EL} – PC_{EL})	15	€/MWh
Total amount of lost hydropower through bypass (E_{BP})	4.4370e+04	MWh/y
Total income from electrical energy delivered to the grid ($Income_{EL}$)	2.5000e+06	€/y

Figure 5.15 shows the operation of the hydrogen system.

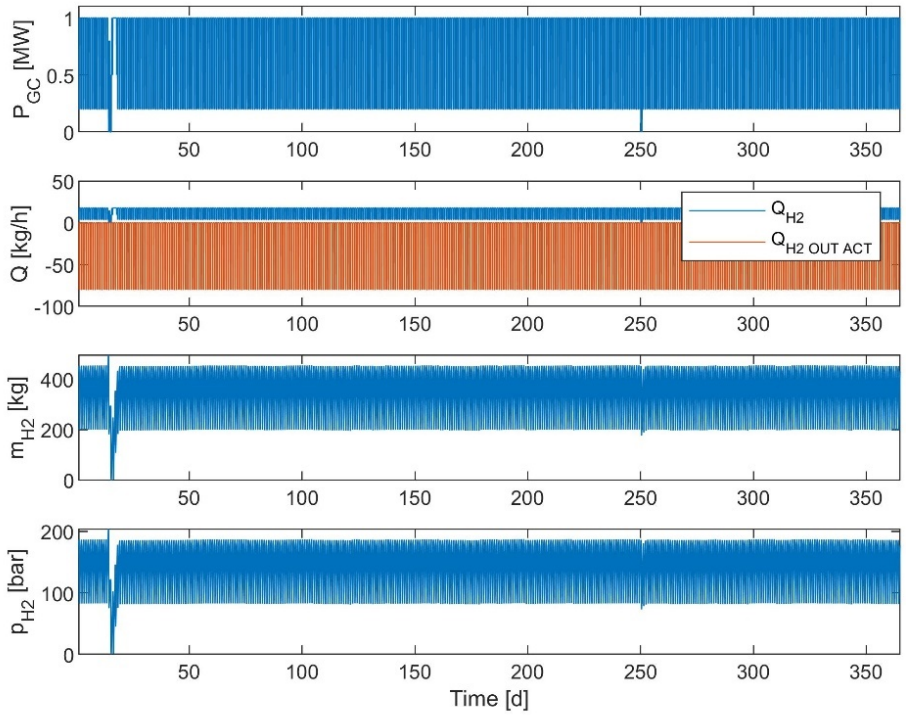

Figure 5.15: Annual hydrogen system's operation.

Table 5.11 shows the summarised annual quantities of the hydrogen system.

Table 5.11: Cumulative annual hydrogen system's operating data.

Parameter	Value	Unit
Total amount of electrical energy consumed for hydrogen generation (electrolysis + compression)	6.5687e+03	MWh/y
Total amount of electrical energy lost during electrolysis and compression	1.9740e+03	MWh/y
Total amount of produced hydrogen	116,610	kg/y
Total amount of consumed hydrogen (consumers)	116,620	kg/y
Hydrogen selling price (SP_{H2})	8	€/kg
Total income from produced hydrogen	2.6022e+05	€/y
Total system operating costs (*operCosts*)	6.7267e+05	€/y

5.2 Hydrogen-System-Configuration Explorer

This section is focused on the simulation-based exploring and optimising of the system parameters, i.e., optimal sizing and parametrisation of the hydrogen system and the photovoltaic power plant. The goal is to find the set of system parameters, that provide the best result according to a selected criterion function (*CF*). In general, the criterion function can be one of the typical key performance indicators (KPIs), such as: profitability,

total amount of produced hydrogen, hydrogen-production cost, hydrogen system utilisation rate, etc.

For this purpose, the **Hydrogen-System-Configuration Explorer** was designed, and represents an important decision-support tool that assists the design and optimal sizing of the system before its actual implementation. The idea and principle are represented in Figure 5.16:

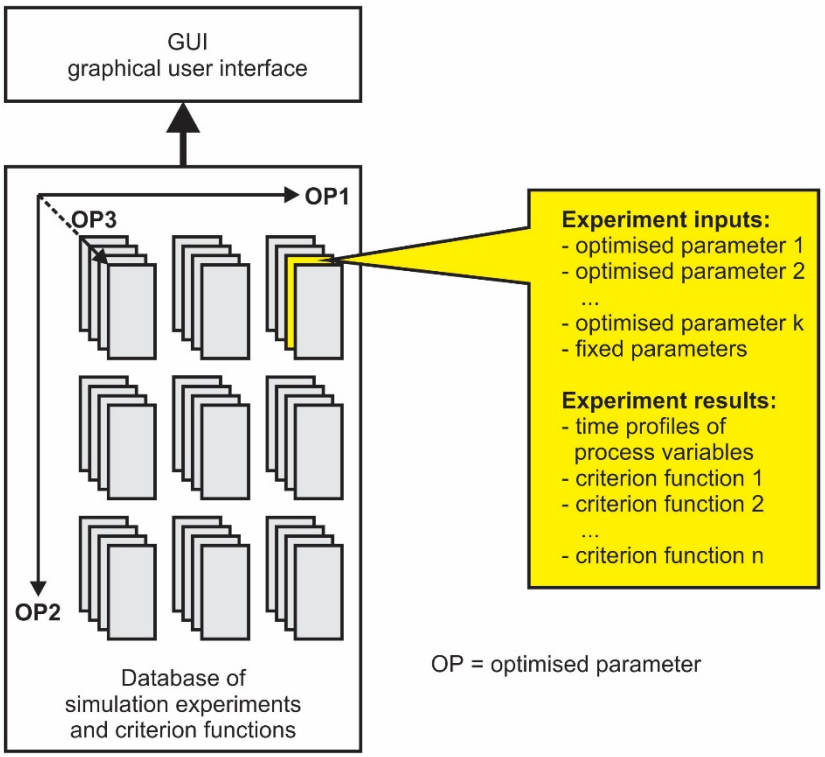

Figure 5.16: Hydrogen-System-Configuration Explorer.

The key idea is to use "exhaustive", also called "brute force", optimisation. This means that the system parameters that are the subject of optimisation are defined and then the system is simulated at all possible combinations of the system's parameters. During each simulation run, a set of criterion functions is calculated.

The developed Hydrogen-System-Configuration Explorer supports a sensitivity analysis, which shows how much and in which way and direction a particular optimised parameter affects the selected criterion function. The Hydrogen-System-Configuration Explorer uses two key features, which are crucial for an efficient and rapid sensitivity analysis:

- *Database of performed simulation experiments and belonging criterion functions, evaluated during each simulation run. Thanks to the database of performed experiments, a quick overview of different parameter combinations is possible, without the need for an online simulation, which can be time consuming.*

- *A graphical user interface (GUI) provides the possibility for a graphical representation of the dependence between the selected criterion function and optimised system parameters. This makes the sensitivity analysis very transparent, didactic and intuitive.*

Among the complete set of system parameters, few (in this case 3 parameters) are the subject of change and optimisation, and they are listed in Table 5.12. In Figure 5.16, they

are denoted as Ops, i.e., optimised parameters. For each parameter, a value range is defined. OPs are adjusted step-wise according to the set of values, defined in Table 5.12.

Table 5.12: Parameters that are the subject of optimisation.

Parameter	Description	Unit	Set of values
OP1: P_{EL_SYS}	Nominal power of the hydrogen system	MW	[0.25 0.50 0.75 1.0 1.25 1.5]
OP2: P_{PV_INST}	Nominal power of the photovoltaic field	MW	[0 1 2 3 4 5 6]
OP3: V_{GEO}	Volume of the hydrogen storage tank	m^3	[10 20 30 40 50 60 70 80]

Beside optimised parameters (OP1, OP2 and OP3), the hydrogen demand ($Q_{H2\_OUT\_DEM}$), expressed in [kg/day], is also varied according to the following predefined values:

Table 5.13: Hydrogen demand.

Parameter	Description	Unit	Set of values
$Q_{H2\_OUT\_DEM}$	Assumed hydrogen consumption	kg/day	[80 160 240 320 400 480 560 640]

The numbers of members in the sets OP1, OP2, and OP3 are 6, 7 and 8, respectively, and 8 in the set $Q_{H2\_OUT\_DEM}$. The simulation run is performed for each combination of values for the optimisation parameters and hydrogen demand, which gives in total $6 \cdot 7 \cdot 8 \cdot 8 = 2688$ combinations and the corresponding simulation runs. By varying more parameters, the number of combinations increases progressively, which leads to increased computational burden and possibly also an unpractically long total simulation time.

The other parameters that are not the subject of the optimisation are set to fixed, predefined values and are listed in Table 5.14 and denoted as "fixed parameters" in Figure 5.16.

The results of each simulation run are:

- *Time profiles of all process variables (mass-flow rates, energy flows, financial flows);*
- *Criterion functions calculated during or after each simulation run on the basis of the process variables. Several different criterion functions are calculated in each simulation run: the amount of hydrogen produced (m_{H2_PROD}), the hydrogen-production costs (PC_{H2}), the utilisation rate of the hydrogen system* (c) *and the income from hydrogen production ($Income_{H2}$).*

Finally, a MATLAB script (multiSim_script, [190]) was created to insert parameters and run a 1-year simulation based on real data.

We used the MATLAB function "parsim" in the script, as it is useful to simulate a dynamic system multiple times in parallel.

The results are saved as a table size of $2688 \cdot 13$, see Table 5.14.

Table 5.14: Variables in the simulation result table (simRes).

N°	Name	MATLAB name	Description	Unit
1	P_{PV_INST}	*PV*	Nominal power of the photovoltaic field	MW
2	P_{EL_SYS}	*P2G*	Nominal power of the hydrogen system	MW
3	V_{GEO}	*H2st*	Volume of the hydrogen storage tank	m^3
4	$Q_{H2\_OUT\_DEM}$	*H2_cons*	Assumed hydrogen consumption per day	kg/d
5	SP_{H2}	*H2 sell price*	Selling price of hydrogen	€/kg
6	*time*	*simDays*	Duration of the simulation in days	d
7	m_{H2_PROD}	*H2_prod*	Annual hydrogen production	kg/y
8	PC_{H2}	*H2prodCost*	hydrogen maximum production flow	€/kg
9	*c*	*P2G_util*	Compression factor	-
10	$Income_{H2}$	*H2Income*	Maximum hydrogen storage capacity	€/y
11	$CapEx_{PV}$	*cpx_PV*	CapEx of the PV filed	€
12	$CapEx_{EL\_SYS}$	*cpx_P2G*	CapEx of the electrolyser system	€
12	$CapEx_{H2\_STOR}$	*cpx_H2st*	CapEx of hydrogen storage	€
14	*CapEx*	*CapEx*	Total hydrogen system CapEx	€

In the table above, variables 1–3 represent the optimisation parameters (current values of the respective simulation run). Variables 7–10 represent the results of the various criteria functions of the respective simulation run. Variables 11–14 represent the financial parameters of the hydrogen and photovoltaic equipment. Parameters 4 and 5 provide information about the assumed hydrogen demand and the duration of the respective simulation run.

To graphically present the simulation results and to be able to manually determine the optimal system configuration, a graphic user interface (GUI) was designed using MATLAB application designer (plotApp, [190]). This interactive GUI application graphically presents the selected criterion variable (CV) as a function of the parameters that are the subject of the optimisation (Table 5.15). The following criterion functions can be presented, depending on the user's preference.

An additional function was added in the GUI script to calculate the payback period (PBP) of the investment in the hydrogen system. The *PBP* values were calculated offline for all simulations performed based on Eq. (5.1),

$$PBP_{SYS} = \frac{CapEx_{SYS}}{(Income_{H2} - OpEx_{SYS})} \tag{5.1}$$

where $Income_{H2}$ represents the annual income from hydrogen production.

The developed GUI offers an insight into the simulation results of all combinations of optimised parameters. The user can select the desired variable for criterion variable (plot variable in the GUI) and a so-called slider variable which can be assigned to one of the three optimised parameters: *PV* ($=P_{PV\_INST}$), *P2G* ($=P_{EL\_SYS}$), or *H2st* ($=V_{GEO}$). The results can then be observed in the form of various 3D or 2D diagrams. The slider allows adjusting the value of the selected variable, which can be one of the following three: 1) nominal power of the photovoltaic field (P_{PV_INST}), 2) nominal power of the electrolyser (P_{EL_SYS}), and 3) hydrogen storage volume (V_{GEO}). Again, different variable names are used in the GUI; therefore, see Table 5.15 for a translation between GUI and model variables.

In the next subsections (5.2.1–5.2.4), several operating cases are simulated. Each case illustrates the effects of the particular variable.

Table 5.15: Variable's translation table.

Criterion function	Name	GUI name	Units
Production cost of hydrogen	PC_{H2}	*H2prodCost*	€/kg
Income from hydrogen production	$Income_{H2}$	*H2Income*	€/y
Hydrogen system utilisation rate	c	*P2Gutil*	-
Hydrogen system payback period	PBP	*PBP*	y
Monthly/annual mass of produced hydrogen	m_{H2_PROD}	*H2_prod*	kg/y
Parameters – subject of optimisation	Name	GUI name	Units
Installed power of PV field	P_{PV_INST}	*PV*	MW
Installed power of hydrogen system	P_{EL_SYS}	*P2G*	MW
Geometrical volume of hydrogen-storage tank	V_{GEO}	*H2st*	m^3
Other parameters shown on GUI	Name	GUI name	Units
Hydrogen demand	$Q_{H2\_OUT\_DEM}$	*H2 cons max*	kg/d
Hydrogen selling price	SP_{H2}	*H2 sell price*	€/kg

5.2.1 Sizing of a Hydrogen System for the Case-Study HPP

To demonstrate the benefit of the developed Hydrogen-System-Configuration Explorer, simulations of hydrogen and electrical power cogeneration in the case-study HPP were performed and the results were observed.

The simulations help to determine the optimal parameters for the hydrogen system according the relevant operating parameters. The simulation results thus help to define the optimal size of the equipment (system components). In the simulations, the following assumptions and limitations were considered:

- *The operation of the hydropower plant must fulfil the prescribed timetable of the supply of electrical power to the grid;*
- *Only the surplus hydro energy and the electrical energy generated by the PV field can be used for the production of hydrogen;*
- *The required hydrogen production is moderate and limited to 320 kg/day;*
- *The price of surplus electrical power generated from excess hydropower, which cannot be accepted by the grid, is considered zero.*
- *The price of electrical power generated that could be delivered to the grid, but is utilised for hydrogen production, is considered to be 38 €/MWh.*
- *The costs of electrical energy generated by the PV is taken into account by considering the CapEx and OpEx of the PV field.*
- *The RUL is evaluated but it is not considered over a period of 1 year of simulations, as its impact is negligible.*

The case-study HPP operates continuously, so the duration of a simulation time to optimise the hydrogen system's parameters must be a whole year. In the course of the year,

there are significant deviations in the water inflow, so we considered the sizing of the hydrogen system in January and November as interesting to show the difference in the operation of the hydrogen system during these two particular months.

The following scenarios are presented by GUI, see Table 5.16.

Table 5.16: List of operating cases presented using GUI.

Scenario	P_{PV_INST} [MW]	Period
Scenario 1	0	January
Scenario 2	6	January
Scenario 3	0	November
Scenario 4	6	November
Scenario 5	0	Annual
Scenario 6	6	Annual
Scenario 7	0	Annual (reduced CapEx)
Scenario 8	6	Annual (reduced CapEx)

For each scenario, the following values are evaluated: $Income_{H2}$ [€], m_{H2} [kg], PC_{H2} [€/kg], c [%], see Sections 5.2.2 – 5.2.3.

5.2.2 Monthly Simulations

As already mentioned, operating conditions strongly depend on the time of the year. For this reason, the month of January was chosen first, since there is little surplus hydropower available for hydrogen production in this period of the year. In the second experimental case, the month of November was chosen, because there is more surplus of hydropower available due to the increased water inflow in the HPP (longer periods of rain).

In both experimental cases, two subcases were simulated, one without the PV field and the other with the PV field with a nominal power of 6 MW. Also, for both experimental cases, the first criterion is the maximum hydrogen income ($Income_{H2}$). Other parameters were as follows: the hydrogen consumption ($Q_{H2\_OUT\_DEM}$) up to 320 kg/day and the hydrogen selling price (SP_{H2}) is 8 €/kg. The following conditions are assumed for hydrogen production [kg/d]: the market can accept up to 320 kg/d, but there are no penalties if a lower amount of hydrogen is generated per day.

5.2.2.1 Simulation Results, January

Figure 5.17 shows the initial simulation results displayed in the GUI. We can see that the maximum monthly income in January, when $P_{PV\_INST} = 0$ MW, can be obtained with a 0.75-MW hydrogen system and a 20 m^3 storage tank. The assumed hydrogen selling price is 8 €/kg.

The resulting income can be as high as 16,269.4 €/month. But in some system configurations, the income can even be negative.

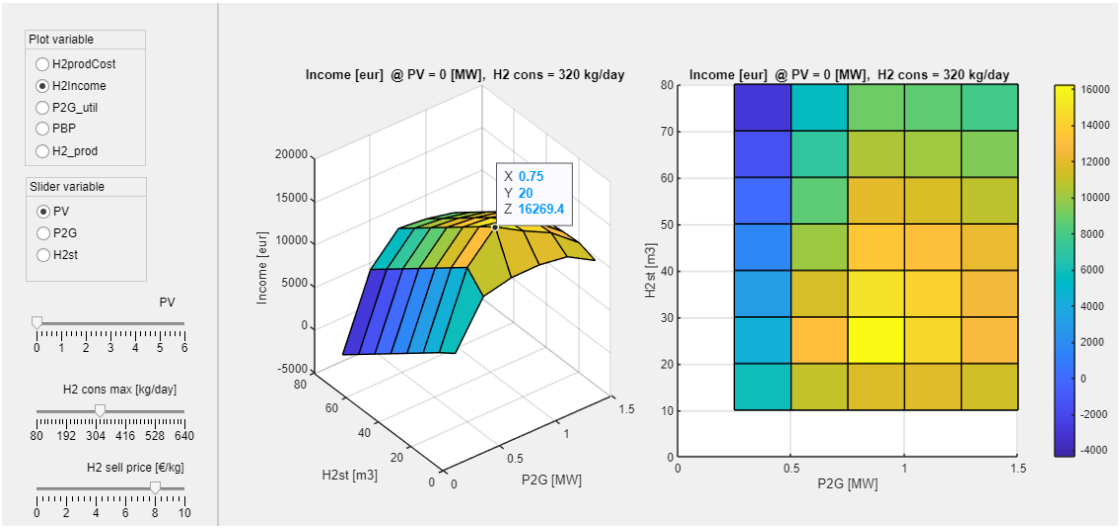

Figure 5.17: Proposed system configuration for maximum income from hydrogen production in January.

Please note that the resulting hydrogen income graphs are shown both in 3D and 2D, as some results are more easily visible in a 2D graph. As there are a lot of figures in this section, all other results are only shown in 3D form.

The chosen hydrogen system configuration results in the amount of total hydrogen production in January (without the additional electrical energy from the photovoltaic field, i.e., $P_{PV\_INST} = 0$ MW) of 4631.16 kg/month, see Figure 5.18. This hydrogen production is only at the expense of the surplus of the water reserve in the accumulation and does not affect regular electrical energy production due to the timetable.

The chosen hydrogen-system configuration results in the amount of total hydrogen production in January (without the additional electrical energy from the photovoltaic field, i.e., PV = 0 MW) of 4631.16 kg/month, see Figure 5.18. This hydrogen is produced using only the excess hydropower and does not affect the timetable of supply of electrical energy to the grid.

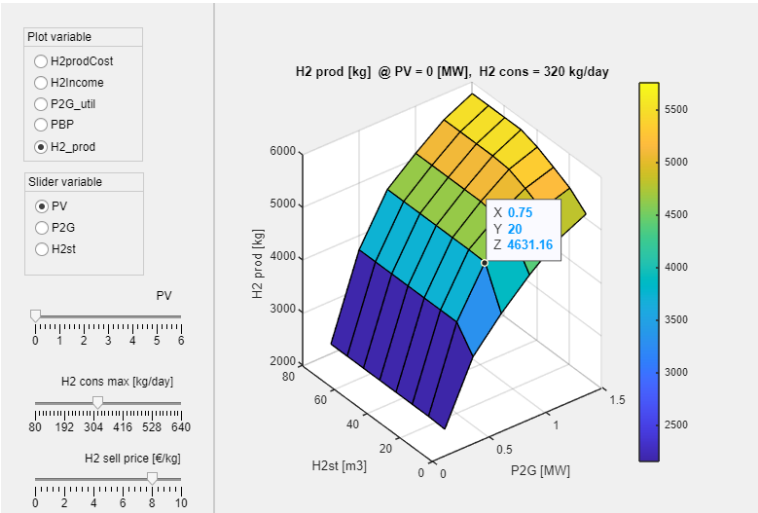

Figure 5.18: Quantity of hydrogen produced in January.

With the same system setup, the production costs of hydrogen were explored. Figure 5.19 shows an example of the representation of the production price of hydrogen in GUI, expressed in €/kg, depending on the installed power of the hydrogen system and the size of the storage tank, for a system without a PV field ($P_{PV\_INST} = 0$) and for the assumed periodic consumption of hydrogen up to 320 kg/day. Note that the hydrogen selling price slider is inactive in this case.

The production costs for hydrogen (PC_{H2}) for the chosen system and an assumed hydrogen demand of up to 320 kg/day are around 4.49 €/kg, see Figure 5.19.

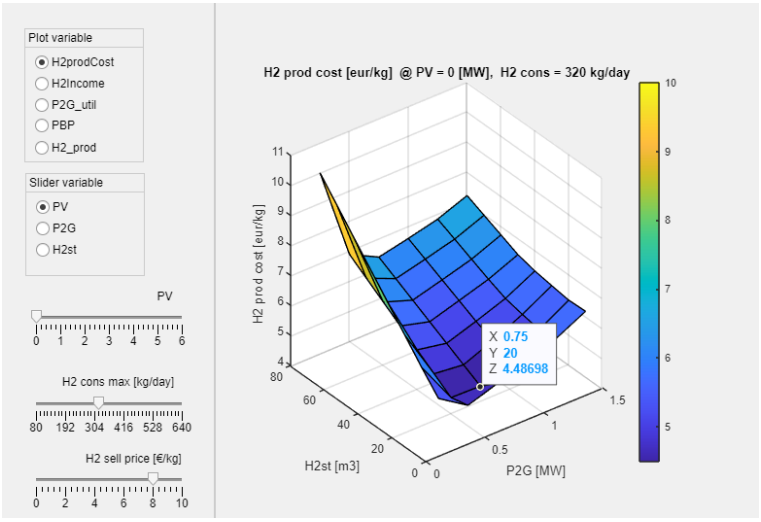

Figure 5.19: Production costs of hydrogen in January with a 0.75-MW hydrogen system, a 20 m^3 hydrogen-storage tank and a hydrogen demand up to 320 kg per day.

Furthermore, the developed GUI can be used as an estimator for the utilisation rate of the hydrogen system in various configurations, see Figure 5.20.

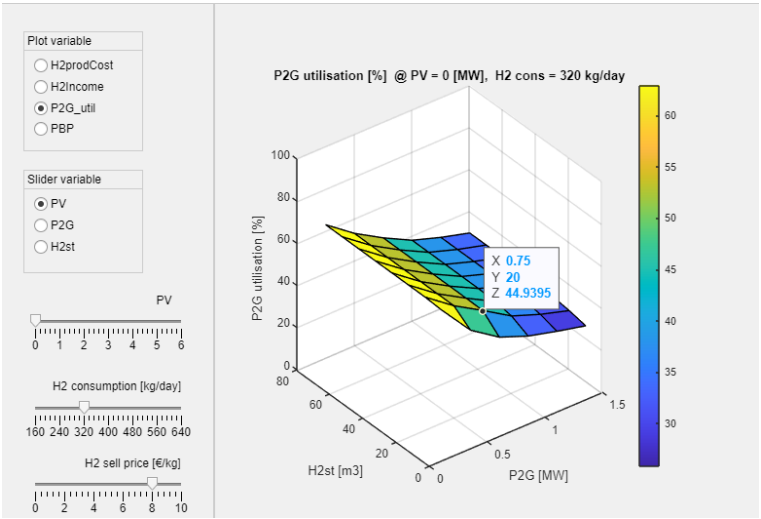

Figure 5.20: Hydrogen-system utilisation rate in January.

In this case, the 0.75-MW electrolyser utilisation rate is around 45%. It can be seen that a smaller hydrogen system increases the hydrogen-system utilisation rate due to low daily hydrogen consumption up to 320 kg/day. Also, the increasing size of the hydrogen storage does not make sense. If the consumption increases, then it is a question of

optimisation as to which subsystem size is more worthwhile. The operation of the electrolyser can be seen in Figure 5.21. In this setup, the electrolyser is underutilised.

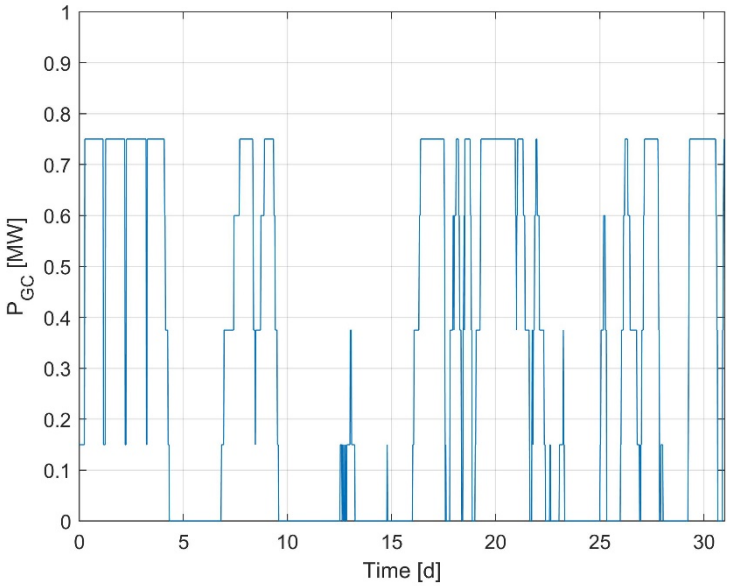

Figure 5.21: Hydrogen system operation in January.

In the next step, the nominal power of the PV field was increased from zero to 6 MW and the income was evaluated, see Figure 5.22. It follows that the hydrogen system with a 0.75-MW electrolyser and 20 m^3 hydrogen storage cannot be profitable in any case, because the relatively small hydrogen system cannot produce enough hydrogen to cover the investment in a large PV field. The income for the proposed system setup is negative. In this system setup, losses of –3341.84 €/month or more are being generated. In nearly all system configurations, the income is negative.

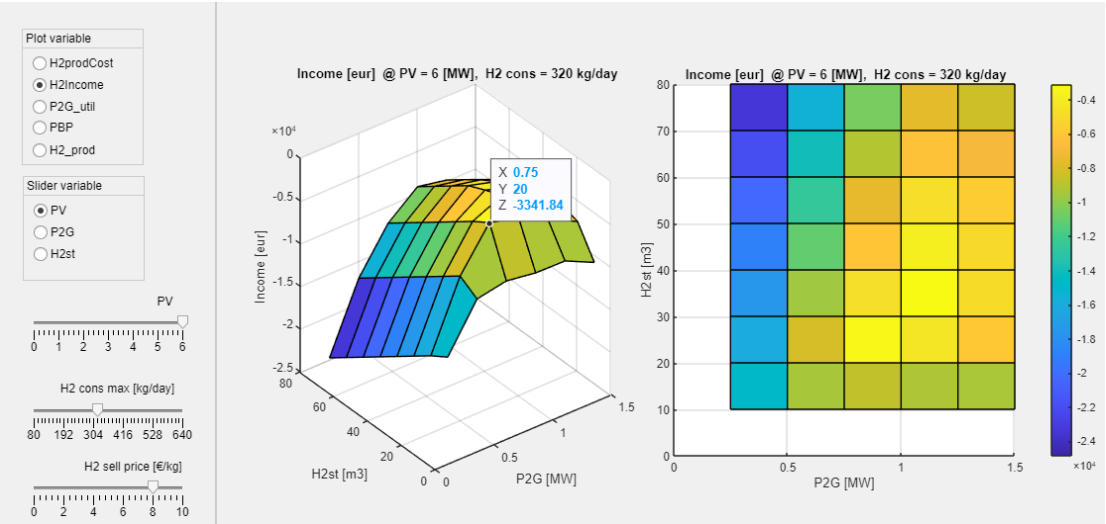

Figure 5.22: Income in January after the inclusion of 6-MW PV field.

The total hydrogen production in this case is 6044.14 kg/month, see Figure 5.18,

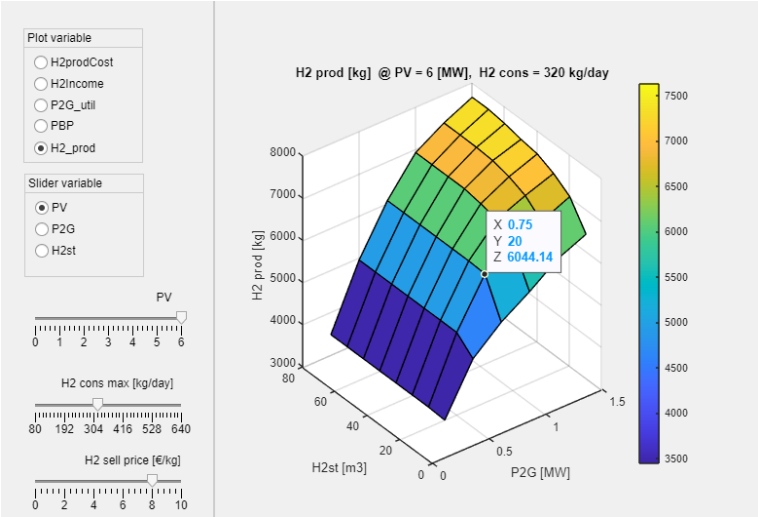

Figure 5.23: Monthly hydrogen mass produced in January.

and the production costs for hydrogen (PC_{H2}) for the chosen system and an assumed hydrogen demand of up to 320 kg/day are around 8.55 €/kg.

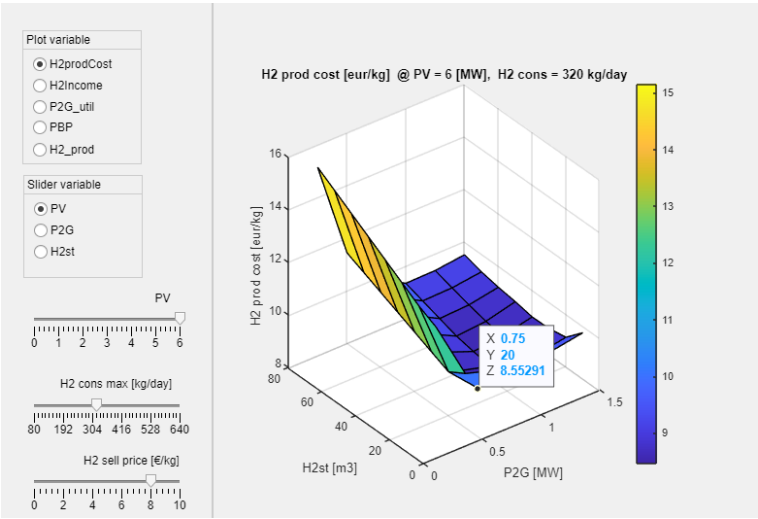

Figure 5.24: Hydrogen-production costs in January after the inclusion of 6-MW PV field.

By increasing the PV field to 6 MW, the utilisation rate of the electrolyser is increased to around 59%, see Figure 5.25. This is because the additional surplus of electrical energy is produced by adding a 6-MW PV field to the system setup.

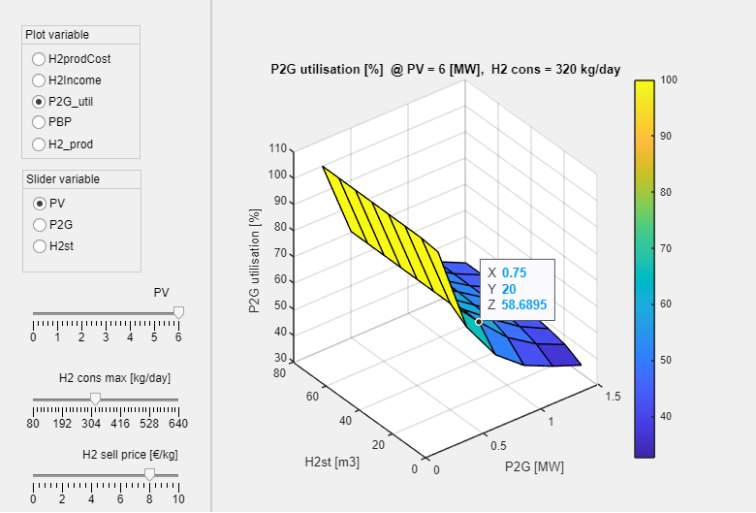

Figure 5.25: Hydrogen system utilisation rate in January after the inclusion of 6-MW PV field.

The operation of the electrolyser can be seen in Figure 5.26.

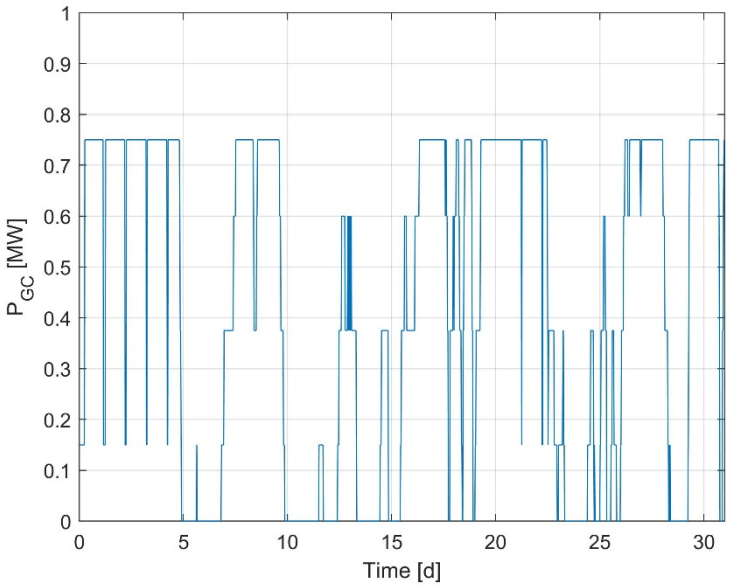

Figure 5.26: Hydrogen system operation in January after the inclusion of 6-MW PV field.

5.2.2.2 Simulation Results, November

The same evaluation procedure for the hydrogen system was followed as in January, but now the month of November has been chosen, because there is a lot of surplus hydro energy due to the increased water inflow in the HPP (longer period of rain). Figure 5.27 shows the simulation results. The maximum income in November without a PV field can be obtained with a 0.75-MW hydrogen system and a 20 m^3 storage tank for the assumed periodic consumption of hydrogen up to 320 kg/day and a hydrogen selling price of 8 €/kg.

The resulting income can be as high as 52,651.5 €/month. In this case, the income is positive in all system configurations.

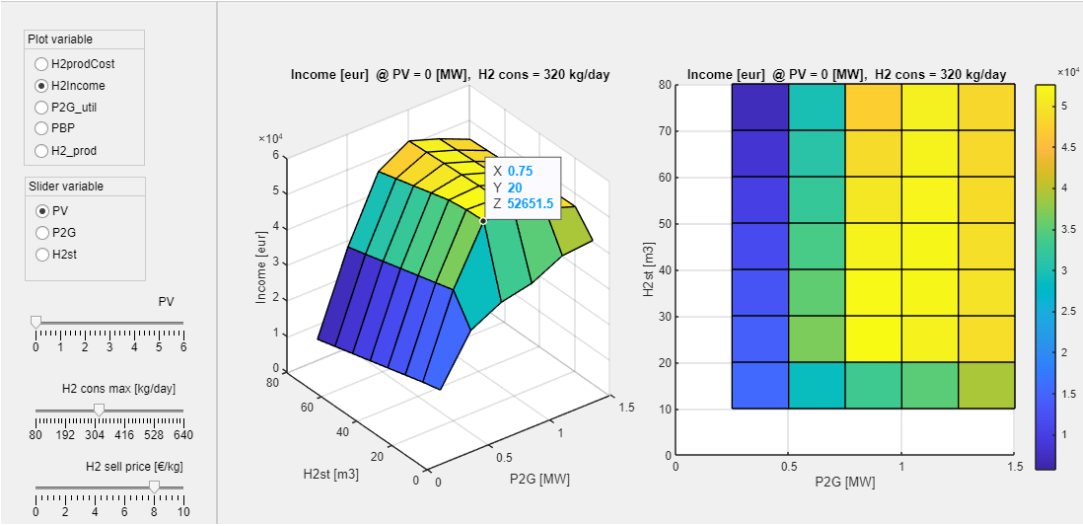

Figure 5.27: Proposed system configuration for maximum income from hydrogen production in November.

The chosen hydrogen-system configuration results in a total hydrogen production in January (without the additional electrical energy from the photovoltaic field, i.e., P_{PV_INST} = 0 MW) of 9095.13 kg/month, see Figure 5.28. This hydrogen production is only at the expense of the surplus of the water reserve in the accumulation and does not affect regular electrical energy production due to the timetable.

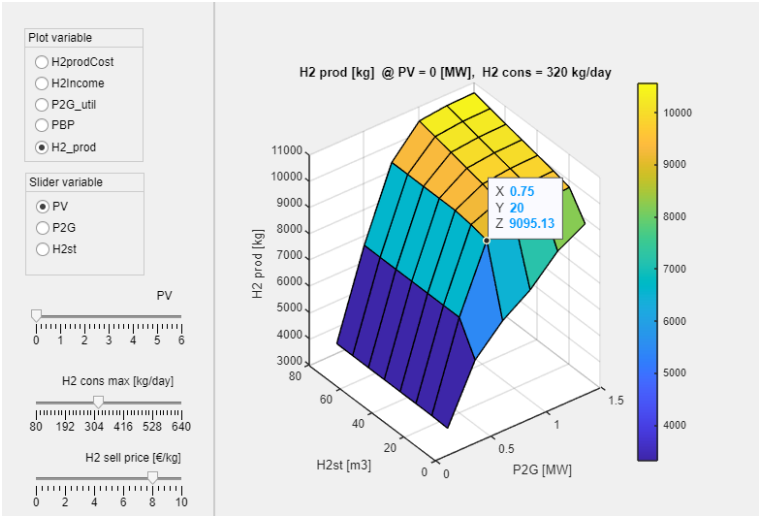

Figure 5.28: Monthly hydrogen quantity produced in November.

With the same system setup, the production costs of hydrogen were explored. Figure 5.29 shows an example of the representation of the production price of hydrogen in the GUI, expressed in €/kg, depending on the installed power of the hydrogen system and the size of the storage tank, for a system without a PV field (P_{PV_INST} = 0 MW) and for the assumed periodic consumption of hydrogen up to 320 kg/day. Note again that the hydrogen-selling-price slider is inactive in this case. The production costs for hydrogen

(PC_{H2}) for the chosen system and an assumed hydrogen demand of up to 320 kg/day are around 2.21 €/kg.

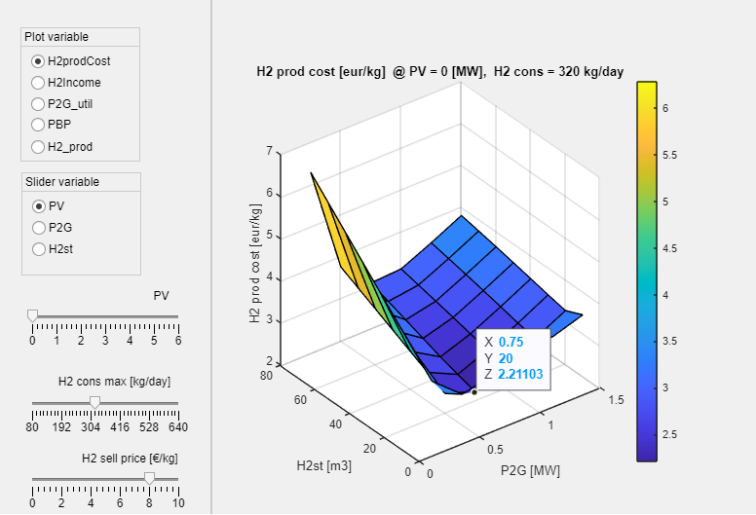

Figure 5.29: Production costs of hydrogen for November with a 0.75-MW hydrogen system and 20 m^3 hydrogen-storage tank.

Furthermore, the developed GUI was used as an estimator for the utilisation rate of the hydrogen system in various configurations, see Figure 5.30.

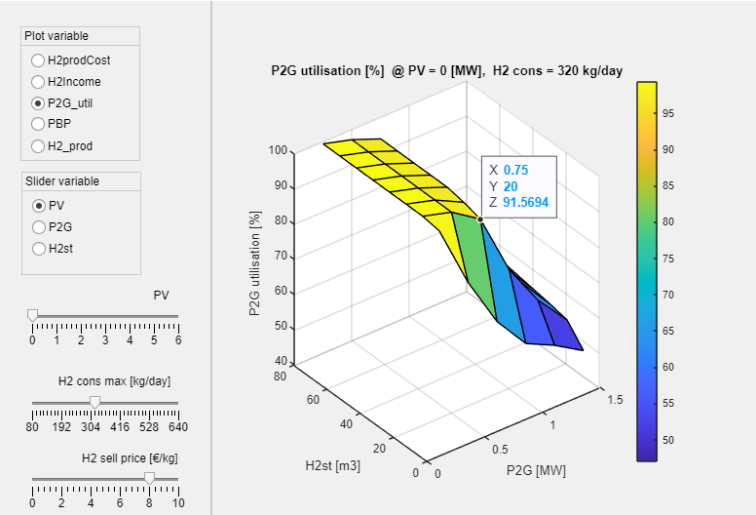

Figure 5.30: Hydrogen-system utilisation rate in November.

The 0.75-MW electrolyser utilisation rate is around 92%. In this case, we see that a smaller hydrogen system increases its utilisation rate due to predefined daily hydrogen consumption up to 320 kg/day. Also, the increasing size of the hydrogen storage does not make sense. If the consumption increases, then it is a question of optimisation regarding which subsystem size is more worthwhile. The operation of the electrolyser can be seen in Figure 5.31.

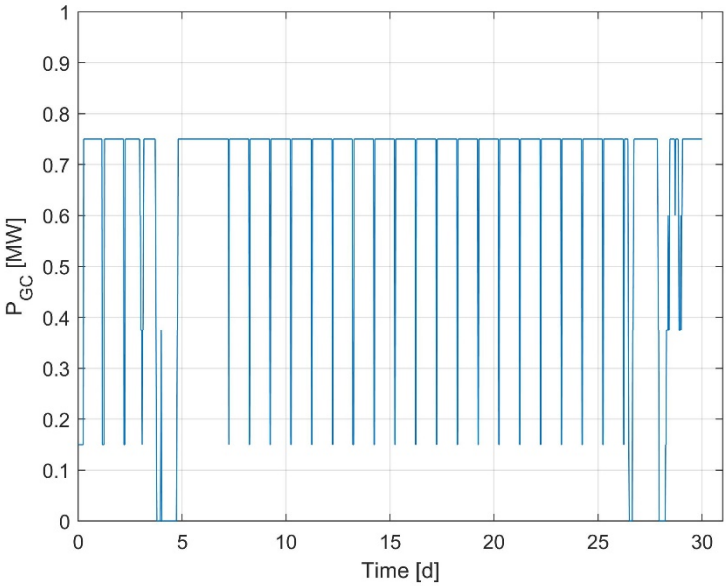

Figure 5.31: Hydrogen system's operation in November.

The income from hydrogen production with a configuration that includes the PV field with a nominal capacity of 6 MW is depicted in Figure 5.32. The hydrogen system with a 0.75-MW electrolyser and 20 m^3 hydrogen storage is only profitable in certain cases, because the relatively small hydrogen system cannot produce enough hydrogen to cover the investment in a large PV field. Further tests carried out with the Simulink model show that an income of 25,774.9 €/month is generated. In some system configurations, income is again negative.

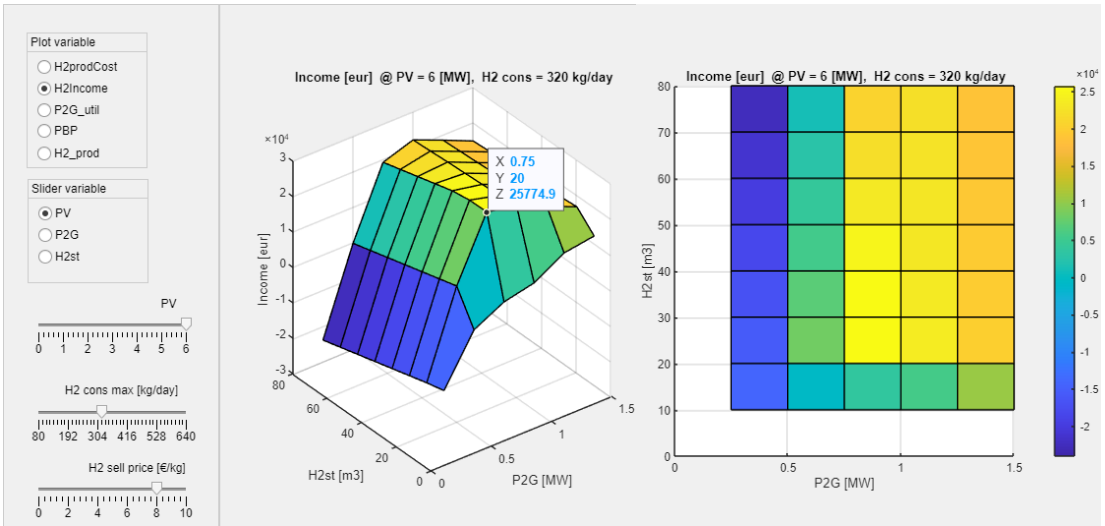

Figure 5.32: Income in November after the inclusion of 6-MW PV field.

Further simulations carried out in Simulink give us a total hydrogen production of 9475.29 kg/month

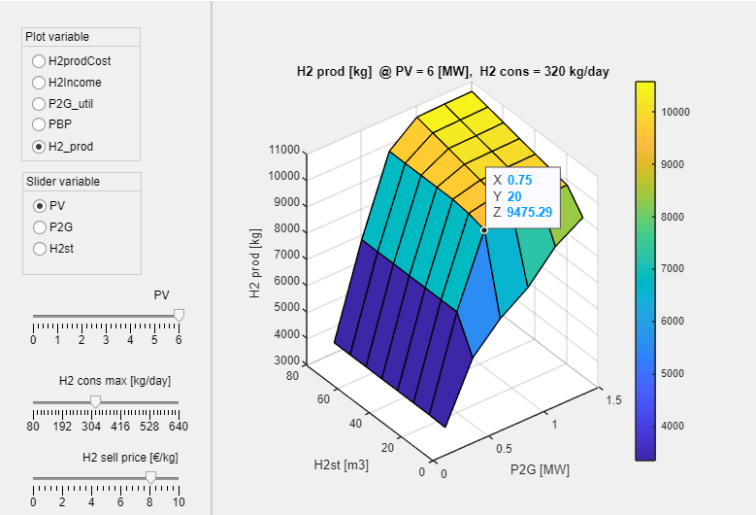

Figure 5.33: Monthly hydrogen quantity produced in November.

and the production costs for hydrogen (PC_{H2}) for the chosen system and an assumed hydrogen demand of up to 320 kg/day are around 5.28 €/kg, see Figure 5.34.

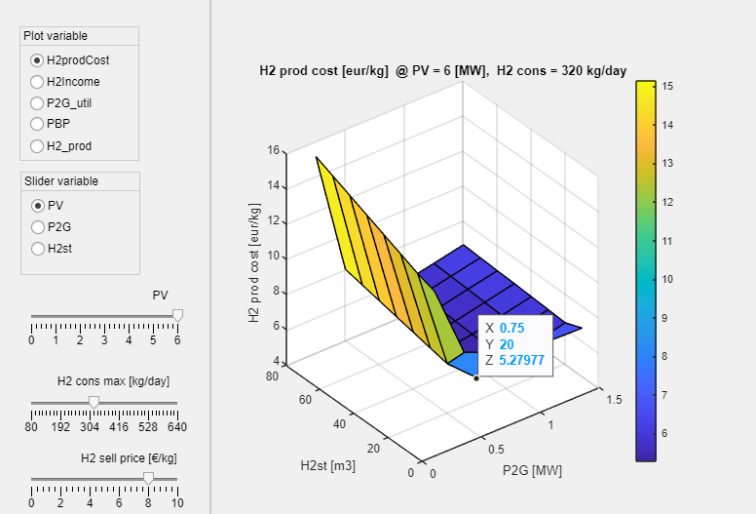

Figure 5.34: Hydrogen production cost in November after the inclusion of 6-MW PV field.

By further increasing the PV field to 6 MW it is possible to increase the utilisation rate of the electrolyser to around 95%, see Figure 5.35.

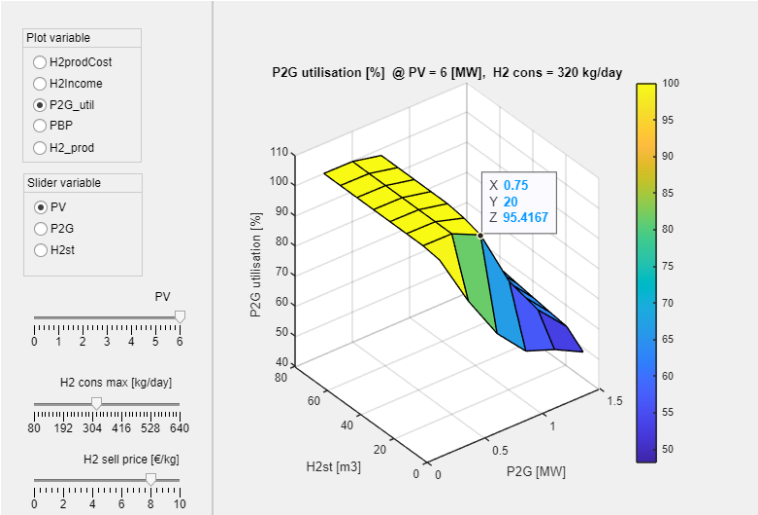

Figure 5.35: Hydrogen system's utilisation rate in November after the inclusion of 6-MW PV field.

The operation of the electrolyser can be observed in Figure 5.36.

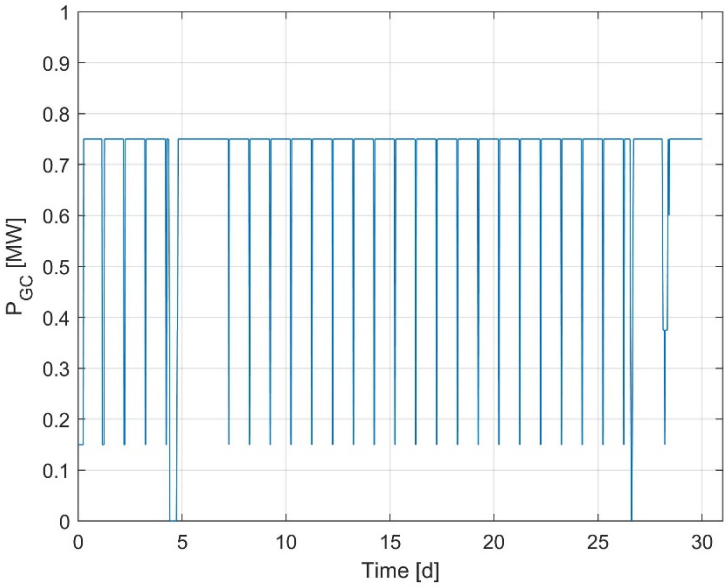

Figure 5.36: Hydrogen system's operation in November after the inclusion of 6 MW PV field.

5.2.3 Annual Simulations

From the above sections we can see that there are significant differences when operating in particular months, which can affect the justification of the investment in the hydrogen system. To get a clear and complete picture of the hydrogen system's operation, a simulation must be performed for the period of 1 year.

5.2.3.1 Simulation Results, Annual

The same procedure has been followed as in January and November, but this time for the period of 1 year. Figure 5.37 and Figure 5.38 show the simulation results. The maximum annual income, when $P_{PV\_INST} = 0$ MW, can be obtained with a 0.75-MW hydrogen system and a 20 m^3 storage tank for the assumed periodic consumption of hydrogen up to 320 kg/day and a hydrogen selling price of 8 €/kg. The resulting income can be as high as 444,042 €/year.

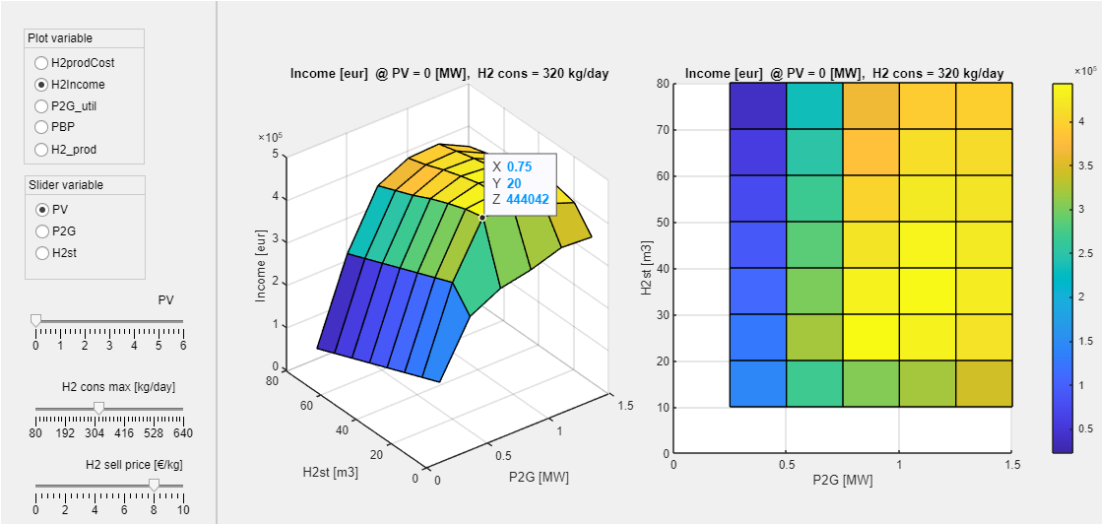

Figure 5.37: Proposed system configuration for maximum annual income from hydrogen production.

If the equipment is inappropriately dimensioned, the criterion function (e.g., $Income_{H2}$) may take on a negative value. This happens in cases where the equipment is oversized, too expensive (high CapEx) or underutilised (low hydrogen-system utilisation rate c). In this case the investment costs exceed the income from the sale of hydrogen. The figure shows such an example.

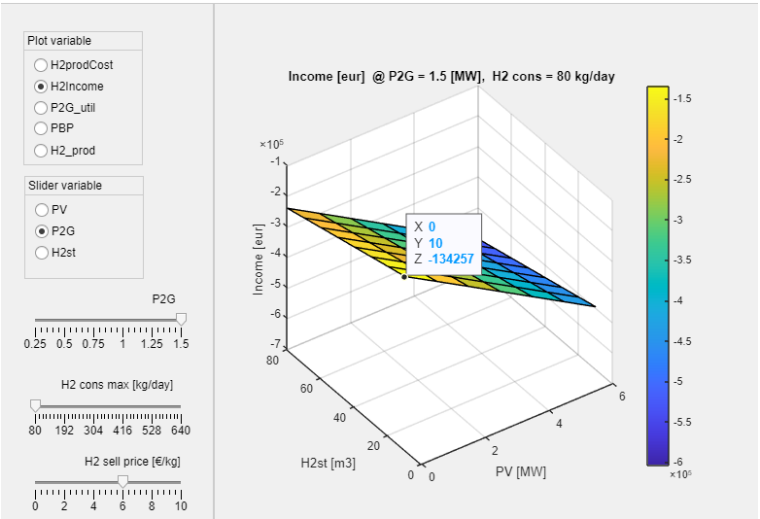

Figure 5.38: Example of over-dimensioned equipment that leads to negative $Income_{H2}$.

The chosen hydrogen-system configuration results in a total annual hydrogen production (without the additional electrical energy from the photovoltaic field, i.e., $P_{PV\_INST} = 0$ MW) of 86,088.6 kg/year, see Figure 5.39. This hydrogen production is only at the expense of the excess hydropower and does not affect the timetable of electrical energy supply to the grid. The simulation confirms that an existing hydro-power surplus appearing during the regular operation of the HPP can result in a moderate annual hydrogen production, see Figure 5.39.

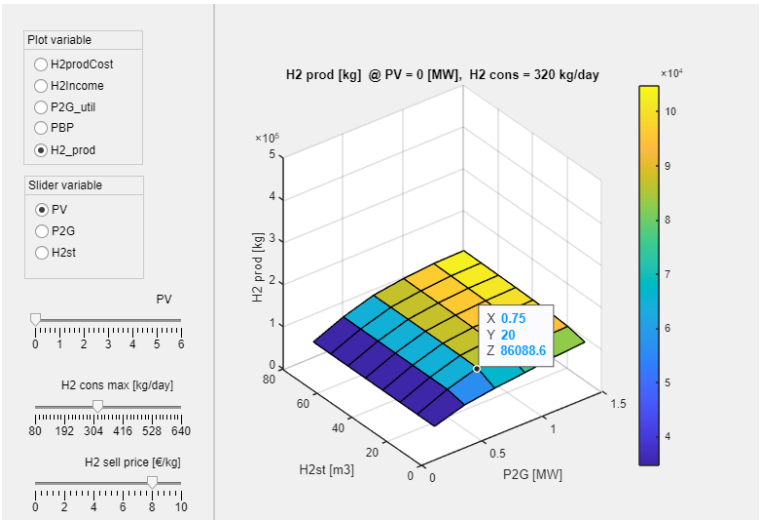

Figure 5.39: Annual hydrogen quantity produced.

With the same system setup, the production costs of hydrogen were explored again. Figure 5.40 shows an example of the representation of the production price of hydrogen in the GUI, expressed in €/kg, depending on the installed power of the hydrogen system and the size of the storage tank, for a system without the PV field ($P_{PV\_INST} = 0$ MW) and for the assumed periodic consumption of hydrogen up to 320 kg/day. The hydrogen-selling-price slider is again inactive in this case. The production costs for hydrogen (PC_{H2}) for the chosen system and an assumed hydrogen demand of up to 320 kg/day are around 2.84 €/kg, Figure 5.40.

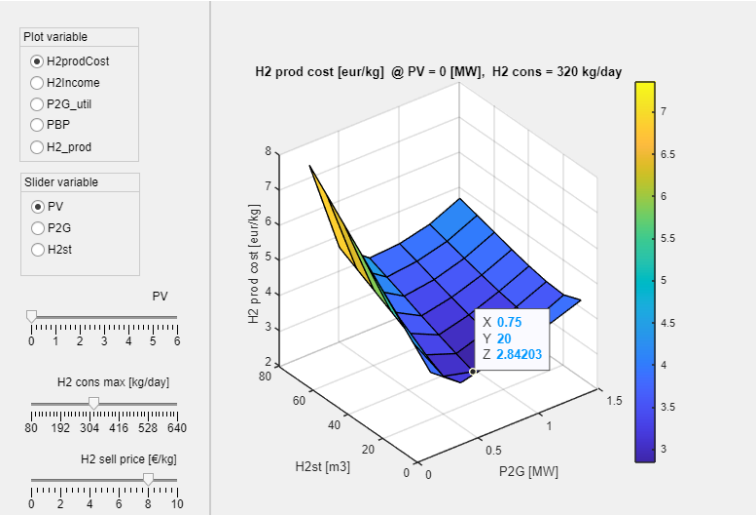

Figure 5.40: Annual production costs of hydrogen with a 0.75-MW hydrogen system, a 20 m^3 hydrogen-storage tank and a hydrogen demand up to 320 kg hydrogen per day.

Furthermore, the Hydrogen-System-Configuration Explorer can be used as an estimator for the utilisation rate of the hydrogen system in various configurations, see Figure 5.41.

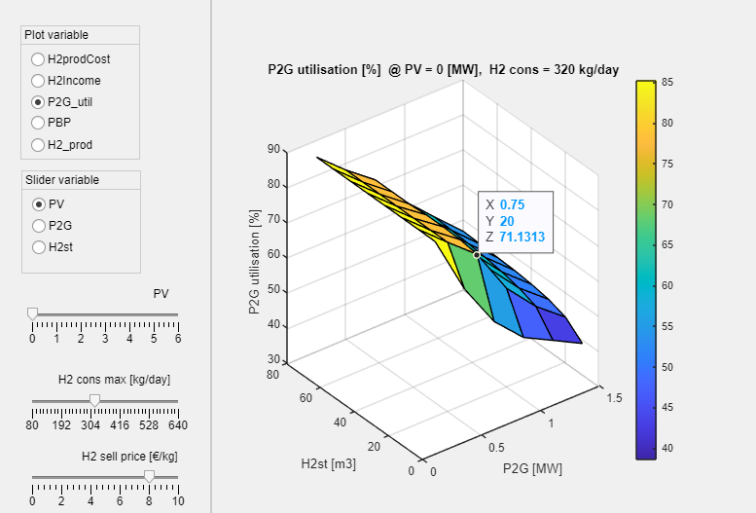

Figure 5.41: Annual hydrogen system's utilisation rate.

The 0.75-MW electrolyser's annual utilisation rate is around 71%. In this case, it was confirmed that a smaller hydrogen system increases the hydrogen system's utilisation rate due to low daily demand for hydrogen consumption. Also, increasing the hydrogen-storage size in this case is neither necessary nor sensible. The operating of the electrolyser can be seen in Figure 5.42.

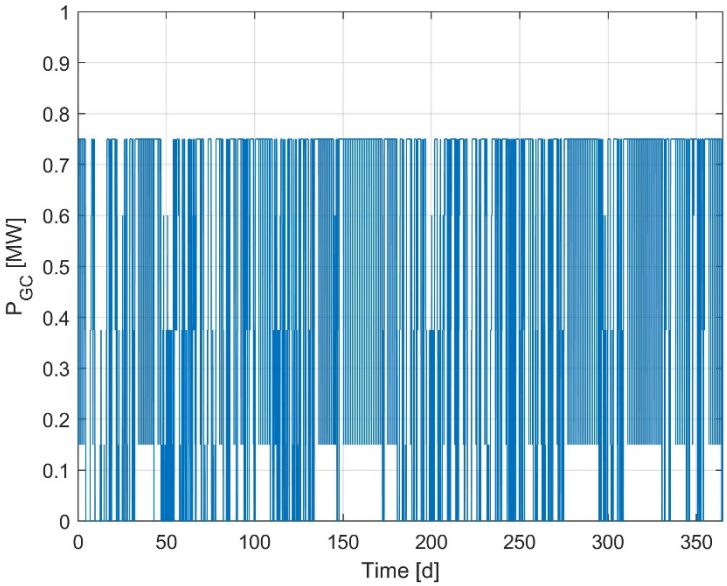

Figure 5.42: Annual hydrogen system's operation.

By increasing the PV field's nominal capacity to 6 MW, the simulated income is depicted in Figure 5.43. We see that the hydrogen system with a 0.75-MW electrolyser and 20 m^3 hydrogen storage cannot be profitable in all configurations (a too small electrolyser cannot produce enough hydrogen to cover the investment in a larger PV field and the income for the proposed system setup is negative). Further tests carried out with the Simulink model show that an income of up to 282,834 €/year is generated.

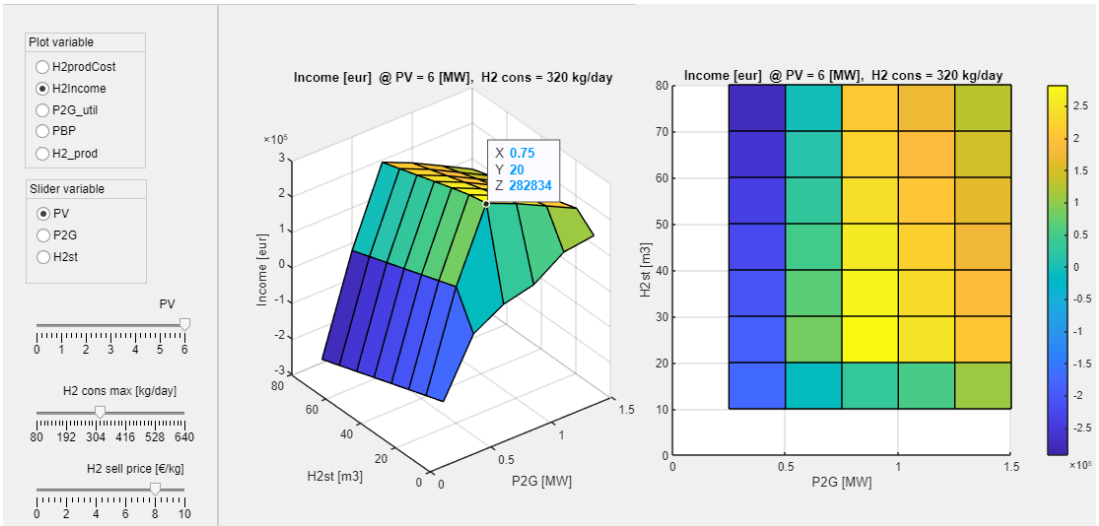

Figure 5.43: Annual income after the inclusion of 6-MW PV field.

Further simulations give a total hydrogen production of 111,438 kg/year,

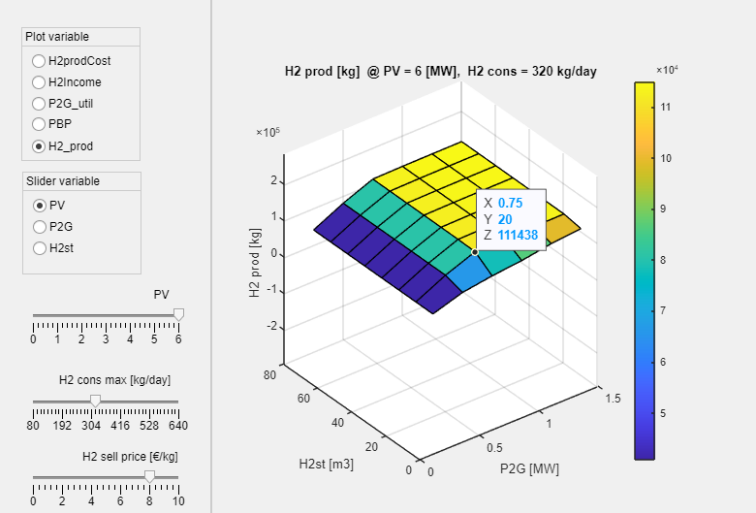

Figure 5.44: Annual hydrogen quantity produced.

and the production costs for hydrogen (PC_{H2}) for the chosen system and an assumed hydrogen demand of up to 320 kg/day are around 5.46 €/kg, see Figure 5.45.

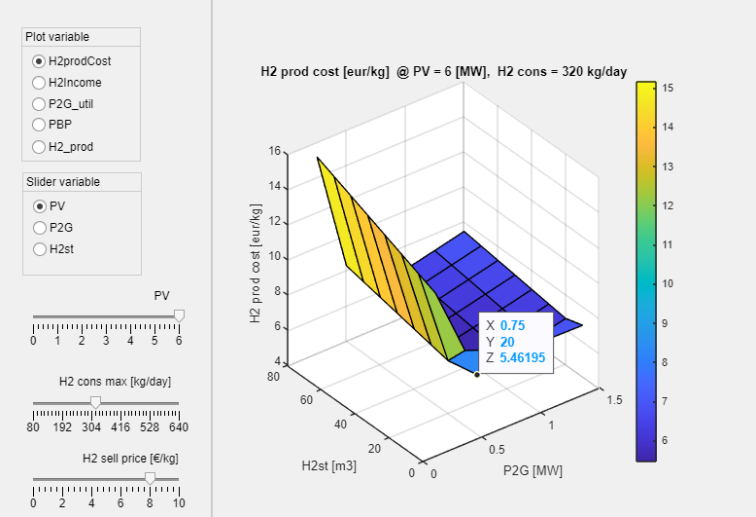

Figure 5.45: Annual hydrogen production costs after the inclusion of 6-MW PV field.

By further increasing the PV field to 6 MW, it is possible to increase the utilisation rate of the electrolyser up to approximately 92%, see Figure 5.46.

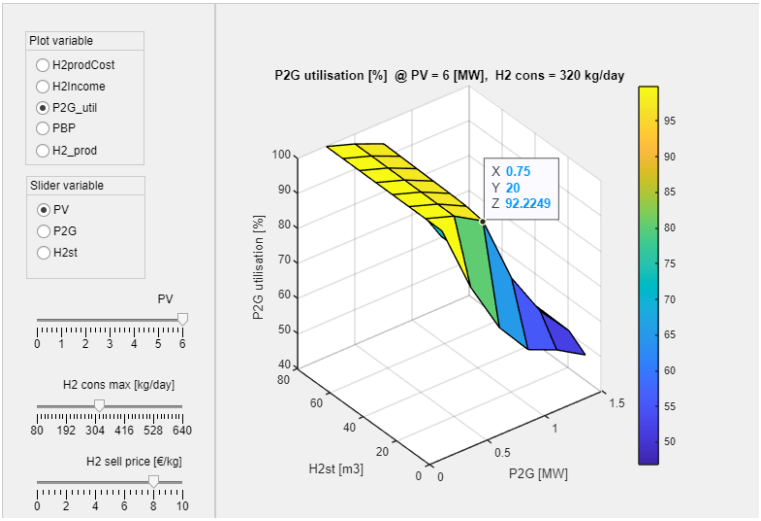

Figure 5.46: Annual hydrogen system's utilisation rate using 0.75 MW electrolyser with the inclusion of 6-MW PV field.

The operation of the electrolyser can be seen in Figure 5.47.

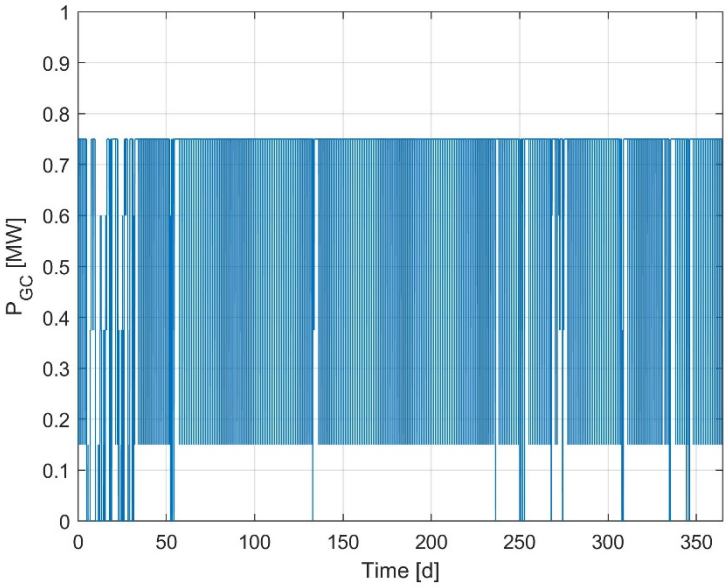

Figure 5.47: Annual hydrogen system's operation after the inclusion of 6-MW PV field.

5.2.3.2 Simulation Results, Annual with Reduced CapEx Costs

To evaluate the assumption that the costs of the equipment can drastically affect the hydrogen system's proposed configuration, we performed simulation runs with half the price of the equipment (a 50% CapEx reduction). In reality, this could be implemented by subsidizing the equipment cost by various governmental subsidies supporting a green transition.

The same procedure has been followed as in the above chapter (an annual simulation), but this time the equipment's CapEx costs have been reduced by half. Figure 5.48 shows

the simulation results. The maximum annual income, when $P_{PV\_INST} = 0$ MW and the CapEx costs are reduced by half, can be obtained with a 1.25 MW hydrogen system and a 70 m^3 storage tank for the assumed periodic consumption of hydrogen up to 320 kg/day and a hydrogen selling price of 8 €/kg. As the hydrogen-production costs are halved, the resulting income can be as high as 609,445 €/year. In this case the income is positive in all system configurations.

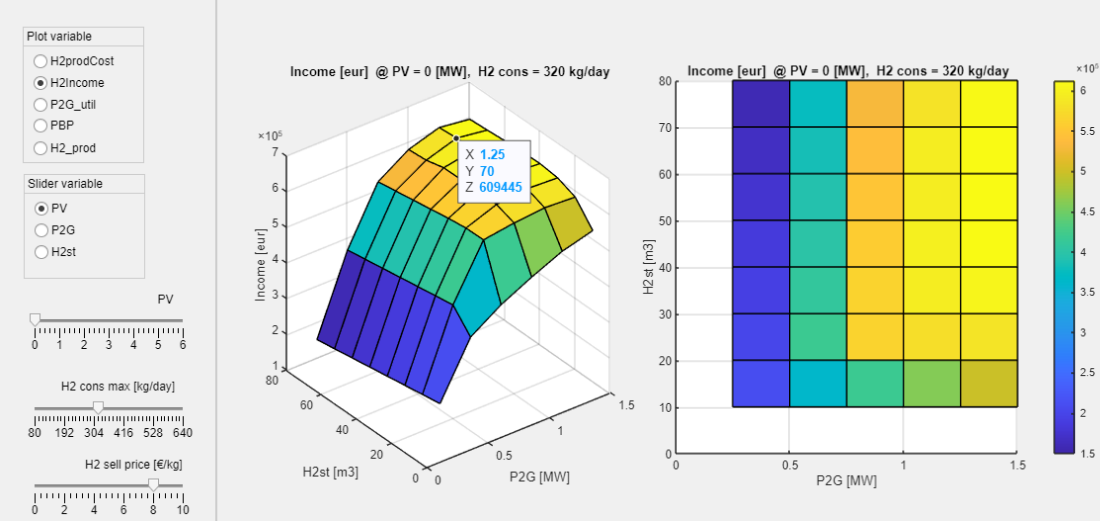

Figure 5.48: Proposed system configuration for maximum annual income from hydrogen production.

The chosen hydrogen system's configuration results in the total annual hydrogen production (without the additional electrical energy from the photovoltaic field, i.e., $P_{PV\_INST} = 0$ MW) of 102,722 kg/year.

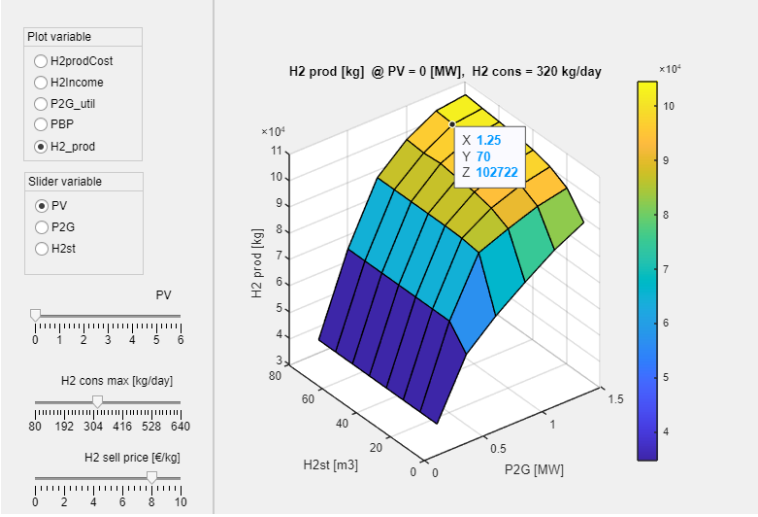

Figure 5.49: Annual quantity of hydrogen produced.

5.2.4 Annual Income Relative to Hydrogen Price

Using a 0.75-MW hydrogen system, a 20 m^3 hydrogen-storage tank, a predefined hydrogen demand of up to 320 kg of hydrogen per day and without including a PV field, the annual

income from the sale of hydrogen at different selling prices was simulated. The results are depicted in Figure 5.50.

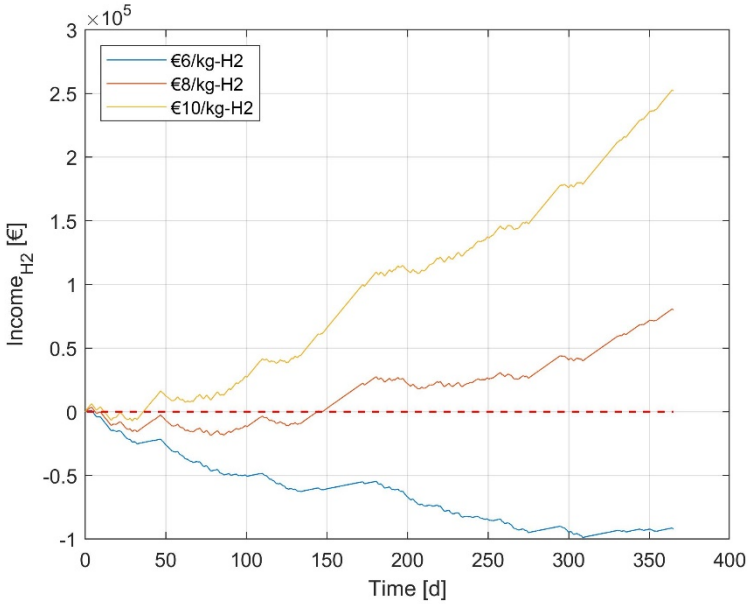

Figure 5.50: Comparison of income at different selling prices of hydrogen, PV = 0 MW.

From Figure 5.50 it follows that the income is negative at the beginning of the year even if hydrogen price is 10 €/kg. The reason is that at the beginning of the year there is no excess of hydropower and therefore no hydrogen is produced and sold. On the other hand, the hydrogen system always generates costs due to CapEx (see Section 3.6). The increase in income from hydrogen generation is also not continuous, as the availability of excess electricity is very volatile.

In addition, the annual income from the sale of hydrogen generated by the same system setup upgraded with a secondary power source (i.e., a 6-MW PV field) was simulated, see Figure 5.51. Due to the integration of the additional energy source, the excess electrical energy is available for almost the entire year. A constant power input (excess electricity) results in a constant hydrogen flow. This is also reflected in the operation of the hydrogen system (see Figure 5.47), and consequently the income from hydrogen generation is more constant than in the previous case.

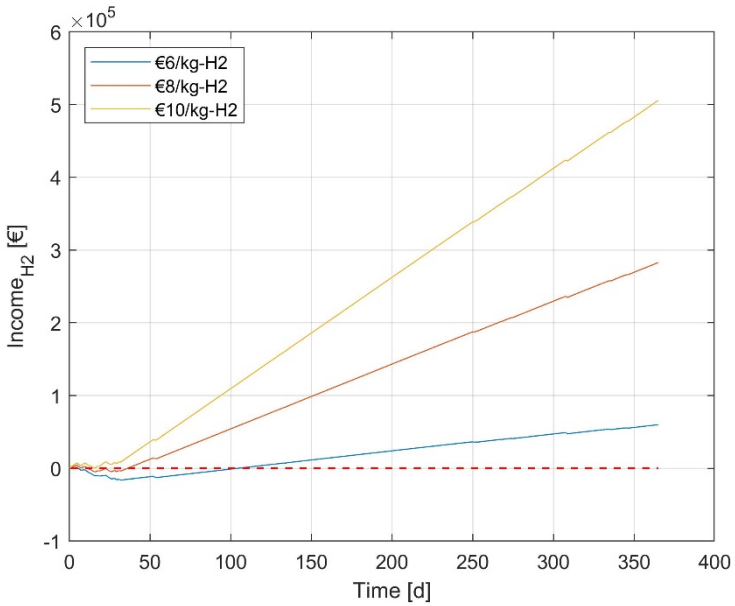

Figure 5.51: Comparison of income at different selling prices of hydrogen, PV = 6 MW.

5.2.5 Payback Period of the Hydrogen System Relative to Hydrogen Price

The calculated payback period (*PBP*) for the implementation of the chosen hydrogen system (0.75-MW electrolyser and 20 m^3 hydrogen-storage tank), and without including a PV field, is between 1.36–2.38 years, depending on the selling price of the hydrogen.

In this case, the utilisation rate of the hydrogen system is around 71%.

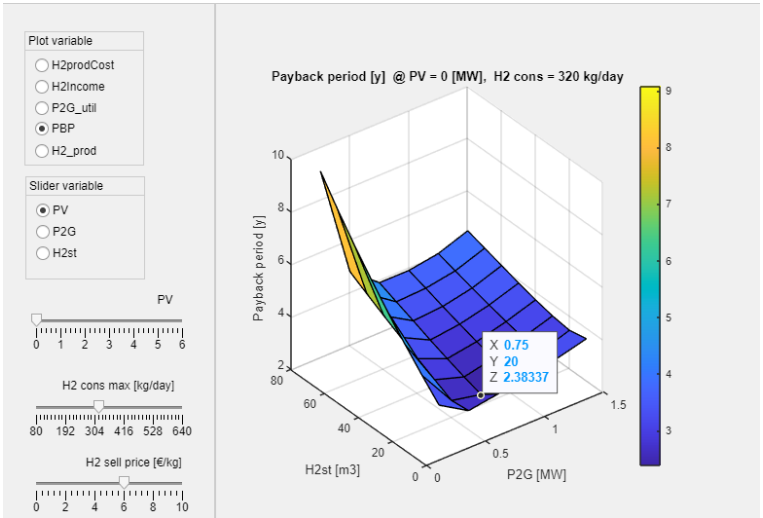

Figure 5.52: Payback period of investment when hydrogen selling price is 6 €/kg.

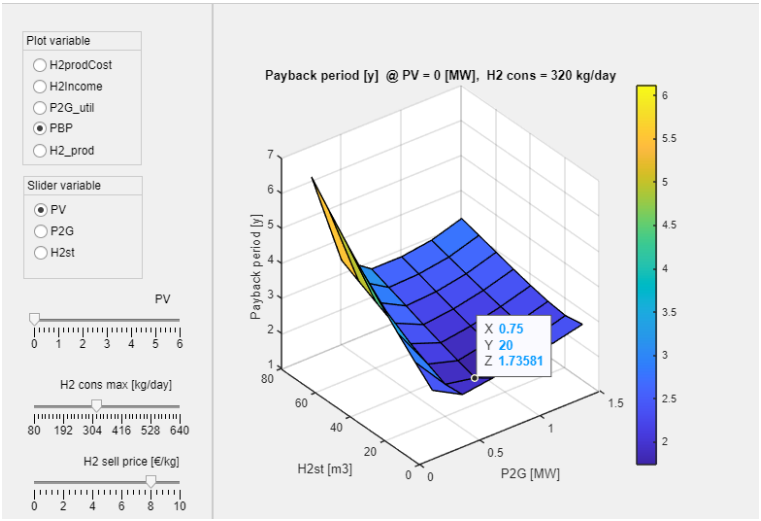

Figure 5.53: Payback period of investment when hydrogen selling price is 8 €/kg.

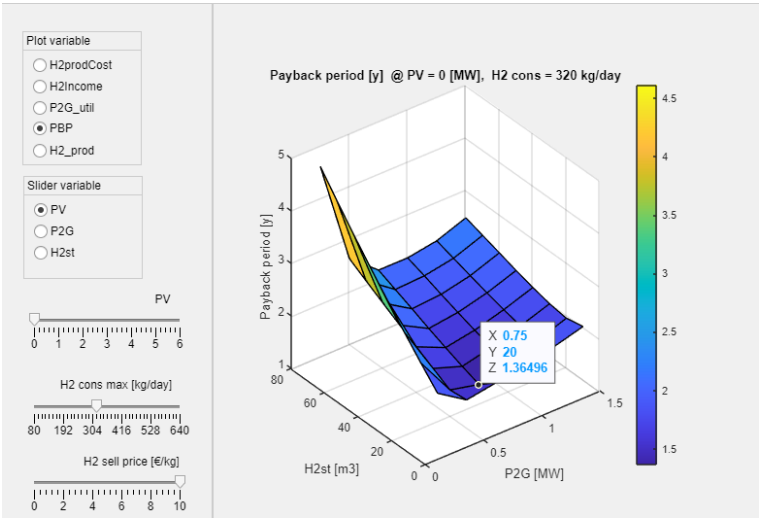

Figure 5.54: Payback period of investment when hydrogen selling price is 10 €/kg.

5.2.6 Conclusions about Hydrogen-System-Configuration Explorer

The developed system model (i.e., Complete Model) together with the Hydrogen-System-Configuration Explorer represents an effective tool for manually sizing the hydrogen system and exploring the effect of particular parameters. It provides an important insight into the operating details and limitations of the hydrogen system's configuration. The above experiments illustrate the potential to quickly evaluate different equipment configurations. In general, we can benefit from a certain amount of manual optimisation, especially at the beginning of the project when we have a general idea of the targeted hydrogen system and its field of application.

5.3 Hydrogen-System-Configuration Optimiser

In the previous Subsection 5.2, a design support tool, the Hydrogen-System-Configuration Explorer, was presented, which provides the possibility to estimate the optimal system parameters for a given objective function. The presented method is based on a number of simulation runs performed over the defined range of process parameters and enables an efficient and transparent sizing of the hydrogen system's main components. It belongs to a class of exhaustive (also called brute-force) optimisation methods, which systematically explore all the potential combinations of parameters in search of the best solution. The Hydrogen-System-Configuration Explorer is a very useful design and decision-support tool; however, some of its certain properties leave room for improvements.

- *Due to the parameter space discretisation, the accuracy of the indicated optimal solution is limited and sometimes more accurate results are needed.*
- *Only a limited number of parameters subjected to optimisation can be included in the simulation to keep the computation acceptable. If the number of optimised parameters is increased, the number of parameter combinations increases progressively and so does the computational burden and simulation time.*
- *In case some parameter, which is not the subject of optimisation, is changed, the whole set of simulations must be repeated, which is time consuming and can in some cases represent a drawback.*

To overcome these challenges, an additional system design tool was prepared (i.e., Hydrogen-System-Configuration Optimiser), which is based on heuristic optimisation methods. The Particle-Swarm Optimisation (PSO) method [191], [192], [193] was selected due to its intuitive algorithm, which can also be understood by engineers not specialised in the field of computational optimisation methods. Alternative methods are Genetic Algorithms, Simulated Annealing and many others [194]. Most importantly, the PSO algorithm does not require the simulation of all combinations of the process parameters and in this way more parameters can be the subject of optimisation while keeping the computational load and optimisation time at an acceptably low level.

In general, the mathematical optimisation problem can be formulated as follows:

$$\min_{x} \quad f(\boldsymbol{x}) \qquad \textit{or} \qquad \max_{x} \quad f(\boldsymbol{x}) \tag{5.2}$$

where $\boldsymbol{x}$ is the vector of parameters subjected to optimisation Eq. (5.2) with their constraints and $f(\boldsymbol{x})$ is an objective function. This means that the method searches for parameter vector $\boldsymbol{x}$, which gives the minimum (or maximum) value of $f(\boldsymbol{x})$. Usually, objective functions such as cost or energy consumption are the subject of minimisation, while objective functions like financial outcome of hydrogen produced are the subject of maximisation.

Note that in our case, $f(\boldsymbol{x})$ is not an analytic function of the parameter vector $\boldsymbol{x}$. For a given vector of parameters $\boldsymbol{x}$, the function $f(\boldsymbol{x})$ is evaluated by performing a simulation run of the complete process over the desired time interval (e.g., 1 year) and then calculating the desired objective function f. In this case, different objective functions are possible, and

they represent different technical or economic key-performance-indicators of hydrogen system's operation.

5.3.1 Particle-Swarm Optimisation

The PSO algorithm can find finding the optimal solution (either local or global) with a relatively small number of system operation simulations [195].

The PSO algorithm consists of a series of proposed solutions (particles) with a random initial position. Each particle represents an instance of parameter vector $\boldsymbol{x}$. The algorithm solves an optimisation problem by using a population (a swarm) of candidate solutions (particles) and by moving these particles around in the search space according to simple mathematical formula over the particle's position and velocity. Two equations are involved in the algorithm. In the equations, i represents the index of an individual particle, i_{TOT} represents the number of all the particles, and n represents the number of current iterations. Eq. (5.3) is called the velocity equation [196].

$$\boldsymbol{v}^i(n+1) = w \cdot \boldsymbol{v}^i(n) + c_1 \cdot r_1 \cdot \left(\boldsymbol{pbest}^i - \boldsymbol{x}^i(n)\right) + c_2 \cdot r_2 \cdot \left(\boldsymbol{gbest}^i - \boldsymbol{x}^i(n)\right) \tag{5.3}$$

It is used to update the velocity (movement) of each particle ($i = 1 \ldots i_{TOT}$) in the n-th step/iteration by using the computed values of the individual and global best solutions and its current position. The velocity in fact represents an increment from the current position $x^i(n)$ to the new position $x^i(n+1)$. The r_1 and r_2 represent user-defined gains between 0 and 1, constants w (inertia), c_1 (self-adjustment weight), and c_2 (social adjustment weight) are the parameters to the PSO algorithm. Personal best $\boldsymbol{pbest}^i$ is the position that gives the best objective function $f(\boldsymbol{x})$ value explored by particle i and global best $\boldsymbol{gbest}^i$ is the best objective function $f(\boldsymbol{x})$ value ever explored by all the particles in the swarm.

The second equation (see Eq. (5.4)) is called the position equation [196], used for updating each particle's position using the calculated velocity from Eq. (5.3):

$$\boldsymbol{x}^i(n+1) = \boldsymbol{x}^i(n) + \boldsymbol{v}^i(n+1) \tag{5.4}$$

Note that each particle's movement is influenced by its local best-known position, but it is also guided towards the best-known positions in the search-space, which are updated as better positions are found by other particles. An iteration of a single particle's shift is illustrated in Figure 5.55.

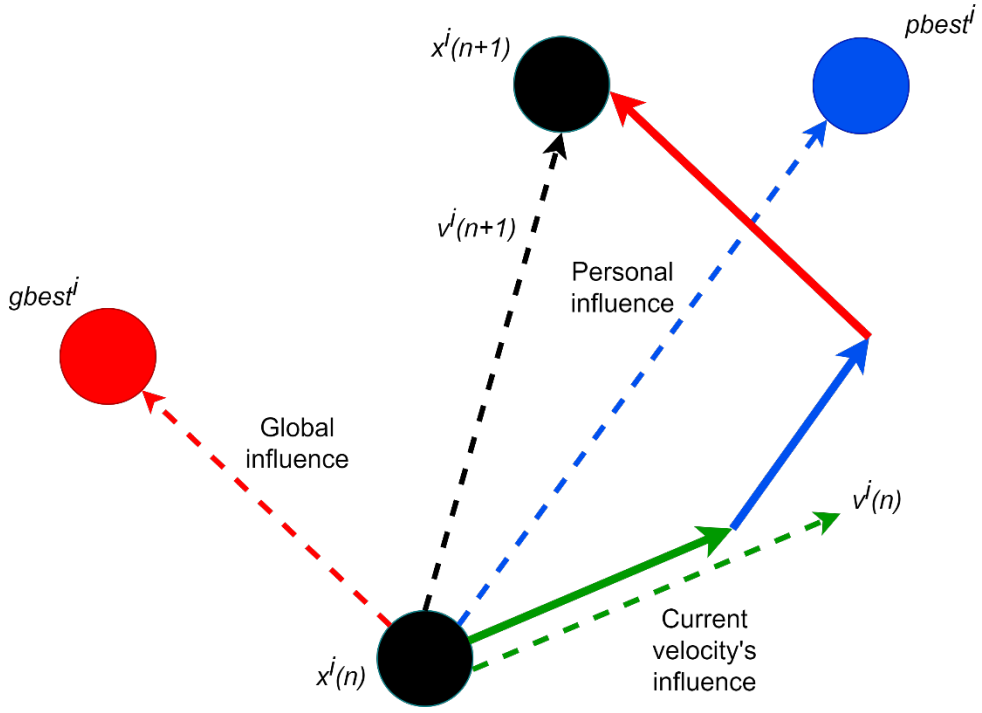

Figure 5.55: Individual particle shift in one iteration [197].

As the number of iterations increases, so will the convergence rate to the best-known position. The result is a heuristic solution because it cannot be proved that the real global optimal solution has been found. The optimisation is complete when the solution is located at a point that appears to be a (local or global) minimum.

In our case, the PSO algorithm was implemented in MATLAB using the *Optimisation Toolbox* and the *fmincon* function to perform the minimisation process, taking into account the constraints. An automation script was also developed (*optim_script,* [190]), which starts the simulation of the model for a given set of system parameters, calculates the selected residuals and enables the automatic search for the optimum for the selected objective function. The whole iterative optimisation procedure is illustrated in Figure 5.56.

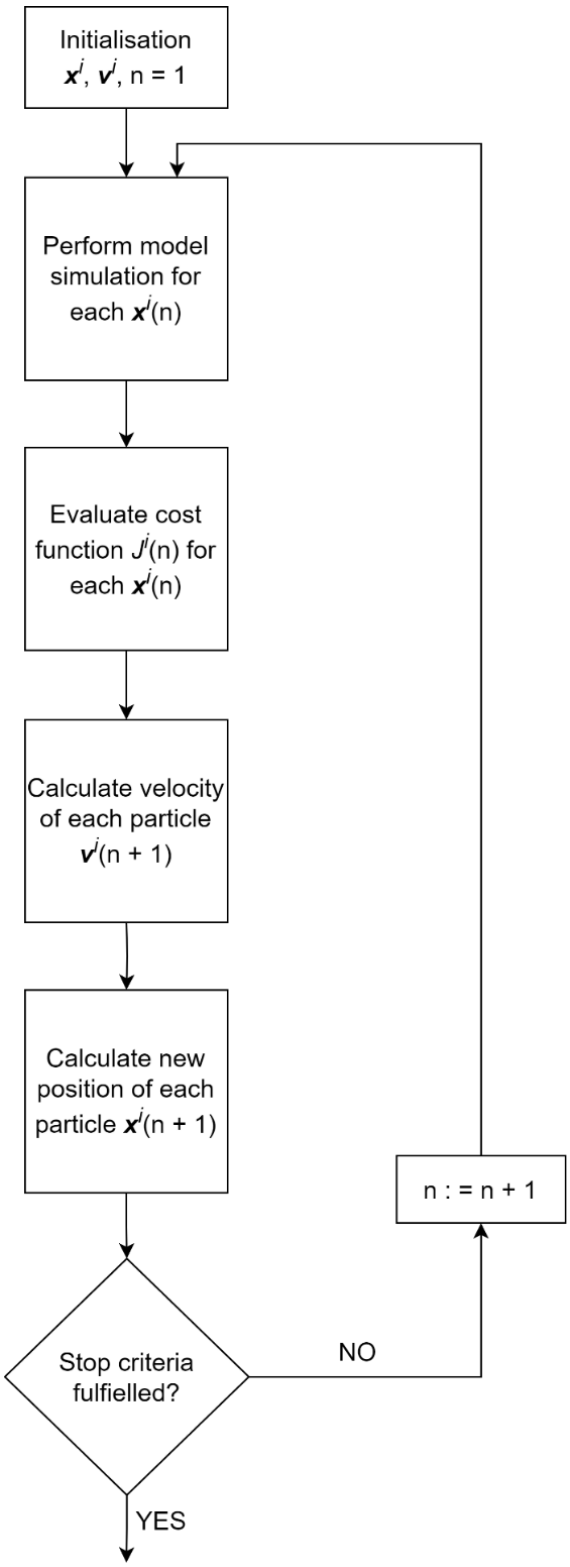

Figure 5.56: Graphical presentation of the *optim_script.*

5.3.2 Optimised Parameters and Objective Functions

Parameters, that are the subject of optimisation, represent the components of vector $\boldsymbol{x}$; ($\boldsymbol{x} = [P_{EL\_SYS}, P_{PV\_INST}, V_{GEO}]$). Table 5.17 shows the range of each parameter (component of the vector $\boldsymbol{x}$).

Table 5.17: List of optimised parameters and their constraints.

Parameter	Description	Range	Units
P_{EL_SYS}	Nominal power of the electrolyser system	[0.25…1.5]	MW
P_{PV_INST}	Nominal power of the photovoltaic field	[0…6]	MW
V_{GEO}	Volume of the hydrogen storage tank	[10…80]	m^3

Table 5.18 shows a list of examples of objective functions, which in general represent technical and economic key-performance indicators. Note that also other kinds of objective functions can also be used, depending on the priorities during the design of a particular hydrogen system and related techno-economic targets. Combinations of several basic objective functions can also be used.

Table 5.18: Examples of objective functions.

Techno-economic target	$J = f(x)$
Maximisation of income (implemented as minimisation of negative income)	$J = -Income_{H2} = -\int_0^{t_{end}} \dot{m}_{IN}(t) \cdot \left(SP_{H2}(t) - PC_{H2}(t)\right) \cdot dt$
Search for hydrogen system's components size to produce the predefined amount of hydrogen	$J = (Q_{H2\_OUT\_DEM} \cdot 365\ [d] - m_{H2\_PROD})^2$
Combination of both objective functions	$J = -k_1 \cdot \left(\frac{Income_{H2}}{Income_{H2_{MAX}}}\right) + k_2 \cdot \left(\frac{m_{H2_{PROD}} - Q_{H2\_OUT\_DEM} \cdot 365\ [d]}{Q_{H2\_OUT\_DEM} \cdot 365\ [d]}\right)^2$

In the following subsections, examples of optimisation are given, and they are performed according to the object functions defined in Table 5.18 above. In all cases, the selling price of the hydrogen SP_{H2} was set to 8 €/kg. The maximum pressure in the tank is assumed to be 350 bar, as defined in previous sections.

5.3.3 Optimisation of Income

As the first example, let the objective function be the annual income from hydrogen production ($J = -Income_{H2}$):

$$J = -Income_{H2} = -\int_{0}^{t_{end}} \dot{m}_{IN}(t) \cdot \left(SP_{H2}(t) - PC_{H2}(t)\right) \cdot dt \tag{5.5}$$

The negative value of $Income_{H2}$ is used, since minimum criteria are used during the optimisation. Minimising a negative value of the income actually means maximising the income.

The solution of this optimisation problem gives the optimal configuration of the hydrogen system for reaching the highest annual income generated by hydrogen production in the case-study HPP.

The constraints of the parameters from Table 5.17 correspond to the ranges of the parameters defined in Table 5.12.

During the iterative optimisation procedure, the selected important output parameters of the model are displayed (Table 5.19).

Table 5.19: Selected important output parameters of the model.

Parameter	Units	Parameter Description
m_{H2_PROD}	kg/y	Annual mass of produced hydrogen
PC_{H2}	€/kg	Production cost of hydrogen
c	%	Utilisation rate of the hydrogen system
$Income_{H2}$	€/kg	Income from the production of hydrogen

The optimisation results show that the optimal configuration for reaching the highest annual income taking into account the installation costs of the hydrogen system and the current operating regime of the case-study HPP is:

- *Hydrogen system's maximum power (*P_{EL_SYS}*): 0.9060 MW*
- *Photovoltaic field's nominal (installed) power (*P_{PV_INST}*): 0 MW*
- *Volume of hydrogen-storage tank (*V_{GEO}*): 28.0098 m*^{3}

Under these conditions, the annual hydrogen production is 76,601.46 kg, the corresponding annual income is 349,290.41 €/y and the hydrogen system's utilisation rate is 75.01 %. It should be noted that in this case the average daily hydrogen consumption is approximately 210 kg/d, which means that the hydrogen demand (320 kg/d) is not completely fulfilled, but this is not penalised. Note that the maximum income may not necessarily mean the maximum production of hydrogen, but the best combination of low system costs and revenue from sold hydrogen.

Table 5.20 gives a further insight into the optimisation procedure by showing the following variables during optimisation iterations:

- *Iteration — Index of current iteration (n in Eq.* (5.3) and Eq. (5.4)*)*
- *f-count — Cumulative number of objective function evaluations (since there are 100 particles in the swarm, the total number of objective function evaluations is increased by 100 in each iteration)*
- *Best f(x) — Best objective-function value (in this case* $Income_{H2}$*)*
- *Mean f(x) — Mean objective-function value over all particles*

- *Stall Iterations — Number of iterations since the last change in Best f(x)*

Table 5.20: Displayed information.

Iteration	f-count	Best f(x)	Mean f(x)	Stall Iteration
0	100	-4.239e+05	-2.364+05	0
1	200	-4.239e+05	-1.676e+05	0
2	300	-4.438e+05	-3.227e+05	0
3	400	-4.442+05	-3.273e+05	0
4	500	-4.455e+05	-3.223e+05	0
5	600	-4.455e+05	-3.075e+05	1
6	700	-4.455e+05	-3.282e+05	2
7	800	-4.455e+05	-3.301e+05	3
8	900	-4.455e+05	-3.233e+05	4
9	1000	-4.455e+05	-3.361e+05	5
10	1100	-4.455e+05	-3.283e+05	6
11	1200	-4.455e+05	-3.749e+05	7
12	1300	-4.46e+05	-4.066e+05	0
13	1400	-4.463e+05	-4.22e+05	0
14	1500	-4.466e+05	-4.353e+05	0
15	1600	-4.467e+05	-4.16e+05	0
16	1700	-4.469e+05	-4.441+05	0
17	1800	-4.469e+05	-4.448e+05	1
18	1900	-4.469e+05	-4.462e+05	2
19	2000	-4.469e+05	-4.464e+05	0
20	2100	-4.469e+05	-4.466e+05	1
21	2200	-4.47e+05	-4.467e+05	0

The term *Stall iteration* defines an iteration where particles were moved, but the best solution of the best particle was not better than the current best global solution. In the table, green fields represent the last best global objective function, while yellow fields show stall iterations, see also Figure 5.57.

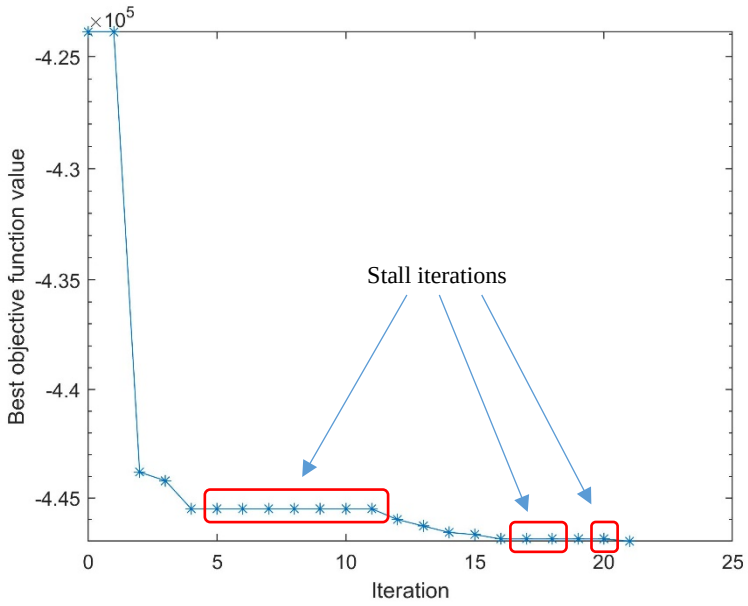

Figure 5.57: Values of the objective function J.

Figure 5.58 shows the "ranges of parameters", which is a characteristic plot of the PSO algorithm and illustrates the convergence of the optimised parameters during the iterations. As mentioned earlier, in each iteration a number of parameter vectors (particles) are moved in search for the optimal solution. Ideally, after a number of iterations, all the particles should converge to the same global optimal solution if it exists for a given optimisation problem. Figure 5.58 contains three plots, since in our case three parameters are the subject of the optimisation (P_{EL_SYS}, P_{PV_INST}, V_{GEO}). Each plot shows the range of a particular parameter, which is the difference between the current maximum and minimum values of a particular parameter in the entire set of particles. At the beginning of the iterations, the ranges of the parameters are large, since parameter vectors (particles) are randomly distributed over the entire parameter space. Later during the iterations, if the parameters converge towards a global optimal solution, the ranges of the parameters converge to zero, indicating that the optimum has been found. The y-axes of the plots are represented on a logarithmic scale to better represent the possible wide ranges of parameters.

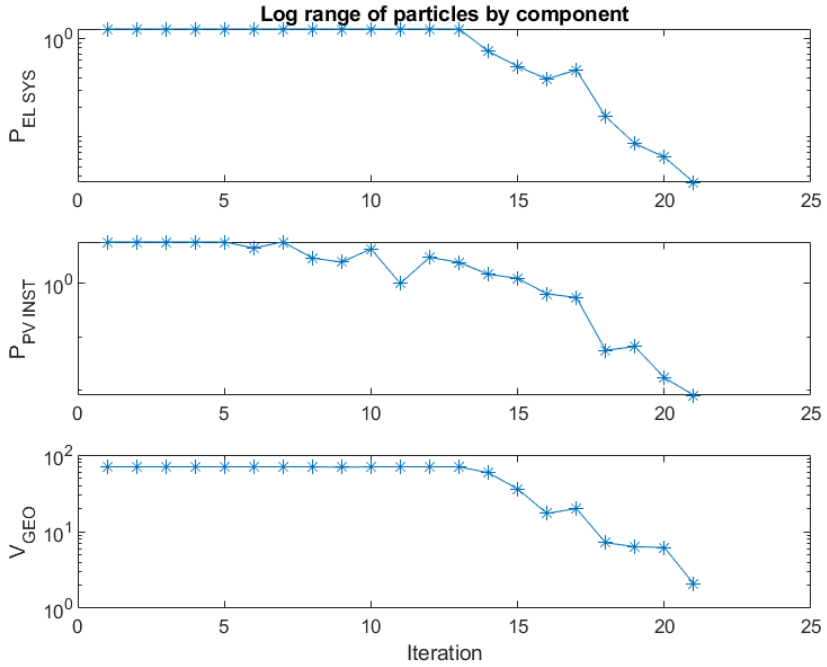

Figure 5.58: Parameter ranges: the top graph shows the maximum power of the hydrogen system, the centre graph the nominal power of the PV field, and the bottom graph the volume of the storage tank.

5.3.4 Optimisation of Hydrogen System's Size to Produce the Predefined Amount of Hydrogen

The next case of sizing the hydrogen-system components by using optimisation methodology is to find the optimal size of the hydrogen-system equipment to match the pre-demanded annual hydrogen production. In fact, we are looking for the size of hydrogen system that has the highest possible utilisation rate (close to 100 %). In this case, the objective function can be defined as:

$$J = f(x) = \left(Q_{H2\_OUT\_DEM} \cdot 365\,[d] - m_{H2\_PROD}\right)^2 \tag{5.6}$$

where in our case the demanded predefined hydrogen production is $Q_{H2\_OUT\_DEM}$ = 160 kg/day.

The results of optimisation show that the (local) optimal configuration for reaching the desired annual production of hydrogen respecting both the installation costs of the hydrogen system and PV field and the current operating regime of the case-study HPP are:

- *Hydrogen system's maximum power (*P_{EL_SYS}*): 0.3551 MW*
- *Photovoltaic field's nominal (installed) power (*P_{PV_INST}*): 6 MW*
- *Volume of hydrogen-storage tank (*V_{GEO}*): 35.2141 m³*

where the annual hydrogen production is 58,400 kg/y (160 kg/d), the hydrogen system utilisation rate is above 98 % and the corresponding annual income is negative (–94,119.66 €/y) due to the high costs of the necessary hydrogen system equipment, the costs of the PV field's installation and low predefined volume of daily hydrogen production. The results are shown in Table 5.21, Figure 5.59 and Figure 5.60.

This example searches for the optimal parameters of the hydrogen system, which result in the required amount of hydrogen being produced, while neglecting the economic issue of operation. As a result, in this case, the annual income is negative. To overcome this, additional criteria can be incorporated into objective function and this is addressed in the next subsection.

Table 5.21: Displayed information.

Iteration	f-count	Best f(x)	Mean f(x)	Stall Iteration
0	100	2.117e+06	1.653e+09	0
1	200	2.117e+06	1.098e+09	0
2	300	5049	5.593e+08	0
3	400	2.648	3.793+08	0
4	500	2.648	4.271e+08	1
5	600	2.648	3.574e+08	2
6	700	2.648	3.271e+08	3
7	800	2.648	3.971e+08	4
8	900	2.648	3.339e+08	5
9	1000	2.648	4.496e+08	6
10	1100	2.648	2.117e+08	7
11	1200	2.648	1.115e+08	8
12	1300	2.648	9.44e+07	9
13	1400	2.648	3.589e+07	10
14	1500	2.648	2.118e+07	11
15	1600	2.648	9.469e+06	12
16	1700	2.099	9.075e+07	0
17	1800	0.009054	1.612e+07	0
18	1900	0.001617	1.056e+07	0
19	2000	9.032e-05	1.177e+07	0
20	2100	7.143e-05	1.311e+07	0
21	2200	4.442e-05	1.163e+07	0
22	2300	7.126e-06	9.693e+06	0
23	2400	5.513e-06	5.647e+06	0
24	2500	4.946e-06	9.4e+06	0
25	2600	3.775e-07	1.076e+07	0
26	2700	4.387e-09	1.041e+07	0
27	2800	4.387e-09	5.928e+06	1
28	2900	4.387e-09	1.079e+07	2
29	3000	4.387e-09	5.05+06	3
30	3100	6.709e-12	5.848e+06	0
31	3200	6.709e-12	6.543e+06	1
32	3300	3.553e-12	1.326e+07	0
33	3400	4.384e-13	5.217e+06	0
34	3500	3.083e-14	4.153e+06	0
35	3600	3.083e-14	3.898e+06	1
36	3700	3.083e-14	17.117e+06	2

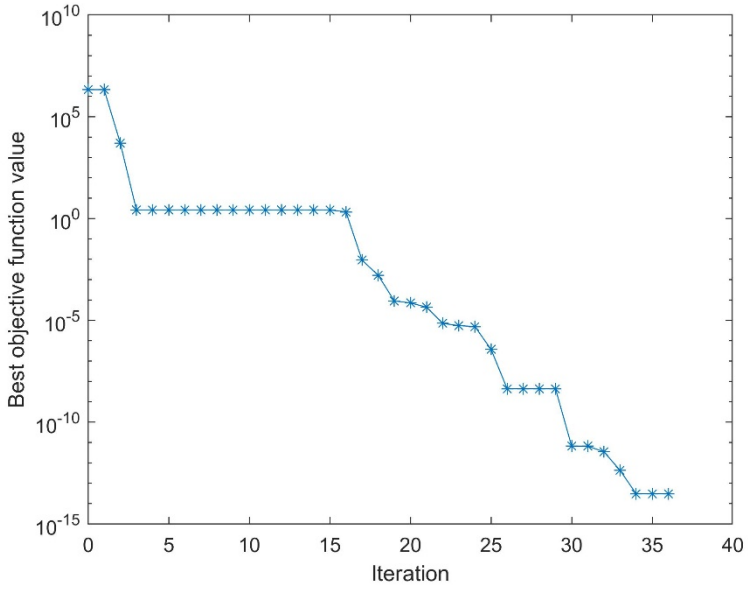

Figure 5.59: Values of the objective function J.

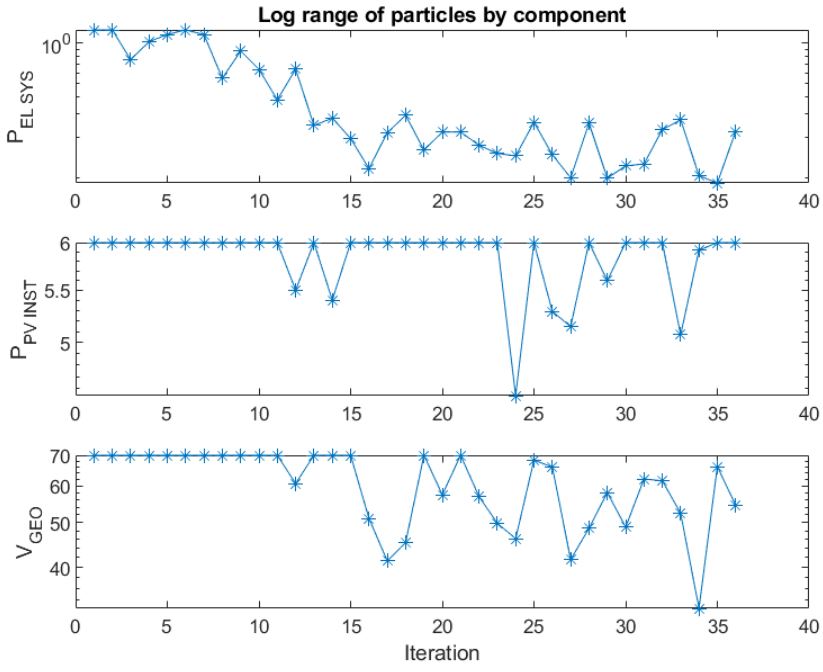

Figure 5.60: Parameter ranges: the top graph shows the maximum power of the hydrogen system, the centre graph the nominal power of the PV field, and the bottom graph the volume of the storage tank.

The same pre-demanded hydrogen production $Q_{H2\_OUT\_DEM} = 160$ kg/day can also be achieved without using the excess energy from the PV field and only by exploiting the

surplus of hydro energy. In this scenario, the optimisation results show that the (local) optimal configuration for reaching the desired annual production of hydrogen is:

- *Hydrogen system's maximum power (*P_{EL_SYS}*): 0.4414 MW*
- *Photovoltaic field's nominal (installed) power (*P_{PV_INST}*): 0 MW*
- *Volume of hydrogen-storage tank (*V_{GEO}*): 58.2813* m^3

where the annual hydrogen production is 58,400 kg/y (160 kg/d), the hydrogen system's utilisation rate is above 79.6444 % and corresponding annual income is 213,785 €/y. In this scenario, a larger electrolyser and a larger hydrogen-storage tank are required due to the more uneven dynamics of the surplus energy for the hydrogen system's operation. The results are shown in Table 5.22, Figure 5.61 and Figure 5.62.

Generally, parameter P_{PV_INST} is an optimised parameter, but in this particular case, we set its upper and lower limits to 0, thus preventing the optimisation of this parameter and leaving it at a value of 0 MW.

Table 5.22: Displayed information.

Iteration	f-count	Best f(x)	Mean f(x)	Stall Iteration
0	100	1.289e+06	1.013e+09	0
1	200	1.289e+06	8.533e+08	0
2	300	3.109e+04	3.93e+08	0
3	400	3507	3.204e+08	0
4	500	3507	2.876e+08	1
5	600	3507	3.252e+08	2
6	700	3507	3.018e+08	3
7	800	3507	3.116e+08	4
8	900	3507	2.678e+08	5
9	1000	3507	2.785e+08	6
10	1100	3507	1.896e+08	7
11	1200	3507	8.642e+07	8
12	1300	378.2	4.949e+07	0
13	1400	19.44	3.155e+07	0
14	1500	19.44	1.876e+07	1
15	1600	19.44	2.598e+07	2
16	1700	19.44	2.471e+07	3
17	1800	3.651	2.365e+07	0
18	1900	0.1272	3.688e+07	0
19	2000	0.1272	3.219e+07	1
20	2100	0.1272	3.001e+07	2
21	2200	0.1272	2.944e+07	3
22	2300	0.02359	3.099e+07	0
23	2400	7.336e-05	1.76e+07	0
24	2500	3.525e-05	2.021e+07	0
25	2600	3.525e-05	2.425e+07	1
26	2700	2.809e-05	1.885e+07	0
27	2800	2.592e-05	1.687e+07	0
28	2900	1.956e-05	1.532e+07	0
29	3000	1.956e-05	2.193e+07	1
30	3100	2.31e-06	1.68e+07	0
31	3200	4.241e-07	1.855e+07	0
32	3300	4.389e-08	1.378e+07	0
33	3400	2.733e-08	1.546e+07	0
34	3500	2.588e-08	1.756e+07	0
35	3600	2.135e-08	1.136e+07	0
36	3700	6.652e-09	1.393e+07	0
37	3800	3.294e-09	1.631e+07	0
38	3900	3.294e-09	1.118e+07	1
39	4000	1.205e-09	2.404e+07	0
40	4100	5.576e-10	2.476e+07	0
41	4200	1.03e-10	3.549e+07	0
42	4300	1.03e-10	2.699e+07	1

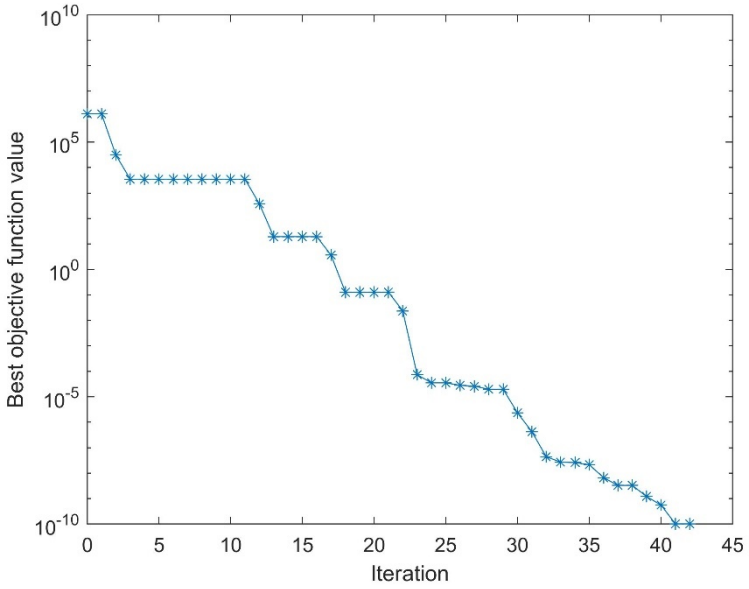

Figure 5.61: Values of the objective function J.

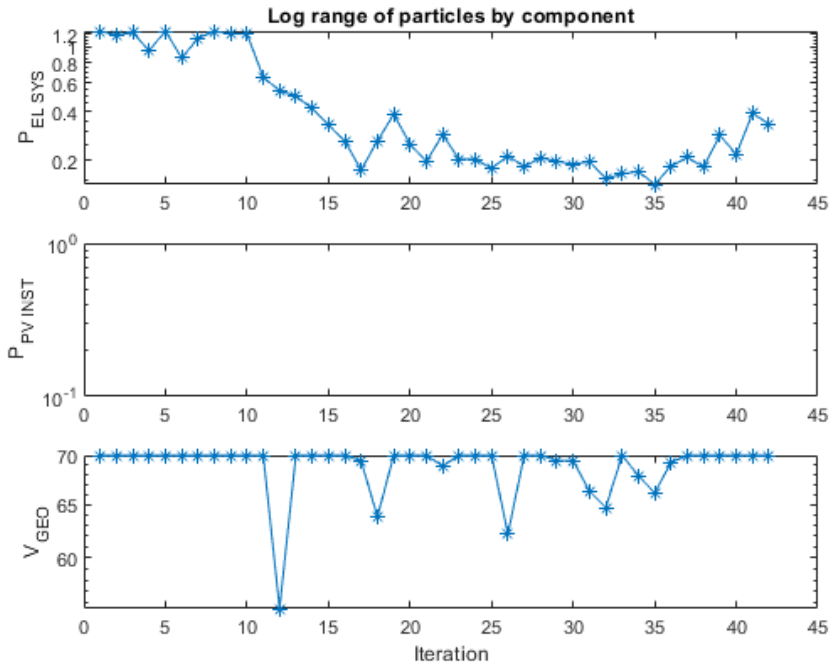

Figure 5.62: Parameter ranges: the top graph shows the maximum power of the hydrogen system, the centre graph the nominal power of the PV field, and the bottom graph the volume of the storage tank.

5.3.5 Combination of Two Objective Functions

To balance the requirements for the volume of hydrogen production and the profitability of its production, two objective functions can be combined:

- *Maximisation of income,*
- *Search for the system size that leads to the required amount of produced hydrogen.*

Mathematically, this is implemented as a linear combination of two separate objective functions, each given its own weight (k_1, k_2). In a linear combination, both objective functions are normalised to enable the equal impact of both demands:

$$J = -k_1 \cdot \left(\frac{Income_{H2}}{Income_{H2_{MAX}}}\right) + k_2 \cdot \left(\frac{m_{H2\_PROD} - Q_{H2_{OUT_{DEM}}} \cdot 365\ [d]}{Q_{H2\_OUT\_DEM} \cdot 365\ [d]}\right)^2 \tag{5.7}$$

In the equation, $Q_{H2\_OUT\_DEM}$ = 160 kg/d and $Income_{H2\_MAX}$ = 425,060.98 €/y, taken from the first example (any other comparable value, e.g., 500,000 €/y could be used here). Table 5.23 comprises the PSO algorithm results for different coefficients k_1 and k_2.

Table 5.23: PSO algorithm results with various coefficients k_1 and k_2, $Q_{H2\_OUT\_DEM}$ = 160 kg/d.

			Results				
Variables	k_1	k_2	P_{EL_SYS} [MW]	P_{PV_INST} [MW]	V_{STOR_MAX} [m³]	$Income_{H2}$ [€/y]	m_{H2_PROD} [kg/y]
	0.75	0.25	0.7352	0	19.2448	398,767.50	95,642.21
	0.50	0.50	0.6534	0	17.2494	392,049.73	83,529.32
	0.25	0.75	0.5119	0	14.1594	264,147.61	66,926.16
	0.10	0.90	0.4643	0	12.5328	296,323.51	59,235.54

The target hydrogen production in this case was 160 kg/d, which is 58,400 kg/year and this value can be compared by m_{H2_PROD} from Table 5.23 to see how well the second objective function was fulfilled. We can see that the second objective function is strongly prioritized (last case in the table above k_1 = 0.1 and k_2 = 0.9), then it fulfils the target value the most.

In the case that the hydrogen demand is doubled ($Q_{H2\_OUT\_DEM}$ = 320 kg/d), the inclusion of the PV field is meaningful. Table 5.24 comprises the PSO algorithm results for different coefficients k_1 and k_2.

It is assumed that all the produced hydrogen is sold at a given price, not only the required amount of hydrogen.

Table 5.24: PSO algorithm results with various coefficients k_1 and k_2, $Q_{H2\_OUT\_DEM}$ = 320 kg/d.

			Results				
Variables	k_1	k_2	P_{EL_SYS} [MW]	P_{PV_INST} [MW]	V_{STOR_MAX} [m³]	$Income_{H2}$ [€/y]	m_{H2_PROD} [kg/y]
	0.75	0.25	1.4903	4.0361	35.3375	490,435.76	117,802.62
	0.50	0.50	1.2987	2.1954	31.4271	580,202.61	135,036.98
	0.25	0.75	1.2434	0.9107	30.3093	537,767.01	119,781.14
	0.10	0.90	1.2143	0.7674	29.0963	545,414.91	117,384.67

From the illustrated examples we can see that the parameters of the hydrogen and photovoltaic system can be successfully optimised according to different objective functions by a heuristic optimisation method, in this particular case the Particle Swarm Optimisation.

When compared to the Hydrogen-System-Configuration Explorer from Section 5.2, which uses exhaustive simulation, the presented automated optimisation method brings the following benefits:

- *The accuracy of the results is higher, since the parameter space is not discretised,*
- *The optimisation procedure can be faster and less computationally demanding, since the number of model simulation runs is smaller.*
- *The number of optimised parameters can be higher.*

The automated optimisation (PSO) and the Hydrogen-System-Configuration Explorer are complementary tools. The Hydrogen-System-Configuration Explorer can be used to obtain the complete picture over the entire parameter space and get rough estimates for the optimal parameters according to the selected objective function. The automated optimisation (PSO), on the other hand, can be used to find more accurate values of optimal parameters, while the results of the Hydrogen-System-Configuration Explorer can be used as initial values of the PSO optimisation.

Chapter 6

Conclusions

Hydrogen is a promising energy vector/carrier and is recognised as one of the main levers for achieving the long-term green transition. However, its today's production method (mostly the steam reforming of natural gas) is not in line with long-term climate and energy goals. Green hydrogen produced by water electrolysis driven by electricity from renewable sources has an extra added value, because its production is CO_2-emission free, and it could make a key contribution to reducing CO_2 emissions, reducing local pollution, ensuring energy independence and helping to achieve sustainable goals.

Since hydropower plants are the most reliable renewable source of green electricity, it makes sense to evaluate the possibilities of cogeneration green hydrogen in this kind of power plant. However, for this kind of upgrading of the operation of hydropower plants, we need new technologies, where the costs of their installation, the optimal selection of the necessary components and the profitability of the operation, have not yet been fully evaluated.

This dissertation is focused on technical and economic analyses of hydrogen technologies in connection with a hydropower plant. The goal is to provide the methodology and tools for:

- *Simulation-based demonstration of the hydrogen system's operation in connection to hydropower plants.*
- *Estimation of the investment and operating costs of hydrogen systems.*
- *Estimation of the possible financial income generated by the hydrogen system's operation.*
- *Optimal sizing of hydrogen system equipment during feasibility studies and system design.*

Therefore, it is believed that this dissertation and its results and tools can contribute to a more effective solution to the above-mentioned challenges. The most important contributions are the following:

- *Implementation of the hydrogen system and hydropower plant model, which enables the simulation of the operation of the entire system using real operating data and evaluates the financial effects.*
- *Assessment of the possibility of cogeneration of green hydrogen, considering the prescribed timetable and possible surpluses of available hydro energy. In addition to the primary role of the hydropower plant, which is the production of electricity according*

to a prescribed timetable, surpluses of hydropower occur from time to time, which can be utilised for the cogeneration of green hydrogen.

- *An assessment of the costs of setting up a hydrogen system and an assessment of the profitability of its operation in terms of hydrogen consumption and its selling price. The basics for calculating the profitability of green-hydrogen production are given, but in future work, attention should be paid to an estimation of the expected consumption of hydrogen and the selling prices of the components of the hydrogen system, which are expected to decrease in the future.*

- *Design and implementation of two tools (Hydrogen-System-Configuration Explorer and Hydrogen-System-Configuration Optimiser) to support decision-making in selecting/sizing the appropriate configuration of the hydrogen system, taking into account the available excess electricity and the expected consumption of green hydrogen. At the current development stage, the developed tools enable the sizing of the main components of the hydrogen system, i.e., the electrolyser, PV field and the hydrogen-storage tank, according to selected criteria (e.g., hydrogen consumption, use of existing equipment, income), but there is potential to add further functionalities.*

- *Implementation of a simple control algorithm, which coordinates the operation of the hydrogen system according to the actual consumption of green hydrogen, the state-of-charge of water accumulation reservoir, the available surplus electrical energy and the state-of-charge of the hydrogen storage tank.*

The simulation experiments on the case-study HPP show that an investment in a hydrogen system could already be justified in certain cases. Considering all the possibilities for producing green hydrogen from surpluses of available hydropower, and taking into account that the costs of the already commercially available components of the hydrogen system will decrease and the demand for green hydrogen will increase, we estimate that it is worth investing in hydrogen technologies.

References

[1] European Commission, Directorate-General for Mobility and Transport, "European Green Deal: Commission proposes transformation of EU economy and society to meet climate ambitions," Brussels, 14 July 2021.

[2] European Commission, Directorate-General for Energy, "Clean energy for all Europeans," Publications Office, 2019, https://data.europa.eu/doi/10.2833/9937.

[3] Vlada Republike Slovenije, "OSNUTEK predloga posodobitve (2024): Celoviti nacionalni energetski in podnebni načrt (NEPN), Nr: 360-7/2023-2430-73," Ljubljana, 22. junij 2023 (in Slovenian language).

[4] ENTSO-E, "Research, Development & Innovation Roadmap 2020 – 2030," https://doi.org/10.13140/RG.2.2.27561.83040, 14 October 2020.

[5] IEA, "Hydropower Special Market Report. Analysis and forecast to 2030, Revised version," June 2021.

[6] M. Yue, H. Lambert, E. Pahon, R. Roche, S. Jemei and D. Hissel, "Hydrogen energy systems: A critical review of technologies, applications, trends and challenges," *Renewable and Sustainable Energy Reviews,* vol. 146, no. 111180; https://doi.org/10.1016/j.rser.2021.111180, 2021.

[7] T. Capurso, M. Stefanizzi, M. Torresi and S. M. Camporeale, "Perspective of the role of hydrogen in the 21st century energy transition," *Energy Conversion and Management,* vol. 251, no. 114898; https://doi.org/10.1016/j.enconman.2021.114898, 2022.

[8] I. Dincer and H. Ishaq, Renewable Hydrogen Production, Amsterdam: Elsevier; https://doi.org/10.1016/C2020-0-02435-7, 2022.

[9] A. Lewandowska-Bernat and U. Desideri, "Opportunities of power-to-gas technology in different energy systems architectures," *Applied Energy,* vol. 228, pp. 57-67; https://doi.org/10.1016/j.apenergy.2018.06.001, 2018.

[10] S. Schiebahn, T. Grube, M. Robinius, V. Tietze, B. Kumar and D. Stolten, "Power to gas: Technological overview, systems analysis and economic assessment for a case study in Germany," *International Journal of Hydrogen Energy,* vol. 40, no. 12, pp. 4285-4294; https://doi.org/10.1016/j.ijhydene.2015.01.123, 2015.

[11] C. Van Leeuwen and M. Mulder, "Power-to-gas in electricity markets dominated by renewables," *Applied Energy,* vol. 232, pp. 258-272; https://doi.org/10.1016/j.apenergy.2018.09.217, 2018.

[12] I. Dincer, "Green methods for hydrogen production," *International Journal of Hydrogen Energy,* vol. 37, no. 2, pp. 1954-1971; https://doi.org/10.1016/j.ijhydene.2011.03.173, 2012.

[13] F. M. Baena-Moreno, Z. Zhang, X. P. Zhang and T. R. Reina, "Profitability analysis of a novel configuration to synergize biogas upgrading and Power-to-Gas," *Energy Conversion and Management,* vol. 224, no. 113369; https://doi.org/10.1016/j.enconman.2020.113369, 2020.

[14] H. Talebian, O. E. Herrera and W. Mérida, "Policy effectiveness on emissions and cost reduction for hydrogen supply chains: The case for British Columbia," *International Journal of Hydrogen Energy,* vol. 46, no. 1, pp. 998-1011; https://doi.org/10.1016/j.ijhydene.2020.09.190, 2021.

[15] J. Wang and S. Matsumoto, "Can subsidy programs lead consumers to select "greener" products?: Evidence from the Eco-car program in Japan," *Research in Transportation Economics,* vol. 91, no. 101066; https://doi.org/10.1016/j.retrec.2021.101066, 2021.

[16] A. Berrada and M. A. Laasmi, "Technical-economic and socio-political assessment of hydrogen production from solar energy," *Journal of Energy Storage,* Vols. 44, Part B, no. 103448; https://doi.org/10.1016/j.est.2021.103448, 2021.

[17] Y. Li, X. Shi and H. Phoumin, "A strategic roadmap for large-scale green hydrogen demonstration and commercialisation in China: A review and survey analysis," *International Journal of Hydrogen Energy,* vol. 47, no. 58, pp. 24592-24609; https://doi.org/10.1016/j.ijhydene.2021.10.077, 2022.

[18] A. Velazquez Abad and P. E. Dodds, "Green hydrogen characterisation initiatives: Definitions, standards, guarantees of origin, and challenges," *Energy Policy,* vol. 138, no. 111300; https://doi.org/10.1016/j.enpol.2020.111300, 2020.

[19] S. McDonagh, S. Ahmed, C. Desmond and J. D. Murphy, "Hydrogen from offshore wind: Investor perspective on the profitability of a hybrid system including for curtailment," *Applied Energy,* vol. 265, no. 114732; https://doi.org/10.1016/j.apenergy.2020.114732, 2020.

[20] M. K. Kazi, F. Eljack, M. M. El-Halwagi and M. Haouari, "Green hydrogen for industrial sector decarbonization: Costs and impacts on hydrogen economy in qatar," *Computers & Chemical Engineering,* vol. 145, no. 107144; https://doi.org/10.1016/j.compchemeng.2020.107144, 2021.

[21] D. Roxby, "Why hydrogen is starting to get the green light in global renewables," Ernst & Young Global Limited, 18 5 2021. [Online]. Available: https://www.ey.com/en_gl/recai/why-hydrogen-is-starting-to-get-the-green-light-in-global-renewables. [Accessed 1 12 2021].

[22] R. Tarkowski and B. Uliasz-Misiak, "Towards underground hydrogen storage: A review of barriers," *Renewable and Sustainable Energy Reviews,* vol. 162, no. 112451; https://doi.org/10.1016/j.rser.2022.112451, 2022.

[23] European Commission, "A Clean Planet for all A European long-term strategic vision for a prosperous, modern, competitive and climate neutral economy," Brussels, 28 November 2018.

[24] Y. Ruf, S. Lange, J. Pfister in C. Droege, „Fuel Cells and Hydrogen for Green Energy in European Cities and Regions,“ Roland Berger GmbH, Munich, 2018.

[25] IEA, “Global demand for pure hydrogen, 1975-2018,” [Online]. Available: https://www.iea.org/data-and-statistics/charts/global-demand-for-pure-hydrogen-1975-2018. [Accessed 14 9 2023].

[26] World Energy Council , “Working Paper: Hydrogen Demand And Cost Dynamics,” World Energy Council , London, 2021.

[27] U. Gupta and U. Turaga, “Hydrogen is back in vogue,” ADI Analytics, [Online]. Available: https://adi-analytics.com/2019/11/12/hydrogen-is-back-in-vogue/. [Accessed 30 8 2022].

[28] C. Acar and I. Dincer, “Selection criteria and ranking for sustainable hydrogen production options,” *International Journal of Hydrogen Energy,* vol. 47, no. 95, pp. 40118-40137; https://doi.org/10.1016/j.ijhydene.2022.07.137, 2022.

[29] M. G. Rasul, M. A. Hazrat, M. A. Sattar, M. I. Jahirul and M. J. Shearer, “The future of hydrogen: Challenges on production, storage and applications,” *Energy Conversion and Management,* vol. 272, no. 116326; https://doi.org/10.1016/j.enconman.2022.116326, 2022.

[30] J. Incer-Valverde, A. Korayem, G. Tsatsaronis and T. Morosuk, ““Colors” of hydrogen: Definitions and carbon intensity,” *Energy Conversion and Management,* vol. 291, no. 117294; https://doi.org/10.1016/j.enconman.2023.117294, 2023.

[31] F. Lubbe, J. Rongé, T. Bosserez and J. A. Martens, “Golden hydrogen,” *Current Opinion in Green and Sustainable Chemistry,* vol. 39, no. 100732; https://doi.org/10.1016/j.cogsc.2022.100732, 2023.

[32] A. Basile, A. Liguori and A. Iulianelli, “Membrane Reactors for Energy Applications and Basic Chemical Production,” in *Energy*, University of Calabria, Rende, Italy, Woodhead Publishing, 2015, pp. 31-59; https://doi.org/10.1016/C2013-0-16489-6.

[33] D. Fraile, J. C. Lanoix, P. Maio, A. Rangel and A. Torres, “Overview of the market segmentation for hydrogen across potential customer groups, based on key application areas,” European Commission, 2015.

[34] A. Mazza, Bompard Ettore and G. Chicco, “Applications of power to gas technologies in emerging electrical systems,” *Renewable and Sustainable Energy Reviews,* vol. 92, pp. 794-806; https://doi.org/10.1016/j.rser.2018.04.072, 2018.

[35] G. Kakoulaki, I. Kougias, N. Taylor, F. Dolci, J. Moya and A. Jäger-Waldau, “Green hydrogen in Europe – A regional assessment: Substituting existing production with electrolysis powered by renewables,” *Energy Conversion and Management,* vol. 228, no. 113649; https://doi.org/10.1016/j.enconman.2020.113649, 2021.

[36] D. Ferrero, M. Gamba, A. Lanzini and M. Santarelli, “Power-to-Gas Hydrogen: techno-economic assessment of processes towards a multi-purpose energy carrier,” *Energy Procedia,* vol. 101, pp. 50-57; https://doi.org/10.1016/j.egypro.2016.11.007, 2016.

[37] M. Sterner and M. Specht, “Power-to-Gas and Power-to-X—The History and Results of Developing a New Storage Concept,” *Energies,* vol. 14, no. 20; https://doi.org/10.3390/en14206594, p. 6594, 2021.

[38] M. Specht, M. Sterner, B. Stuermer, V. Frick and B. Hahn, "Energieversorgungssystem und Betriebsverfahren". Germany Patent Patent 10 2009 018 126.1, 9 April 2009.

[39] M. Thema, F. Bauer and M. Sterner, "Power-to-Gas: Electrolysis and methanation status review," *Renewable and Sustainable Energy Reviews,* vol. 112, pp. 775-787; https://doi.org/10.1016/j.rser.2019.06.030, 2019.

[40] X. Xing, J. Lin, Y. Song, Y. Zhou, S. Mu and Q. Hu, "Modeling and Operation of the Power-to-Gas System for Renewables Integration: A Review," *Journal of Power and Energy Systems,* vol. 4, no. 2; https://doi.org/10.17775/CSEEJPES.2018.00260, 2018.

[41] IEA, "Electrolysers: Technology deep dive," September 2022. [Online]. Available: https://www.iea.org/reports/electrolysers. [Accessed 27 3 2023].

[42] A. Z. Arsad, M. A. Hannan, A. Q. Al-Shetwi, R. A. Begum, M. J. Hossain, P. J. Ker and T. M. Indira Mahlia, "Hydrogen electrolyser technologies and their modelling for sustainable energy production: A comprehensive review and suggestions," *International Journal of Hydrogen Energy,* vol. 48, no. 72, pp. 27841-27871; https://doi.org/10.1016/j.ijhydene.2023.04.014, 2023.

[43] IEA (2023), "Tracking Clean Energy Progress 2023, IEA," Paris https://www.iea.org/reports/tracking-clean-energy-progress-2023, License: CC BY 4.0.

[44] Hydrogen Insights 2023, "An update on the state of the global hydrogen economy, with a deep dive into North America," Hydrogen Council, McKinsey & Company, 2023.

[45] D. Borge-Diez, E. Rosales-Asensio, E. Açıkkalp and D. Alonso-Martínez, "Analysis of Power to Gas Technologies for Energy Intensive Industries in European Union," *Energies,* vol. 16(1), no. 538; https://doi.org/10.3390/en16010538, 2023.

[46] M. McPherson, N. Johnson and M. Strubegger, "The role of electricity storage and hydrogen technologies in enabling global low-carbon energy transitions," *Applied Energy,* vol. 216, pp. 649-661; https://doi.org/10.1016/j.apenergy.2018.02.110, 2018.

[47] O. Schmidt, A. Gambhir, I. Staffell, A. Hawkes, J. Nelson and S. Few, "Future cost and performance of water electrolysis: An expert elicitation study," *International Jurnal of Hydrogen Energy,* vol. 42, no. 52, pp. 30470-30492; https://doi.org/10.1016/j.ijhydene.2017.10.045, 2017.

[48] IRENA (2020), "Green hydrogen cost reduction: Scaling up electrolysers to meet climate goal 1.5°C climate goal," International Renewable Energy Agency, Abu Dhabi.

[49] A. Pozio, F. Bozza, G. Nigliaccio and M. Platter, "Development perspectives on low-temperature electrolysis," *Energia, ambiente e innovazione,* 2021; https://doi.org/10.12910/EAI2021-014.

[50] S. Shiva Kumar and H. Lim, "An overview of water electrolysis technologies for green hydrogen production," *Energy Reports,* vol. 8, pp. 13793-13813; https://doi.org/10.1016/j.egyr.2022.10.127, 2022.

[51] S. Zhang and N. Zhang, "Review on integrated green hydrogen polygeneration system——Electrolysers, modelling, 4 E analysis and optimization," *Journal of*

Cleaner Production, vol. 414, no. 137631; https://doi.org/10.1016/j.jclepro.2023.137631, 2023.

[52] M. N. I. Salehmin, T. Husaini, J. Goh and A. B. Sulong, "High-pressure PEM water electrolyser: A review on challenges and mitigation strategies towards green and low-cost hydrogen production," *Energy Conversion and Management,* vol. 268, no. 115985; https://doi.org/10.1016/j.enconman.2022.115985, 2022.

[53] S. Shiva Kumar and V. Himabindu, "Hydrogen production by PEM water electrolysis – A review," *Materials Science for Energy Technologies,* vol. 2, no. 3, pp. 442-454; 10.1016/j.mset.2019.03.002, 2019.

[54] P. Muthukumar, A. Kumar, M. Afzal, S. Bhogilla, P. Sharma, A. Prida, S. Jana, E. Anil Kumar, R. K. Pai and I. P. Jain, "Review on large-scale hydrogen storage systems for better sustainability," *International Journal of Hydrogen Energy,* no. In Press, Corrected Proof: https://doi.org/10.1016/j.ijhydene.2023.04.304, 2023.

[55] G. K. Karayel, N. Javani and I. Dincer, "A comprehensive assessment of energy storage options for green hydrogen," *Energy Conversion and Management,* vol. 291, no. 117311; https://doi.org/10.1016/j.enconman.2023.117311, 2023.

[56] M. R. Usman, "Hydrogen storage methods: Review and current status," *Renewable and Sustainable Energy Reviews,* vol. 167, no. 112743; https://doi.org/10.1016/j.rser.2022.112743, 2022.

[57] K. Nejc, I. Grimmer, F. Winkler, M. Sartory and A. Trattner, "A review on metal hydride materials for hydrogen storage," *Journal of Energy Storage,* Vols. 72, Part B, no. 108456; https://doi.org/10.1016/j.est.2023.108456, 2023.

[58] NEL, "Containerized PEM Electrolyser," NEL, [Online]. Available: https://nelhydrogen.com/product/m-series-containerized/. [Accessed 2 2 2021].

[59] F. Grüger, O. Hoch, J. Hartmann, M. Robinius and D. Stolte, "Optimized electrolyzer operation: Employing forecasts of wind energy availability, hydrogen demand, and electricity prices," *International Journal of Hydrogen Energy,* vol. 44, no. 9, pp. 4387-4397; https://doi.org/10.1016/j.ijhydene.2018.07.165, 2019.

[60] G. Squadrito, A. Nicita and G. Maggio, "A size-dependent financial evaluation of green hydrogen-oxygen co-production," *Renewable Energy,* vol. 163, pp. 2165-2177; https://doi.org/10.1016/j.renene.2020.10.115, 2021.

[61] D. Parra and M. K. Patel, "Techno-economic implications of the electrolyser technology and size for power-to-gas systems," *International Journal of Hydrogen Energy,* vol. 41, no. 6, pp. 3748-3761; https://doi.org/10.1016/j.ijhydene.2015.12.160, 2016.

[62] S. M. Saba, M. Müller, M. Robinius and D. Stolten, "The investment costs of electrolysis - A comparison of cost studies from the past 30 years," *International Journal of Hydrogen Energy,* vol. 43, no. 3, pp. 1209-1223; https://doi.org/10.1016/j.ijhydene.2017.11.115, 2018.

[63] E. Tzimas, C. Filiou, S. D. Peteves and J. B. Veyet, "Hydrogen storage: State-of-the-art and future perspective," Directorate General Joint Research Centre (DG JRC), Institute for Energy, Petten, 2003.

[64] M. Zghaibeh and e. al., "Optimization of green hydrogen production in hydroelectric-photovoltaic grid connected power station," *International Journal of Hydrogen*

Energy, Vols. In Press, Corrected Proof, no. https://doi.org/10.1016/j.ijhydene.2023.06.020, 2023.

[65] O. Ruhnau, "How flexible electricity demand stabilizes wind and solar market values: The case of hydrogen electrolyzers," *Applied Energy,* vol. 307, no. 118194; https://doi.org/10.1016/j.apenergy.2021.118194, 2022.

[66] D. Bellotti, M. Rivarolo and L. Magistri, "A comparative techno-economic and sensitivity analysis of Power-to-X processes from different energy sources," *Energy Conversion and Management,* vol. 260, no. 115565; https://doi.org/10.1016/j.enconman.2022.115565, 2022.

[67] S. Krishnan, V. Koning, M. T. de Groot, A. de Goot, P. Grandoz Mendoza, M. Junginger and G. J. Kramer, "Present and future cost of alkaline and PEM electrolyser stacks," *International Journal of Hydrogen Energy,* vol. 48, no. 83, pp. 32313-32330; https://doi.org/10.1016/j.ijhydene.2023.05.031, 2023.

[68] A. M. Villarreal Vives, R. Wang, S. Roy and A. Smallbone, "Techno-economic analysis of large-scale green hydrogen production and storage," *Applied Energy,* vol. 346, no. 121333;https://doi.org/10.1016/j.apenergy.2023.121333, 2023.

[69] D. J. Jovan, G. Dolanc and B. Pregelj, "Cogeneration of green hydrogen in a cascade hydropower plant," *Energy Conversion and Management: X,* vol. 10, no. 100081; https://doi.org/10.1016/j.ecmx.2021.100081, 2021.

[70] Agora Industry and Umlaut (2023), "Levelised cost of hydrogen. Making the application of the LCOH concept more consistent and more useful.".

[71] D. J. Jovan and G. Dolanc, "Can Green Hydrogen Production Be Economically Viable under Current Market Conditions," *Energies,* vol. 13, no. 24, 6599; https://doi.org/10.3390/en13246599 , 2020.

[72] M. Castañeda, A. Cano, J. Francisco, H. Sánchez and L. M. Fernández, "Sizing optimization, dynamic modeling and energy management strategies of a stand-alone PV/hydrogen/battery-based hybrid system," *International Journal of Hydrogen Energy,* vol. 38, no. 10, pp. 3830-3845; https://doi.org/10.1016/j.ijhydene.2013.01.080, 2013.

[73] S. Abid and A. Ammous, "Modeling, Control, and Simulation of a Solar Hydrogen/Fuel Cell Hybrid Energy System for Grid-Connected Applications," *Advances in Power Electronics,* no. 352765; https://doi.org/10.1155/2013/352765, 2013.

[74] J. G. G. Clúa, R. J. Mantz and H. De Battista, "Hybrid control of a photovoltaic-hydrogen energy system," *International Journal of Hydrogen Energy,* vol. 33, no. 13, pp. 3455-3459; https://doi.org/10.1016/j.ijhydene.2007.12.046, 2008.

[75] G. A. de Andrade, J. G. García-Clúa, P. R. Mendes and J. E. Normey-Rico, "Optimal Control of a Grid Assisted Photovoltaic-Hydrogen Production System," *IFAC-PapersOnLine,* vol. 52, no. 1, pp. 1012-1017; https://doi.org/10.1016/j.ifacol.2019.06.195, 2019.

[76] Ø. Ulleberg, "The importance of control strategies in PV–hydrogen systems," *Solar Energy,* vol. 76, no. 1-3, pp. 323-329; https://doi.org/10.1016/j.solener.2003.09.013, 2004.

[77] A. H. Schrotenboer, A. A. Veenstra, M. A. uit het Broek and E. Ursavas, "A Green Hydrogen Energy System: Optimal control strategies for integrated hydrogen storage and power generation with wind energy," *Renewable and Sustainable Energy Reviews,* vol. 168, no. 112744; https://doi.org/10.1016/j.rser.2022.112744, 2022.

[78] M. A. Hossain, M. R. Islam, M. A. Hossain and M. J. Hossain, "Control strategy review for hydrogen-renewable energy power system," *Journal of Energy Storage,* Vols. 72, Part A, no. 108170; https://doi.org/10.1016/j.est.2023.108170, 2023.

[79] A. Cano, F. Jurado, H. Sánchez, L. M. Fernández and M. Castañeda, "Optimal sizing of stand-alone hybrid systems based on PV/WT/FC by using several methodologies," *Journal of the Energy Institute,* vol. 87, no. 4, pp. 330-340; https://doi.org/10.1016/j.joei.2014.03.028, 2014.

[80] P. Puranen, A. Kosonen and J. Ahola, "Technical feasibility evaluation of a solar PV based off-grid domestic energy system with battery and hydrogen energy storage in northern climates," *Solar Energy,* vol. 213, pp. 246-259; https://doi.org/10.1016/j.solener.2020.10.089, 2021.

[81] K. Farrukh, I. Dincer, M. A. R. Rosen and M. A. Rosen, "Analysis and assessment of an integrated hydrogen energy system," *International Journal of Hydrogen Energy,* vol. 41, no. 19, pp. 7960-7967; https://doi.org/10.1016/j.ijhydene.2015.12.221, 2016.

[82] W. Zhang, "Optimization with a simulated annealing algorithm of a hybrid system for renewable energy including battery and hydrogen storage," *Energy,* vol. 163, pp. 191-207; https://doi.org/10.1016/j.energy.2018.08.112, 2018.

[83] G. Yang and X. Zhai, "Optimization and performance analysis of solar hybrid CCHP systems under different operation strategies," *Applied Thermal Engineering,* vol. 133, pp. 327-340; https://doi.org/10.1016/j.applthermaleng.2018.01.046, 2018.

[84] A. Maleki and F. Pourfayaz, "Optimal sizing of autonomous hybrid photovoltaic/wind/battery power system with LPSP technology by using evolutionary algorithms," *Solar Energy,* vol. 115, pp. 471-483; https://doi.org/10.1016/j.solener.2015.03.004, 2015.

[85] R. Kherzi and A. Mahmoudi, "Review on the state-of-the-art multi-objective optimisation of hybrid standalone/grid-connected energy systems," *IET journals,* 2020; https://doi.org/10.1049/iet-gtd.2020.0453.

[86] S. C. Bhatia, Advanced Renewable Energy Systems, Woodhead Publishing India PVT. Ltd, 2014.

[87] D. S. Tarnay, "Hydrogen production at hydro-power plants," *International Journal of Hydrogen Energy,* vol. 10, no. 9; https://doi.org/10.1016/0360-3199(85)90032-1, pp. 577-584, 1985.

[88] F. Posso, J. L. Espinoza, J. Sanchez and J. Zalamea, "Hydrogen from hydropower in Ecuador: Use and impacts in the transport sector," *International Journal of Hydrogen Energy,* vol. 40, no. 45, pp. 15432-15447; https://doi.org/10.1016/j.ijhydene.2015.08.109, 2015.

[89] H. Liu, T. Brown, G. B. Andersen, D. P. Schlachtberger and M. Greinera, "The role of hydro power, storage and transmission in the decarbonization of the Chinese

power system," *Applied Energy,* vol. 239, pp. 1308-1321; https://doi.org/10.1016/j.apenergy.2019.02.009, 2019.

[90] G. K. Karayel, N. Javani and I. Dincer, "Hydropower for green hydrogen production in Turkey," *International Journal of Hydrogen Energy,* vol. 48, no. 60, pp. 22806-22817; https://doi.org/10.1016/j.ijhydene.2022.04.084, 2023.

[91] S. R. Andrus, R. J. Diffely and T. L. Alford, "Theoretical analysis of green hydrogen from hydropower: A case study of the Northwest Columbia River system," *International Journal of Hydrogen Energy,* vol. 48, no. 22, pp. 7993-8001; https://doi.org/10.1016/j.ijhydene.2022.11.027, 2023.

[92] Y. G. Son, H. G. Kwag, S. H. Lee and S. Y. Kim, "Marginal fixed premium for clean hydrogen portfolio standard (CHPS) considering techno-economic analysis of clean hydrogen production based on hydropower plants," *Energy Reports,* vol. 10, pp. 1356-1368; https://doi.org/10.1016/j.egyr.2023.08.004, 2023.

[93] S. R. Andrus, R. J. Diffely and T. L. Alford, "Theoretical analysis of green hydrogen from hydropower: A case study of the Northwest Columbia River system," *International Journal of Hydrogen Energy,* vol. 48, no. 22, pp. 7993-8001; https://doi.org/10.1016/j.ijhydene.2022.11.027, 2023.

[94] M. Lynch, M. T. Devine and V. Bertsch, "The role of power-to-gas in the future energy system: Market and portfolio effects," *Energy,* vol. 185, pp. 1197-1209; https://doi.org/10.1016/j.energy.2019.07.089, 2019.

[95] R. Qiu, H. Zhang, G. Wang, Y. Liang and Y. Jinyue, "Green hydrogen-based energy storage service via power-to-gas technologies integrated with multi-energy microgrid," *Applied Energy,* vol. 350, no. 121716; https://doi.org/10.1016/j.apenergy.2023.121716, 2023.

[96] Y. Li and F. Taghizadeh-Hesaryc, "The economic feasibility of green hydrogen and fuel cell electric vehicles for road transport in China," *Energy Policy,* vol. 160, no. 112703; https://doi.org/10.1016/j.enpol.2021.112703, 2022.

[97] B. Motealleh, Z. Liu, R. I. Masel, J. P. Sculley, Z. R. Ni and L. Meroueh, "Next-generation anion exchange membrane water electrolyzers operating for commercially relevant lifetimes," *International Journal of Hydrogen Energy,* vol. 46, no. 5, pp. 3379-3386; https://doi.org/10.1016/j.ijhydene.2020.10.244, 2021.

[98] A. Ursúa, L. M. Gandía and P. Sanchis, "Hydrogen production from water electrolysis: current status and future trends," *Proceedings IEEE,* vol. 100, no. 2, pp. 410-426; https://doi.org/10.1109/JPROC.2011.2156750, 2012.

[99] M. Götz, J. Lefebvre, F. Mörs, A. McDaniel Koch, F. Graf, S. Bajohr, R. Reimert and T. Kolb, "Renewable Power-to-Gas: A technological and economic review," *Renewable Energy,* vol. 85, pp. 1371-1390; https://doi.org/10.1016/j.renene.2015.07.066, 2016.

[100] L. Grond, P. Schulze and J. Holstein, "Systems Analyses Power to Gas. Deliverable 1: Technology Review. Final report," DNV KEMA Energy & Sustainability; GCS 13.R.23579, Groningen, June 2019.

[101] F. Meylan, V. Moreau and S. Erkman, "Material constraints related to storage of future European renewable electricity surpluses with CO2 methanation," *Energy Policy,* vol. 94, pp. 366-376; https://doi.org/10.1016/j.enpol.2016.04.012, 2016.

[102] T. Skoczylas, "Securing high-purity hydrogen," *Compound Semiconductor magazine,* vol. 24, no. 8, 2018.

[103] I. Dincer and C. Zamfirescu, Sustainable Hydrogen Production, Amsterdam: Elsevier; https://doi.org/10.1016/C2014-0-00658-2, 2016.

[104] K. S. Gabriel, R. S. El-Emam and C. Zamfirescu, "Technoeconomics of large-scale clean hydrogen production - A review," *International Journal of Hydrogen Energy,* vol. 47, no. 72, pp. 30788-30798; https://doi.org/10.1016/j.ijhydene.2021.10.081, 2022.

[105] R. Bhandari and R. R. Shak, "Hydrogen as energy carrier: Techno-economic assessment of decentralized hydrogen production in Germany," *Renewable Energy,* vol. 177, pp. 915-931; https://doi.org/10.1016/j.renene.2021.05.149, 2021.

[106] IRENA (2018), "Hydrogen from renewable power: Technology outlook for the energy transition, International Renewable Energy Agency," International Renewable Energy Agency, Abu Dhabi.

[107] ARUP, "Assessment of Electrolysers: Final Report," 23 9 2022. [Online]. Available: https://www.gov.scot/publications/assessment-electrolysers-report/. [Accessed 3 14 2023].

[108] D. S. Falcão and A. M. F. R. Pinto, "A review on PEM electrolyzer modelling: Guidelines for beginners," *Journal of Cleaner Production,* vol. 261, no. 121184; https://doi.org/10.1016/j.jclepro.2020.121184, 2020.

[109] P. Oliver, C. Bourasseau and B. Bouamama, "Modelling, simulation and analysis of a PEM electrolysis system," *IFAC-PapersOnLine,* vol. 49, no. 12, pp. 1014-1019; https://doi.org/10.1016/j.ifacol.2016.07.575, 2016.

[110] Z. Ma, L. Witteman, J. A. Wrubel and G. Bender, "A comprehensive modeling method for proton exchange membrane electrolyzer development," *International Journal of Hydrogen Energy,* vol. 46, no. 34, pp. 17627-17643; https://doi.org/10.1016/j.ijhydene.2021.02.170, 2021.

[111] M. Persson, D. Mignard and D. Hogg, "Insights on performance and an improved model for full scale electrolysers based on plant data for design and operation of hydrogen production," *International Journal of Hydrogen Energy,* vol. 45, no. 56, pp. 31396-31409; https://doi.org/10.1016/j.ijhydene.2020.08.255, 2020.

[112] K. Hu, J. Fang, X. Ai, Z. Zhong, D. Huang, C. Wang, Y. Ying and X. Yang, "Grid-Oriented multiphysics model of Power-to-Hydrogen electrolyzers," *Energy Conversion and Management,* vol. 270, no. 116264; https://doi.org/10.1016/j.enconman.2022.116264, 2022.

[113] H-TEC SYSTEMS GmbH, "High efficiency electrolyzers," [Online]. Available: https://www.h-tec.com/en/products/. [Accessed 14 9 2023].

[114] ITM Power PLC, "Our leading PEM electrolysers," [Online]. Available: https://itm-power.com/products. [Accessed 14 9 2023].

[115] T. Amirthan and M. S. A. Perera, "The role of storage systems in hydrogen economy: A review," *Journal of Natural Gas Science and Engineering,* vol. 108, no. 104843; https://doi.org/10.1016/j.jngse.2022.104843, 2022.

[116] Z. Abdin, K. Khalilpour and K. Catchpole, "Projecting the levelized cost of large scale hydrogen storage for stationary applications," *Energy Conversion and Management,* vol. 270, no. 116241; https://doi.org/10.1016/j.enconman.2022.116241, 2022.

[117] J. Li, J. Zhao, Y. Chen, L. Mao, K. Qu and F. Li, "Optimal sizing for a wind-photovoltaic-hydrogen hybrid system considering levelized cost of storage and source-load interaction," *International Journal of Hydrogen Energy,* vol. 48, no. 11, pp. 4129-4142; https://doi.org/10.1016/j.ijhydene.2022.10.271, 2023.

[118] J.-Q. Li, J.-C. Li, K. Park, S.-J. Jang and J.-T. Kwon, "An Analysis on the Compressed Hydrogen Storage System for the Fast-Filling Process of Hydrogen Gas at the Pressure of 82 MPa," *Energies,* vol. 14, no. 9, 2635; https://doi.org/10.3390/en14092635, 2021.

[119] N. S. Muhammed, M. B. Haq, D. A. Al Shehri, A. Al-Ahmed, M. M. Rahman, E. Zaman and S. Iglauer, "Hydrogen storage in depleted gas reservoirs: A comprehensive review," *Fuel,* vol. 337, no. 127032; https://doi.org/10.1016/j.fuel.2022.127032, 2023.

[120] A. M. Elberry, J. Thakur, A. Santasalo-Aarnio and M. Larmi, "Large-scale compressed hydrogen storage as part Large-scale compressed hydrogen storage as part," *International Journal of Hydrogen Energy,* vol. 46, no. 29, pp. 15671-15690; https://doi.org/10.1016/j.ijhydene.2021.02.080, 2021.

[121] A. Trattner, M. Höglinger, M. G. Macherhammer and M. Sartory, "Renewable Hydrogen: Modular Concepts from Production over Storage to the Consumer," *Chemie Ingenieur Technik,* vol. 93, no. 4, pp. 706-716; https://doi.org/10.1002/cite.202000197, 2021.

[122] G. Squadrito, G. Maggio and A. Nicita, "The green hydrogen revolution," *Renewable Energy,* vol. 216, no. 119041; https://doi.org/10.1016/j.renene.2023.119041, 2023.

[123] O. Faye, J. Szpunar and U. Eduok, "A critical review on the current technologies for the generation, storage, and transportation of hydrogen," *International Journal of Hydrogen Energy,* vol. 47, no. 29, pp. 13771-13802; https://doi.org/10.1016/j.ijhydene.2022.02.112, 2022.

[124] L. Schorer and S. Schmitz, "Onsite hydrogen generation and hydrogen recycling for refuelling FCEVs using an electrochemical hydrogen compressor," in *30th Electric Vehicle Symposium - EVS30*, Stuttgart, 2017.

[125] T. Mohammad-Reza, "Recent advances in hydrogen compressors for use in large-scale renewable energy integration," *International Journal of Hydrogen Energy,* vol. 47, no. 83, pp. 35275-35292; https://doi.org/10.1016/j.ijhydene.2022.08.128, 2023.

[126] I. Pivac, A. Stoilova Pavasović and F. Barbir, "Recent advances and perspectives in diagnostics and degradation of electrochemical hydrogen compressors," *International Journal of Hydrogen Energy,* In Press, Corrected Proof; https://doi.org/10.1016/j.ijhydene.2023.01.281, 2023.

[127] G. N. B. Durmus, C. O. Colpan and Y. Devrim, "A review on the development of the electrochemical hydrogen compressors," *Journal of Power Sources,* vol. 494, no. 229743; https://doi.org/10.1016/j.jpowsour.2021.229743, 2021.

[128] M. Trégaro, M. Rhandi, F. Druart, J. Deseure and M. Chatenet, "Electrochemical hydrogen compression and purification versus competing technologies: Part II. Challenges in electrocatalysis," *Chinese Journal of Catalysis,* vol. 41, no. 5, pp. 770-782; https://doi.org/10.1016/S1872-2067(19)63438-8, 2020.

[129] P. Fragiacomo and M. Genovese, "Developing a mathematical tool for hydrogen production, compression and storage," *International Journal of Hydrogen Energy,* vol. 45, no. 35, pp. 17685-17701; https://doi.org/10.1016/j.ijhydene.2020.04.269, 2020.

[130] A. Zulfhazli, A. R. Keeley, S. Takeda and S. Managi, "A systematic review of the techno-economic assessment of various hydrogen production methods of power generation," *Frontiers in Sustainability,* vol. 3; https://doi.org/10.3389/frsus.2022.943145, 2022.

[131] A. Patonia and R. Poudineh, "Cost-competitive green hydrogen: how to lower the cost of electrolysers?," Oxford Institute for Energy Studies, Oxford, 2022.

[132] R. Y. Kannah, S. Kavitha, O. P. Karthikeyan, G. Kumar, N. V. Dai-Viet and J. R. Banu, "Techno-economic assessment of various hydrogen production methods – A review," *Bioresource Technology,* vol. 319, no. 124175; https://doi.org/10.1016/j.biortech.2020.124175, 2021.

[133] IRENA (2022), "Geopolitics of the Energy Transformation: The Hydrogen Factor," International Renewable Energy Agency , Abu Dhabi.

[134] IEA, "The Future of Hydrogen: IEA G20 Hydrogen report: Assumptions annex".

[135] L. Viktorsson, J. T. Heinonen, J. B. Skulason and R. Unnthorsson, "A Step towards the Hydrogen Economy—A Life Cycle Cost Analysis of A Hydrogen Refueling Station," *Energies,* vol. 10, no. 6, 763; https://doi.org/10.3390/en10060763, 2017.

[136] A. Hassan, M. K. Patel and D. Parra, "An assessment of the impacts of renewable and conventional electricity supply on the cost and value of power-to-gas," *International Journal of Hydrogen Energy,* vol. 44, no. 19, pp. 9577-9593; https://doi.org/10.1016/j.ijhydene.2018.10.026, 2019.

[137] C. Blazquez-Dias, "Techno-economic modelling and analysis of hydrogen fuelling stations," *International Journal of Hydrogen Energy,* vol. 44, no. 2, pp. 495-510; https://doi.org/10.1016/j.ijhydene.2018.11.001, 2019.

[138] J. Proost, "State-of-the art CAPEX data for water electrolysers, and their impact on renewable hydrogen price settings," *International Journal of Hydrogen Energy,* vol. 44, no. 9, pp. 4406-4413; https://doi.org/10.1016/j.ijhydene.2018.07.164, 2019.

[139] I. Maynard and A. Abdulla, "Assessing benefits and costs of expanded green hydrogen production to facilitate fossil fuel exit in a net-zero transition," *Renewable Energy Focus,* vol. 44, pp. 85-97; https://doi.org/10.1016/j.ref.2022.12.002, 2023.

[140] A. H. Reksten, M. S. Thomassen, S. Møller-Holst and K. Sundseth, "Projecting the future cost of PEM and alkaline water electrolysers; a CAPEX model including electrolyser plant size and technology development," *International Journal of Hydrogen Energy,* vol. 47, no. 90, pp. 38106-38113; https://doi.org/10.1016/j.ijhydene.2022.08.306, 2022.

[141] Energy.Gov, "Technical Targets for Proton Exchange Membrane Electrolysis," The Office of Energy Efficiency and Renewable Energy (EERE), 2023. [Online].

Available: https://www.energy.gov/eere/fuelcells/technical-targets-proton-exchange-membrane-electrolysis. [Accessed 10 8 2023].

[142] FCHJU, "Clean Hydrogen Joint Undertaking Work Programme 2023: ANNEX to GB decision no CleanHydrogen-GB-2022-13," 2022.

[143] European Commission, "A hydrogen strategy for a climate-neutral Europe," Brussels, 2020.

[144] S. Craen, "Financing a world scale hydrogen export project," Oxford Institute for Energy Studies, Oxford, 2023.

[145] G. Fambri, C. Diaz-Londono, A. Mazza, M. Badami, T. Sihvonen and R. Weiss, "Techno-economic analysis of Power-to-Gas plants in a gas and electricity distribution network system with high renewable energy penetration," *Applied Energy,* vol. 312, no. 118743; https://doi.org/10.1016/j.apenergy.2022.118743, 2022.

[146] J. Yates, R. Daiyan, R. Patterson, R. Egan, R. Amal, A. Ho-Baille and N. L. Chang, "Techno-economic Analysis of Hydrogen Electrolysis from Off-Grid Stand-Alone Photovoltaics Incorporating Uncertainty Analysis," *Cell Reports Physical Science,* vol. 1, no. 10; https://doi.org/10.1016/j.xcrp.2020.100209, 2020.

[147] V. Walter, L. Göransson, M. Taljegard, S. Öberg and M. Odenberger, "Low-cost hydrogen in the future European electricity system – Enabled by flexibility in time and space," *Applied Energy,* Vols. 330, Part B, no. 120315; https://doi.org/10.1016/j.apenergy.2022.120315, 2023.

[148] R. Li, X. Jin, P. Yang, X. Sun, G. Zhu, Y. Zheng, M. Zheng, L. Wang, M. Zhu, Y. Qi, Z. Huang, Z. Luyao, D. Wang and W. Yung, "Techno-economic analysis of a wind-photovoltaic-electrolysis-battery hybrid energy system for power and hydrogen generation," *Energy Conversion and Management,* vol. 281, no. 116854; https://doi.org/10.1016/j.enconman.2023.116854, 2023.

[149] Deep Source, "Observing the renewable energy transition from a European perspective," [Online]. Available: https://deepresource.wordpress.com/2019/01/14/largest-hydrogen-electrolyser-plant-in-the-world-135-167-mw/. [Accessed 22 9 2023].

[150] S. Kasahara, Water Electrolysis from: Nuclear Hydrogen Production, CRC Press, 28 Mar 2011.

[151] V. A. Panchenko, Y. V. Daus, A. A. Kovalev, I. V. Yudaev and Y. V. Litti, "Prospects for the production of green hydrogen: Review of countries with high potential," *International Journal of Hydrogen Energy,* vol. 48, no. 12, pp. 4551-4571; https://doi.org/10.1016/j.ijhydene.2022.10.084, 2023.

[152] "Hydrospider plans first Swiss commercial hydrogen production," *Fuel Cells Bulletin,* vol. 2019, no. 8, p. 9, 2019.

[153] Hydro Review, "Hydrogen production facility to be powered by Reichenau hydropower plan," [Online]. Available: https://www.hydroreview.com/business-finance/business/hydrogen-production-facility-to-be-powered-by-reichenau-hydropower-plant/#gref. [Accessed 22 9 2023].

[154] H2 Energy AG, "The first electrolyzer plant in Switzerland generating hydrogen from renewable power at the run-of-the-river plant in Aarau," [Online]. Available:

https://h2energy.ch/wp-content/uploads/2017/06/Brochure-First-Swiss-Hydropower-electrolysis-system-hydrogen.pdf. [Accessed 2021 3 18].

[155] Renewable Energy World, "Landsvirkjun to build hydrogen production facility at 16-MW Ljosifoss hydropower," 6 9 2020. [Online]. Available: https://www.renewableenergyworld.com/hydrogen/landsvirkjun-to-build-hydrogen-production-facility-at-16-mw-ljosifoss-hydropower/#gref. [Accessed 18 3 2021].

[156] ThyssenKrupp AG, "A perfect match: hydropower plants & water electrolysis," [Online]. Available: https://www.thyssenkrupp.com/en/stories/sustainability-and-climate-protection/fits-perfectly-hydropower-and-green-hydrogen. [Accessed 12 9 2023].

[157] Varennes Carbon Recycling (VCR), "A biofuel plant for green economy," [Online]. Available: https://rcv-vcr.com/. [Accessed 19 3 2024].

[158] ARSO, "Arhiv meritev (eng. Measurement archive)," Slovenian Environment Agency, [Online]. Available: https://meteo.arso.gov.si/met/sl/archive/. [Accessed 17 3 2023].

[159] R. A. Naghizadeh, S. Jazebi and B. Vahidi, "Modeling Hydro Power Plants and Tuning Hydro Governors as an Educational Guideline," *International Review on Modelling and Simulations,* vol. 5, no. 4, 2012.

[160] N. Kishor, R. P. Saini and S. P. Singh, "A review on hydropower plant models and control," *Renewable and Sustainable Energy Reviews,* vol. 11, no. 5, pp. 776-796; https://doi.org/10.1016/j.rser.2005.06.003, 2007.

[161] A. Acakpovi, E. B. Hagan and F. X. Fifatin, "Review of Hydropower Plant Models," *International Journal of Computer Applications,* vol. 108, no. 18, 2014.

[162] J. Garrido, Á. Zafra and F. Vázquez, "Object oriented modelling and simulation of hydropower plants with run-of-river scheme: A new simulation tool," *Simulation Modelling Practice and Theory,* vol. 17, no. 10, pp. 1748-1767; https://doi.org/10.1016/j.simpat.2009.08.007, 2009.

[163] G. A. Munoz-Hernandez, S. P. Mansoor and D. I. Jones, Modelling and Controlling Hydropower Plants, New York: London Dordrecht Heidelberg, 2013.

[164] S. Heimerl and N. Schwiersch, "Dynamic Water-Level Regulation at Run-of-River Hydropower Plants to Increase Efficiency and Generation," *Water,* vol. 13, no. 21, 2983; https://doi.org/10.3390/w13212983, 2021.

[165] D. Tsuanyo, B. Amougou, A. Aziz, B. N. Nnomo, D. Fioriti and J. Kenfack, "Design models for small run-of-river hydropower plants: a review," *Sustainable Energy Research,* vol. 10, no. 3; https://doi.org/10.1186/s40807-023-00072-1, 2023.

[166] The Institution of Engineering and Technology (IET), Modeling and Dynamic Behaviour of Hydropower Plants, London: The Institution of Engineering and Technology, 2017.

[167] D. J. Jovan, G. Dolanc and B. Pregelj, "Utilization of excess water accumulation for green hydrogen production in a run-of-river hydropower plant," *Renewable Energy,* vol. 195, pp. 780-794; https://doi.org/10.1016/j.renene.2022.06.079, 2022.

[168] P. Punys, A. Dumbrauskas, E. Kasiulis, G. Vyčienė and L. Šilinis , "Flow Regime Changes: From Impounding a Temperate Lowland River to Small Hydropower

Operations," *Energies,* vol. 8, pp. 7478-7501; https://doi.org/10.3390/en8077478, 2015.

[169] J. Amezcua Medina, *Modeling of a power-to-hydrogen system based on hydro energy = Modeliranje sistema za napajanje z vodikom na osnovi hidroenergije : a Master's thesis of the second-cycle master's study programme in Mechanical Engineering / Joel Amezcua Medina, M.S. thesis,* University of Ljubljana, Faculty of Mechanical Engineering. Available: https://plus.cobiss.net/cobiss/adz/sl/bib/21934595, 2020.

[170] Cristóbal Rodríguez, Marco, *Feasibility study of the operation of Brežice hydro power plant for the implementation of hydrogen electrolyzers = Študija izvedljivosti delovanja hidroelektrarne Brežice za vgradnjo elektrolizerjev : a Bachelor's thesis of the first-cycle bachelor's stud,* University of Ljubljana, Faculty of Mechanical Engineering. Available: https://plus.cobiss.net/cobiss/adz/sl/bib/22004739, 2018.

[171] X. Mei, Z.-j. Dai, P. Van Gelder and J. Gao, "Linking Three Gorges Dam and downstream hydrological regimes along the Yangtze River, China," *Earth and Space Science,* vol. 2, no. 4; https://doi.org/10.1002/2014EA000052, 2015.

[172] F. Pappenberger, P. Matgen, K. J. Beven, L. Pfister and P. De Fraipont, "Influence of uncertain boundary conditions and model structure on flood inundation predictions," *Advances in Water Resources,* vol. 29, no. 10, pp. 1430-1449; https://doi.org/10.1016/j.advwatres.2005.11.012, 2006.

[173] B. Kim, T. Lee and T. B. M. J. Ouarda, "Total least square method applied to rating curves," *Hydrological Processes,* vol. 28, no. 13; https://doi.org/10.1002/hyp.9944, 2014.

[174] M. Rhandi, M. Trégaro, F. Druart, J. Deseure and M. Chatenet, "Electrochemical hydrogen compression and purification versus competing technologies: Part I. Pros and cons," *Chinese Journal of Catalysis,* vol. 41, no. 5, pp. 756-769; https://doi.org/10.1016/S1872-2067(19)63404-2, 2020.

[175] P. J. Bouwman, J. Konink, D. Semerel, L. Raymakers, M. Koeman, W. Kout, W. Dalhujsen, E. Milacic and M. J. J. Mulder, "Electrochemical Hydrogen Compression," *ECS Transactions,* vol. 64, no. 3, pp. 1009-1018; https://doi.org/10.1149/06403.1009ecst, 2014.

[176] Engineering ToolBox, "Universal and Individual Gas Constants," [Online]. Available: https://www.engineeringtoolbox.com/individual-universal-gas-constant-d_588.html. [Accessed 10 3 2022].

[177] M. J. Ginsberg, M. Venkatraman, D. V. Esposito and V. M. Fthenakis, "Minimizing the cost of hydrogen production through dynamic polymer electrolyte membrane electrolyzer operation," *Cell Reports Physical Science,* vol. 3, no. 6, 100935; https://doi.org/10.1016/j.xcrp.2022.100935, 2022.

[178] J. Davies, F. Dolci and E. Weidner Ronnefeld, "Historical Analysis of FCH 2 JU Electrolyser Projects," EUR 30648 EN, Publications Office of the European Union, Luxembourg, 2021, ISBN 978-92-76-32441-6, doi:10.2760/951902, JRC121704.

[179] G. Papakonstantinou, G. Algara-Siller, D. Teschner, T. Vidaković-Koch, R. Schlögl and K. Sundmacher, "Degradation study of a proton exchange membrane water electrolyzer under dynamic operation conditions," *Applied Energy,* vol. 280, no. 115911; https://doi.org/10.1016/j.apenergy.2020.115911, 2020.

[180] hpem2gas, “Technical Highlight: Increase in Hydrogen Production Rate,” [Online]. Available: https://hpem2gas.eu/itm-power-technical-highlight/. [Accessed 15 11 2022].

[181] M. Suermann, B. Bensmann and R. Henke-Rauschenbach, “Degradation of Proton Exchange Membrane (PEM) Water Electrolysis Cells: Looking Beyond the Cell Voltage Increase,” *Journal of The Electrochemical Society,* vol. 166, no. 10, pp. 645-652; https://doi.org/10.1149/2.1451910jes, 2019.

[182] HESS d.o.o., “HE Brežice,” [Online]. Available: https://www.he-ss.si/eng/he-brezice-general-info.html.

[183] HESS d.o.o., “Letno poročilo družbe HESS, do.o. in skupine HESS za leto 2020,” Družba Hidroelektrarne na Spodnji Savi, d.o.o. , Brežice, 2020.

[184] D. Požun, “Izgradnja in obratovanje verige HE na spodnji Savi,” Družba HESS, d.o.o., Brežice, 2013.

[185] Zelena Slovenija, “Hibridni sistem sonca in vode kot vzorčni primer lokalno vodenega mešanega vira – ESG 181,” 3 8 2023. [Online]. Available: https://www.zelenaslovenija.si/esg/hibridni-sistem-sonca-in-vode-kot-vzorcni-primer-lokalno-vodenega-mesanega-vira-esg-181/. [Accessed 20 10 2023].

[186] S. Sagaria, R. C. Neto and P. Baptista, “Assessing the performance of vehicles powered by battery, fuel cell and ultra-capacitor: Application to light-duty vehicles and buses,” *Energy Conversion and Management,* vol. 229, no. 113767: https://doi.org/10.1016/j.enconman.2020.113767, 2021.

[187] A. Ajanovic, A. Glatt and R. Haas, “Prospects and impediments for hydrogen fuel cell buses,” *Energy,* vol. 235, no. 121340: https://doi.org/10.1016/j.energy.2021.121340, 2021.

[188] H. Kim, N. Hartmann, M. Zeller, R. Luise and T. Soylu, “Comparative TCO Analysis of Battery Electric and Hydrogen Fuel Cell Buses for Public Transport System in Small to Midsize Cities,” *Energies,* vol. 14, no. 14, 4384: https://doi.org/10.3390/en14144384, 2021.

[189] Ballard, “Hydrogen Fueling for Fuel Cell Bus Fleets,” June 2019. [Online]. Available: https://www.ballard.com/.

[190] D. J. Jovan, B. Pregelj and G. Dolanc, “Hydrogen system optimisation tool: (MATLAB scripts),” IJS delovno poročilo, 14617, Ljubljana, 2024.

[191] P. B. de Moura Oliveira, E. J. Solteiro Pires, J. Boaventura Cunha and D. Vrančić, (2009). Multi-Objective Particle Swarm Optimization Design of PID Controllers. In: Omatu, S., et al. Distributed Computing, Artificial Intelligence, Bioinformatics, Soft Computing, and Ambient Assisted Living. IWANN 2009. Lecture Notes in Computer Science.

[192] P. B. de Moura Oliveira and D. Vrančić, "Swarm Design of Series PID Cascade Controllers," 2018 13th APCA International Conference on Automatic Control and Soft Computing (CONTROLO), Ponta Delgada, Portugal, 2018, pp. 276-281, doi: 10.1109/CONTROLO.2018.8516417.

[193] P. B. de Moura Oliveira and D. Vrančić, (2017). Grey Wolf, Gravitational Search and Particle Swarm Optimizers: A Comparison for PID Controller Design. In:

Garrido, P., Soares, F., Moreira, A. (eds) CONTROLO 2016. Lecture Notes in Electrical Engineering, vol 402. Springer, Cham. https://doi.org/.

[194] X.-S. Yang, Nature-Inspired Optimization Algorithms (Second Edition), London, United Kingdom: Middlesex University London, School of Science and Technology, https://doi.org/10.1016/B978-0-12-821986-7.00002-0, 2021.

[195] MathWorks®, "Particle swarm optimization," [Online]. Available: https://www.mathworks.com/help/gads/particleswarm.html. [Accessed 26 5 2023].

[196] A. P. Engelbrecht, "Chapter 16: Particle Swarm Optimization," in *Computational Intelligence: An Introduction (2nd Edition)*, Hoboken, John Wiley & Sons, Ltd, 2007, pp. 289-358.

[197] M. Jain, V. Saihjpal, N. Singh and S. B. Singh, "An Overview of Variants and Advancements of PSO Algorithm," *Applied Sciences,* vol. 12, no. 17; 8392; https://doi.org/10.3390/app12178392, 2022.

Bibliography

Publications Related to the Thesis

Journal Articles

[1] David Jure Jovan, Gregor Dolanc, Boštjan Pregelj, *"Utilization of excess water accumulation for green-hydrogen production in a run-of-river hydropower plant"*, Renewable energy, [Print ed.], 2022, vol. 195, august, pages 780-794, ISSN 0960-1481, DOI: 10.1016/j.renene.2022.06.079.

[2] David Jure Jovan, Gregor Dolanc, Boštjan Pregelj, *"Cogeneration of green hydrogen in a cascade hydropower plant"*, Energy conversion and management. X., 2021, vol. 10, str. 100081-1-100081-12, ISSN 2590-1745, DOI: 10.1016/j.ecmx.2021.100081.

[3] David Jure Jovan, Gregor Dolanc, *"Can green-hydrogen production be economically viable under current market conditions"*, Energies, 2020, vol. 13, no. 24, str. 6599-1-6599-17, ISSN 1996-1073, DOI: 10.3390/en13246599.

Conference Paper

[4] Boštjan Pregelj, David Jure Jovan, Gregor Dolanc, Boštjan Drobnič, *"Modeliranje in simulacija hidroelektrarne s sistemom za soproizvodnjo vodika in sončno elektrarno"*, In: Zbornik enaintridesete mednarodne Elektrotehniške in računalniške konference ERK 2022 = Proceedings of the 31st International Electrotechnical and Computer Science Conference ERK 2022 : Portorož, Slovenija, 19. - 20. september 2022.

[5] David Jure Jovan, Gregor Dolanc, Boštjan Pregelj, *"Kogeneracija zelenega vodika v pretočni hidroelektrarn"*, In: AIG.si 21 : 8. april 2021 : zbornik dvanajste konference Avtomatizacija v industriji in gospodarstvu, Nenad Muškinja (ed.), Milan Rotovnik (ed.), Elektronska izd., Ljubljana: Društvo avtomatikov Slovenije, 2021.

Other Publications

[6] David Jure Jovan, Boštjan Pregelj, Gregor Dolanc. Hydrogen system optimisation tool : (MATLAB scripts). 2024. IJS delovno poročilo, 14617.

[7] David Jure Jovan, *"Activities on the field of hydrogen technologies",* presented at Slovenian - German Hydrogen Day, 31st Jan. 2023.

[8] David Jure Jovan, Boštjan Pregelj, Gregor Dolanc, Vladimir Jovan. "*Matlab/Simulink model HE Brežice",* 2022. IJS delovno poročilo, 13767.

[9] Vladimir Jovan, David Jure Jovan, Gregor Dolanc. *"Izhodišča za proizvodnjo in uporabo zelenega vodika v Sloveniji*", 2021. IJS delovno poročilo, 13571.

[10] Vladimir Jovan, Gregor Dolanc, David Jure Jovan. *"Ekonomika in stroški obratovanja Power-to-gas (P2G) sistema v Hidroelektrarni Brežice",* 2020. IJS delovno poročilo, 13140.

[11] David Jure Jovan, Vladimir Jovan, Gregor Dolanc. *"Ocena možnosti uvedbe P2G sistema v HE Brežice : (proizvodnja zelenega vodika)",* 2020. IJS delovno poročilo, 13279, zaupno.

[12] David Jure Jovan, Gregor Dolanc, Vladimir Jovan. *"Pregled komercialnih dobaviteljev opreme za vodikove tehnologije",* 2020. IJS delovno poročilo, 13137.

[13] David Jure Jovan, Gregor Dolanc, Vladimir Jovan. *"Pregled trenutnega stanja in potencialov vodikove ekonomije v svetu",* 2020. IJS delovno poročilo, 13139.

Biography

David Jure Jovan was born on the 23nd of March, 1985 in Ljubljana, the Republic of Slovenia. He holds a BSc in Chemical Technology from the University of Ljubljana, Faculty of Chemistry and Chemical Technology, and an MSc in Information and Communication Technologies from the Jožef Stefan International Postgraduate School.

After graduation, he worked in the industry for more than 9 years. He gained a lot of professional experience as a process and development engineer in a company producing acrylic sheets, and later as a senior technical sales representative in a company that is a leading supplier of water treatment technologies in Slovenia.

Leading various project teams allowed him to develop management skills and gain an insight into the entire development process. In parallel with his work, he remained connected to science by further developing the control of the pre-polymerisation reactor, the temperature control of the polymerisation pools and the post-polymerisation furnaces. He also introduced automatic pliers for the acrylic sheets moulding line and helped to introduce numerous methods to control the feedstock for the polymerisation process and develop new formulations for acrylics that improved the quality of the final product. During his regular employment, the company also funded his postgraduate studies. As part of his research, he developed a new method for online viscosity estimation using a soft sensor during prepolymer production. After a job change in 2017, he managed to sell and commission four drinking water treatment plants (one of them in Kenya) and completed his master's thesis entitled: Estimation of dissolved organic matter in surface waters using data-based modelling and simulation.

Jovan is currently working in the Department of Systems and Control at the Jožef Stefan Institute. His research interests include hydrogen technologies with a focus on green-hydrogen production. As a chemical technologist, he is particularly interested in new chemical technologies and their transfer to industrial practise.

He was also actively involved in various research projects during his studies, such as:

HYPER - An electrochemically produced oxidiser for modular, onsite generation of HYdrogen PERoxide.

L2-1832 (B) - from the ARIS records: Optimization based control of P2G converter connected to hydro power plant.

L2-4456 (B) - from the ARIS records: Multifunctional hydrogen technologies supporting power system balancing, energy storage and market.